2015

TARGET-DIRECTED BIOSYNTHETIC EVOLUTION: REDIRECTING PLANT EVOLUTION TO GENOMICALLY OPTIMIZE A PLANT'S PHARMACOLOGICAL PROFILE

Dustin Paul Brown
University of Kentucky, dpbrow2@uky.edu

STUDENT AGREEMENT:

I represent that my thesis or dissertation and abstract are my original work. Proper attribution has been given to all outside sources. I understand that I am solely responsible for obtaining any needed copyright permissions. I have obtained needed written permission statement(s) from the owner(s) of each third-party copyrighted matter to be included in my work, allowing electronic distribution (if such use is not permitted by the fair use doctrine) which will be submitted to UKnowledge as Additional File.

I hereby grant to The University of Kentucky and its agents the irrevocable, non-exclusive, and royalty-free license to archive and make accessible my work in whole or in part in all forms of media, now or hereafter known. I agree that the document mentioned above may be made available immediately for worldwide access unless an embargo applies.

I retain all other ownership rights to the copyright of my work. I also retain the right to use in future works (such as articles or books) all or part of my work. I understand that I am free to register the copyright to my work.

REVIEW, APPROVAL AND ACCEPTANCE

The document mentioned above has been reviewed and accepted by the student's advisor, on behalf of the advisory committee, and by the Director of Graduate Studies (DGS), on behalf of the program; we verify that this is the final, approved version of the student's thesis including all changes required by the advisory committee. The undersigned agree to abide by the statements above.

Dustin Paul Brown, Student

Dr. Greg A. Gerhardt, Major Professor

Dr. Wayne A. Cass, Director of Graduate Studies

TARGET-DIRECTED BIOSYNTHETIC EVOLUTION: REDIRECTING PLANT EVOLUTION TO GENOMICALLY OPTIMIZE A PLANT'S PHARMACOLOGICAL PROFILE

DISSERTATION

A dissertation submitted in partial fulfillment of the
requirements for the degree of Doctor of Philosophy in the
College of Medicine
at the University of Kentucky

By
Dustin Paul Brown

Lexington, Kentucky

Director: Dr. Greg A. Gerhardt, Professor of Anatomy and Neurobiology

Lexington, Kentucky

2015

ABSTRACT OF DISSERTATION

TARGET-DIRECTED BIOSYNTHETIC EVOLUTION: REDIRECTING PLANT EVOLUTION TO GENOMICALLY OPTIMIZE A PLANT'S PHARMACOLOGICAL PROFILE

The dissertation describes a novel method for plant drug discovery based on mutation and selection of plant cells. Despite the industry focus on chemical synthesis, plants remain a source of potent and complex bioactive metabolites. Many of these have evolved as defensive compounds targeted on key proteins in the CNS of herbivorous insects, for example the insect dopamine transporter (DAT). Because of homology with the human DAT protein some of these metabolites have high abuse potential, but others may be valuable in treating drug dependence. This dissertation redirects the evolution of a native *Lobelia* species toward metabolites with greater activity at this therapeutic target, i.e. the human DAT. This was achieved by expressing the human DAT protein in transgenic plant cells and selecting gain-of-function mutants for survival on medium containing a neurotoxin that is accumulated by the human DAT. This created a sub-population of mutants with increased DAT inhibitory activity. Some of the active metabolites in these mutants are novel (i.e. not detectable in wild-type cells). Others are cytoprotective, and also protect DAergic neurons against the neurotoxin. This provides proof-of-concept for a novel plant drug discovery platform, which is applicable to many different therapeutic target proteins and plant species.

KEYWORDS: Plant secondary metabolites, *Lobelia cardinalis*, human dopamine transporter, target-directed biosynthetic evolution, drug dependence

Dustin Paul Brown

Student's Signature

10-10-2015

Date

TARGET-DIRECTED BIOSYNTHETIC EVOLUTION: REDIRECTING PLANT EVOLUTION TO GENOMICALLY OPTIMIZE A PLANT'S PHARMACOLOGICAL PROFILE

By

Dustin Paul Brown

Dr. Greg A. Gerhardt

Co-Director of Thesis

Dr. John M. Littleton

Co-Director of Thesis

Dr. Wayne A. Cass

Director of Graduate Studies

10-10-2015

Date

For my father, Paul Darwin Brown, for without your unconditional love and belief in me I would have never come to be the man I am today, and none of my life's achievements would have every been possible. And for my loving fiancée, Cassie Kate Starr, the one true love I my life that has always been by my side. All that I do is for you two, and I am doing all I can to be the kind of person you wanted me to Dad, someone who can contribute and give back to society…

ACKNOWLEDGEMENTS

I cannot thank my co-mentors, Dr. Greg Gerhardt and Dr. John Littleton, enough for all of the help and insight you have provided during my years as a graduate student. Your guidance has truly been invaluable. My first experience with research in Dr. Littleton's lab was invaluable, as it led my realization of the love I have for their career path. Dr. Gerhardt, our conversations were truly a pleasure, and I thank you helping guide me along the path, and contributing to my understanding of the research field and things in life in general. The same can be said for Dr. Littleton, as well. Each of you have been instrumental, enabling me to gain the technical knowledge required to perform quality research, as well as knowing how to balance all our commitments in life. These men are not only fantastic mentors, but also great friends, and I look forward to our continuing relationship. After all, you all are my "mentors for life." I couldn't have chosen better. I would also like to thank my committee members. Your insight and guidance is truly appreciated.

I would also like to thank my family and friends for all the support and belief in me. It truly made a difference. The critical role my father, Paul Darwin Brown, played in my life cannot be put into words. Since elementary school, he has stressed the importance of acquiring an education, and through the good and the bad, he has always been by my side. I love you Dad. As you've told me before, some flowers may bloom latter than others, but they are every bit as beautiful as the rest. The path bringing me to where I am today required a significant amount of time, but it was all worth it, and I look forward to the day when you truly have the opportunity to see me "bloom." That is, the day I obtain my PhD and MD. I will always be there for you Dad, just as you have been for me. And for my loving fiancé, Cassie Kate Starr, I will always be thankful that you were there by my side, through thick and thin supporting me along the way. I'm sure it hasn't always been pleasant having someone up banging on the keyboard until the sun rises, but you've never complained. I look forward to our life together more than you know.

TABLE OF CONTENTS

LIST OF TABLES

LIST OF FIGURES

Chapter 1

Introduction

1.1. Plants as a source of drugs and drug leads

Plant-derived medicines have been used to treat human disease for millennia. Their utilization likely predates even the earliest records signifying the therapeutic utilization of plants, such as Sumerian artifacts dating back to 5000 B.C. indicating the clinical use of opium [1]. Plant-derived small molecule natural products (SMNPs) continue to be used in modern medicine in fields ranging from neurology (e.g. galantamine) to oncology (e.g. vincristine) [2]. Furthermore, pharmacotherapies and drug leads continue to be discovered from plant sources [3]. Undoubtedly, plants are an excellent source of novel drug leads. However, there are a number of challenges and limitations associated with plant-based drug discovery including low yields of bioactive metabolites, identifying which of the thousands of plant species in existence contain metabolites with a desired bioactivity, the isolation of a single bioactive metabolite of interest from potentially thousands in a single extract, and threats of extinction to plant species, to name a few [4, 5].

In the last quarter of the 20th century, many drug discovery programs largely discontinued screening of plant SMNPs in favor of synthetics as a source of structurally diverse drug leads [2, 4, 6]. This was largely due to the advent of combinatorial chemistry (CC) and high-throughput pharmacological screening (HTPS), as well as the perceived difficulties associated with plant-based drug discovery [2, 4]. The transition seemed logical. The development of CC gave medicinal chemists the capacity to generate thousands of novel molecules in a relatively short period of time, which could be rapidly screened for a given biological activity using HTPS [2, 7]. Thus, the coupling of CC to HTPS (CC-

HTPS) enabled drug discovery programs to rapidly sort through thousands of synthetics to identify novel drug leads. However, CC-HTPS fell short of expectations, yielding a single small molecule of complete synthetic origin approved by the FDA for use in humans over the 30 year span between 1981 and 2010 [6]. During that same span of time, 64% of small molecules approved by the FDA for use in humans were natural products, or natural product derived, despite reductions in revenue, facilities, and manpower contributed to this effort [4, 6]. The disparity between the success rates of synthetics and SMNPs, or derivatives thereof, compelled researchers to investigate the physiochemical properties of each as compared to those of FDA-approved small molecule therapeutics. This led to the consensus that SMNPs, including those from plant sources, share a greater degree of physiochemical similarity to FDA approved small molecule therapeutics leading to greater “druggability” of bioactive SMNPs [8, 9]. Furthermore, plant SMNPs must have a certain degree of biocompatibility to exist in living cells, bioavailability in order to reach and interact with their target/s in other organisms, and bioactivity to elicit a response upon reaching their target/s, all of which contribute to the inherent “druggability” of bioactive plant secondary metabolites [9, 10].

Numerous investigators have made efforts to overcome obstacles encountered in plant-based drug discovery [5, 11]. Recent advances in analytical chemistry will undoubtedly facilitate the isolation and structural elucidation of bioactive plant SMNPs [4, 7]. Progress in the fields of plant molecular biology and plant sciences are also addressing challenges associated with plant-based drug discovery [5, 7, 11]. For example, the expression of genes encoding biosynthetic enzymes to generate transgenic rice containing Vitamin A was one of the greatest, and most successful efforts to reduce blindness caused by malnutrition in countries where rice is the major grain consumed by humans [12]. An example of the use of plant cell cultures for the purpose of drug discovery is the growth of hairy roots to obtain precursors for the semi-synthesis of the chemotherapeutic Taxol [13]. Another breakthrough in plant molecular biology enabling the generation of stable, “gain-of-function” mutants, known as activation

tagging mutagenesis (ATM), has been used to generate mutants with increased yields of therapeutically valuable plant secondary metabolites [14, 15]. Herein, “gain-of-function” mutation refers to mutations that cause enhanced gene transcription. “Gain-of-function” mutations are induced by transforming plant cells with agrobacterial strains harboring binary vectors carrying a tetramer of the enhancer element from the Cauliflower Mosaic Virus (CaMV) 35S promoter gene [14, 16-19]. Successful transformation and integration of the enhancer tetramer into the plant genome “activates” flanking genes 10-kb upstream and downstream of the integration site [14, 18]. Using ATM, Littleton (2007) generated activation tagged *Nicotiana tabacum* mutants with increased yields of nicotine, as well as putatively “novel” nicotinic acetylcholine receptor ligands that were undetectable in the wild-type plant [14, 15]. Utilization of *Agrobacterium tumifaciens* in the former study was less than ideal, since the resulting neoplastic callus cultures are undifferentiated leading to a reduction in their biosynthetic capacity [19]. However, transformation of plant cells with *A. rhizogenes* carrying ATM vectors induces the formation of stable, gain-of-function hairy roots, which develop from a single transformed cell, are clonal in nature, and are differentiated retaining much of the biosynthetic capacity of an intact plant [19]. Hairy roots are easy to culture, do not require hormones to sustain growth, and methods are available to scale-up the growth of hairy root cultures [19]. However, the use of ATM alone requires the generation and maintenance of thousands of mutants to saturate a plant’s genome, as well as the preparation and screening of extracts from each mutant [14, 15]. The use of ATM alone for the purpose of drug discovery is inefficient (“positive hit” rate, ~1/1000), timely, and laborious, limitations we seek to overcome by combining ATM with artificial selection favoring the survival of mutants with a genotype of interest [14, 15].

The majority of medicinal compounds derived from plants are secondary metabolites, molecules of astonishing complexity and diversity which evolved to enable plants to react and respond to stimuli arising from abiotic and biotic sources in their local environment [13, 20]. Over plants’ ~3 billion year existence, natural selection has optimized the interactions between plant secondary

metabolites and macromolecules present in co-existing prokaryotic and eukaryotic organisms to elicit a required biological response [3, 10, 13, 14]. Plants containing SMNPs with optimal function had a survival advantage, thus natural selection favored the retention of such molecules and their respective biosynthetic pathways [3, 4, 13]. The evolutionary process is essentially analogous to optimization and screening of compound libraries during drug discovery and development [4]. Variation in plants' metabolomes and biosynthetic pathways, arising from sexual reproduction, mutations, and horizontal gene transfer, leads to the genesis of new metabolites and/or numerous congeners of a single molecule (optimization), which are retained or lost through the process of natural selection (screening) depending on the survival advantage a metabolite/s affords a plant [3, 4, 13]. The evolutionary plasticity of plants, their remarkable biosynthetic capacity, and "experience" arising from their ~3 billion year existence gives plants a tremendous advantage over medicinal chemists [2, 7, 10, 14].

Given biosynthesis plant secondary metabolites, including those of medicinal value, evolved via natural selection, it should be possible to devise artificial selection conditions favoring the survival of plants with pharmacologically optimized genotypes, and resultant phenotypes. Here, we present a novel approach aimed to overcome the challenges and limitations associated with drug discovery from plant sources, outlined above, by applying the principles of natural selection and evolution to harness the biosynthetic capacity of plants to generate SMNPs with desirable drug-like properties that are active at molecular targets of interest. Essentially, the evolution of a plant species is redirected to encourage synthesis of metabolites designed to interact with a specific human target protein, coined target-directed biosynthesis. This is accomplished by generating a heterogeneous population of gain-of-function mutant plant cells expressing a human protein that is a therapeutic molecular target. The aforementioned population of mutant plant cells is subject to selection conditions such that survival is contingent upon beneficial mutations that increase yields and/or cause biosynthesis of novel metabolites with a desired/required

therapeutic activity. Therefore, we are able to select individual cultures with optimized pharmacological genotypes/phenotypes, and thereby massively accelerate the evolution of plant secondary metabolism. This innovative approach redirects plant biosynthetic evolution to produce molecules with a specific human target and related potential therapeutic activity. In the example described below, we have generated mutant cultures of *Lobelia cardinalis* which are overproducing inhibitors of the human dopamine transporter, a molecular target for therapeutics in drug dependence.

1.2. Plants as a source of novel drug leads for the treatment of drug abuse

The vast majority of pharmacotherapies implemented for the treatment of drug abuse, including those used for the treatment of nicotine use disorders and opioid dependence, are natural products, natural product-derived, and/or were inspired by the structure of natural products. Plant-derived SMNPs, such as nicotine and cytisine, are approved in the United States and many countries in Eastern Europe, respectively, as smoking cessation agents [20, 21]. Varenicline, another FDA-approved smoking cessation agent, was inspired by the structure of cytisine [20-22]. Varenicline and cytisine function as $\alpha_4\beta_2$-nicAchR partial agonists, whereas nicotine is a full agonist at $\alpha_4\beta_2$-nicAchRs [22]. The aforementioned nicAchR ligands are utilized as substitution therapies for nicotine use disorders [20-22]. However, cytisine and varenicline are unique from nicotine in that they have the capacity to blunt the rewarding effects associated with smoking by functionally antagonizing the effect of nicotine [21]. Bupropion is a DAT inhibitor based on the structure of cathinone, an alkaloid present in khat, which is also approved by the FDA as a smoking cessation agent [23-26]. Buprenorphine is a structural analogue of thebaine, a naturally occurring alkaloid present in *Papaver somniferum* [27]. Buprenorphine is a μ-opioid receptor partial agonist FDA-approved for the treatment of opioid addiction [27]. The structure of methadone, which is also utilized as a substitution therapy for opioid dependence, is derived from the structural backbone of atropine, a naturally

occurring alkaloid present in *Atropa belladonna* [20]. Furthermore, the structure of the μ-opioid receptor antagonists, naltrexone and naloxone, were inspired by that of the alkaloid oripavine (also present in *P. somniferum*), and are approved by the FDA for the management of opioid dependence and overdose, respectively [27]. A summary of select pharmacotherapeutics used for the treatment of drug abuse, as well as SMNPs on which their structure is based, and the SMNPs' plant origin, is presented in **Table 1.1**. Indeed, plant metabolites' structural scaffolds may possess the "blueprints" necessary to develop promising drug leads for the treatment of drug abuse, including psychostimulant addiction.

Plants are an invaluable source of medicines and novel drug leads, and plant's repository of SMNPs arguably represents one of the most structurally complex and diverse small molecule libraries in existence [14, 20, 28]. However a question remains: why are plant SMNPs biologically active in humans? It would be egocentric, and quite naïve to think that plants evolved molecules with therapeutic effects for the sole purpose of curing human disease. A recent review by Kennedy and Wightman (2012) addressing this topic provides compelling evidence that natural selection arising from plant's interaction with co-existing organisms led to the evolution of SMNPs that are bioactive in humans [13, 14]. Given humans only came into existence relatively recently in evolutionary time, their impact on the evolution of plant biosynthesis is relatively negligible [13, 14]. The major culprits accredited underlie the evolution of plant SMNPs having bioactivity in the human CNS are herbivorous insects [13, 14]. Plants and herbivorous insects have co-existed for 400 million years [13]. Furthermore, plant-insect interactions occur at a greater frequency owing to the tremendous number insect species [13]. To date, insect species represent greater than half of the multicellular species identified on earth, and nearly half of existing insect species are herbivorous [13]. Additionally, the collective biomass of insects outweighs that of vertebrates by a factor of 10 to 1 [13]. The co-existence of plants and insects necessitated the evolution of defense strategies ensuring the continuing existence of plants, despite threats imposed by herbivorous insects [13, 14]. Since plants are sessile, their primary means of deterring herbivorous

insects is the synthesis of chemical defenses in the form of secondary metabolites [13, 14]. Plant secondary metabolites are not required for plants' primary metabolism, and thus evolved enabling plants to respond and react to changes in their local environment [13, 14]. Well-known examples of defensive metabolites synthesized by plants include nicotine and cocaine [13, 14, 29, 30]. Waxy substances exuded by plant cells immobilize and/or suffocate herbivorous insects, whereas chemical attractants are released from plants attracting predators of insects that pose as threats [13]. In order to address the genesis of plant SMNPs bioactive in the human CNS, a closer examination of insect neurotransmission and similarity shared between key proteins present in the human and insect CNS is required.

The major excitatory neurotransmitter in the insect CNS is acetylcholine, which activates nicotinic acetylcholine receptors (nicAchR) [14]. Given the importance of cholinergic neurotransmission in insects, the disruption of signaling at insect nicAchRs presents an excellent target for plant chemical defenses [13, 14]. A variety of nicAchR ligands have been identified in plants, which are primarily believed to function as natural insecticides, including nicotine and cytisine [13, 14, 29]. For example, ingestion of nicotine by insects produces aversive stimuli, paralysis, and/or death, via activation of insect nicAchRs [14, 29]. Acetylcholine is also a prominent excitatory neurotransmitter in the human CNS, which influences the activity of numerous neurotransmitter systems via the modulation of nicAchRs [31, 32]. NicAchRs present in the human and insect CNS share structural homology due to their common evolutionary ancestry [13, 14]. Courtesy of their shared homology, nicAchR ligands synthesized by plants display bioactivity across Phyla, modulating the activity of nicAchRs present in the insect CNS, and their human counterparts [13, 14]. This holds true for a variety of proteins essential for regulation of human and insect neurotransmission, including the DAT [33, 34].

In contrast to humans, insect DAergic neurotransmission is strongly implicated with aversive learning [13, 35]. Increased DAergic neurotransmission in insects has also been reported to signal satiety, attenuate negative geotaxis,

and even induce convulsions and death in insects [36, 37]. Any of the aforementioned affects, which can be elicited by cocaine, would deter insects from feeding on plants containing metabolites that augment DAergic neurotransmission. Thus, inhibition of the DAT represents a viable mechanism to increase DAergic tone in the insect CNS, thereby preventing insect herbivory [30, 35-37]. As such, natural selection would be predicted to favor the biosynthesis of metabolites that function as DAT inhibitors, given plants possessing such compounds would have a survival advantage increasing their evolutionary fitness [3, 4, 13]. Genes encoding the biosynthetic machinery responsible for the synthesis of DAT inhibitors would thereby be retained by the forces of natural selection, and further optimized over time by the forces of evolution [3, 4, 13]. Cocaine, a well-known example of a DAT inhibitor synthesized by the plant *Erythroxylum coca,* functions as a natural insecticide [30].

1.3. Psychostimulant drug abuse

Psychostimulant drug abuse is a major public health concern in the United States and around the world. The abuse of psychostimulants, such as cocaine and methamphetamine, is associated with a significant socioeconomic burden arising from healthcare costs, crime, and lost productivity [38, 39]. Detrimental health effects caused by short-term psychostimulant abuse include hypertension, tachycardia, cardiac arrhythmia, heart attack, stroke, convulsions, paranoia, and/or psychosis [38, 39]. Their long-term use can potentially lead to psychosis, mood disturbances, and/or infection potentially causing death due to bowel ischemia, amongst other adverse health effects [38, 39]. In 2012, 1.2 million individuals reported the use of methamphetamine alone in the past year (National Survey on Drug Use and Health), with an estimated $23.4 billion cost associated with its abuse in 2005 (RAND report, 2009) [38, 39]. Despite years of research and substantial effort on the behalf of scientific investigators, at present there is no pharmacotherapy approved by the United States Food and Drug Administration (FDA) for the treatment of psychostimulant addiction, a significant

unmet medical need [23-25, 40-42]. Multiple lines of evidence indicate the reinforcing effects of cocaine and methamphetamine result from augmentation of dopaminergic (DAergic) neurotransmission in the mesocorticolimbic DAergic pathway [43-45]. Increased DAergic tone in the nucleus accumbens, in particular, is highly implicated in mediating the positive rewarding effects of psychostimulants and other drugs of abuse [43-45].

The dopamine transporter (DAT) is the primary regulator of DAergic tone in the striatum and nucleus accumbens, and is recognized as a key molecular target of cocaine and methamphetamine [33, 43, 46-55]. Cocaine is an inhibitor of the DAT, and enhances vesicular DA release [23, 45]. Methamphetamine is a substrate of the DAT, which competitively inhibits DA reuptake, and also redistributes vesicular DA leading to an increase in cytosolic DA [23, 25, 45]. Subsequently, cytosolic DA is released via methamphetamine-induced reversal of DAT function [23, 25, 45]. As such, the use of both psychostimulants has a common outcome: increased DAergic tone in brain regions densely innervated by DAergic neurons, including the nucleus accumbens [23, 25, 43-45, 56].

Multiple lines of evidence indicate that modulation of DAT function underlies the locomotor and hedonic effects of cocaine and methamphetamine [43-45, 57, 58]. In homozygous DAT knockout mice, cocaine and amphetamine fail to increase locomotor activity above baseline, and do not produce stereotypy [43]. In homozygous mutant knock-in mice expressing a cocaine-insensitive DAT (CI-DAT), cocaine failed to produce locomotor stimulation, conditioned place preference, or an increase in DA levels in the NAcc, yet these effects of amphetamine are preserved supporting the notion that the interaction of the two psychostimulants with the DAT are distinct [57]. Of note, cocaine actually produced conditioned place aversion and suppressed locomotor activity in CI-DAT mice [57, 58]. Expression of the wild-type DAT (wtDAT) in adult CI-DAT mice using adeno-associated viral expression vectors restored cocaine's ability to produce psychomotor stimulation and reward [58]. Furthermore, in animal models of cocaine abuse, "atypical" DAT inhibitors (e.g. JHW-007) reduce psychostimulant self-administration and display low abuse liability (*see section*

1.4 for further details on "atypical" DAT inhibitors) [59, 60]. These observations led to a renewed interest in the development of DAT ligands capable of inducing a conformational change in the DAT that attenuates the reinforcing effects of cocaine [59-62]. DAT inhibitors with the aforementioned profile represent potentially novel pharmacotherapies for the treatment of cocaine addiction [59]. "Atypical" DAT inhibitors (e.g. JHW-007) also reduce self-administration of methamphetamine in animal models [59]. Therefore, DAT ligands capable of antagonizing the hedonic effects of psychostimulants, which possess minimal abuse potential and acceptable side effect profiles, represent potential novel pharmacotherapies for the treatment of psychostimulant abuse [63]. Clinical utilization of pharmacotherapeutic agents with the latter profile would be analogous to the treatment of opioid dependence with methadone, thus a delayed rate of onset and a prolonged duration of action would be desirable [42, 59-61, 64, 65]. DAT ligands with the aforementioned profile would not necessarily have to be devoid of reinforcing effects, as this would likely increase compliance and reduce attrition rates [41, 65, 66].

The efficacy of a variety of treatment modalities has been evaluated in an effort to develop effective approaches to combat psychostimulant addiction. These include cognitive behavioral therapy, pharmacotherapeutic intervention, and combinations thereof, none of which has been demonstrated as an efficacious approach to increase abstinence in individuals addicted to cocaine or methamphetamine [23]. However, of the various pharmacotherapeutic agents examined in human trials, DAT inhibitors have arguably demonstrated the most success.

Modafinil, an "atypical" DAT inhibitor that also enhances glutamatergic neurotransmission, reduced the subjective hedonic effects of cocaine in naïve human subjects [23, 24, 64, 67]. In cocaine-dependent individuals, modafinil decreased cocaine intake, and improved the efficacy of cognitive behavioral therapy [23-25]. Bupropion is a DA reuptake inhibitor that was reported to decrease the subjective effects of methamphetamine and reduced drug craving in a Phase I clinical trial [23-25, 41, 67]. In a Phase II clinical study, bupropion

effectively increased abstinence rates in low-to-moderate methamphetamine abusers, but was not efficacious in heavy users [23-25, 41, 67]. Methylphenidate is a selective DAT inhibitor commonly used to treat attention-deficit/hyperactivity disorder, which has been reported as an effective treatment for cocaine and amphetamine addiction [23, 25, 40, 68]. Despite these observations, none of the aforementioned medications has displayed the level of efficacy necessary to merit approval by the FDA for the indication of treating psychostimulant addiction [23-25, 40-42].

Numerous structural analogues of cocaine and benztropine have been synthesized and investigated for their ability to decrease cocaine and/or methamphetamine self-administration [59, 61, 69]. The “atypical” DAT inhibitor JHW-007 is a structural congener of benztropine that reduces cocaine and methamphetamine self-administration in animal models of psychostimulant abuse [59, 67]. The cocaine analogue RTI-336 antagonized cocaine intake, as well, although the dose of RTI-336 required to reduce cocaine self-administration reduced water and food intake [63]. In contrast, JHW-007’s ability to decrease psychostimulant self-administration occurred at doses that did not significantly reduce the seeking of natural rewards (e.g. food intake) [59, 70]. A variety of phenylpiperazine derivatives were also synthesized in an attempt to develop DAT ligands capable of antagonizing the hedonic effects of cocaine and/or amphetamine [61, 69]. GBR12909 was perhaps one of the most promising, and thoroughly investigated phenylpiperazines [56, 59, 61, 63]. In animal models of psychostimulant abuse, GBR12909 reduced self-administration of cocaine and methamphetamine at doses that had little effect on the seeking of natural rewards [42, 56, 59, 61, 63, 66]. Although each of the these DAT inhibitors demonstrated promise in preclinical models of psychostimulant abuse, their development was halted due to the realization of undesirable effects unveiled in latter studies, as described below.

One of the most commonly encountered problems limiting the development of DAT inhibitors for the treatment of psychostimulant abuse was their potential abuse liability. GBR12909 and RTI-336 readily are self-

administered by non-human primates, and produce discriminative stimulus effects similar to those observed for cocaine [59, 65, 66]. Furthermore, GBR12909 prolonged the QT interval, which increases the risk of potentially fatal ventricular arrhythmia [59, 63]. In a Phase I clinical study GBR12909 produced QT interval prolongation in 5 out of 5 human subjects, leading to the termination of the clinical trial [63]. This effect of GBR12909 arose due to the inhibition of the hERG channel [59]. Given ventricular arrhythmia is associated with hERG inhibition, binding and inhibitory activity at this channel has received increased attention by drug discovery programs [71]. Given both 4-chlorobenztropine and 4,4-dichlorobenztropine bind the hERG channel, molecules structurally related to these compounds (e.g. JHW-007) are also likely to interact with the ion channel [72]. As such, a deviation from the structural scaffolds commonly utilized to synthesize DAT inhibitors may be necessary to identify and develop DAT inhibitors for the treatment of psychostimulant abuse, which are both effective and lack potentially fatal adverse effects.

1.4. The dopamine transporter

The DAT is the primary regulator of extracellular DAergic tone, and is a member of the neurotransmitter sodium symporter (NSS) superfamily [33, 43, 46-55]. NSSs couple the energetically unfavorable “uphill” (up concentration gradient) movement of their respective substrate/s to the “downhill” (down concentration gradient) movement of Na^+ to drive substrate translocation [33, 47, 48, 50-52, 54, 55, 73]. As such, NSS transporters are electrochemically-coupled secondary active transporters [33, 47, 54, 55]. Members of the NSS superfamily (the SLC6 gene family) include transporters for dopamine, norepinephrine (NET), serotonin (SERT), glycine (GlyT1 and GlyT2), and gamma-aminobutyric acid (GAT1-4) [33, 48, 49, 51, 52, 54, 73].

Jardetzky proposed one of the first mechanistic models for secondary active transporters [54]. This model hypothesized that secondary active transporters must meet three general criteria to have the capacity to translocate

substrate: 1) the transporter much have a central binding cavity at it's core of sufficient and appropriate structure to enable binding interaction between the transporter and it's substrate/s, 2) the transporter must be capable of adopting at least two conformational states, an extracellular-facing (outward-facing) conformation and an intracellular facing (inward-facing) conformation, and 3) the extracellular and intracellular facing conformations of the transporter must have differing affinities for substrate/s, the extracellular facing conformation having higher binding affinity than the intracellular facing conformation [54]. Based on this model, the outward-facing conformation of the transporter initially binds extracellular substrate at it's core, a conformational change occurs upon binding substrate shifting the transporter to a substrate-bound inward-facing conformation, then substrate dissociates from transporter to the intracellular environment due to decreased binding affinity for substrate associated with the transition to the inward-facing conformation [54]. The release of substrate to the intracellular environment then triggers a shift back to the outward-facing conformation [54]. Indeed, this proposed mechanism was quite close to the current theoretical conformational states that the DAT adopts throughout its translocation cycle. At present, there are five proposed conformational states of the transporter which occur in the following stepwise fashion: 1) Na^+ and Cl^- bind to the transporter stabilizing the outward-facing conformation priming the transporter for DA binding, 2) DA binds to the outward facing conformation promoting a transition to, 3) the occluded conformation in which the transporter is closed to both the extracellular and intracellular milieu with substrate and accompanying ions sheltered in its central core, 4) a transition to the inward-facing conformation and subsequent dissociation of substrate and bound ions occurs, and then 5) the transporter adopts an inward-facing ligand-free conformation [54]. The low intracellular concentrations of Na^+ and Cl^- favors their dissociation, and that of an accompanying DA molecule, after which the outward facing conformation is promoting due to high extracellular Na^+ and Cl^- concentrations, which stabilize the outward-facing conformation of the DAT [54]. Thus, the transporter adopts the outward-facing conformation, after which Na^+

and Cl^- associate with their respective binding sites priming the DAT to accept another DA molecule [54].

Translocation of DA is accompanied by the import of two Na^+ ions and one Cl^- ion [33, 47, 52, 54, 55, 74]. As such, translocation of DA by DAT is associated with the net import of two positive charges [33, 47, 52, 54, 55]. The electrogenic nature of the DAT led to the future realization that DAT influences membrane potential and neuronal excitability [47, 55, 74]. In addition to inward currents associated with the translocation of DA, DAT also functions in a channel-like mode [33, 47, 74]. A non-selective ion current is potentiated by arachidonic acid (AA), which is inhibited by pretreatment with cocaine [33, 74]. AA also decreases the rate of DA uptake, as has been observed for other polyunsaturated fatty acids (PUFAs), including docosahexaenoic acid, linoleic acid, and oleic acid [74, 75]. A higher the degree of unsaturation leads to an increased DAT inhibitory potency in such PUFAs [75].

As mentioned above, the DAT is the primary regulator of extracellular DAergic tone [33, 43, 46-54]. A number of studies have been performed, all of which support the DAT as the key mechanism governing extracellular DA concentration. In striatal slices from DAT knockout mice, DA's extracellular lifetime, monitored using fast-scanning cyclic voltammetry, increased ~100-fold, in which case diffusion would account for the "disappearance" of DA [43]. Furthermore, in *in vivo* studies measuring extracellular DA clearance in the rat striatum or nucleus accumbens using Nafion coated carbon-fiber microelectrodes coupled to high-speed chronoamperometry, selective DAT inhibitors, but not select selective serotonin or norepinephrine transporter (SERT and NET, respectively) inhibitors, significantly prolonged the extracellular lifetime of DA [46]. Additionally, after producing lesions with the selective DAergic neurotoxin 6-OHDA, thereby destroying DAergic terminals expressing the DAT, DA clearance was again due to diffusion alone [46]. These studies strongly support the role of the DAT as the primary regulator of extracellular DAergic tone, particularly in regions receiving dense DAergic innervation, such as the dorsal striatum and nucleus accumbens [33, 43, 46-55].

The DAT is a glycoprotein comprised of 12 transmembrane-spanning domains, with both its amino- and carboxyl- termini located on the intracellular face of the membrane, modification of which influences DAT function [48, 51, 52, 55]. The importance of DAT is further illustrated by the complexity of its regulatory mechanisms. DAT substrates and inhibitors are capable of regulating DAT function [33, 47, 48, 51, 55]. Brief exposure (~30 seconds) to DAT substrates, such as DA or amphetamine, causes a transient increase in transporter expression, followed by a downregulation of DAT function after prolonged exposure intervals (~1 hour) [48]. DAT inhibitors, such as cocaine, cause an increase in DAT expression [33, 47, 48, 51, 55]. The effects of substrates are accompanied by a decrease in V_{max}, whereas the K_D is unaffected, indicating trafficking of the transporter away from the plasma membrane is responsible for substrate-induced downregulation of the DAT [47, 48]. These effects are believed to occur, in part, via enzymatic post-translational modifications to the transporter (e.g. phosphorylation by kinases) [47, 48, 55]. Activation of protein kinase C (PKC) by phorbol esters causes a downregulation of DAT expression, which is associated with endocytic trafficking of the transporter via a clathrin-dependent mechanism [47, 48, 55]. Amphetamine-induced internalization of the DAT is prevented by PKC inhibition, supporting the notion that substrates decrease DAT activity via internalizing the transporter [47, 48, 55].

The tertiary structure of the DAT is also an important determinant of DAT protein expression [33, 48, 49, 51, 55, 73, 76]. Mutations to residues that prevent the oligomerization of NSSs prevent trafficking of the transporter to the plasma membrane [33, 48, 49, 51, 55, 73]. Amphetamine also causes a shift, disrupting the association of DAT oligomers with a subsequent increase in monomeric DAT, which is believed to contribute to amphetamine-induced internalization [48, 49, 76].

Numerous proteins influence DAT function. As outlined above, PKC activation leads to increased phosphorylation of DAT and an accompanying decrease in DAT surface expression [33, 47, 48, 51-53, 55, 77]. A number of

other kinases influence DAT activity, including phosphatidylinositol-3-kinase (PI3K), protein tyrosine kinase (PTK), and mitogen-activated kinase (MAPK) families [33, 48, 51, 52, 55]. Activation of PI3K and MAPK respective signaling pathways leads to an increase in DAT activity [33, 48, 51, 52, 55]. Activation of TrkB, a PTK, by BDNF leads to increased DAT activity, as well [48, 51]. Increased activity of the DAT by PI3K, MAPK, and TrkB is mediated by an increase in DAT surface expression [33, 48, 51, 52, 55]. Furthermore, activation of the presynaptic DA D2 receptor, a G protein coupled receptor, increases DAT activity [33, 47, 48, 51, 52, 78]. The intricacy of the regulatory mechanisms that influence DAT function highlight's the importance of the transporter in controlling DAergic neurotransmission.

"Atypical" DAT inhibitors are another class of DAT ligands that alter the activity of the transporter, and are of particular interest in the development of treatments for psychostimulant abuse [60, 67]. In contrast to traditional DAT inhibitors, such as cocaine and methylphenidate, "atypical" DAT inhibitors are not associated with significant abuse potential despite inhibiting DA reuptake [79]. "Atypical" DAT inhibitors preferentially bind to the inward-facing conformation of the DAT transporter, whereas traditional DAT inhibitors prefer the outward-facing DAT [79]. Examples of "atypical" DAT inhibitors include GBR-12909, JHW-007, and modafinil, all of which decrease cocaine self-administration in animal models at doses that minimally influence seeking of natural rewards (e.g. food intake) [23, 60]. Binding studies with traditional and "atypical" DAT inhibitors were performed with mutant variants of the human DAT (hDAT) whose conformational equilibrium was shifted favoring either the inward- or outward-facing conformer [79]. In these studies, as indicated above, traditional DAT inhibitors interacted more favorably with outward-facing mutant variants, while "atypical" DAT inhibitors preferentially bound the inward-facing DAT [79]. As such, "atypical" DAT ligands that bind DAT stabilizing a conformation that minimizes cocaine's ability to influence the transporter, while minimally affecting normal transport function, could serve as novel leads to develop treatments for psychostimulant abuse [61, 62]. Considering "atypical" DAT inhibitors have been

demonstrated to decrease self-administration of both psychostimulants in animal models, this holds true for both cocaine and methamphetamine abuse [59, 60].

1.5. Target-directed biosynthetic evolution

Plant-derived medicines have been used to treat human disease for millennia. Given plant secondary metabolites evolved via natural selection, it should be possible to design artificial selection pressures to redirect the evolution of a plant biosynthesis [13, 14]. For drug discovery, selection pressures should favor the survival of genetically optimized medicinal plants with increased yields therapeutically valuable SMNPs and/or novel metabolites with a desired/required bioactivity. Note that plant secondary metabolites evolved to target macromolecules present in organisms other than humans, given species of the Genus *Homo* have only come into existence relatively recently in evolutionary time [13, 14]. Therefore, human's impact on the evolution of plant secondary metabolism is negligible (a limited number of exceptions exist, such as increased yields of nicotine in tobacco as the result of human cultivation) [10, 13]. Bioactivity of plant metabolites in humans arises due to homology that exists between human macromolecules and those present in other organisms with which plant secondary metabolites were intended to target and elicit a biological response [13]. Thus, leads from natural sources often require structural optimization by medicinal chemists to fine-tune their pharmacologic profile making them suitable for use in humans [10]. Our approach is designed to redirect the evolution of plants with medicinal value favoring the biosynthesis of metabolites meant to interact with human macromolecules. This could potentially reduce and/or eliminate the need for further optimization of novel chemical entities to tailor their activity to human systems.

To provide proof-of-concept for this innovative approach to plant-based drug discovery, coined target-directed biosynthesis, the human dopamine transporter (hDAT) was functionally expressed in *Lobelia cardinalis*. *L. cardinalis* contains the complex binitrogenous alkaloid lobinaline, which is a relatively low

potency DAT inhibitor and cannot be synthesized in the laboratory. Although tracer studies have shed light on the precursors for lobinaline biosynthesis *in planta,* methods for the total synthesis of the alkaloid remain elusive [80]. Additionally, the yield of lobinaline from *L. cardinalis* plant material is low and purification via recrystallization is particularly challenging [81]. Thus, *L. cardinalis* was an ideal candidate species for proof-of-concept studies utilizing target-directed biosynthesis. Transgenic *L. cardinalis* primary hairy roots expressing the hDAT (hDAT-1°HRs) display increased susceptibility to dopaminergic (DAergic) neurotoxins that are DAT substrates, including 1-methyl-1,2,3,6-tetrahydropyridine (MPTP) and 6-hydroxydopamine (6-OHDA) [82, 83]. The selective DAT inhibitor GBR12909 attenuates MPTP-induced cytotoxicity in hDAT-1°HRs [84-88]. *L. cardinalis* transgenic plant cells expressing the hDAT were activation tagged, generating transgenic gain-of-function plant cells expressing the hDAT. These cells were generated on selection medium containing 1-methly-4-phenylpyridinium (MPP^+), a cytotoxic DAT substrate, such that selection should favor the survival of cells with beneficial gain-of-function mutations enabling MPP+-resistance [89, 90]. MPP^+ is a selective DAergic neurotoxin used to model Parkinson's disease (PD), which is accumulated in DAergic neurons by the DAT, causing subsequent impairment of mitochondrial function and ultimately neuronal death [89-92].

To date, 120 gain-of-function mutants functionally expressing the hDAT that are resistant to MPP^+ have been generated. Theoretically, these mutants may be resistant to MPP^+ due to gain-of function mutations causing: 1) increased synthesis of lobinaline and/or other more potent DAT inhibitors preventing MPP^+ accumulation and subsequent toxicity, 2) synthesis of cytoprotective metabolites, and/or 3) activation of cytoprotective genes that prevent MPP^+ toxicity (see **Figure 1.1**). Analysis of DAT inhibitory activity of extracts from MPP^+-resistant gain-of-function mutants expressing the hDAT revealed that the population was greatly enriched with individuals whose extracts inhibit DAT much more potently than extracts from the wild-type plant, or controls. Chemical analysis by gas chromatography-mass spectrometry (GC-MS) led to the identification of mutants

that synthesize increased yields and/or novel metabolites undetectable in the wild-type plant or controls. Furthermore, individuals were identified which had increased yields of squalene and/or linoleic acid, a natural products that attenuate MPP^+-induced neurodegeneration in models of PD [93, 94]. DAT inhibitors generated in the current study may hold therapeutic value in the treatment of DAergic neurodegeneration, psychostimulant abuse, nicotine use disorders, ADHD/ADD, depression, and/or other neuropsychiatric disorders [54, 95-104]. Mitochondrial protectants and/or other molecules that prevent intracellular mechanisms of MPP^+ toxicity are of potential therapeutic value in the treatment of neurodegenerative disorders in which mitochondrial dysfunction is implicated in the pathogenesis of disease, including PD [92, 105-126]. This novel approach to re-direct evolution of plant biosynthetic machinery has the potential to revitalize plant-based drug discovery, and feed the pipelines of many drug discovery programs.

Table 1.1.
FDA-approved pharmacotherapeutics inspired by plant SMNPs used for the treatment of drug abuse

Medication	Clinical Application	Plant SMNP	Plant Source[#] (common name)
Nicotine*	Smoking cessation[1, 2]	--------	*Nicotiana tabacum* (Tobacco)
Cytisine*	Smoking cessation[1, 2]	--------	*Cytisus laborinum* (Golden Rain acacia)
Varenicline	Smoking cessation[1, 2, 3]	Cytisine	*Cytisus laborinum* (Golden Rain acacia)
Bupropion	Smoking cessation[4, 5, 6, 7]	Cathinone	*Catha edulis* (Khat)
Buprenorphine	Opioid dependence[8]	Thebaine	*Papaver somniferum* (Poppy)
Methadone	Opioid dependence[1]		
Naltrexone	Opioid dependence[8] Alcohol use disorder[8]	Oripavine	*Papaver somniferum* (Poppy)
Naloxone	Opioid overdose[8]	Oripavine	*Papaver somniferum* (Poppy)

*Molecule is a naturally occurring plant SMNP
[#]Plant SMNP occurs naturally in other plant species
[1]Salim et al. (2008) [20]
[2]Leaviss et al. (2014) [21]
[3]Daly (2005) [22]
[4]Vocci et al. (2007) [23]
[5]Montoya et al. (2008) [24]
[6]Karila et al. (2010) [25]
[7]Appendino et al. (2014) [26]
[8]Hostzafi (2014) [27]

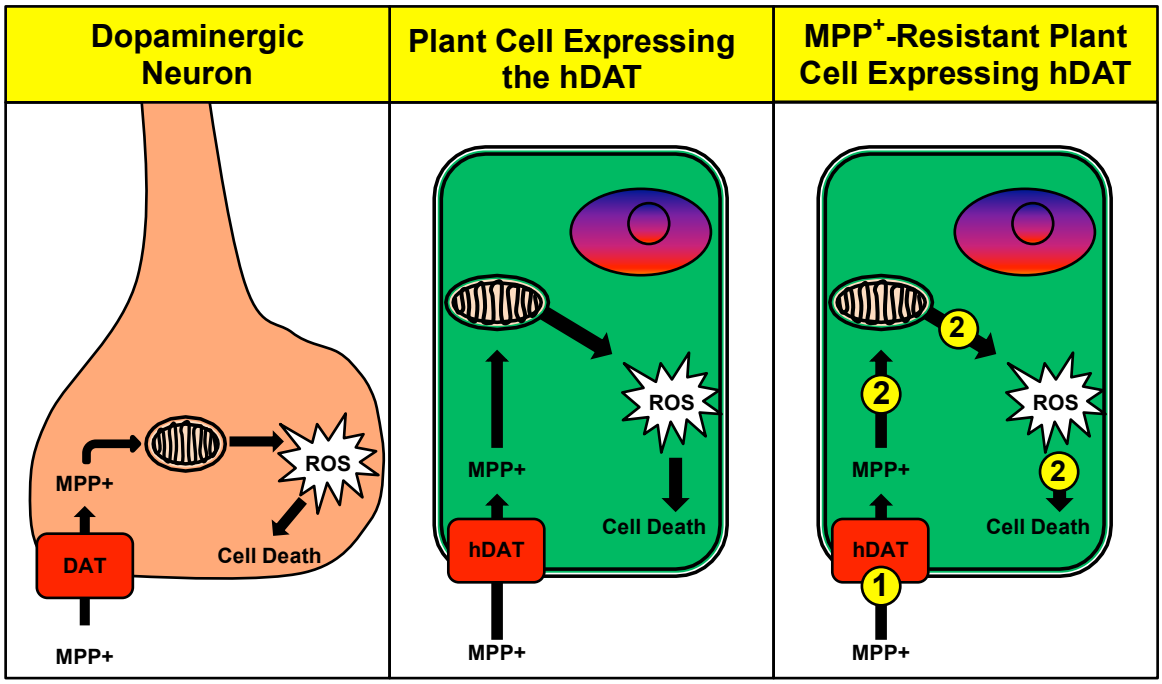

Figure 1.1. Schematic of selection process. A) MPP^+ is translocated to the interior of DAergic neurons via DAT-mediated uptake. Inside the DAergic terminal, MPP^+ inhibits complex-I of the electron transport chain causing excessive production of reactive oxygen species (ROS), which causes cytotoxicity and ultimately cell death. B) The plant cell's phenotype is made to resemble that of DAergic neurons on a fundamental level: the hDAT is expressed in transgenic plant cells rendering them vulnerable to MPP^+. MPP^+-induced cytotoxicity theoretically ensues by the same/similar mechanism/s as described in DAergic neurons. C) Activation tagging mutagenesis (ATM) creates stable gain-of-function mutations randomly throughout plant genome that should confer resistance to MPP^+ via: 1) inducing increased biosynthesis of DAT inhibitors (lobinaline and/or "novel" DAT inhibitors of greater potency) preventing intracellular accumulation of MPP^+ and ensuing cytotoxicity and/or 2) biosynthesis of metabolites that interfere with MPP^+ toxicity intracellularly.

Chapter 2

General methodology

2.1. Chemicals and Supplies

Methanol, hexane, chloroform, ethyl acetate, butanol, acetonitrile, (-)-nicotine (NIC), methyllycaconitine (MLA) citrate salt hydrate, mecamylamine (MEC) hydrochloride, nomifensine, (-)-lobeline hydrochloride, and 2,2-diphenyl-1-picrylhydrazyl (DPPH) were purchased from Sigma Aldrich (St. Louis, MO, USA). Streptomycin (10,000 µg/ml), penicillin (10,000 units/ml), fetal bovine serum (FBS), and Dulbecco's Modified Eagle Medium (DMEM) were purchased from Life Technologies Corporation (Grand Island, NY, USA). Quercetin was purchased from Chromadex (Irvine, CA, USA). [^{3}H]-epibatidine (S.A. = 30 Ci/mmol), [^{3}H]-cytisine (S.A. = 16 Ci/mmol), [^{3}H]-MLA (S.A. = 60 Ci/mmol), [^{3}H]-GBR12935 (S.A. = 40 Ci/mmol), $^{45}CaCl_2$ (S.A. = 12.05 mCi/mg), and [^{3}H]-DA (S.A. = 60 Ci/mmol) were purchased from American Radiolabeled Chemicals, Inc. (St. Louis, MO, USA). All other chemicals and materials were purchased from Fisher Scientific (Pittsburgh, PA, USA), unless otherwise stated.

2.2. Animals

Adult, male Sprague-Dawley rats (200 – 250 g) purchased from Harlan Laboratories (Indianapolis, IN, USA) were housed in cages in groups of 3 – 4 at the Division of Laboratory Animal Resources at the University of Kentucky. Animals had access to food and water *ad libitum*. All protocols for the handling, care, and use of animals were approved by the Institutional Animal Care and Use Committee (IACUC) at the University of Kentucky and were performed in

accordance with the National Institute of Health's Guide for Care and Use of Laboratory Animals.

2.3. Collection of Plant Material

Plant samples were collected as previously described by Littleton et al. (2005) [15]. Briefly, plant samples were collected from field sites by a highly qualified botanist. GPS coordinates were recorded for each accession. Samples were snap-frozen with liquid nitrogen immediately after field collection, and stored at -80°C prior to solvent extraction. Reference samples of each species were deposited at the University of Kentucky Herbarium. *Lobelia cardinalis* was grown at the University of Kentucky Spindletop Farm to obtain plant material in bulk.

2.4. Aqueous plant extract library

A library of aqueous plant extracts was prepared as previously described [15]. Briefly, snap-frozen plant samples collected from the field were removed from storage at -80°C, immediately freeze-dried using a lyophilizer, and finely powdered. Powdered plant material was extracted (100 mg/ml) by suspending samples in aqueous solution (100% Milli-Q H_2O) and placing them on a shaker overnight. The following day, aqueous extracts were collected via vacuum filtration, and freeze-dried using a lyophilizer. The resulting residue was re-suspended in an appropriate volume of assay buffer to achieve a final concentration of 100 mg/ml. When necessary, dimethylsulfoxide (DMSO) was added (<0.05%) to promote solubility of samples in aqueous solution. The resulting aqueous extracts were stored at -80°C prior to pharmacological screening.

2.5. HTPS: Differential smart screen

HTPS was conducted on a library of aqueous plant extracts prepared from ~1,000 species native to the Southeastern United States, completing the screening of the library previously described by Littleton et al. (2005) [15]. HTPS was performed using a Packard Multiprobe liquid handling system in a 96-well plate format (350 µl well volume) as previously described, with minor modifications [15, 127-129]. An innovative assay design, coined "differential smart screening" (DSS), was employed to identify extracts that contained nicAchR ligands with a pharmacological profile unlike that of nicotine [15]. Briefly, pure compounds or plant extracts were prepared, and dissolved in a volume of Krebs-Ringers buffer (120 mM NaCl, 3.9 mM KCl, 650 µM $MgSO_4$, 510 µM $CaCl_2$, 190 µM $NaHPO_4$, 100 µM pargyline, 2 mg/ml glucose, 0.2 mg/ml ascorbic acid, 20 mM HEPES, pH 7.4, saturated with 95% O_2/5% CO_2) necessary to prepare a 100 mg/ml stock solution (*see section 2.4*). Dilutions of the stock solution were prepared for screening (1:10, 1:20, 1:50, 1:100, 1:200, 1:500, 1:1,000, 1:2,000). Samples were evaluated over this concentration range to determine the dilution that effectively displaced 50% of [^{3}H]-epibatidine (168 pM, 3 hour incubation period) from rat cortical membranes (ID_{50}). [^{3}H]-epibatidine is a potent, high affinity nicAchR ligand with similar binding affinity at most nicAchRs present in the mammalian CNS [130, 131]. Determination of a plant species' ID_{50} enabled the identification of extracts containing nicAchR ligands, and provided a "reference point" for subsequent binding studies [15]. Plant extracts that inhibited [^{3}H]-epibatidine binding were tested for their ability to displace [^{3}H]-cytisine (1 nM, 1 hour incubation) and [^{3}H]-MLA (2 nM, 2 hour incubation) at a concentration equal to their ID_{50} for [^{3}H]-epibatidine displacement. [^{3}H]-cytisine and [^{3}H]-MLA displacement studies were performed in rat cortical and hippocampal membranes, respectively. [^{3}H]-cytisine is a β_2-subtype selective ligand, and thus will reflect mainly $\alpha_4\beta_2$-nicAchR binding in the mammalian CNS, whereas [^{3}H]-MLA is α_7-nicAchR selective ligand [22, 128, 132, 133]. The final protein concentration of membrane preparations in HTPS assays was 150 µg/ml. After

reaching equilibrium, membranes were harvested onto 96-well GF/B filtration plates (PerkinElmer Inc., Waltham, MA, USA) and rapidly washed three times with ice-cold 50 mM Tris-HCl buffer (pH 7.4). Filtration plates were allowed to dry overnight before adding 35 µl of scintillation fluid (Microscint 20, Packard Inc.). Plates were then kept in the dark for 2 hours, after which radioactivity was measured using a Packard TopCount® NXT™ microplate scintillation counter. Non-specific binding was measured in the presence of excess NIC (300 µM) and total binding was measured in the presence of radioligand alone. Total specific binding and specific binding in the presence of competitors was calculated by subtracting non-specific binding. Specific binding in the presence of a competitor was expressed as a percentage to total specific binding. Dividing the percentage displacement of [^{3}H]-cytisine by that of [^{3}H]-MLA at a concentration equal to the ID_{50} for [^{3}H]-epibatidine displacement yields a "differential displacement ratio" (DDR) indicative of nicAchR subtype selectivity. DDR values > 5 indicate the plant extract contains metabolites selective for $\alpha_4\beta_2$-nicAchRs, while DDR values < 1 indicate the presence of metabolites selective for α_7-nicAchR, as previously described [14, 15]. Likewise, the DDR can also be used to identify plant extracts containing metabolites with equipotent binding activity at $\alpha_4\beta_2$- and α_7-nicAchRs. In theory, a DDR value of ~3 should indicate the presence of nicAchR ligands with equipotent binding affinity at $\alpha_4\beta_2$- and α_7-nicAchRs. In support of this hypothesis, anabasine, a nicAchR ligand with relatively equipotent binding affinity at $\alpha_4\beta_2$- and α_7-nicAchRs (K_i = 65 and 58 nM, respectively), was previously reported to have a DDR value of 4.16 [15, 22]. Similarly, aqueous extracts from *Nicotiana* species with greater amounts of nicotine than anabasine produce DDR values of > 5, whereas those having greater quantities of anabasine produce a DDR value of ~3 (*see* ***Table 2.1*** *for comparison*) [15, 134]. Therefore, plant extracts that produced DDR values of ~3 were predicted to contain metabolites with equipotent binding affinity at $\alpha_4\beta_2$- and α_7-nicAchRs, thus warranting further investigation in the present study. Aqueous extracts from species of interest were evaluated *in vitro* for their ability to activate nicAchRs and inhibit the DAT (*see sections 2.12 and 2.13*). Plant species whose extracts displayed a combination of

the aforementioned pharmacological activities (presence of a ligand with similar binding affinity at $\alpha_4\beta_2$- and α_7-nicAchRs, ability to activate nicAchRs, and inhibition of the DAT) were prioritized for further evaluation.

2.6. Fractionation of the L. cardinalis crude methanolic extract

Air-dried aerial portions of *L. cardinalis* were ground to a coarse powder, and extracted with 9 volumes of methanol (3 volumes per extraction, 24 hours per extraction). The methanolic extract obtained was dried under vacuum using a rotary evaporator, resuspended in water, and partitioned with organic solvents of increasing polarity in the order that follows: hexane, chloroform ($CHCl_3$), ethyl acetate, and butanol. Sodium sulfate was added to the organic fractions obtained to remove any residual water, removed by vacuum filtration, and each organic fraction was dried under vacuum. The remaining aqueous phase was freeze-dried using a lyophilizer. Fractions were resuspended in modified Krebs-Ringers buffer (final concentration, 100 mg/ml) and assessed in the DSS (*see section 2.5*). Additionally, fractions were re-suspended in uptake buffer (final concentration, 100 mg/ml) and assessed for their ability to inhibit DAT-mediated [^{3}H]-DA uptake in rat striatal synaptosomes (*see section 2.13*).

2.7. pHPLC sub-fractionation of the L. cardinalis $CHCl_3$ fraction.

The $CHCl_3$ fraction obtained from the *L. cardinalis* crude methanolic extract was sub-fractionated via pHPLC using a Waters XBridge Prep C_{18} (5 µm OBD, 19 x 150 mm) column attached to a Waters 600E Multisolvent Delivery System coupled to a Waters 2998 Photodiode Array Detector and Waters 2767 Sample Manager, Injector, and Collector. The pHPLC instrument was operated using Waters MassLynx Software (Version 4.1) and FractionLnyx Collection Control Software (Version 4.1). The mobile phase consisted of a mixture of Solvent A (100% Milli-Q water, pH 7.0) and Solvent B (100% acetonitrile, HPLC grade). Separation was performed with the following gradient at a flow rate of 7

ml/minute: initial conditions, 1% B in A; 0 – 6 minutes, linear gradient, 1 – 20% B in A; 6 – 12 minutes, linear gradient, 20 – 40% B in A; 12 – 18 minutes, linear gradient, 40 – 50% B in A; 18 – 24 minutes, linear gradient, 50 – 75% B in A; 24 – 30 minutes, linear gradient, 75 – 95% B in A; 30 – 35 minutes, linear gradient, 95 – 100% B in A; 35 – 43 minutes, isocratic gradient, 100% B. Sub-fractions were dried, and then re-suspended in modified Krebs-Ringer's buffer or uptake buffer (333 µg/ml) for nicAchR binding studies and [^{3}H]-DA uptake studies, respectively (*see section 2.13*).

2.8. Isolation of lobinaline

The $CHCl_3$ fraction was obtained from *L. cardinalis*, as described above. Acid-base extraction was performed on the $CHCl_3$ fraction to obtain lobinaline. Briefly, 100 mg of the dried $CHCl_3$ fraction was dissolved in 50 ml of $CHCl_3$. The solution was acidified with 1 M HCl (final pH, 2 – 3), shaken gently, and the organic phase was discarded. The remaining aqueous phase was washed 2 – 3 times with $CHCl_3$. The aqueous phase was subsequently basified with ammonium hydroxide (final pH, 10 – 12), partitioned between $CHCl_3$ and water, and the resulting organic phase was collected. The basified aqueous layer was extracted two additional times with $CHCl_3$, and each of the organic phases obtained from the basified aqueous phase were combined. Sodium sulfate was added to the combined organic phases to remove any residual water, removed by vacuum filtration, and the organic phase was dried under vacuum using a rotary evaporator. Lobinaline obtained using this method was analyzed using gas chromatographic-mass spectrometric (GC-MS) methods (*see section 2.9).*

2.9. GC-MS analysis

GC-MS analyses were performed using a Hewlett Packard 6890 Gas Chromatogram interfaced to a Hewlett Packard 5973 Series Mass Selective Detector, an Agilent Technologies 7683 Series Injector, and a Hewlett Packard

7683 Series Autosampler. ChemStation Software (Version 1.02.06) and the Wiley Spectral Database (Version 4.0) were used for instrument control, data analysis, and structural elucidation. Separation was performed on a HP-5MS column ((5%-phenyl)-methylpolysiloxane; 30.0 m x 320 µm x 0.25 µm). Ultra-high purity helium (flow rate of 1.2 ml/minute) served as the carrier gas. Sample volumes of 1 µl were injected in split mode (split ratio, 10.0:1; split flow 12.3 ml/minute) at an inlet pressure of 1.60 psi. The inlet temperature was held at 250°C. The oven was operated using the following parameters: initial temperature, 80°C; 80°C, 2 minute hold; 10°C/minute to 160°C, 1 minute hold; 60°C/minute to 275°C, 12 minute hold; 60°C/min to 60°C, 0 minute hold; total runtime, 28.50 minutes. The transfer line temperature was held at 280°C. The *L. cardinalis* $CHCl_3$ pHPLC sub-fraction of interest (based on its DDR value and DAT inhibitory activity) was analyzed via GC-MS to identify the most abundant constituent/s present. Lobinaline isolated from crude plant material was injected at 2 mg/ml, two runs per sample. Purity of the alkaloid was determined by integrating the area under the curve (AUC) of lobinaline's chromatographic peak (GC-MS run in TIC mode). The identity of the alkaloid was confirmed based on previously reported MS fragmentation data for lobinaline [135].

2.10. [^{3}H]-Epibatidine, [^{3}H]-cytisine, and [^{3}H]-MLA binding

Radioligand displacement studies with pure compounds were performed using methods previously described [136]. Briefly, adult male Sprague-Dawley (200 – 250 g) rats were anesthetized with CO_2 and decapitated. Hippocampal and cortical tissues were rapidly dissected, placed in 10 volumes of ice-cold sucrose buffer (0.32 M sucrose, 1 mM EDTA, 0.1 mM phenylmethylsulfonyl fluoride, 0.01% w/v sodium azide, pH 7.4), and homogenized in a glass homogenization tube with a Teflon pestle. The homogenate was centrifuged at 1,000 x g for 10 minutes at 4°C, and the supernatant was placed on ice. The pellet was re-suspended in sucrose buffer, and centrifuged again at 1,000 x g for 10 minutes at 4°C. The two supernatants were combined and the pellet was

discarded. The combined supernatants were centrifuged at 50,000 x g for 10 minutes at 4°C. The resulting supernatant was discarded, and the pellet was washed twice with assay buffer (50 mM Tris-HCl, 144 mM NaCl, 1.5 mM KCl, 2 mM $CaCl_2$, 1 mM $MgSO_4$, 20 mM HEPES, pH 7.4). The total protein content was measured using the bicinchoninic acid kit (Sigma Aldrich). The final protein concentration was adjusted to 3 mg/ml with assay buffer, and membranes were stored at -80°C prior to further experimentation.

One the day on which competition binding studies were performed, membrane preparations were removed from storage at -80°C and thawed on ice. Lobinaline (final concentration, 3.4 mM – 3.4 nM) was dissolved in assay buffer. DMSO (< 0.1%) was added to promote solubility. Solutions containing lobinaline were mixed with membrane (final protein concentration, 1 mg/ml) and radioligand (168 pM [^{3}H]-epibatidine, 3 hour incubation; 2 nM [^{3}H]-cytisine, 2 hour incubation; 2 nM [^{3}H]-MLA, 2 hour incubation) in individual wells in a 96-well plate format. Experiments were performed at room temperature. After reaching equilibrium (2 – 3 hours), membranes were harvested onto 96-well GF/B filter plates (PerkinElmer Inc., Waltham, MA, USA) by vacuum filtration, and rapidly washed three times with ice-cold 50 mM Tris-HCl buffer (pH 7.4). Filter plates were allowed to dry overnight. The following day, 35 µl of scintillation fluid was added to each well (Mircoscint 20, Packard Inc.) and plates were placed in the dark for two hours. Afterward, radioactivity was measured by scintillation counting (2 minutes per well) using a Packard TopCount® NXT™ microplate scintillation counter. In each plate, non-specific binding was measured in the presence of excess NIC (final concentration, 300 µM) and total binding was measured with radioligand alone. Total specific binding and specific binding in the presence of lobinaline was calculated by subtracting non-specific binding. Specific binding in the presence of lobinaline was expressed as a percentage of total specific binding. Binding studies with pHPLC sub-fractions were conducted with essentially the same methods with the exception that only [^{3}H]-MLA binding was performed, whereas the displacement of all three nicAchR ligands was characterized for lobinaline. The $CHCl_3$ sub-fraction that was the most effective at

displacing [^{3}H]-MLA was analyzed via GC-MS (*see section 2.9*) to determine the major constituent/s present.

2.11. [^{3}H]-GBR12935 binding

Competition binding studies were conducted using previously described methods with minor modifications [84, 86, 137]. Membranes were prepared as described (*see section 2.10*) with the exception that striatal tissue was collected, homogenized in ice-cold homogenization buffer (120 mM NaCl, 50 mM Tris-HCl, pH = 7.4), centrifuged at 25,000 x g for 20 minutes at 4°C, then washed thrice with assay buffer (120 mM NaCl, 50 mM Tris-HCl, 0.01% FBS, pH 7.4). Each wash was performed by re-suspending the pellet 10 volumes of assay buffer followed by centrifugation at 25,000 x g for 20 minutes at 4°C. Total protein content was measured using the bicinchoninic acid kit (Sigma Aldrich). The final protein concentration was adjusted to 3 mg/ml with assay buffer. Striatal membranes were stored at -80°C prior to further experimentation.

One the day binding experiments were performed, membranes were removed from storage at -80°C and thawed on ice. Lobinaline (final concentration, 0.1 nM – 1.0 mM) was dissolved in assay buffer. DMSO (< 0.1%) was added to promote solubility. Solutions containing lobinaline were mixed with membrane (final protein concentration, 1 mg/ml) and incubated for 15 minutes prior to the addition of radioligand (1 nM [^{3}H]-GBR12935, 1 hour incubation) in a 96-well plate format. Experiments were performed at room temperature. After reaching equilibrium, membranes were harvested onto 96-well GF/B filter plates (PerkinElmer Inc., Waltham, MA, USA) by vacuum filtration, and rapidly washed three times with ice-cold 50 mM Tris-HCl buffer (pH 7.4). Filter plates were pretreated with a solution of 0.1% polyethyleneimine 1 hour prior to harvesting membranes to reduce non-specific binding. Filter plates were allowed to dry overnight. The following day, 35 µl of scintillation fluid (Microscint 20, Packard Inc.) was added to each well and plates were placed in the dark for two hours. Afterward, radioactivity was measured by scintillation counting (2 minutes per

well) using a Packard TopCount® NXT™ microplate scintillation counter. In each plate, non-specific binding was measured in the presence of excess GBR12909 (final concentration, 10 μM) and total binding was measured with radioligand alone. Total specific binding and specific binding in the presence of lobinaline was calculated by subtracting non-specific binding. Specific binding in the presence of lobinaline was expressed as a percentage of total specific binding.

2.12. $^{45}Ca^{2+}$ entry in SH-SY5Y cells

Cell-based assays evaluating functional activity of pure compounds or extracts at nicAchRs were conducted using previously described methods with modifications [138-140]. SH-SY5Y human neuroblastoma cells were sub-cultured in polylysine coated petri dishes containing culture medium (DMEM supplemented with 10% FBS, 1 mM glutamine, 50 units/ml penicillin, and 50 μg/ml streptomycin) and maintained in an incubator at 37°C in a humidified atmosphere (95% O_2/5% CO_2). The day prior to performing $^{45}Ca^{2+}$ entry studies, SH-SY5Y cells were plated onto 24-well polylysine coated plates containing 300 μl of culture medium at a seeding density of 20,000 cells/well and placed back in the incubator. After allowing 24 hours for cells to adhere, culture medium was aspirated and replaced with 300 μl of assay buffer (130 mM NaCl, 5 mM KCl, 6 mM glucose, 20 mM HEPES, and 1 mM $CaCl_2$, pH 7.4). Pure compounds or extracts were dissolved in assay buffer to allow direct addition to wells. DMSO (final concentration, < 0.1%) was added to promote solubility of extracts or compounds. Control and treatment groups were performed in quadruplicate on each plate. SH-SY5Y cells were pretreated with vehicle, pure compounds, and/or extracts for 1 minute prior to the addition of $^{45}Ca^{2+}$ (~5 μCi). $^{45}Ca^{2+}$ entry was terminated by aspirating assay buffer, and then washing cells thrice with 1 ml of ice-cold assay buffer. Cells were lysed overnight by the addition 0.5 M NaOH (0.5 ml/well). Lysates were pooled for each group, and two 100 μl aliquots were counted per group. Radioactivity was measured by scintillation counting using a Packard Tri-Carb Liquid Scintillation Counter (Gaithersberg, MD, USA). Basal

$^{45}Ca^{2+}$ entry was designated as that observed in vehicle treated cells. $^{45}Ca^{2+}$ entry in treatment groups was normalized to that observed in vehicle treated controls.

2.13. DAT-mediated [^{3}H]-DA uptake in rat striatal synaptosomes

In vitro [^{3}H]-DA uptake was performed as previously described with minor modifications [57]. Briefly, adult male Sprague-Dawley rats (200 – 250 g) were anesthetized with CO_2 and decapitated. Striata were rapidly dissected and immediately placed into 10 volumes of ice-cold uptake buffer (120 mM NaCl, 3.9 mM KCl, 650 µM $MgSO_4$, 510 µM $CaCl_2$, 190 µM $NaHPO_4$, 100 µM pargyline, 2 mg/ml glucose, 0.2 mg/ml ascorbic acid, 20 mM HEPES, pH 7.4, saturated with 95% O_2/5% CO_2) containing 0.32 M sucrose. Striatal tissue was homogenized in a glass homogenization tube with a Teflon pestle. The homogenate was centrifuged at 1,000 x g for 10 minutes at 4°C. The resulting supernatant was collected and centrifuged at 16,000 x g for 20 minutes at 4°C. The resulting pellet was washed twice with ice-cold uptake buffer and re-suspended in 10 ml of uptake buffer (synaptosome preparation). Synaptosomes (100 µl) were added to individual wells in a 96-well plate and incubated at 37°C for 10 minutes. Lobinaline was dissolved in 100% DMSO, then diluted with uptake buffer (0.3 nM – 3.0 mM). The final concentration of DMSO in uptake studies never exceeded 1.0%, which had no significant effect on radiotracer uptake using methods outlined in the present study. Lobinaline (100 µl; final concentration, 0.1 nM – 1.0 mM) was co-incubated with synaptosomes for 10 minutes at 37°C prior to the addition of [^{3}H]-DA (100 µl). After the 10-minute co-incubation, [^{3}H]-DA was added to each well (final concentration, 15 – 30 nM) and uptake was allowed to proceed for 5 minutes at 37°C. Uptake was terminated by placing 96-well plates on ice, and then immediately harvesting synaptosomes onto 96-well GF/C filter plates (PerkinElmer Inc.) by vacuum filtration, followed by three rapid washes with ice-cold 50 mM Tris-HCl buffer (pH 7.4). After allowing filtration plates to dry overnight, 35 µl of scintillation fluid (Microscint 20, Packard Inc.) was added to

each well and the plate was kept in the dark for 2 hours. Subsequently, radioactivity was measured by scintillation counting using a Packard TopCount® NXT™ microplate scintillation counter. Total uptake was measured in the presence of [^{3}H]-DA alone. Non-specific uptake was determined in the presence of 10 µM GBR-12909. Total specific uptake and specific uptake in the presence of inhibitor was calculated by subtracting non-specific uptake from each, respectively. Specific uptake in the presence of inhibitor was expressed as a percentage of total specific uptake. [^{3}H]-DA uptake studies with conducted with extracts, fractions, or $CHCl_3$ sub-fractions were conducted using the same methods. The $CHCl_3$ sub-fraction that most potently inhibited the DAT was analyzed via GC-MS (*see section 2.9*) to determine the major constituent/s present.

2.14. DPPH free radical scavenging assay

Lobinaline's capacity to scavenge free radicals was examined using the DPPH free radical scavenging assay. The DPPH assay was performed as previously described with minor modifications [141]. Briefly, a DPPH stock solution (600 µM) and stock solutions (1 mg/ml) of lobinaline, lobeline, and the reference compound quercetin were prepared by dissolving compounds in methanol. Stock solutions of DPPH and test compounds were prepared fresh on the day of the experiment. The assay was performed in a 96-well plate format. DPPH solution (final concentration, 300 µM), or DPPH solution and solutions of pure compounds were (final concentration, 1 – 500 µg/ml) added to each plate in quadruplicate. Plates were immediately covered and placed in the dark for 5 minutes. After 5 minutes, the reaction mixture's absorbance at 517 nm was measured using a Wallac 1420 VICTOR plate reader (PerkinElmer Inc., MA, USA). DPPH free radical scavenging activity was calculated using the following equation:

DPPH Free Radical Scavenging Activity (%) = $((Abs_1 – Abs_2) / Abs_1) \times 100$

,where Abs_1 is the absorbance of the solution containing DPPH only and Abs_2 is the absorbance of the solution containing DPPH and pure compounds.

2.15. Fractional [^{3}H] release from [^{3}H]-DA preloaded striatal slices

The ability of lobinaline to evoke fractional [^{3}H] release from [^{3}H]-DA preloaded striatal slices was examined as previously described, with minor modifications [142, 143]. Briefly, coronal slices of rat striatum (500 µm, 6 – 8 mg) were incubated in Krebs' buffer (118 mM NaCl, 4.7 mM KCl, 1.2 mM $MgCl_2$ 1.0 mM NaH_2PO_4, 1.3 mM $CaCl_2$, 11.1 mM glucose, 25 mM $NaHCO_3$, 0.11 mM ascorbic acid, and 0.004 mM EDTA, pH 7.4, saturated with 95%O_2/5%CO_2) for 30 minutes in a metabolic shaker at 34°C. Afterward, slices were incubated in Krebs' buffer containing 0.1 µM [^{3}H]-DA (6 – 8 slices/3 ml) for 30 minutes at 34°C. Subsequently, slices were rinsed and transferred to a glass superfusion chamber maintained at 34°C. Slices were superfused with oxygenated Krebs' buffer containing the monoamine oxidase (MAO) inhibitor pargyline (10 µM) and the DAT inhibitor nomifensine (10 µM) at 1 ml/minute. The inclusion of a MAO inhibitor reduced [^{3}H] signal arising from [^{3}H]-DA metabolites, and the DAT inhibitor prevented the release of [^{3}H]-DA via DAT reversal, promoting the measurement of fractional [^{3}H] release via exocytosis of [^{3}H]-DA from vesicular stores [143, 144]. Slices were superfused for 60 minutes, and then five 4-minute samples (4 ml) were collected in scintillation vials to determine the level of basal [^{3}H] outflow ensuring baseline was stable.

In studies assessing the lobinaline's ability to concentration-dependently evoke fractional [^{3}H] release, a single concentration of lobinaline (10, 100, or 1000 µM) was perfused through an individual superfusion chamber after collection of basal samples. Slices treated with lobinaline were superfused with a single concentration of the alkaloid for the remainder of the experiment. In each experiment, one chamber was superfused with vehicle only throughout the entire course of the experiment. After the addition of lobinaline, superfusate samples

were collected at 4-minute intervals. A repeated-measures design was utilized for superfusion studies to establish a concentration-response for lobinaline-evoked fractional [^{3}H] release.

After establishing a concentration-response for lobinaline in fractional [^{3}H] release studies, experiments were performed to determine whether MEC (10 μM) could antagonize lobinaline-evoked fractional [^{3}H] release. A repeated-measures design was used for studies evaluating the effect of MEC on lobinaline-evoked fractional [^{3}H] release. Slices were perfused for 60 minutes prior to the collection of two 4-minute samples to determine basal [^{3}H] overflow ensuring baseline was stable. After collection of basal samples, chambers were superfused with vehicle or Krebs' buffer containing MEC (10 μM) for 20 minutes. After being superfused with vehicle or MEC for 20 minutes, lobinaline (100 μM) was added to a single chamber for the remainder of the experiment. In each experiment performed, one chamber was superfused with vehicle only throughout the entire course of the experiment. Superfusate samples were collected in scintillation vials at 4-minute intervals.

Upon completion of each superfusion experiment, slices were carefully removed from superfusion chambers and solubilized with 1 ml of TS-2 in scintillation vials. The volume and pH of solubilized striatal slices were adjusted to match that of superfusate samples. Radioactivity in the samples collected during superfusion studies was measured by liquid scintillation using a Packard Tri-Carb Liquid Scintillation Counter (Gaithersberg, MD, USA). Fractional [^{3}H] release was calculated by expressing [^{3}H] collected in superfusate samples as a percentage of [^{3}H] present in solubilized striatal slices upon completion of each superfusion study. Fractional [^{3}H] release evoked by various treatments was compared to vehicle treated control slices.

2.16. In vivo electrochemical studies

In vivo electrochemical studies were conducted using previously described methods to evaluate lobinaline's ability to modulate DAT function in the dorsal

striatum of anesthetized rats [46, 83]. Briefly, high-speed chronoamperometric (HSC) measurements were performed using a FAST-16 system (Quanteon, L.L.C., Nicholasville, KY, USA). Square wave pulses, 0.00 V to +0.55 V vs. Ag/AgCl reference electrodes, were applied for 100 milliseconds at a frequency of 5 Hz. Oxidation and reduction currents were integrated during the last 80 milliseconds of each pulse and averaged over 1 second. Carbon-fiber microelectrodes (Quanteon, L.L.C., Nicholasville, KY, USA), constructed as previously described, consisted of a single carbon-fiber (outer diameter, 30 – 33 μm) passed through and sealed in a glass capillary tube (exposed fiber length, ~150 μm). Nafion (5% solution, Aldrich Chemical Co., Milwaukee, WI) coating of the exposed carbon-fiber tip (2 – 3 coats cured in a 200°C-oven, 5-minute cure interval per coat) provided excellent selectivity for DA over other anionic interferents (DA over ascorbic acid ≥ 100:1; DA over DOPAC ≥ 100:1), as previously reported [145]. Microelectrodes were calibrated *in vitro* in phosphate buffered saline (0.05 M) to generate calibration curves for DA (slope > 0.2 nA/μM and L.O.D < 50 nM) for each microelectrode prior to *in vivo* studies. Electrode responses to DA were linear ($r^2 \geq 0.997$). Lobinaline was evaluated *in vitro* prior to *in vivo* studies to determine whether the alkaloid was electroactive. For *in vivo* studies, micropipette-microelectrode assemblies were constructed using sticky wax (Kerr, Orange, CA, USA) to affix double-barrel micropipettes (A-M System, Sequim, WA) to the microelectrodes. The distance between micropipette and electrode tips ranged from 250 – 350 μm. Care was taken to ensure parallel, vertical alignment of micropipettes and microelectrodes. Double-barrel micropipettes contained a solution of DA (200 μM in 0.9% saline, pH 7.4) in one micropipette and lobinaline (1 mM in 0.9% saline solution containing 0.1% DMSO, pH 7.4; vehicle containing DMSO did not affect DA dynamics) in the second micropipette. Animals were anesthetized using isoflurane (1 – 3%) and placed securely in a stereotaxic frame. Body temperature was maintained at 37°C throughout the experiment using a heating pad coupled to a rectal thermometer. Ag/AgCl reference electrodes were implanted in the brain parenchyma at a region remote to recording sites through a burr hole and

secured using dental acrylic. Skin overlying the cranium of rats was reflected, and the skull and dura overlying recording sites were removed bilaterally. Micropipette-microelectrode assemblies were implanted in the striatum under stereotactic control using the following coordinates: anterior-poster, +1.5 mm; medial-lateral, ±2.2 mm; dorsal-ventral, -3.8 to -5.4 mm. The atlas of Paxinos and Watson (2007) was used to determine coordinates for stereotaxic placement [146]. Solutions of DA (ejection volume, ~100 nl) or lobinaline (ejection volume, ~250 nl) were pressure ejected using a Picospritzer III (Parker instrumentation) and the volume ejected was monitored with a dissecting microscope equipped with a 10 mm reticule [147]. After implantation, the micropipette-microelectrode assembly was left undisturbed to achieve baseline (~30 minutes) before starting the experiment. DA was then pressure ejected at 5-minute intervals until three reproducible signals were obtained (±10%) at each recording site. Lobinaline was then applied slowly (10 – 15 seconds) to minimize disturbance of electrochemical signals. DA was ejected 1 minute following the lobinaline application, and then at 5-minute intervals thereafter (4 – 5 times). The micropipette-microelectrode assembly was lowered 0.5 mm to obtain additional recordings (4 – 6 recordings per hemisphere). Responses to DA were averaged from each animal and data were analyzed using FAST analysis software (Version 6.0; Quanteon, L.L.C., Nicholasville, KY, USA). Two DA signal parameters were obtained: 1) the T_{80} (80% decay time from peak response), and 2) the clearance rate, the first order rate of decay of the DA signal multiplied times the peak amplitude. The T_{80} and the clearance rate reflect alterations in DAT function, rather than diffusion or metabolism [83, 148]. Comparisons were made between amplitude matched DA signals pre- and post-lobinaline application.

2.17. Assessment of lobinaline's oral "druggability"

The oral "druggability" of a molecule is commonly evaluated using Lipinski's "Rule of Five" [149]. These criteria enable prediction of a lead molecule's potential as a drug candidate based on its physiochemical properties.

Assessment of lobinaline's druggability based on these criteria was assessed using data readily available at the PubChem website (https://pubchem.ncbi.nlm.nih.gov/) [150, 151].

2.18. Statistical analysis

Statistical analyses, curve fitting, and graphical presentation of data were performed using GraphPad Prism software (Version 6.0; GraphPad Software, San Diego, CA, USA). The statistical significance of treatment-induced $^{45}Ca^{2+}$ entry in SH-SY5Y cells was determined using a one-tailed Student's t-test. The statistical significance of DAT inhibition caused by pretreatment of rat striatal synaptosomes with the LC_{aq} and the LC_{CHCl3} was determined with a one-tailed Student's t-test. ID_{50}, IC_{50}, and EC_{50} values for high-throughput DSS, [^{3}H]-DA uptakes studies, and DPPH free radical scavenging assays, respectively, were calculated using nonlinear regression analysis to fit data to a variable slope, sigmoidal dose-response curve. K_i values were calculated using the Cheng-Prusoff equation for radioligand binding studies using nonlinear regression analysis to fit data to a one-site competition binding model, sigmoidal concentration-response curve. Repeated-measures, two-way analysis of variance (ANOVA) was performed (lobinaline x time interaction) to determine whether lobinaline evoked a significant, dose-dependent increase in fractional [^{3}H] release from [^{3}H]-DA preloaded striatal slices. Repeated-measures, two-way ANOVA was performed (treatment x time interaction) to determine whether lobinaline-evoked fractional [^{3}H] release was MEC-sensitive. Bonferroni's post-hoc analysis was used to determine time points at which fractional [^{3}H] release was statistically different from vehicle treated controls. DA signals from *in vivo* electrochemical studies were obtained using Fast Analysis Software (Version 6.0; Quanteon, L.L.C., Nicholasville, KY, USA) and GraphPad Prism software was used for graphical presentation of data. DAT inhibitors consistently increase the T_{80}, whereas the clearance rate may increase or decrease depending on experimental conditions [148]. Thus, a paired one-tailed Student's t-test and a

paired two-tailed Student's t-test were performed to determine the significance of lobinaline's effects on the aforementioned DA signal parameters, respectively. All data are expressed as the mean ± the standard error of the mean (S.E.M.), unless otherwise stated. A p-value < 0.05 was defined as statistically significant.

Table 2.1.
DDR values, anabasine, and nicotine content of select *Nicotiana* species

Species	Nicotine : Anabasine, % of total alkaloids[1]	DDR Value[2]
N. tabacum	94.8 : 0.3	9.5
N. undulate	95.3 : 1.3	6.7
N. velutina	2.8 : 8.1	2.9

[1]Alkaloid content reported by Saitoh et al. (1984) [134]
[2]DDR values reported by Littleton et al. (2005) [15]

Chapter 3

Identification of *Lobelia cardinalis* and the isolation of lobinaline

3.1. Introduction

Plants are a rich source of nicotinic acetylcholine receptor (nicAchR) ligands used as medicines, drug leads, and/or pharmacological probes [22]. In plants, metabolites active at nicAchRs are believed to function as chemical defenses against herbivorous insects [13, 14, 29]. Nicotine is a well-known example of a naturally occurring insecticide present in *Nicotiana tabacum* (tobacco) that, upon ingestion, targets and activates nicAchRs present in the insect central nervous system (CNS) producing aversive stimuli and/or death [14, 29]. Nicotine also activates nicAchRs present in the human CNS, which underlies its rewarding and neuroprotective properties [14, 152]. The latter effect has generated interest in the development of nicAchR agonists as neuroprotective agents [153-160]. Nicotine itself is undergoing evaluation in the NIC-PD trial funded by the Michael J. Fox Foundation to assess its therapeutic efficacy in the early stage of Parkinson's disease (PD) patients (https://www.michaeljfox.org/) [153].

The neuroprotective effects of nicAchR ligands are primarily a function of agonist activity at $\alpha_4\beta_2$- and α_7-nicAchR subtypes [153, 154, 156-161]. Considering plants are known to synthesize nicAchR ligands of astonishing complexity and diversity, the screening of plant extracts to discover novel nicAchRs ligands with potential as neuroprotective drug leads seems logical [15, 22]. However, the majority of nicAchR ligands that have been isolated from plant sources are either $\alpha_4\beta_2$-nicAchRs selective agonists (e.g. cytisine), or selective antagonists at α_7-nicAchRs (e.g. methyllycaconitine) [22, 128, 132, 133]. Agonists selective for $\alpha_4\beta_2$-nicAchRs are likely to induce dependence, whereas

α_7-nicAchR selective antagonism is associated with toxicity [15, 132, 162-164]. Therefore, development of a screen that enables rapid identification of plant extracts, which contain metabolites with appropriate nicAchR selectivity is necessary to efficiently discover novel neuroprotective drug leads from plant sources [15].

In the present study, high-throughput pharmacological screening (HTPS) was performed on a library of aqueous plant extracts prepared from ~1,000 species in an effort to discover novel nicAchR ligands with greater therapeutic potential as neuroprotective agents, as compared to previously investigated ligands. The "differential smart screen" employed in the present study, as previously described by Littleton et al. (2005), measures a plant extract's binding activity at $\alpha_4\beta_2$- and α_7-nicAchRs, yielding a differential displacement ratio (DDR) indicative of nicAchR selectivity [15]. The DDR was previously utilized to identify plant extracts containing metabolites selective for α_7-nicAchRs, although it can be readily applied to identify extracts containing metabolites with equipotent binding activity at $\alpha_4\beta_2$- and α_7-nicAchRs (*see section 2.5*) [15]. The latter may fully exploit neuroprotection afforded by nicAchR agonists via activation of both receptor subpopulations associated with nicotine's neuroprotective effects [154, 158, 160, 161].

Several previously uninvestigated plant species were identified in the HTPS as having activity meriting further investigation. *Lobelia cardinalis* was one of these displaying activity indicative of the presence of metabolites with equipotent binding activity at $\alpha_4\beta_2$- and α_7-nicAchRs. Furthermore, the extract from *L. cardinalis* induced $^{45}Ca^{2+}$ uptake via nicAchR activation in SH-SY5Y cells, indicating the metabolite/s present functioned as an agonist/s [111]. *Lobelia* alkaloids have previously been described as inhibitors of the dopamine transporter (DAT), thus the extract from *L. cardinalis* was screened for this activity [143, 165, 166]. Indeed, the extract significantly inhibited DAT-mediated [^{3}H]-dopamine (DA) uptake in rat striatal synaptosomes. This combination of pharmacological activities is potentially of considerable value for the development of neuroprotective agents targeted on the dopaminergic (DAergic)

neurodegeneration that occurs in PD, and psychostimulant-induced DAergic neurotoxicity [95-99, 102, 103, 153-160, 167].

Native Americans knew the potential medicinal value of *L. cardinalis*, although the uses show no clear relation to the pharmacology described herein. Formulations of the plant were consumed by tribes for a wide variety of purposes, ranging from its use as an emetic, a remedy for the treatment of typhoid, and even as a "love potion" [168]. In addition, a close relative of *L. cardinalis*, *L. inflata*, is the source of lobeline [166]. Lobeline has been generated interest as a treatment for neurodegenerative disorders, such as PD and Alzheimer's disease, as well as neuropsychiatric disease including psychostimulant dependence and attention deficit hyperactivity disorder [166]. Bioactive metabolites originating from species of the Genus *Lobelia* may hold therapeutic potential for a variety of neurological disorders. Here, we describe the putative identification of the major bioactive metabolite present in *L. cardinalis*, lobinaline, and the subsequent isolation of the alkaloid.

3.2. Identification of L. cardinalis as a "species of interest" using the high-throughput DSS

In the present study, a library of aqueous plant extracts was screened to identify extracts that contained nicAchR ligands with relatively equipotent binding affinity at $\alpha_4\beta_2$- and α_7-nicAchRs. This was accomplished utilizing an innovative HTPS previously described by Littleton et al. (2005), coined "differential smart screening" (DSS) [15]. As described above, this translated into the prioritization of extracts with a DDR value of ~3 in the DSS (*see section 2.5*). An extract's DDR value was calculated (*see section 2.5*) by dividing the percentage displacement of [^{3}H]-cytisine by that of [^{3}H]-MLA at a concentration equal to the ID_{50} for [^{3}H]-epibatidine displacement [15]. The aqueous extract from *L. cardinalis* (LC_{aq}) displaced [^{3}H]-epibatidine from rat cortical membranes (ID_{50} = 1:300, 333 µg/ml), and exhibited a DDR value of 2.96. Thus, *L. cardinalis* was designated as

a “species of interest,” since its DDR value indicated the presence of a nicAchR ligand(s) with relatively equipotent binding affinity at $\alpha_4\beta_2$- and α_7-nicAchRs.

3.3. The LC_{aq} activates nicAchRs and inhibits the DAT

The LC_{aq} activated nicAchRs and inhibited the DAT in functional studies performed *in vitro* (**Figure 3.1**). In a variety of neuronal and non-neuronal cell types, acute treatment with nicAchR agonists (e.g. NIC and DMPP) has been reported to increase $^{45}Ca^{2+}$ entry [140, 169]. In contrast, basal levels of intracellular Ca^{2+} are generally unaltered by treatment with nicAchR antagonists, such as MEC or MLA [111, 140, 169, 170]. Here, $^{45}Ca^{2+}$ entry studies were conducted with SH-SY5Y cells due to their neuronal properties, catecholaminergic phenotype, and utility as an *in vitro* model of DAergic neurotoxicity [123, 124]. Furthermore, SH-SY5Y cells express β_2-subunit containing and α_7-nicAchRs, reported to mediate many of the neuroprotective effects of nicAchR agonists, as well as $\alpha_3\beta_4$-nicAchRs that are believed to indirectly modulate the activity of the mesolimbic DAergic pathway [111, 153, 154, 156-161, 170]. Ca^{2+} entry elicited by nicAchR ligands and extracts was measured using $^{45}Ca^{2+}$, rather than calcium fluorimetry, to eliminate signal arising from other sources of Ca^{2+}, such as that released from intracellular stores via Ca^{2+}-induced Ca^{2+} release [111, 169]. In the SH-SY5Y cells, NIC (10.0 μM) significantly increased $^{45}Ca^{2+}$ entry (374% increase above basal, $p = 0.0001$). $^{45}Ca^{2+}$ entry was unaffected by MEC (1.0 μM), a non-selective nicAchR antagonist, in agreement with previous studies [111, 140, 143, 169-171]. The LC_{aq} (1.0 mg/ml) significantly increased $^{45}Ca^{2+}$ entry (137% increase above basal, $p < 0.001$), and this effect was completely blocked by MEC. $^{45}Ca^{2+}$ entry was significantly increased in SH-SY5Y cells concomitantly treated with the LC_{aq} and NIC (1.0 mg/ml and 10 μM, respectively; 232% increase above basal, $p < 0.001$), yet the effect was significantly less ($p = 0.0143$) than that observed in SH-SY5Y cells treated with NIC alone. The NIC-evoked increase in Ca^{2+} entry in the current study is consistent with previous studies reporting nicAchR agonist-

evoked Ca^{2+} entry in SH-SY5Y cells, measured using fluorimetric techniques [111]. These results suggest the LC_{aq} likely contains a metabolite(s) that functions as a nicAchR partial agonist. Consistent with this view, the LC_{aq} displays intrinsic activity at nicAchRs present on SH-SY5Y cells, but functions as a nicAchR antagonist in the presence of a nicAchR full agonist (i.e. NIC) [170, 172, 173]. Furthermore, in rat striatal synaptosomes the LC_{aq} significantly and dose-dependently inhibited DAT-mediated [^{3}H]-DA uptake. The LC_{aq} significantly inhibited DAT-mediated [^{3}H]-DA uptake at concentrations of 74.1 µg/ml (35% uptake, $p < 0.001$), 151.3 µg/ml (12% uptake, $p < 0.001$) and 3.3 mg/ml (2% uptake, $p < 0.001$). The unique combination of pharmacological effects (i.e. nicAchR partial agonism and DAT inhibition) merited further investigation of *L. cardinalis* with the aim of identifying a metabolite or metabolites responsible for the aforementioned activities.

3.4. Putative identification of a multifunctional alkaloid present in L. cardinalis

A crude methanolic extract prepared from air-dried aerial portions of *L. cardinalis* was subject to bioassay-guided fractionation. Fractions obtained were evaluated in the DSS and for their ability to inhibit the DAT *in vitro*. The $CHCl_3$ fraction thus obtained displaced [^{3}H]-epibatidine from rat cortical membranes (ID_{50} = 1:60,000, 1.67 µg/ml), and exhibited a DDR value of 1.59 in the DSS, indicative of the presence of a ligand(s) with comparable affinity at $\alpha_4\beta_2$- and α_7-nicAchRs, as compared to nicotine or lobeline (DDR values of 13.00 and 6.27, respectively) [15]. The $CHCl_3$ fraction also caused a significant, dose-dependent inhibition of DAT-mediated [^{3}H]-DA uptake in rat striatal synaptosomes (**Figure 3.2**) at 33.3 µg/ml (38% uptake, $p < 0.001$) and 3.3 µg/ml (90% uptake, $p = 0.0013$). Thus, pHPLC sub-fractionation of the $CHCl_3$ fraction was performed in an effort to identify a multifunctional plant metabolite responsible for the aforementioned activities. A single $CHCl_3$ sub-fraction was the most effective at displacing [^{3}H]-MLA from rat hippocampal membranes, and was also the most potent inhibitor of the DAT in rat striatal synaptosomes. These results indicated

the presence of a putatively novel multifunctional plant metabolite. GC-MS analysis of the $CHCl_3$ sub-fraction revealed lobinaline, the major alkaloid present in *L. cardinalis*, as the most abundant constituent (AUC = 70%) of the sub-fraction [80, 81, 135, 174, 175]. The identity of lobinaline, a complex binitrogenous alkaloid, was confirmed based on previously reported structural and MS data [135, 174, 175].

3.5. Isolation of lobinaline

The crude methanolic extract prepared from air-dried aerial portions of *L. cardinalis* was fractionated to obtain the $CHCl_3$ fraction. Acid-base extraction was performed on the $CHCl_3$ fraction, yielding lobinaline (purity ≥ 95%). The identity of the alkaloid was confirmed based on previously reported MS data, and its purity was determined by integration of the AUC of the chromatographic peak corresponding to lobinaline on the GC trace [135]. Lobinaline (**Figure 3.3**) was stored in the dark at -20°C prior to further experimentation.

3.6 Discussion

Plants are a rich source of multifunctional drug leads, as described in recent reviews [13, 176, 177]. The complex alkaloid lobinaline was putatively identified as the major bioactive metabolite present in *L. cardinalis* [80, 81, 135, 174, 175]. The alkaloid was presumably responsible for nicAchR agonism and DAT inhibition caused by *L. cardinalis* extracts. NicAchR agonists and DAT inhibitors attenuate DAergic neurotoxicity in animal models of PD and psychostimulant abuse [95-99, 102-104, 119, 153-160, 167, 178-182]. Thus, lobinaline may prove to be a particularly valuable lead for the development of multifunctional neuroprotective therapeutics aimed to prevent DAergic neurotoxicity if, indeed, it is responsible for the aforementioned pharmacological effects.

Initially, HTPS was conducted on a library of aqueous plant extracts from ~1,000 species in an effort to identify a novel nicAchR agonist with equipotent binding affinity at $\alpha_4\beta_2$- and α_7-nicAchRs. Using the DSS previously described by Littleton et al. (2005), the *L. cardinalis* aqueous extract (LC_{aq}) produced a DDR value of 2.96 signifying the extract contained a metabolite/s with similar binding affinity at $\alpha_4\beta_2$- and α_7-nicAchRs, as described above (*see section 2.5*) [14, 15]. In SH-SY5Y cells, the LC_{aq} (1.0 mg/ml) significantly increased $^{45}Ca^{2+}$ entry. The LC_{aq}-induced increase in $^{45}Ca^{2+}$ entry was abolished by MEC (1.0 μM), indicating the effect was mediated by nicAchR activation [111, 140, 143, 169-171]. Furthermore, the LC_{aq} significantly reduced NIC-induced $^{45}Ca^{2+}$ entry in SH-SY5Y cells. Collectively, these results indicated the LC_{aq} contained a metabolite/s that functioned as a nicAchR partial agonist with relatively equipotent affinity for $\alpha_4\beta_2$- and α_7-nicAchRs [170, 172, 173]. This is in contrast to "typical" nicAchR ligands from plant sources, the majority of which are $\alpha_4\beta_2$-nicAchR selective agonists (e.g. cytisine) or α_7-nicAchR antagonists (e.g. MLA) [22, 128, 132, 133]. Additionally, the extract inhibited DAT-mediated [^{3}H]-DA uptake in rat striatal synaptosomes. This was an intriguing observation since, to the best of our knowledge, all plant metabolites reported to inhibit the DAT and modulate nicAchRs act as antagonists at the latter [22, 143, 144, 183].

Bioassay-guided fractionation of the *L. cardinalis* methanolic extract, followed by pHPLC sub-fractionation, indicated both activities resided in a single $CHCl_3$ sub-fraction. GC-MS analysis of the sub-fraction revealed lobinaline was the major constituent present (AUC = 70%), the identity of which was confirmed based on previously reported MS data [135]. Lobinaline, the alkaloid putatively responsible for multifunctional pharmacological effects of *L. cardinalis*, was subsequently isolated (purity ≥ 95%). Studies then were conducted to characterize the pharmacology of lobinaline, confirming the multi-target effects of the alkaloid.

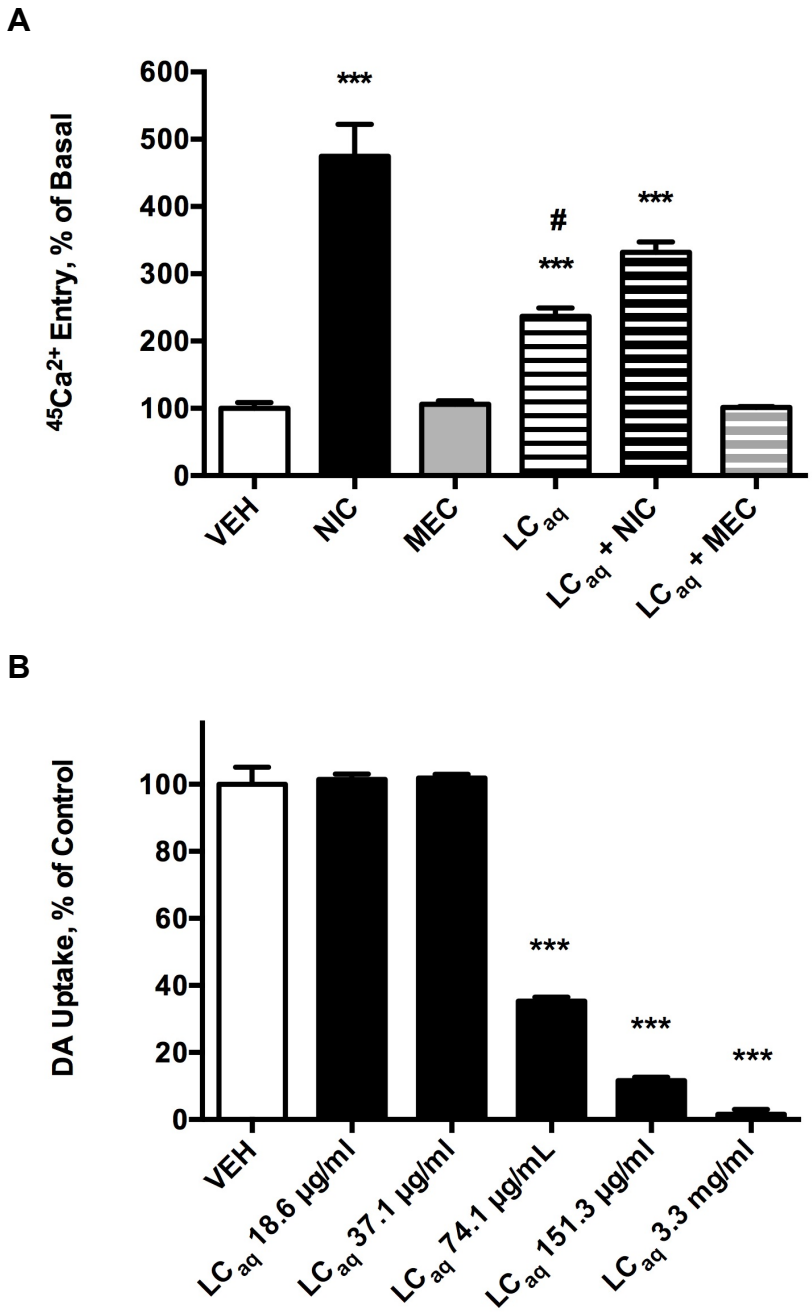

Figure 3.1. Modulation of $^{45}Ca^{2+}$ entry in SH-SY5Y cells and DAT-mediated [^{3}H]-DA uptake in rat striatal synaptosomes by the LC_{aq}. Data expressed as the mean ± S.E.M. A) NIC (10.0 µM) and the LC_{aq} (1.0 mg/ml) significantly increased $^{45}Ca^{2+}$ entry in SH-SY5Y cells. The LC_{aq} significantly attenuated NIC-induced $^{45}Ca^{2+}$ entry, and MEC (1.0 µM) pretreatment completely abolished LC_{aq}-induced $^{45}Ca^{2+}$ entry. *** $p < 0.001$ vs. vehicle (VEH), Student's one-tailed t-test; # $p < 0.05$ compared to cells treated with NIC alone, Student's one-tailed t-test. B) DAT-mediated [^{3}H]-DA uptake is significantly and dose-dependently inhibited by the LC_{aq}. *** $p < 0.001$ vs. VEH, one-tailed Student's t-test. n = 3 - 4.

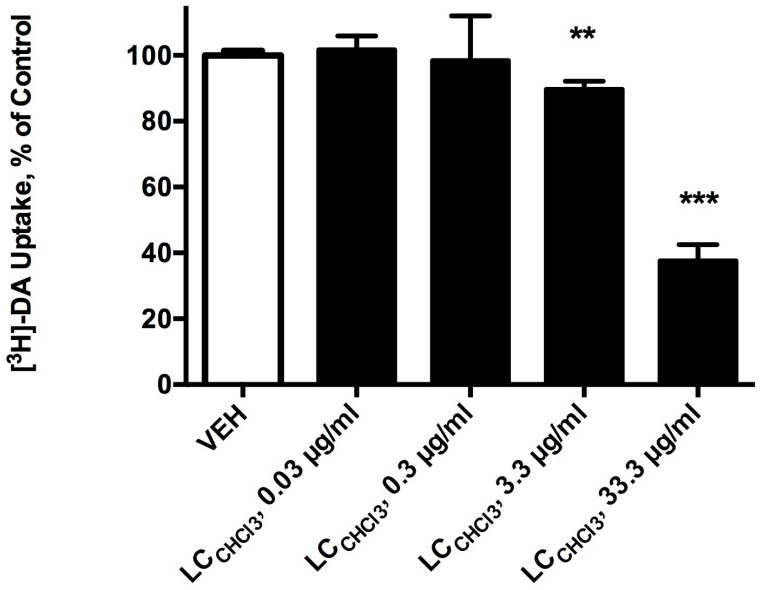

Figure 3.2. Modulation of DAT-mediated [^{3}H]-DA uptake in rat striatal synaptosomes. Data expressed as the mean ± S.E.M. The *L. cardinalis* chloroform fraction (LC_{CHCl3}) significantly and dose-dependently inhibited the DAT. ** $p < 0.01$, *** $p < 0.001$ vs. vehicle (VEH), one-tailed Student's t-test. n = 4.

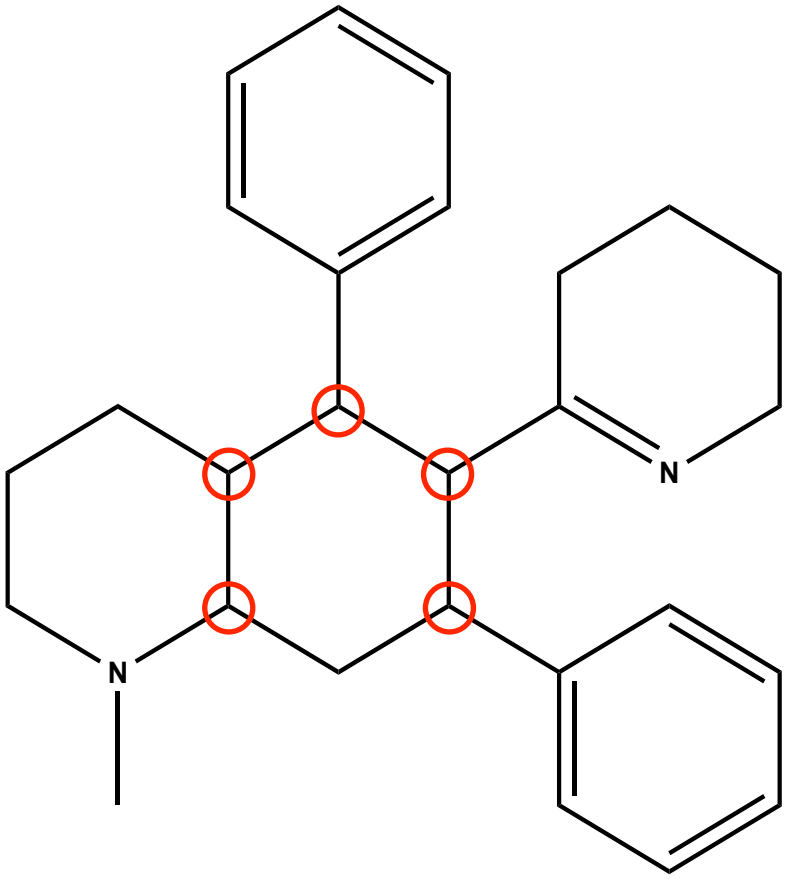

Figure 3.3. The structure of lobinaline. Red circles denote chiral centers.

Chapter 4

Pharmacological characterization of lobinaline

4.1 Introduction

Lobinaline was putatively identified as the major bioactive metabolite present in *L. cardinalis*. Here, the multifunctional pharmacology of the complex decahydroquinoline alkaloid is described, as well as its potential therapeutic applications. The alkaloid possesses a unique polypharmacological profile functioning as a nicAchR agonist, DAT inhibitor, and free radical scavenger. These pharmacological effects of lobinaline are previously unreported, and to the best of our knowledge, the alkaloid is the only natural product with a combination of the aforementioned activities. NicAchR agonists, DAT inhibitors, and free radical scavengers attenuate DAergic neurotoxicity in animal models of PD and psychostimulant abuse [95-99, 102-104, 119, 153-160, 167, 178-182]. Thus, lobinaline may be a particularly valuable lead for the development of multifunctional neuroprotective therapeutics aimed to prevent DAergic neurotoxicity.

Here, the *in vitro* pharmacological characterization major bioactive metabolite present in *L. cardinalis*, lobinaline, is described. The alkaloid's effects on DA uptake *in vivo* were examined by measuring the clearance of exogenous DA locally applied in the striatum of isoflurane-anesthetized rats using Nafion-coated carbon fiber microelectrodes in combination with high-speed chronoamperometry (HSC) [46, 78, 83, 184-187]. Since excessive free radical production contributes to DAergic neurotoxicity seen in PD and psychostimulant abuse, lobinaline's capacity to scavenge free radicals was evaluated in the 1,1-diphenyl-2-picrylhydracyl (DPPH) free radical scavenging assay [97, 98, 104, 167, 188, 189]. All of the data presented suggest lobinaline is a potential lead

compound for the development of multifunctional neuroprotective agents to prevent DAergic neurotoxicity.

4.2. Lobinaline displaces radioligands selective for nicAchRs and the DAT

Lobinaline concentration-dependently inhibited [^{3}H]-epibatidine, [^{3}H]-cytisine, and [^{3}H]-MLA binding at nicAchRs (K_i = 16.2, 1.1, and 67.5 μM, respectively; **Figure 4.1 A – C**). Radioligand binding studies with the aforementioned nicAchR ligands were performed as described previously [15, 136]. Competition binding studies with [^{3}H]-epibatidine and [^{3}H]-cytisine were conducted in rat cortical membranes. The former nicAchR ligand is relatively non-selective at neuronal nicAchR subtypes, while the latter is selective for $\alpha_4\beta_2$-nicAchRs [22, 128, 130, 131]. Competition binding studies with the α_7-nicAchR selective ligand [^{3}H]-MLA were conducted in rat hippocampal membranes [128, 132]. In contrast to nicotine and lobeline, lobinaline has similar affinity at $\alpha_4\beta_2$- and α_7-nicAchRs (*see* ***Table 4.1*** *for comparison*) [190, 191]. Lobinaline produced a DDR value of 1.32, virtually identical to that produced by the $CHCl_3$ fraction, indicating lobinaline was the main metabolite responsible for the fraction's nicAchR binding activity. Lobinaline also inhibited binding of [^{3}H]-GBR12935, a highly selective DAT ligand, in rat striatal membranes (K_i = 2.5 μM; **Figure 4.2**) [84, 86].

4.3. Lobinaline activates nicAchRs and inhibits the DAT in vitro

Lobinaline's functional effect at nicAchRs was evaluated by assessing its ability to modulate $^{45}Ca^{2+}$ entry in SH-SY5Y cells (**Figure 4.3 A**). In these experiments, NIC (10.0 μM) significantly increased $^{45}Ca^{2+}$ entry (197% increase above basal, p = 0.0008). Treatment of cells with MEC alone (1.0 μM) did not affect $^{45}Ca^{2+}$ entry. At the concentration tested in the current study, lobinaline (1.0 mM) significantly increased $^{45}Ca^{2+}$ entry (42% increase above basal, p = 0.0011). Lobinaline-induced $^{45}Ca^{2+}$ entry in SH-SY5Y cells was completely

abolished by MEC. Concomitant treatment of SH-SY5Y cells with lobinaline and NIC (1.0 mM and 10 μM, respectively) significantly increased $^{45}Ca^{2+}$ entry (116% increase above basal, $p < 0.001$). Similar to the LC_{aq}, concomitant treatment of SH-SY5Y cells with lobinaline and NIC significantly reduced $^{45}Ca^{2+}$ entry ($p = 0.0347$), as compared to cells treated with NIC alone. The observation of nicAchR activation by lobinaline, in combination with its ability to attenuate NIC-induced $^{45}Ca^{2+}$ entry, is consistent with the view that lobinaline functions as a partial agonist at nicAchRs expressed by SH-SY5Y cells [170, 172, 173]. In order to assess lobinaline's efficacy as an inhibitory modulator of the DAT, [^{3}H]-DA uptake was performed in rat striatal synaptosomes. DAT-mediated [^{3}H]-DA uptake was inhibited by lobinaline (IC_{50} = 12.0 μM; **Figure 4.3 B**). Based on these results, and data obtained from binding studies, lobinaline functions as a multifunctional alkaloid with unique pharmacological profile, acting as a nicAchR partial agonist and an inhibitor of the DAT.

4.4. Lobinaline is a relatively potent DPPH free radical scavenger

Multiple lines of evidence indicate excessive free radical production contributes to DAergic neurotoxicity seen in PD and psychostimulant abuse [97, 98, 104, 167, 188, 189]. The DPPH free radical scavenging assay is commonly utilized to assess a molecule's ability to quench free radicals [141]. Lobinaline acted as a potent free radical scavenger (EC_{50} = 18.0 μM), as did quercetin (EC_{50} = 11.2 μM), a plant metabolite previously reported to potently scavenge DPPH free radicals (**Figure 4.4**) [141]. In contrast, lobeline was a weak DPPH free radical scavenger (EC_{50} = 228.8 μM). Although quercetin's EC_{50} is greater than previously reported (6.22 μM), this was expected given the concentration of DPPH used in the present study (300 μM) was 6-fold greater than the former (50 μM) [141].

4.5. Lobinaline dose-dependently evokes fractional [^{3}H] release from [^{3}H]-DA preloaded rat striatal slices

The modulation of nicAchRs by lobinaline was also examined by monitoring its ability to evoke fractional [^{3}H] release from rat striatal slices preloaded with [^{3}H]-DA. Superfusion studies were performed in the presence of pargyline (10.0 μM) and nomifensine (10.0 μM). The inclusion of a MAO inhibitor reduced the contribution of [^{3}H]-DA metabolites to the [^{3}H] signal recorded, and the use of a DAT inhibitor promoted measurement of [^{3}H]-DA released from vesicular stores, rather than efflux of [^{3}H]-DA via reversal of the DAT [143, 144]. Lobinaline caused a significant, concentration-dependent increase in fractional [^{3}H] release from rat striatal slices preloaded with [^{3}H]-DA (**Figure 4.5 A**). Repeated measures, two-way ANOVA revealed a significant main effect of concentration ($F_{(3,26)} = 15.5$, $p < 0.001$), a significant main effect of time ($F_{(11, 286)} = 4.9$, $p < 0.001$), and a significant concentration x time interaction ($F_{(33, 286)} = 3.6$, $p < 0.001$). The lowest concentration of lobinaline that evoked a significant increase in fractional [^{3}H] release compared to vehicle was 100 μM. At concentrations of 100 μM and 1000 μM, lobinaline-evoked fractional [^{3}H] release reached significance ($p < 0.05$ and $p < 0.001$, respectively) 8 minutes after treatment (the second sample collected after lobinaline treatment). Fractional [^{3}H] release evoked by 1000 μM lobinaline reached a maximum (494% greater than vehicle treated, $p < 0.001$) 8 minutes post-treatment. Fractional [^{3}H] release evoked by 100 μM lobinaline reached a maximum (186% greater than vehicle treated, $p < 0.001$) 12 minutes post-treatment, and was no longer significantly different from vehicle treated slices 16 minutes after treatment. In contrast, fractional [^{3}H] release evoked by 1000 μM lobinaline remained significantly elevated above that of vehicle treated slices for the remainder of the experiment (28 minutes).

After establishing lobinaline's ability to concentration-dependently evoke fractional [^{3}H] release, studies were performed to evaluate the contribution of nicAchR stimulation to lobinaline-evoked fractional [^{3}H] release. Striatal slices

preloaded with [^{3}H]-DA were pretreated with MEC (10.0 μM) for 20 minutes prior to the addition of lobinaline (100 μM). Fractional [^{3}H] release from vehicle treated striatal slices served as a control. MEC significantly attenuated lobinaline-evoked fractional [^{3}H] release indicating activation of nicAchRs contributes to fractional [^{3}H] release evoked by the alkaloid (**Figure 4.5 B**) [143]. Repeated measures, two-way ANOVA revealed a significant main effect of treatment ($F_{(2, 9)}$ = 9.683, p = 0.0057) and a significant main effect of time ($F_{(13, 117)}$ = 2.465, p = 0.0053). The treatment x time interaction was not significant ($F_{(26, 117)}$ = 1.488, p = 0.0793). In this set of experiments, the effect of lobinaline (100 μM) alone was generally in agreement with initial studies, albeit the time course of its effect was slightly prolonged. That is, lobinaline-evoked fractional [^{3}H] release reached significance 8 minutes after treatment (160% greater than vehicle, $p < 0.05$), and was no longer significantly different from vehicle treated slices after 24 minutes. Additionally, the maximal increase in fractional [^{3}H] release occurred 16 minutes after lobinaline treatment and the maximum (262% greater than vehicle treated controls, $p < 0.001$) was greater than that observed in initial studies. When comparing fractional [^{3}H] release from vehicle treated slices and slices pretreated with MEC prior to lobinaline, no significant difference was observed at any time point. These results indicate lobinaline's effect was MEC-sensitive, providing additional evidence that the alkaloid is a nicAchR agonist. This is in contrast to lobeline, which evokes fractional [^{3}H] release from rat striatal slices that is MEC-insensitive, and was reported to antagonize nicAchRs [143, 144].

4.6. Lobinaline inhibits DA uptake in vivo in the striatum of isoflurane-anesthetized rats

In vivo electrochemical studies were performed to evaluate modulation of DA uptake in isoflurane-anesthetized rats. In agreement with *in vitro* [^{3}H]-DA uptake studies, local application of lobinaline in the dorsal striatum significantly prolonged the clearance rate of exogenous DA. A representative trace of exogenous DA clearance recorded pre- and post-lobinaline application is

depicted in **Figure 4.6 A**. The alkaloid significantly increased the T_{80} (76.3 ± 39.5 sec., p = 0.0203) and significantly decreased the clearance rate (0.09 ± 0.05 μM/sec., p = 0.0459) 1-minute post-application, as compared to the T_{80} (33.7 ± 12.5 sec.) and clearance rate (0.13 ± 0.07 μM/sec.) pre-application (**Figure 4.6 B and C**). The effects of lobinaline on the aforementioned DA signal parameters are indicative of DAT inhibition. Lobinaline's effects on DA clearance are short acting, as they are no longer significant 3 – 5 minutes after lobinaline ejection. Lobinaline's effects on DA clearance are somewhat like those observed after local application of nomifensine in the dorsal striatum of urethane-anesthetized Sprague-Dawley rats, but were not as efficacious, which is consistent with *in vitro* studies of nomifensine in synaptosomes [84, 148]. *In vitro* electrochemical studies confirmed lobinaline itself was not electroactive by chronoamperometric recordings used to measure endogenous DA (*data not shown*). *In vivo*, lobinaline had no direct effects when locally applied from a micropipette (n = 10; *data not shown*). Given lobinaline prolonged exogenous DA clearance and failed to cause DA release, the alkaloid appears to act as a DAT inhibitor, rather than a DAT substrate/releasing agent.

4.7. Lobinaline fits the criteria set forth by Lipinski's "Rule of Five"

The oral "druggability" of lobinaline, based on its physiochemical properties, was assessed according to Lipinski's "Rule of Five" [149]. These data are readily available the PubChem website (https://pubchem.ncbi.nlm.nih.gov/) [150, 151]. Lobinaline did not violate any of the criteria set forth by Lipinski's "Rule of Five": molecular weight = 386, hydrogen bond donors = 0, hydrogen bond acceptors = 2, cLogP = 4.8, molar fractivity = 82.47. Additionally, based on previously reported *in vivo* studies, lobinaline displays appropriate pharmacokinetics and low mammalian toxicity in mice relative to lobeline, the most widely studied *Lobelia* alkaloid [81].

4.8. Discussion

Plants are a rich source of multifunctional drug leads [13, 176, 177]. The multifunctional alkaloid lobinaline was identified as the major bioactive metabolite present in *L. cardinalis* [80, 81, 135, 174, 175]. The alkaloid possesses a unique polypharmacological profile functioning as a nicAchR agonist, DAT inhibitor, and free radical scavenger. These pharmacological effects of lobinaline are previously unreported, and to the best of our knowledge, the alkaloid is the only natural product with a combination of the aforementioned activities. NicAchR agonists, DAT inhibitors, and free radical scavengers attenuate DAergic neurotoxicity in animal models of PD and psychostimulant abuse [95-99, 102-104, 119, 153-160, 167, 178-182]. Thus, lobinaline may be a particularly valuable lead for the development of multifunctional neuroprotective therapeutics aimed to prevent DAergic neurotoxicity.

Lobinaline inhibited binding of the $\alpha_4\beta_2$-nicAchR selective ligand [^{3}H]-cytisine (K_i = 1.1 μM), and the α_7-nicAchR selective ligand [^{3}H]-MLA (K_i = 67.5 μM), in rat cortical and hippocampal membranes, respectively, and produced a DDR value of 1.32 [22, 128, 132, 133]. Compared to other plant metabolites, such as nicotine and lobeline, lobinaline is relatively non-selective with respect to $\alpha_4\beta_2$- and α_7-nicAchRs (*see* ***Table 4.1*** *for comparison*) [190, 191]. The plant metabolite anabasine is also non-selective at $\alpha_4\beta_2$- and α_7-nicAchRs (K_i = 65 nM and 58 nM at $\alpha_4\beta_2$- and α_7-nicAchRs, respectively) [22]. However, anabasine is teratogenic, limiting its clinical utility [192]. In SH-SY5Y cells, lobinaline significantly increased $^{45}Ca^{2+}$ entry, an effect that was blocked by MEC. Lobinaline also significantly reduced NIC-induced $^{45}Ca^{2+}$ entry in SH-SY5Y cells. The ability of lobinaline to activate nicAchRs and functionally antagonize the effect of a nicAchR full agonist (i.e. NIC) suggests the alkaloid may be a nicAchR partial agonist [170, 172, 173]. Lobeline, on the other hand, antagonizes nicAchRs in a variety of experimental models [143, 144]. Based on these data, lobinaline appears to be distinct from nicotine and lobeline in terms of its selectivity and functional effects at nicAchRs. Electrophysiological studies (e.g.

two-electrode voltage clamping) assessing lobinaline's efficacy at nicAchRs are necessary to confidently designate lobinaline as a nicAchR partial agonist.

Lobinaline was further evaluated *in vitro* for its ability to interact with and modulate the DAT. In rat striatal membranes, binding of the highly selective DAT ligand [^{3}H]-GBR12935 was inhibited by lobinaline (K_i = 2.5 μM), and the alkaloid dose-dependently attenuated DAT-mediated [^{3}H]-DA uptake (IC_{50} = 12.0 μM) in rat striatal synaptosomes [84, 86]. Lobeline also inhibits the DAT, but is less potent (IC_{50} = 28.2 – 80.0 μM) than lobinaline [143, 190]. In contrast, nicotine is inactive at the DAT in rat striatal synaptosomes [143]. However, in *in vivo* electrochemical studies performed in rats, systemic administration of nicotine enhanced DAT function [193]. The latter study suggests an intact neurological system is required to examine modulation of DAT activity by nicotinic agonists.

As described above, lobinaline exerts pleiotropic pharmacological effects relevant to the prevention and/or reduction of DAergic neurotoxicity seen in PD and psychostimulant abuse, including nicAchR activation and DAT inhibitory modulation [95, 98, 99, 102, 103, 153-157, 160, 167]. Since multiple lines of evidence indicate excessive free radical production contributes to DAergic neurotoxicity seen in the aforementioned pathologies, lobinaline was assessed for its capacity to scavenge free radicals [97, 98, 104, 167, 188, 189]. In the DPPH free radical scavenging assay, lobinaline acted as a potent scavenger of free radicals (EC_{50} = 18.0 μM), as compared to quercetin (EC_{50} = 11.2 μM), a natural product known for its free radical scavenging and antioxidant activity [119, 141, 177, 182]. Lobeline's capacity to scavenge DPPH free radicals was relatively poor (EC_{50} = 228.8 μM). Given quercetin's neuroprotective effects in cellular and animal models of PD, lobinaline may exert similar effects warranting future investigation of the alkaloid in models of PD [119, 182].

In superfusion studies, lobinaline caused a significant, dose-dependent increase in fractional [^{3}H] release from rat striatal slices preloaded with [^{3}H]-DA. The buffer used in superfusion studies contained a MAO inhibitor and a DAT inhibitor to reduce signal arising from [^{3}H]-DA metabolites and [^{3}H]-DA release via reversal of the DAT, respectively [143, 144]. At the highest concentration

examined in the current study (1000 μM), lobinaline-evoked fractional [^{3}H] release remained significantly greater than control for the duration of the experiment. This effect mirror's that observed for high concentrations of lobeline (10.0 – 1000 μM) under essentially identical experimental conditions [143]. In contrast, nicotine's effect on fractional [^{3}H] release is transient, even at high concentrations, likely due to desensitization of nicAchRs [143]. Subsequent experiments revealed lobinaline-evoked fractional [^{3}H] release was MEC-sensitive, providing additional evidence that the alkaloid is an agonist at nicAchRs. Based on these observations, stimulation of nicAchRs underlies lobinaline's ability to evoke fractional [^{3}H] release from [^{3}H]-DA preloaded striatal slices. Lobeline, on the other hand, is reported to antagonize nicAchRs, and evokes fractional [^{3}H] release that is MEC-insensitive and Ca^{2+}-independent [143].

Lobinaline's ability to affect vesicular monoamine transporter type-2 (VMAT-2) activity, inhibition of which is believed to underlie lobeline's effect in similar superfusion studies, was not examined [143]. Furthermore, the [^{3}H] signal measured in studies examining lobeline-evoked fractional [^{3}H] release from [^{3}H]-DA preloaded rat striatal slices was reported to arise predominantly from an increase in [^{3}H]-DOPAC release, rather than [^{3}H]-DA [143]. The authors reached this conclusion upon measuring lobeline-evoked endogenous DA and DOPAC release from rat striatal slices via HPLC coupled with electrochemical detection (HPLC-ECD). Lobinaline's ability to modulate VMAT-2 and endogenous DA/DOPAC release from rat striatal slices, measured using HPLC-ECD, remain to be explored.

The effect of lobinaline on DAT function was examined *in vivo* in the striatum of isoflurane-anesthetized rats using HSC coupled to local applications of exogenous DA. This technique allows measurement of DA dynamics *in vivo* in an intact neurological system with a high degree of spatial and temporal resolution, and has been used extensively to characterize effects of DAT inhibitors [46, 78, 148, 184, 194]. Consistent with *in vitro* [^{3}H]-DA uptake studies, lobinaline significantly prolonged the clearance rate of exogenous DA 1-minute

post-application. Local application of the alkaloid in the dorsal striatum significantly increased the T_{80} and significantly reduced the clearance rate when compared to amplitude matched DA signals pre-lobinaline application. These observations demonstrate lobinaline's ability to inhibit DAT function *in vivo*, although the alkaloid's effects are transient and are no longer significant 3 – 5 minutes post-application. Alterations in the T_{80} and the clearance rate reflect modulation of DAT activity, as has been characterized for other DAT inhibitors [46, 148, 195]. Effects somewhat like those of lobinaline were observed following local application of the DAT inhibitor nomifensine in the dorsal striatum of Sprague-Dawley rats, albeit lobinaline was less efficacious, which is consistent with *in vitro* studies of nomifensine in synaptosomes [84, 148]. In isoflurane-anesthetized rats, lobinaline locally applied in the striatum had no direct effects. DAT substrate-releasing agents, such as amphetamines, induce endogenous DA release [196, 197]. Thus, lobinaline likely functions as a DAT inhibitor, rather than a substrate, although the results are not conclusive. The transient nature of lobinaline's effects *in vivo* may result from the alkaloid's relatively low affinity and/or potency at the DAT. Conformational changes resulting from lobinaline's interaction with the DAT and mechanism/s underlying lobinaline's effects on DAergic neurotransmission and DAT function *in vivo* remain to be thoroughly elucidated.

The multifunctional pharmacological effects of lobinaline are somewhat expected in view of the structural complexity and functional groups present in the decahydroquinoline alkaloid. For example, lobinaline meets all criteria of the "refined" pharmacophore proposed by Inamdar (2011) for DAT inhibitors: 1) ionizable nitrogen, 2) aromatic ring, 3) hydrogen bond acceptor, and 4) two hydrophobic groups [198]. Although these requirements are not absolute, an ionizable nitrogen within ~6 Å of a phenyl moiety is present in the vast majority of DAT inhibitors [198, 199]. Illustrating this point, the lack of a phenyl and/or benzyl substituent in nicotine and anabasine seems to be a reasonable explanation for their inability to inhibit DAT, especially given their structural similarity to the competitive DAT inhibitor/substrate 1-methyl-4-phenlypiperidinium [22, 151, 200].

On the other hand, structural features common to lobinaline and the alkaloids anabasine and anabaseine likely explain lobinaline's selectivity and activity at select nicAchR subtypes. The 3-(2-piperidyl)pyridine alkaloids anabasine and anabaseine, the latter having a 1,2-unsaturated piperidyl group, are nicAchR agonists with similar affinity for $\alpha_4\beta_2$- and α_7-nicAchRs [22, 200]. Although lobinaline lacks a pyridyl functional group, the aromatic character of its phenyl substituents in the vicinity of the 1,2-dehydropiperidine functional group may suffice to create a physiochemical environment adequate to engender similar interactions with nicAchRs. The agonist activity lobinaline displays at nicAchRs is of note, given other decahydroquinolines studied to date antagonize nicAchRs, possibly due to the lack of a tetrahydropiperidyl substituent in those previously investigated [201, 202].

A question becomes apparent when considering the pharmacological actions of lobinaline, and the amount of energy that is likely required to synthesize a molecule of its complexity: What benefit does lobinaline afford to the plant? One explanation relates to the effects of nicAchR agonists and DAT inhibitors on insect behavior. Both classes of compounds have been reported to function as naturally occurring insecticides, nicotine and cocaine representing examples of the former and latter [14, 29, 30]. Additionally, modulating two molecular targets may be more effective, due to synergistic effects. Targeting nicAchRs and the DAT also ensures protection against herbivorous insects resistant to one mode-of-action, or the other. Thus, having a "shotgun" approach to fend off herbivorous threats is potentially "safer" for the plant. Furthermore, lobinaline's ability to function as an antioxidant should reduce oxidative stress arising from excessive exposure to ultraviolet radiation, or free radical species that are generated during normal metabolism [13]. All in all, synthesis of a multifunctional molecule is potentially a more efficient strategy, given a single biosynthetic pathway and resulting metabolite addresses each of the challenges plants encounter, outlined above. Given evolution favors efficiency and effectiveness, natural selection would likely favor the retention and optimization

of multifunctional molecules, such as lobinaline, and their respective biosynthetic pathways.

Only one other molecule which activates nicAchRs and inhibits the DAT has been reported, a synthetic analogue of cocaine, cocaine methiodide (CMI) [22, 183, 203]. However, the clinical utility of CMI is severely limited due its toxic peripheral effects [203]. Previously, a limited number of *in vivo* studies were performed with lobinaline [81]. Intravenous administration of lobinaline in cats and rabbits was reported to lower blood pressure, whereas respiration was unaffected by the alkaloid [81]. The authors reported minimal lethal doses of 800 and 300 mg/kg for lobinaline and lobeline, respectively, following subcutaneous administration in mice [81]. These initial studies indicate the alkaloid's pharmacokinetic (PK) and toxicity profile are acceptable for a drug lead, especially considering complications arising from PK and toxicity reportedly underlie failure of ~30% of NCEs in clinical development [204, 205]. Additionally, lobinaline does not violate criteria outlined by Lipinski's "Rule of Five," a common assessment used to predict a molecule's oral "druggability" based on its physiochemical properties [149]. Thus, lobinaline holds considerable value as a potential lead molecule for the development of therapeutics with its combination of effects. One hurdle that may stall optimization of the alkaloid via traditional medicinal chemistry is the lack of a method for the total synthesis of lobinaline, limiting access to a pure starting material [8, 20, 206]. Although tracer studies examining lobinaline biosynthesis *in planta* indicate phenylalanine and lysine are the likely precursors of the alkaloid, a method for the total synthesis of lobinaline remains elusive [80]. Also the presence of five chiral centers in lobinaline would necessitate the separation of enantiomers likely to arise during chemical optimization, creating additional challenges and costs [8]. To address this problem, our group is currently developing a novel plant-based drug discovery platform that favors evolution of plant biosynthetic pathways yielding molecules with desirable interactions at a protein which is a therapeutic molecular target. Proof-of-application studies are being conducted using the hDAT as the molecular target, and *L. cardinalis* as the candidate plant species.

Lobinaline, or congeners with similar pharmacological effects represent promising multifunctional drug leads to prevent DAergic neurotoxicity seen in PD or psychostimulant abuse. For example, DAT inhibitors prevent uptake of endogenous and exogenous neurotoxic substrates of the transporter thought to contribute to DAergic neuron loss in PD, and DAT inhibitors alleviate specific parkinsonian symptoms in rodent and nonhuman primate models of PD [95-101]. NicAchR agonists selective for $\alpha_4\beta_2$- or α_7-nicAchRs are neuroprotective in cellular and animal models of PD, and reduce drug-induced dyskinesia caused by therapeutics used to treat PD [153-160, 207]. In models of psychostimulant abuse, $\alpha_4\beta_2$- and α_7-nicAchR selective agonists, as well as DAT inhibitors, attenuate neurotoxicity caused by amphetamines [99, 102-104, 153, 154, 156, 159, 160, 167]. In animal models of cocaine and amphetamine abuse, “atypical” DAT inhibitors (e.g. JHW-007) reduce psychostimulant self-administration and display low abuse liability [59, 60, 65, 66, 70, 79]. DAergic neurotoxicity caused by psychostimulants and neurotoxic DAT substrates utilized to model PD is attenuated by pre-treatment with antioxidants, including ubiquinol (coenzyme Q_{10}) and flavonoids (e.g. baicalein) [119, 178-182]. Thus multifunctional molecules, such as lobinaline, which activate $\alpha_4\beta_2$- and α_7-nicAchRs, inhibit the DAT, and function as free radical scavengers may be superior DAergic neuroprotectants that act via a single mechanism of action. This notion is supported by recent reviews indicating multifunctional leads have a higher probability of displaying efficacy with minimal side effects [177, 204, 208]. Furthermore, high affinity binding is not required for multifunctional drugs presumably due to synergistic and/or additive effects arising from their multi-target activities, and this relative lack of potency at a single molecular target may reduce adverse effects [177, 204, 208]. Collectively, the data presented herein indicate lobinaline’s potential as a lead to develop multifunctional neuroprotective therapeutics for neurological disorders involving DAergic neurodegeneration and/or psychostimulant abuse.

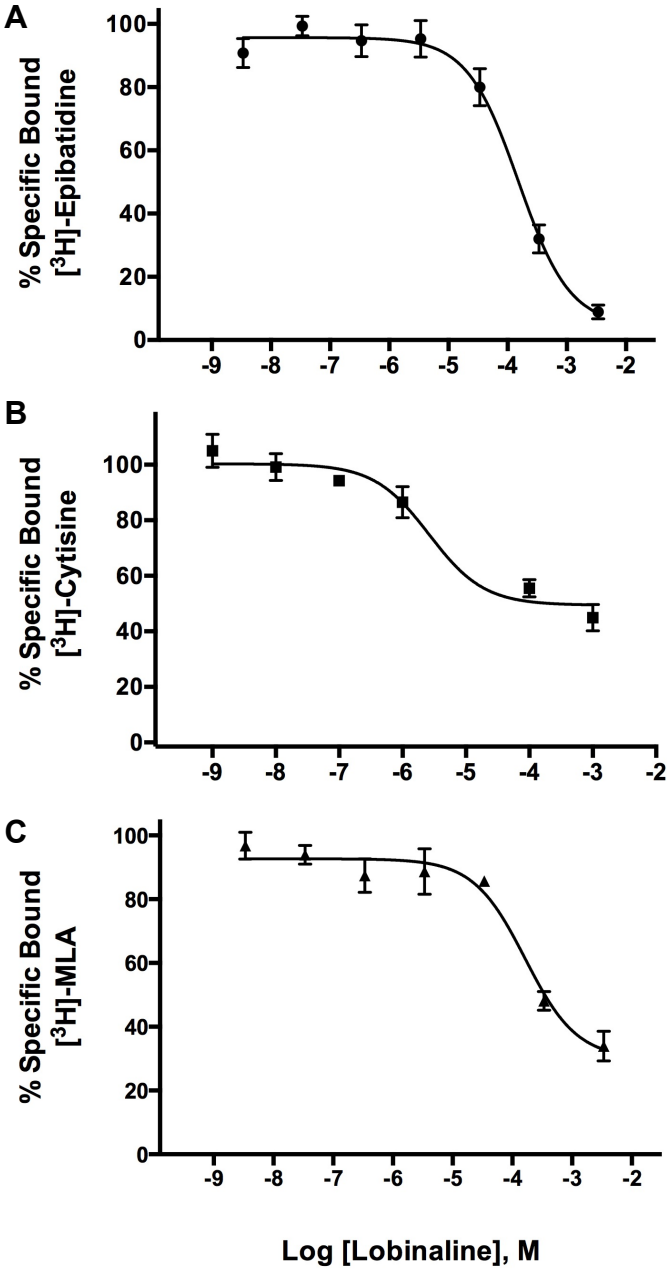

Figure 4.1. Lobinaline displaces nicAchR-selective radioligands. Data are expressed as the mean ± S.E.M. Concentration-dependent inhibition of A) [^{3}H]-epibatidine (K_i = 16.2 µM) and B) [^{3}H]-cytisine (K_i = 1.1 µM) binding at nicAchRs by lobinaline in rat cortical membranes. C) Concentration-dependent inhibition of [^{3}H]-MLA binding (K_i = 67.5 µM) at nicAchRs in rat hippocampal membranes. n = 3 – 4.

Table 4.1.
NicAchR selectivity of lobinaline, lobeline, and nicotine at $\alpha_4\beta_2$- and α_7-nicAchRs

	K_i µM		NicAchR Selectivity	
Compound	$\alpha_4\beta_2$-nicAchR	α_7-nicAchR	(-fold difference)[5]	DDR value
Lobinaline	1.1	67.5	63	1.32
Lobeline[3]	4.0×10^{-3}	6.26	1565	6.27[6]
Nicotine[4]	9.6×10^{-4}	1.448	1508	13.00[6]

[3]Ki's previously reported by Hojahmat et al. (2010) [209]
[4]Ki's previously reported by Rueter et al. (2006) [191]
[5]Selectivity based on comparison of K_i's
[6]DDR values previously reported by Littleton et al. (2005) [15]

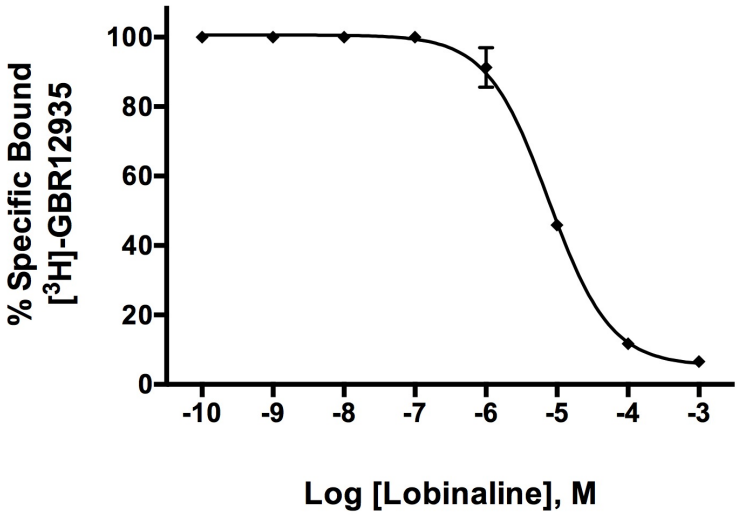

Figure 4.2. Lobinaline displays affinity for the DAT. Data expressed as the mean + S.E.M. A.) Lobinaline concentration-dependently displaces [^{3}H]-GBR12935 (K_i = 2.5 μM) from rat striatal membranes. n = 4.

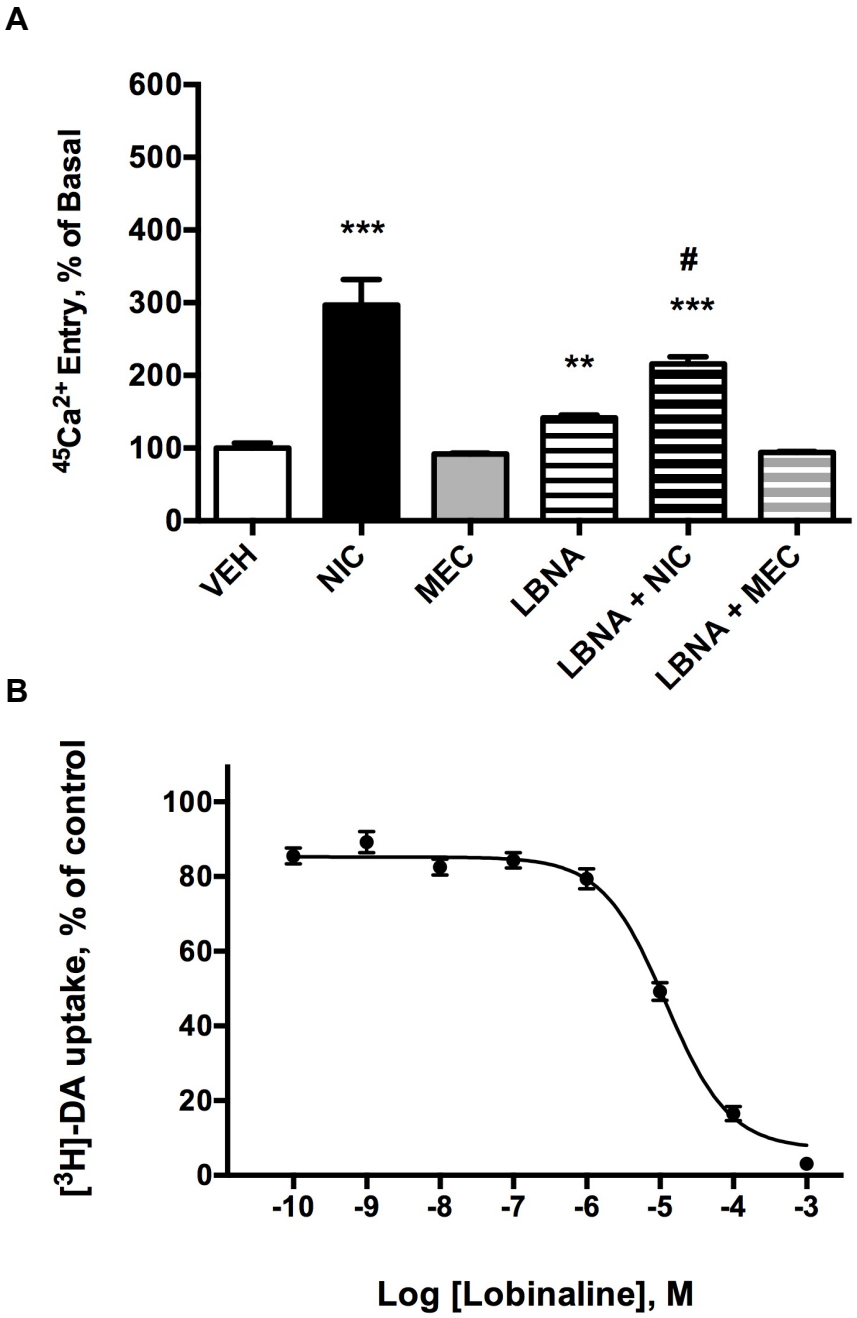

Figure 4.3. Lobinaline (LBNA) activates nicAchRs and inhibits the DAT. Data expressed as the mean ± S.E.M. A) NIC (10.0 μM) and LBNA (1.0 mM) significantly increase $^{45}Ca^{2+}$ entry in SH-SY5Y cells. LBNA significantly attenuates NIC-induced $^{45}Ca^{2+}$ entry, and MEC (1.0 μM) pretreatment completely abolishes LBNA-induced $^{45}Ca^{2+}$ entry. ** $p < 0.01$, *** $p < 0.001$ vs. vehicle (VEH), Student's one-tailed t-test. # $p < 0.05$ vs. cells treated with NIC alone, Student's one-tailed t-test. n = 3 – 4. B.) Lobinaline dose-dependently inhibits the DAT (IC_{50} = 12.0 μM). n = 3 – 4.

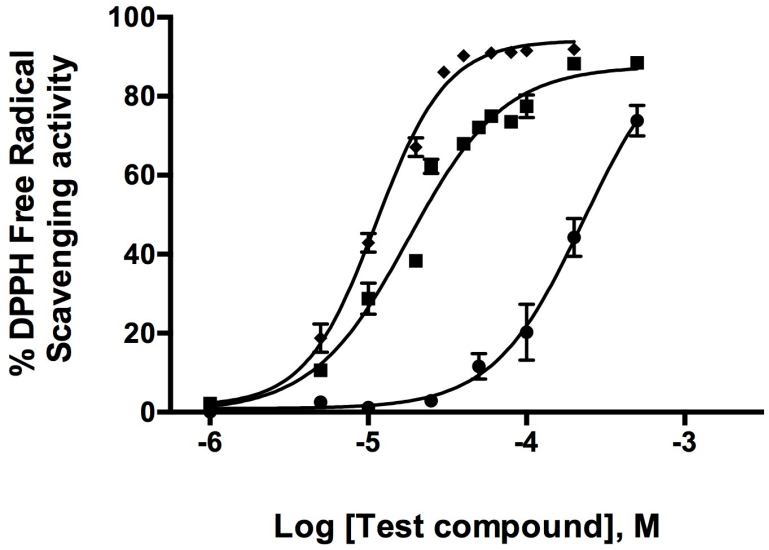

Figure 4.4. DPPH free radical scavenging activity. Data expressed as the mean ± S.E.M. Quercetin (◆) and lobinaline (■) are potent DPPH free radical scavengers (EC_{50} = 11.2 and 18.0 μM, respectively). Lobeline (●) is a relatively poor scavenger of DPPH free radicals (EC_{50} = 228.8 μM). n = 3 - 5.

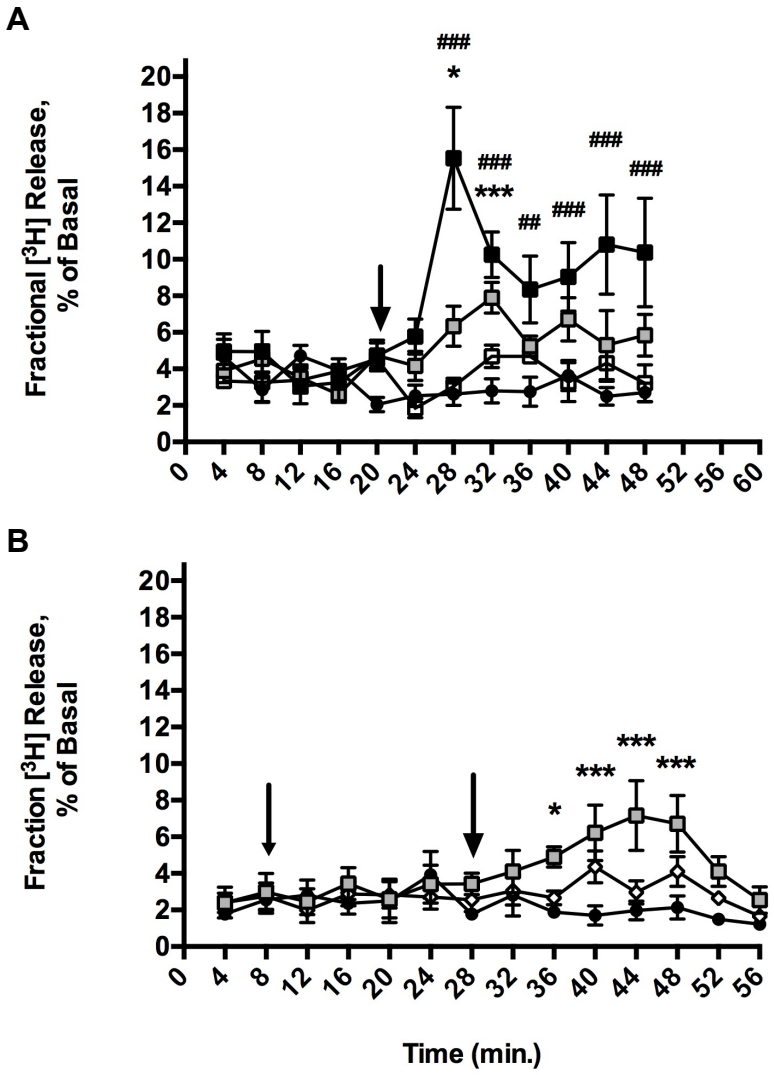

Figure 4.5. Time course of lobinaline-evoked fractional [^{3}H] release from [^{3}H]-DA preloaded rat striatal slices. Data expressed as the mean ± S.E.M. A) Lobinaline significantly, and dose-dependently increased fractional [^{3}H] release at 100 μM (□) and 1,000 μM (■) vs. vehicle treated controls (●). Fractional [^{3}H] release was not significantly increased by 10 μM (□) lobinaline. Lobinaline was added immediately after the collection of the fifth sample, as indicated by the arrow. * $p < 0.05$, *** $p < 0.001$, 100 μM lobinaline vs. vehicle treated slices; ## $p < 0.01$, ### $p < 0.001$, 1,000 μM lobinaline vs. vehicle treated slices; Two-way ANOVA, Bonferroni's post-hoc test. n = 4 – 10 rats. B) Effect of MEC on the time course of lobinaline-evoked fractional [^{3}H] release from [^{3}H]-DA preloaded rat striatal slices. Fractional [^{3}H] release was significantly increased by 100 μM lobinaline (□). Fractional [^{3}H] release from striatal slices pretreated with 10 μM MEC prior to the addition of 100 μM lobinaline (◇) was not significantly different from vehicle treated slices (●). MEC was added immediately after the collection of the second sample (small arrow). Lobinaline was added immediately after collection of the seventh sample (large arrow). * $p < 0.05$, *** $p < 0.001$, 100 μM lobinaline vs. vehicle treated slices; Two-way ANOVA, Bonferroni's post-hoc test. n = 4.

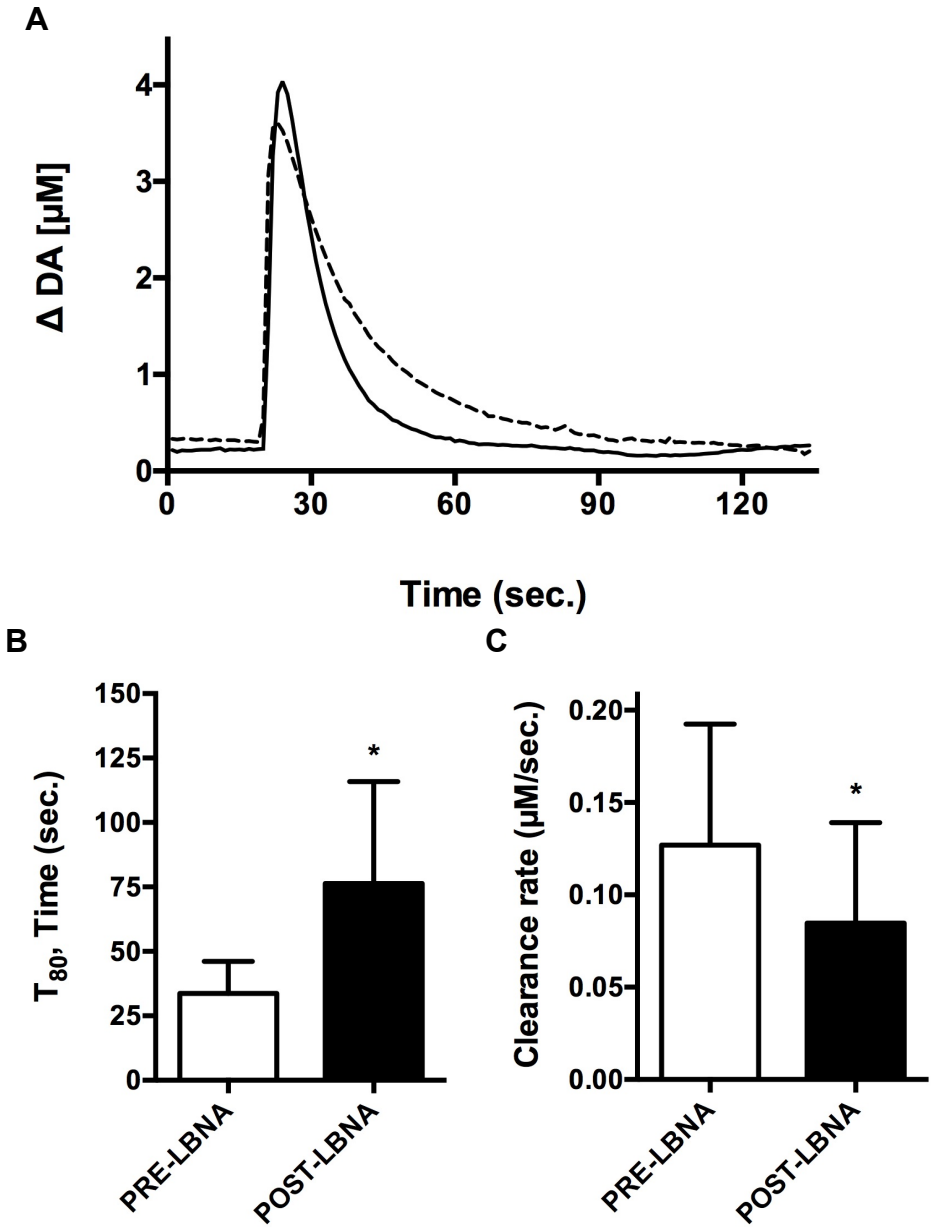

Figure 4.6. Effects of lobinaline (LBNA) on exogenous DA clearance in isoflurane-anesthetized rats measured using HSC. Data are expressed as the mean ± S.E.M. A) Representative trace of exogenous DA clearance pre- (solid line) and post-LBNA (dashed line) application. B) LBNA significantly increased ($p = 0.0203$) the T_{80} 1-minute post application (76.3 ± 39.5 sec.), as compared to the T_{80} pre-application (33.7 ± 12.5 sec.). * $p < 0.05$, pre- vs. post-lobinaline application, paired one-tailed Student's t-test. C) LBNA significantly decreased ($p = 0.0459$) the clearance rate 1-minute post-application (0.09 ± 0.05 μM/sec.), as compared to the clearance rate pre-application (0.13 ± 0.07 μM/sec.). * $p < 0.05$, pre- vs. post-LBNA application, paired two-tailed Student's t-test. n = 6.

Chapter 5

Hairy root methodology

5.1. Chemicals and supplies

Methanol, hexane, and chloroform were purchased from Sigma Aldrich (St. Louis, MO, USA). [^{3}H]-GBR12935 (S.A. = 40 Ci/mmol) and [^{3}H]-DA (S.A. = 60 Ci/mmol) were purchased from American Radiolabeled Chemicals, Inc. (St. Louis, MO, USA). All other chemicals and materials were purchased from Fisher Scientific (Pittsburgh, PA, USA), unless otherwise stated. In all instances, the use of water (preparation of media, aqueous solutions, etc.) refers to the use of Milli-Q® H_2O (Millipore, Billerica, Massachusetts, USA). Sterile water refers to Milli-Q H_2O sterilized by autoclaving at 120°C for 20 minutes.

5.2. Selection of candidate plant species

The selection of the candidate plant species for proof-of-concept studies aimed to demonstrate the use target-directed biosynthesis to optimize a plant's pharmacological genotype/phenotype was identified based on the following characteristics: 1) biological activity of interest, 2) bioactivity arising from a structurally complex metabolite that was not amenable to pharmacological optimization via traditional approaches used by medicinal chemist, 3) amenable to genetic transformation using well-established methodology to generate stable transgenic cultures, and 4) transgenic cultures generated from the candidate species which are readily maintained *in vitro*. In the present study, this translated to each of the following, respectively: 1) inhibitory modulation of the DAT, 2) bioactivity arising due to a metabolite having for which no published method for total synthesis exists which possessed a high degree of structural complexity

rendering total synthesis unfeasible, 3) amenable to *A. rhizogenes*-mediated genetic transformation, and 4) resultant transgenic hairy root cultures having a rapid rate of growth using conventional *in vitro* methodology for plant cell culture. These characteristics were required and/or desirable to increase the feasibility of successfully demonstrating proof-of-concept.

5.3. Bacterial and plant cell culture media formulations

All bacterial cultures were grown using lysogeny broth (LB; pH 7.0), prepared as previously described [210]. LB media was autoclaved at 121°C for 20 minutes. Solid LB medium was prepared by adding a gelling agent (agar, 15 g/l) prior to autoclaving. Autoclaved media was placed in a water bath, allowed to reach 55°C, and then filter sterilized (0.45 µm pore size) solutions of antibiotics were added as required. The following LB media compositions were used during the course of the study: liquid LB supplemented with kanamycin (50 mg/ml) or ampicillin (100 mg/ml), and solid LB supplemented with kanamycin (50 mg/ml) or ampicillin (100 mg/ml). Solid LB used to isolate transformed *E. coli* bacterial colonies carrying pGEM-T vectors was prepared using instructions provided with the p-GEMT Easy Vector System (Promega, Madison, WI, USA). Transformed *A. rhizogenes* strains carrying pCambia1301-based binary vectors were selected solidified LB supplemented with kanamycin, whereas strains carrying the binary vector pKYLX80 or pPCVICE4hpt were selected on solidified LB containing ampicillin.

In vitro plant growth media was prepared using hormone-free half-strength Murashige and Skoog salts containing B vitamins (½ MS), supplemented with sucrose (30 g/l) and MES hydrate (0.5 g/l), adjusted to a pH of 5.8. Solid media was prepared by adding Gelrite (3.875 g/l) prior to autoclaving. All media was sterilized by autoclaving at 121°C for 20 minutes. After autoclaving and allowing media to cool to 55°C in a water bath, filter sterilized (0.45 µm pore size) solutions of antibiotics (cefotaxime) and selection agents (MPTP or MPP^+) were added to achieve required media formulations. The following media were used

during the course of experimentation: antibiotic-free liquid ½ MS, liquid ½ MS supplemented with cefotaxime (800 mg/ml), antibiotic-free solid ½ MS, solid ½ MS supplemented with cefotaxime (800 mg/ml or 400 mg/ml), and solid ½ MS supplemented with cefotaxime (400 mg/ml) and MPTP or MPP^+ (final concentration, 100 µM).

5.4. Binary vectors and the construction of pCambia1301-hDAT

Binary vectors mobilized into *A. rhizogenes* for the purpose of hairy root induction, including their respective reporter genes, genes of interest, and selectable marker genes, are summarized in **Table 6.1**. Human brain total reference RNA obtained from Ambion RNA Company (Life Technologies, Grand Island, NY, USA) was used to isolate cDNA via reverse transcription. Full-length cDNA coding for the hDAT (1.8-kb pairs) was PCR amplified (forward primer: 5'-AAGCTTATGAGTAAGAGCAAATGCTC-3'; reverse primer: 5'-TCTAGACTACA-CCTTGAGCCAGTGGC-3'), and cloned into the p-GEMT Easy Vector System (Promega, Madison, WI, USA) using methods provided by the manufacturer. HindIII and XbaI restriction enzyme sites were added to the 5'-end of the forward and reverse primers, respectively (underlined above). Authenticity of the gene was confirmed via sequencing. Full-length cDNA encoding the hDAT was sub-cloned into the binary vector pKYLX80 downstream of the CaMV 35S promoter using a directional cloning strategy using the restriction enzymes HindIII and Xba1, thus creating pKYLX80-hDAT. The CaMV 35S promoter, multiple cloning site, and rbcs 3' terminator sequence was restricted from pKYLX80 using EcoR1 and Cla1, then sub-cloned into the multiple cloning site of pBluescript SK- creating a modified pBluescript SK- (mpBluescript SK-). The CaMV 35S promoter and cDNA encoding the hDAT were excised from pKYLX80-hDAT with EcoR1 and Xba1 restriction enzymes, and ligated into mpBluescript SK- upstream of the rbcs 3' terminator, creating hDATmpBluescript SK-. The expression cassette consisting of the CaMV 35S promoter, full length cDNA coding for the hDAT, and the rbcs 3' terminator was excised from hDATmpBluescript SK- using EcoR1 and

Sal1 restriction enzymes, and ligated into the binary vector pCabmia1301, ultimately obtaining pCambia1301-hDAT. The presence of the hDAT expression cassette in pCambia1301-hDAT was confirmed via PCR amplification (forward primer: 5'-ATGAGTAAGAGCAAATGCTCCGTGGG-3'; reverse primer: 5'-CTACACCTTGAGCCAGTGGCGGAG-3').

5.5. Agrobacterial strains and transformation

In the present study, *A. rhizogenes* strain R1000 (AR1000) was used to generate hairy roots. Competent cells of AR1000 were transformed with binary vectors using the freeze-thaw method, as previously described [210]. AR1000 carrying pCambia1301, pCambia1301-hDAT, pKM24GFP, or pPCVICE4hpt was thus obtained (AR1000-C, AR1000-hDAT, AR1000-GFP, and AR1000-ATM, respectively). Agrobacterial strains were stored at -80°C in 60% glycerol. Fresh agrobacterial stocks retrieved from storage at -80°C and grown overnight were used for all plant transformation experiments. Fresh agrobacterial stocks were prepared every 6 months to conserve the viability and integrity of bacterial strains their respective vectors.

5.6. Plant growth conditions

In vitro grown plant cultures were maintained in a plant growth chamber at 25°C ± 2°C on a 12-hour light/dark cycle under commercially available fluorescent lights (light intensity, 45 µmol • m^{-2} • sec^{-1}). All *in vitro* grown plants, wild-type roots, and hairy root cultures were maintained under aseptic conditions. *In vitro* grown plants, wild-type roots, and hairy root cultures were subcultured onto fresh medium every 4 – 6 weeks, unless otherwise stated.

5.7. Germination of L. cardinalis seedlings and induction hairy roots: primary hairy root induction

L. cardinalis seeds obtained from the Prairie Moon Nursery (Winona, MN, USA) were surface sterilized with an aqueous 30% bleach solution for 15 minutes, washed three times with sterile water, then stored at 4°C in 10 volumes of sterile water. Under aseptic conditions, sterilized seeds were aspirated into a sterile 9-inch pipette, plated onto antibiotic-free solid ½ MS, and then placed in a plant growth chamber. Care was taken to distribute the seeds evenly over the surface of the medium. Seeds generally germinated within 4 – 8 weeks.

Hairy roots were generated using methods previously described for *L. erinus*, with minor modifications [211, 212]. Briefly, AR1000-hDAT was grown overnight to an OD_{600} of ~0.6 in liquid LB supplemented with kanamycin (100 mg/ml). The following day, the bacterial suspension was centrifuged at 4,000 x g for 8 minutes. The resulting pellet was re-suspended 25 ml of antibiotic-free liquid ½ MS. Plant tissue explants used for hairy root induction consisted of hypocotyl segments (length, ~1.5 cm) prepared by excising and discarding cotyledons and radicles from 4 – 6 week old seedlings grown *in vitro* under aseptic conditions. Explants were placed in antibiotic-free liquid ½ MS containing agrobacteria, punctured three times with a sterile hypodermic needle, and allowed to soak for 20 minutes in presence of agrobacteria. Explants were then removed from the solution containing agrobacteria, blotted on sterile filter paper, placed on antibiotic-free solid ½ MS, and kept in the dark in a plant growth chamber for a 3-day co-cultivation period. Afterward, explants were transferred to a 50 ml conical tube containing 40 ml of liquid ½ MS supplemented with cefotaxime (1,000 mg/ml) for 30 minutes. The conical tubes were gently shaken (~30 seconds) at 5-minute intervals. Explants were then removed, blotted on sterile filter paper, placed on solid ½ MS supplemented with cefotaxime (800 mg/ml), and subcultured onto fresh medium every 3 – 5 days for 2 weeks. Next, explants were transferred to and maintained on solid ½ MS supplemented with cefotaxime (400 mg/ml), and subcultured onto fresh medium every 1 – 2 weeks. Hairy roots

emerged from explants within 4 – 6 weeks. Upon reaching a length ≥ 1.5 cm, hairy roots were excised and maintained on solid ½ MS supplemented with cefotaxime (400 mg/ml). Control hairy roots were induced using essentially identical methods, with the exception of being transformed with AR1000-C. Hairy roots generated directly from *L. cardinalis* hypocotyls herein are referred to as primary hairy roots (1°HRs). Two populations of 1°HRs were thus obtained: 1) transgenic primary hairy roots expressing the hDAT (hDAT-1°HRs) and 2) control primary hairy roots (Ctrl-1°HRs).

5.8. β-glucuronidase (GUS) histochemical staining assay

Successful transformation of *L. cardinalis* hairy roots induced with AR1000-C or AR1000-DAT was confirmed using the GUS histochemical staining assay, as previously described [210]. Briefly, a stock solution of GUS staining buffer (50 mM Na_3PO_4, 0.5 mM $K_3Fe(CN)_6$, 0.5 mM $K_4Fe(CN)_6$, 10 mM EDTA, and 0.05% Triton X-100 dissolved in 150 ml of water, pH 7.0) was prepared and 15 ml aliquots of the stock were stored at -20°C. For GUS staining, a 15 ml aliquot of stock GUS staining buffer was thawed, diluted with water (final volume, 100 mL), and then 35 mg of 5-bromo-4-chloro-3-indolyl-β-D-glucuronide (X-Gluc) dissolved in 150 µl of DMF was added to the diluted stock buffer. Hairy roots (length, ~3 – 4 cm) were divided into equal halves with a sterile surgical blade. Hairy root apices were maintained on solid ½ MS supplemented with cefotaxime (400 mg/ml). Basal portions of hairy roots were incubated in GUS staining buffer containing X-Gluc for a 24-hour period at 37°C. The formation of a blue precipitate indicated successful integration of T-DNA. Hairy root apices corresponding to basal portions that tested positive for GUS reporter gene expression were maintained for use in later studies.

5.9. Conformation of cDNA encoding the hDAT in hDAT-1°HRs

Total RNA was isolated from Ctrl- and hDAT-1°HRs that tested positive for GUS reporter gene expression. RNA (1 µg) from each sample was reversely transcribed and subsequently amplified using a cDNA synthesis kit from Invitrogen and 0.5 mmol of both sense and antisense primers specific to the hDAT gene sequence. Ten-fold dilutions (initial concentration, 100 ng) of pCambia1301-hDAT plasmid DNA was used as positive control (standard). Standards and samples were simultaneously PCR amplified for 30 cycles in a thermocycler. After amplification, the PCR products were run in agarose gel-based electrophoresis and visualized after ethidium bromide staining. The amplified PCR products were analyzed under UV light in a Gel-Doc system. The following primer sequences were used for PCR amplification: forward, 5'-ATGAGTAAGAGCAAATGCTCCGTGGG-3'; reverse, 5'-CTACACCTTGAGCCA-GTGGCGGAG-3'. hDAT-1°HRs that tested positive for cDNA encoding the hDAT were maintained for use in later studies.

5.10. [^{3}H]-GBR12935 binding in transgenic L. cardinalis hairy root membranes

Radioligand binding studies were conducted in 1°HR membrane preparations with the highly selective DAT ligand [^{3}H]-GBR12935 [84, 86]. Membranes were prepared as previously described, with minor modifications [213]. Briefly, plant tissue from Ctrl- or hDAT-1°HRs that tested positive for cDNA encoding the hDAT was flash frozen with liquid nitrogen and lyophilized. Freeze-dried tissue was ground to a fine powder and homogenized in 10 volumes of buffer (0.1 M Na_2HPO_4, 0.5 M mannitol, 50 mM ascorbic acid, 5 mM EDTA, 40 mM 2-mercaptoethanol, 0.5 M PMSF, 10 µg/ml leupeptin, 4.4 µg/ml aprotenin and 2.5 µg/ml bacitracin). The resulting homogenates were centrifuged at 10,000 x g for 15 minutes at 4°C, the resulting pellet was discarded, and the supernatant was centrifuged at 50,000 x g for 30 minutes at 4°C. The resulting pellet was resuspended in buffer (20 mM HEPES, 20 mM NaCl, 1 mM $MgCl_2$, 1 mM EDTA,

30% glycerol, 0.2 mM PMSF, 10 µg/ml leupeptin, 4.4 µg/ml aprotenin, 2.5 µg/ml bacitracin), washed 3 times, then pelleted again at 50,000 x g for 30 minutes at 4°C. The resulting membrane isolates (final tissue concentration, 3.3 µg/ml) were incubated with [^{3}H]-GBR12935 (final concentration, 0 – 250 nM) in assay buffer (50 mM Na_2PO_4, 120 mM NaCl, 10 µM ZnCl, adjusted to pH 7.4) for 2 hours in a 96-well plate format (final reaction volume, 300 µL). Experiments were performed at room temperature. After reaching equilibrium, membranes were harvested onto 96-well GF/B filter plates (PerkinElmer Inc., Waltham, MA, USA) by vacuum filtration, and rapidly washed three times with ice-cold 50 mM Tris-HCl buffer (pH 7.4). Filter plates were pretreated with a solution of 0.1% polyethyleneimine 1 hour prior to harvesting membranes to reduce non-specific binding. Filter plates were allowed to dry overnight. The following day, 35 µL of scintillation fluid (Microscint 20, Packard Inc.) was added to each well and plates were placed in the dark for two hours. Afterward, radioactivity was measured by scintillation counting (2 minutes per well) using a Packard TopCount® NXT™ microplate scintillation counter. Total binding was measured in the presence of radioligand alone, and non-specific binding was measured in the presence of excess GBR12909 (final concentration, 10 µM). Specific binding was calculated by subtracting non-specific binding from total binding. hDAT-1°HRs that tested positive for hDAT protein expression were maintained for use in subsequent experiments.

5.11. [^{3}H]-DA uptake studies in L. cardinalis 1°HRs

Radiotracer uptake studies were performed with apices from Ctrl- or hDAT-1°HRs. Briefly, excised 1°HR apices (n = 20 per group; total mass, ~100mg) were incubated in uptake buffer (120 mM NaCl, 3.9 mM KCl, 650 µM $MgSO_4$, 510 µM $CaCl_2$, 190 µM $NaHPO_4$, 100 µM pargyline, 2 mg/ml glucose, 0.2 mg/ml ascorbic acid, 20 mM HEPES, pH 7.4), uptake buffer containing the highly selective DAT inhibitor GBR12909 (final concentration, 100 µM), or Na^+-free uptake buffer at 37°C for 15 minutes prior to the addition of [^{3}H]-DA (final

concentration, 20 – 30 nM) [84-88]. Initial experiments were performed at a single time point, terminating uptake 4 minutes after the addition of [^{3}H]-DA. Experiments examining the time-dependence of [^{3}H]-DA uptake were performed by incubating Ctrl- or hDAT-1°HRs in uptake buffer at 37°C for 15 minutes, after which [^{3}H]-DA was added. Uptake in time course studies was terminated 1 – 30 minutes after the addition of [^{3}H]-DA. In a final set of experiments, Ctrl- or hDAT-1°HRs were incubated in uptake buffer, or uptake buffer containing GBR12909 (final concentration, 10 µM or 100 µM) for 15 minutes at 37°C, after which [^{3}H]-DA was added, and uptake was allowed to proceed for 5 or 25 minutes. The final concentration of [^{3}H]-DA was consistent in all uptake studies. Uptake in all experiments was terminated by washing 1°HR apices thrice with ice-cold uptake buffer after the removal of solution containing [^{3}H]-DA. After removing the last wash, 1°HR apices were flash frozen with liquid nitrogen, lyophilized, and ground to a fine powder. Ground hairy root tissue was extracted with 300 µl of uptake buffer containing cellulase enzyme (1,500 units/ml) for 24 hours, then centrifuged at 20,0000 x g for 20 minutes at 4°C. Aliquots (100 µl) from the supernatants of various treatment groups were added to scintillation fluid and radioactivity was measured by scintillation counting using a Packard Tri-Carb Liquid Scintillation Counter (Gaithersberg, MD, USA). Data were expressed as the rate of uptake per unit mass of hairy root tissue per unit time (CPM/mg tissue/minute).

5.12. 6-OHDA- and MPTP/MPP$^+$-induced cytotoxicity

Wild-type roots (WT-Rs), Ctrl-1°HRs, and hDAT-1°HRs were exposed to cytotoxic DAT substrates, 6-hydroxydopamine (6-OHDA) and 1-methyl-4-phenyl-1,2,3,6-tetrahydropyridine (MPTP), which are neurotoxins used to model PD [43, 89-92, 114, 214]. The oxidative metabolite of MPTP, 1-methyl-4-phenylpyridinium (MPP$^+$), is a cytotoxic DAT substrate [89, 90]. Hairy root apices (n = 5 per treatment group; total mass, ~ 120 mg total) were placed in conical tubes containing 5 ml of liquid ½ MS (vehicle), or liquid ½ MS containing MPTP or 6-OHDA (final concentration, 100 µM and 50 µM, respectively), and then incubated

at room temperature for 24 hours in the dark. Cell viability was normalized to that of WT-Rs. In a separate set of experiments, Ctrl- or hDAT-1°HR apices were placed in conical tubes containing 5 mL of liquid ½ MS (vehicle) or liquid ½ MS containing GBR12909 (final concentration, 10 µM or 100 µM) for 1 hour prior to being treated with MPTP or 6-OHDA, as described above. In the latter experiments, only hDAT-1°HR apices were treated with GBR12909 and/or neurotoxins. Cell viability was normalized to that of vehicle treated Ctrl-1°HRs.

After the 24-hour treatment period, root apices were stained with trypan blue to visualize dead or dying cells, as previously described with modifications [215]. Briefly, treatment solutions were removed and discarded, then root apices were washed 3 times with liquid ½ MS. The final wash was removed, replaced with 5 ml of trypan blue stain (0.4%), and the staining solution was vacuum infiltrated for 30 minutes. Root apices were then incubated at 90°C for 2 hours, the trypan blue staining solution was then removed, and replaced with an aqueous solution (5 ml) of chloral hydrate (final concentration, 2.5 g/ml). Roots were incubated in the solution of choral hydrate at room temperature overnight in the dark. The following day, root apices were placed on a microscope slide and visualized at 32x magnification using a dissecting microscope. Images were captured with a digital camera affixed to the microscope. Trypan blue staining intensity was quantified with ImageJ software and converted to an index of cell viability.

5.13. Sequential hairy root transformation: induction of secondary hairy roots

Sequential transformation of hairy roots was accomplished using essentially the same protocol as that described to induce 1°HRs (*see section 5.7*), with the exception that 1°HRs served as a source of explants. Explants (length, ~1.5 – 2 cm) excised from Ctrl-1°HRs that tested positive for GUS reporter gene expression (*see section 5.8*) were co-cultured with AR1000-GFP. Secondary hairy roots (2°HRs) emerged ~2 – 4 weeks later at cut surfaces and wound sites on the lateral surfaces of explants created with a sterile hypodermic

needle. Individual hairy roots were tested for both GFP and GUS reporter gene expression via florescent microscopy (equipment, wave length of excitation, etc.) and histochemical staining, respectively. Initially, 2°HRs were evaluated for GFP reporter gene expression, since GUS staining would preclude GFP imaging. The transformation frequency was determined by dividing the total number of 2°HRs emerging from the each 1°HR explant by the number of 2°HRs that tested positive for both GUS and GFP reporter gene expression.

5.14. Induction and selection of transgenic gain-of-function hairy roots functionally expressing the hDAT

Explants (length, ~1.5 – 2 cm) obtained from hDAT-1°HRs functionally expressing the hDAT were co-cultured with AR1000-ATM for 3 days, using methods for sequential hairy root induction described above. Following the co-cultivation period, hairy root explants were soaked in liquid ½ MS supplemented with cefotaxime (1,000 mg/ml) for 30 minutes, blotted on sterile filter paper, and placed on solid ½ MS supplemented with cefotaxime (800 mg/ml). Explants were subcultured every 3 days onto fresh medium for 1 week. Nodules indicating the initiation of 2°HR formation began form at cut surfaces and wound sites on the lateral surfaces of explants ~2 weeks after co-culture. Explants were then transferred to selection medium, solid ½ MS supplemented with cefotaxime (400 mg/ml) and a neurotoxin/selection agent, MPTP or MPP^+ (final concentration, 100 μM). During the first month of selection, explants were subcultured onto fresh selection medium weekly. Subsequently, explants were subcultured onto fresh selection medium every 4 – 6 weeks. Fully differentiated secondary gain-of-function transgenic hairy roots expressing the hDAT which were resistant to the selection agent (toxin resistant secondary hairy roots, TR-2°HRs) emerged 4 – 6 weeks later, and were excised from hDAT-1°HR explants after reaching a length ≥ 1.5 cm. Excised TR-2°HRs were maintained on selection medium ≥ 4 months prior to being transferred to solid ½ MS supplemented with cefotaxime (400 mg/ml) only. TR-2°HRs that were initially selected on medium containing MPTP

were transferred to and maintained on selection medium containing MPP^+ for ≥ 4 months prior to be transferred to solid ½ MS supplemented with cefotaxime (400 mg/ml) only. MPP^+ was used as a selection agent, rather than MPTP, in later studies since differences in MPTP susceptibility could have arisen due to variations in 2°HRs' ability to oxidize MPTP to MPP^+. Selection with MPP^+ also prevented resistance that could have arisen from mutations leading synthesis of oxidase inhibitors and/or reduction of oxidase activity. Therefore, MPP^+ selection was more selective for the survival of TR-2°HRs having mutations leading to increased hDAT inhibitory modulation. A separate population of secondary gain-of-function transgenic hairy roots expressing the hDAT was generated, but was not selected on medium containing a cytotoxic DAT substrate (ATMhDAT-2°HRs).

5.15. Hairy Root Populations and Tissue collection

Four hairy root populations were established: Ctrl-1°HRs (n = 68), hDAT-1°HRs (n = 77), ATMhDAT-2°HRs (n = 72), and RHRs (n = 109). Root apices (length, ~1.5 cm) were placed on fresh medium to propagate individual cultures when hairy root populations were subcultured. All remaining tissue from individual hairy root cultures was placed in 15 ml conical tubes labeled with the corresponding population and hairy root number, then stored at -20°C prior to use in subsequent experiments.

5.16. Preparation of hairy root MeOH extracts and the isolation of lobinaline

Tissue samples collected from individual hairy roots were removed from storage at -20°C, immediately freeze-dried, ground to a coarse powder, and extracted with 3 volumes of methanol overnight in the dark. The following day, samples were centrifuged at 10,000 RPM for 30 minutes. Equal volumes of the resulting supernatants were aliquoted into two pre-weighed, labeled 1.5 ml conical tubes, dried using a CentriVap, and the masses conical tubes containing

dried extract were determined. The mass of a dried extract was calculated by subtracting the mass of the conical tube and from that of a conical tube containing dried extract. One aliquot from each individual hairy root was assessed in pharmacological assays. The other was subject to gas chromatographic-mass spectrometric (GC-MS) analysis. Lobinaline was isolated as previously described (*see section 3.5*). Lobinaline thus obtained was analyzed using GC-MS methods described below (*see section 5.18)*, and the purity of the alkaloid was determined by integrating the area under the curve (AUC) of lobinaline's chromatographic peak (GC-MS run in TIC mode; purity ≥ 95%). The identity the alkaloid was confirmed based on previously reported MS fragmentation data for lobinaline [135]. Dried methanolic (MeOH) hairy root extracts and lobinaline were stored at -20°C prior to further experimentation.

5.17. Pharmacological analysis of hairy root MeOH extracts: inhibition of DAT-mediated [^{3}H]-DA uptake

The DAT inhibitory activity of MeOH extracts from individual hairy roots was examined by performing [^{3}H]-DA uptake in rat striatal synaptosomes. *In vitro* [^{3}H]-DA uptake was performed as previously described with minor modifications [57]. Briefly, adult male Sprague-Dawley rats (200-250 g) were anesthetized with CO_2 and decapitated. Striata were rapidly dissected and immediately placed into 10 volumes of ice-cold uptake buffer (120 mM NaCl, 3.9 mM KCl, 650 µM $MgSO_4$, 510 µM $CaCl_2$, 190 µM $NaHPO_4$, 100 µM pargyline, 2 mg/ml glucose, 0.2 mg/ml ascorbic acid, 20 mM HEPES, pH 7.4, saturated with 95% O_2/5% CO_2) containing 0.32 M sucrose. Striatal tissue was homogenized in a glass homogenization tube with a Teflon pestle. The homogenate was centrifuged at 1,000 x g for 10 minutes at 4°C. The resulting supernatant was collected and centrifuged at 16,000 x g for 20 minutes at 4°C. The resulting pellet was washed twice with ice-cold uptake buffer and re-suspended in 10 ml of uptake buffer (synaptosome preparation). Synaptosomes (100 µl) were added to individual wells in a 96-well plate and incubated at 37°C for 10 minutes. Hairy root MeOH

extracts were dissolved in uptake buffer containing 1.0% DMSO. Lobinaline was dissolved in 100% DMSO, then diluted with uptake buffer (0.3 nM – 3 mM). The final concentration of DMSO in uptake studies never exceeded 1.0%, which had no significant effect on radiotracer uptake using methods outlined in the present study. Hairy root MeOH extracts (100 µl; final concentration 200 or 100 µg/ml) or lobinaline (100 µl; final concentration, 0.1 nM – 1 mM) were co-incubated with synaptosomes for 10 minutes at 37°C prior to the addition of [^{3}H]-DA (100 µl). After the 10-minute co-incubation, [^{3}H]-DA was added to each well (final concentration, 15 – 30 nM) and uptake was allowed to proceed for 5 minutes at 37°C. Uptake was terminated by placing 96-well plates on ice, and then immediately harvesting synaptosomes onto a 96-well GF/C filter plates (PerkinElmer Inc.) by vacuum filtration, followed by three rapid washes with ice-cold 50 mM Tris-HCl buffer (pH 7.4). After allowing filtration plates to dry overnight, 35 µl of scintillation fluid (Microscint 20, Packard Inc.) was added to each well and the plate was kept in the dark for 2 hours. Subsequently, radioactivity was measured by scintillation counting using a Packard TopCount® NXT™ microplate scintillation counter. Total uptake was measured in the presence of [^{3}H]-DA alone. Non-specific uptake was determined in the presence of 10 µM GBR-12909. Total specific uptake and specific uptake in the presence of extract or lobinaline was calculated by subtracting non-specific uptake from each, respectively. Specific uptake in the presence of inhibitor was expressed as a percentage of total specific uptake. Each extract's inhibitory activity at the DAT was expressed as lobinaline equivalents, extrapolated from the lobinaline dose-response curve. DAT inhibitory activity (mean ± S.E.M) of each hairy root population was calculated. The frequencies of "highly active DAT inhibitors," designated as hairy roots whose extract produced DAT inhibition ≥ 2 S.D. above mean DAT inhibition observed for the hDAT-1°HR population, were calculated for ATMhDAT- and TR-2°HR populations.

5.18. GC-MS analysis of hairy root MeOH extracts

MeOH extracts from individual hairy roots were analyzed via GC-MS. GC-MS analyses were performed using a Hewlett Packard 6890 Gas Chromatograph interfaced to a Hewlett Packard 5973 Series Mass Selective Detector, an Agilent Technologies 7683 Series Injector, and a Hewlett Packard 7683 Series Autosampler. ChemStation Software (Version 1.02.06) and the Wiley Spectral Database (Version 4.0) were used for instrument control, data analysis, and structural elucidation. Separation was performed on a HP-5MS column ((5%-phenyl)-methylpolysiloxane; 30.0 m x 320 µm x 0.25 µm). Ultra-high purity helium (flow rate of 1.2 ml/minute) served as the carrier gas. Sample volumes of 1 µl were injected in split mode (split ratio, 10.0:1; split flow 12.3 ml/minute) at an inlet pressure of 1.60 psi. The inlet temperature was held at 250°C. The oven was operated using the following parameters: initial temperature, 80°C; 80°C, 2 minute hold; 10°C/minute to 160°C, 1 minute hold; 60°C/minute to 275°C, 12 minute hold; 60°C/min. to 60°C, 0 minute hold; total runtime, 28.50 minutes. The transfer line temperature was held at 280°C. Lobinaline content of each extract was quantified. A concentration-response curve for lobinaline was generated by dissolving the alkaloid in methanol (concentrations prepared, 10 µg/ml, 25 µg/ml, 50 µg/ml, 100 µg/ml, 250 µg/ml, 500 µg/ml, and 1,000 µg/ml), and then analyzing duplicate samples at each concentration. The abundances of the peak corresponding to m/z = 186 in the MS extracted from lobinaline's chromatographic peak were averaged at each concentration. Data were analyzed using linear regression, and response to lobinaline over this concentration range displayed excellent linearity (r^2 = 0.9965, x-intercept = 1.8 µg/ml). Lobeline was dissolved in methanol (final concentration, 10 – 1000 µg/ml), and subject to GC-MS analysis using the same chromatographic conditions to identify and determine the retention time of it's chromatographic peaks (two prominent peaks were observed, presumably due to decomposition of lobinaline in the instrument prior to reach the MSD). In the present study, chromatographic peaks indicating the presence of lobeline were not detected in

any of the MeOH extracts prepared from *L. cardinalis* hairy roots. Dried MeOH extracts obtained from individual hairy roots were resuspended in methanol (final concentration, 4 mg/ml), and then each sample was analyzed in duplicate. The peak abundance (m/z = 186) in the MS extracted from the lobinaline's chromatographic peak was averaged for each individual hairy root. The concentration of lobinaline present was calculated from the lobinaline calibration curve. The mean lobinaline content of each hairy root population was calculated. The frequencies of "lobinaline overproducers," designated as hairy roots whose extract's lobinaline content was ≥ 2 S.D. above the mean lobinaline content observed for the hDAT-1°HR population, were calculated for ATMhDAT- and TR-2°HR populations.

Qualitative examination of GC traces from individual hairy roots from each population was carried out to determine whether the "fingerprint" of metabolites (i.e. chromatographic peaks) present in extracts within a given population were consistent and reproducible. Qualitative analysis of GC traces from ATMhDAT-2°HRs and TR-2°HRs was also performed to identify of chromatographic peaks that were present, which were undetectable in 1°HR populations. When possible, structural elucidation of metabolites present in increased yields and/or "novel" metabolites was carried out using the software described above.

5.19. Data Analysis

Statistical analyses, curve fitting, and graphical presentation of data were performed using GraphPad Prism software (Version 6.0; GraphPad Software, San Diego, CA, USA). B_{max} and K_d values for [^{3}H]-GBR12935 binding in hDAT-1°HR membranes were calculated using nonlinear regression analysis to fit radioligand binding data to a one-site saturation binding model. One-way analysis of variance (ANOVA) followed by Tukey's post-hoc analysis was performed to determine whether hDAT expression significantly increased [^{3}H]-DA uptake in hDAT-1°HRs, and to determine whether GBR12909 or Na^+-free conditions significantly affected radiotracer uptake in Ctrl- and hDAT-1°HRs at 4-

minutes. Two-way ANOVA was performed (time x phenotype interaction) to determine if hDAT expression significantly increased [^{3}H]-DA uptake in time course studies. Bonferroni's post-hoc analysis was used to determine time points at which the magnitude of [^{3}H]-DA uptake in Ctrl- and hDAT-1°HRs was significantly different. One-way ANOVA followed by Dunnett's post-hoc analysis was performed to determine the time points at which [^{3}H]-DA uptake in Ctrl- or hDAT-1°HRs was significantly different than that measured in respective groups at 1-minute. Two-way ANOVA (time x phenotype interaction) followed by Bonferroni's post-hoc analysis was performed to determine whether [^{3}H]-DA uptake measured at 5- and 25-minutes was significantly increased by hDAT expression, and to determine if uptake at 25-minutes was significantly greater than that observed at 5-minutes in Ctrl- and hDAT-1°HRs. Two-way ANOVA (treatment x phenotype interaction) followed by Bonferroni's analysis was performed to determine whether GBR12909 significantly inhibited [^{3}H]-DA uptake in Ctrl- and hDAT-1°HRs at 5- and 25-minutes. One-way ANOVA followed by Tukey's post-hoc analysis was performed to determine whether susceptibility to cytotoxic DAT substrates was significantly affected by hairy root phenotype and/or hDAT expression. One-way ANOVA followed by Tukey's post-hoc analysis was performed to determine whether GBR12909 significantly attenuated toxicity caused by cytotoxic DAT substrates in hDAT-1°HRs. One-way ANOVA followed by Tukey's post-hoc analysis was performed to determine whether the mean inhibitory DAT activity and the mean lobinaline content of hairy root populations were significantly different. Two-tailed Chi-Square analysis and Fisher's exact test were performed to determine whether ATM combined with selection significantly increased the frequency of "highly active DAT inhibitors" and/or "lobinaline overproducers" when compared to the use of ATM alone. All data are expressed as the mean ± the standard error of the mean (S.E.M.), unless otherwise stated. A p-value < 0.05 was defined as statistically significant.

Table 5.1. Binary vectors mobilized into *A. rhizogenes*

Vector	Reporter genes, genes of interest	Selectable marker gene*
pCamiba1301	GUS reporter gene	KanR, kanamycin resistance
pCambia1301-hDAT	GUS reporter gene cDNA encoding the hDAT	KanR, kanamycin resistance
pKM24GFP	GFP	KanR, kanamycin resistance
pPCVICE4hpt	CaMV 35S enhancer tetramer	AmpR, ampicillin resistance

*Selectable marker genes used to isolate transformed bacterial colonies

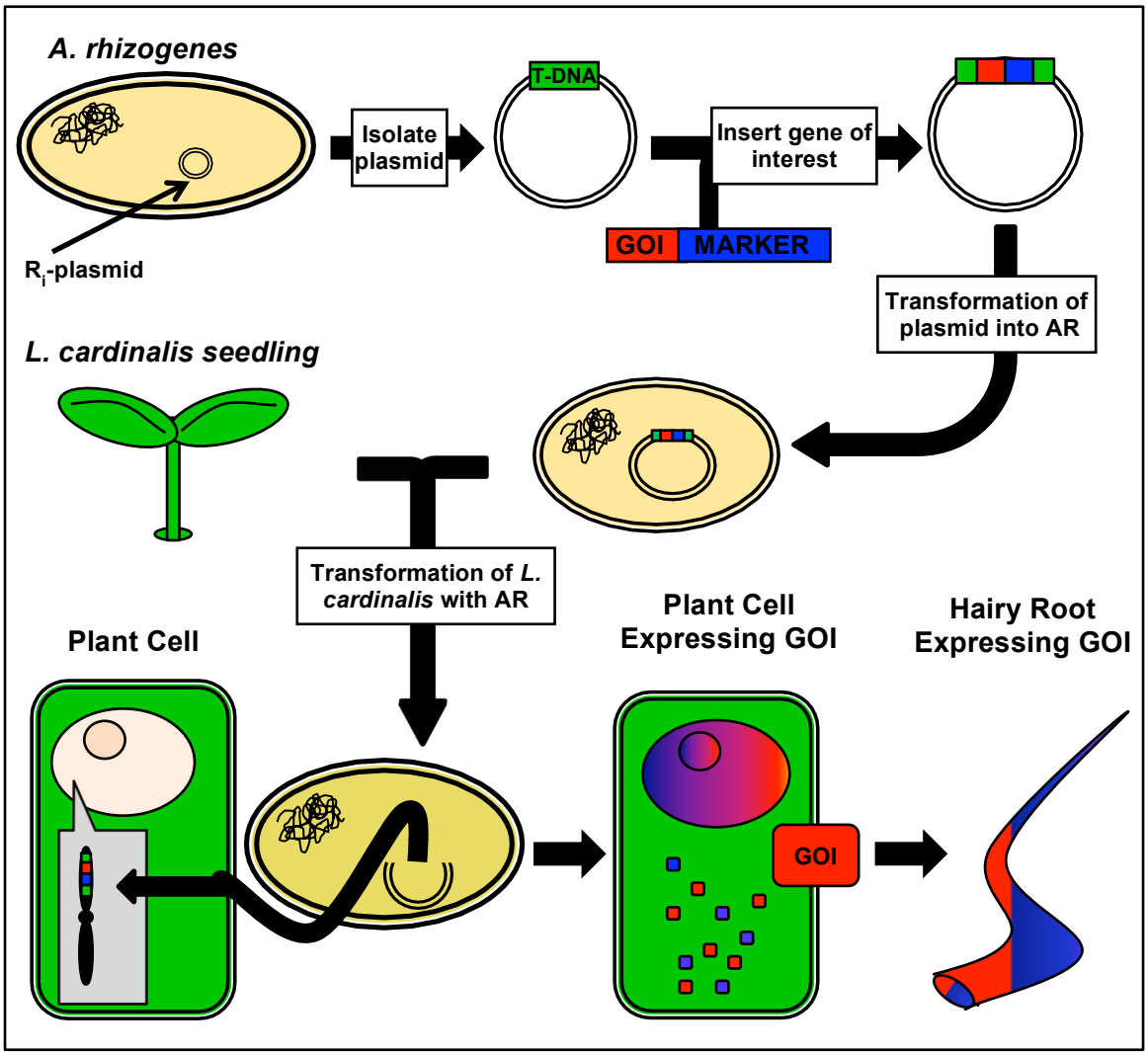

Figure 5.1. Expression of foreign genes in plant cells via *A. rhizogenes*-medicated genetic transformation. *A. rhizogenes* carrying the root inducing plasmid (R_i-plasmid) is capable of transforming plant cells leading the induction of hairy roots. Transfer DNA (T-DNA) present in the R_i-plasmid is transferred and integrated into the genome of host plant species, which encodes genes responsible for hairy root formation. The R_i-plasmid is isolated and genes of interest (GOI), along with a maker gene, are cloned into the borders of the T-DNA. The R_i-plasmid, containing GOI and a marker gene within the borders of the T-DNA, is transformed into *A. rhizogenes*. Transformation of plant seedlings with *A. rhizogenes* harboring the newly constructed R_i-plasmid leads to the induction hairy roots, which arise from a single transformed plant cell. The resulting hairy root is comprised of cells that are clonal in nature, each expressing the GOI and the marker gene, which is utilized to confirm successful transformation. In the present study, *L. cardinalis* hypocotyl explants were transformed with AR1000-hDAT, harboring the binary vector pCambia 1301-hDAT, leading to the induction of hDAT-1°HRs.

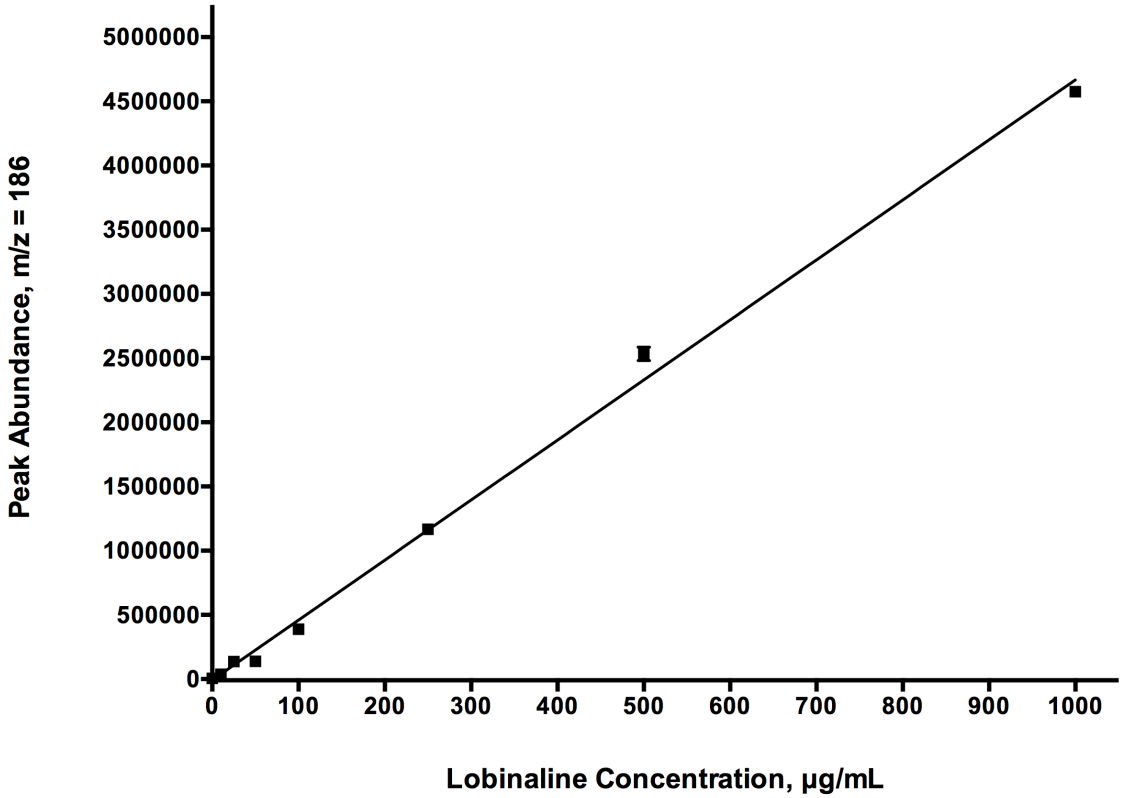

Figure 5.2. Lobinaline calibration curve. Data expressed as the mean ± S.E.M. The lobinaline concentration-response displayed excellent linearity (r^2 = 0.9965) over the concentration range examined (10 – 1000 µg/ml). Each concentration was prepared in duplicate. X-intercept = 1.8 µg/ml.

Chapter 6

Functional Expression of the hDAT in transgenic *L. cardinalis* hairy roots

6.1. Introduction

Lobinaline is structurally complex binitrogenous alkaloid present in *L. cardinalis*, which inhibits the DAT, albeit with low potency (IC_{50} = 12.0 μM). There is no published method for the total synthesis of lobinaline, and the alkaloid is obtained in low yields when purified from plant material, preventing access to sufficient quantities of lobinaline required for pharmacological optimization via traditional approaches [8, 20, 206]. In order to generate a library of *L. cardinalis* plant cell cultures whose pharmacological profile was genomically optimized, the human dopamine transporter (hDAT) was functionally expressed in transgenic *L. cardinalis* hairy "primary" root cultures (hDAT-1°HRs). Here, "primary" refers to hairy roots induced directly from wild-type plant, *L. cardinalis*, in contrast to "secondary" hairy roots generated directly from hairy root explants via sequential transformation.

The purpose of expressing the hDAT protein in transgenic plant cells was two-fold. One, to enable the selection of gain-of-function mutant transgenic plant cells expressing the hDAT on selection medium containing cytotoxic DAT substrates, which was predicted to favor mutants with increased yields of lobinaline and/or "novel" DAT inhibitors. Two, to favor biosynthesis of "novel" DAT ligands whose structure was optimized to interact with a specific human target protein. The former was desirable since mutants with increased yields of lobinaline could be utilized for the production of the alkaloid, whereas mutants with "novel" DAT inhibitors served as a repository of leads for the development of novel DAT ligands. The latter should theoretically enable one to redirect plant evolution favoring biosynthesis of molecules meant to interact with a human

target protein. This is in contrast to naturally occurring plant metabolites, which evolved to interact with molecular targets present in organisms more frequently encountered by plants, such as microbes or herbivorous insects [13, 14].

6.2. Candidate plant species: Lobelia cardinalis

L. cardinalis was selected as the candidate species for proof-of-concept studies using target-directed biosynthesis. Lobinaline (*see* ***Figure 3.3***), the major alkaloid present in *L. cardinalis*, inhibits the DAT and scavenges free radicals (*see sections 4.3 and 4.4, respectively*). However, there is no published method for the total synthesis of the complex decahydroquinoline alkaloid, rendering lobinaline a poor candidate for pharmacological optimization via traditional methods used by medicinal chemist. In preliminary studies, *L. cardinalis* was readily transformed using *A. rhizogenes*-mediated genetic transformation. The resulting hairy root cultures displayed a rapid rate of growth and were easily maintained *in vitro* on solid ½ MS medium. These characteristics of the *L. cardinalis*, *L. cardinalis* hairy root cultures, and lobinaline were ideal for proof-of-concept studies using target-directed biosynthesis to optimize the plant's pharmacological activity at the hDAT. Here, optimized activity at the hDAT refers to: 1) increased yields of lobinaline and/or 2) biosynthesis of "novel" metabolites that are more potent DAT inhibitors.

6.3. Construction of pCambia1301-hDAT and the establishment of L. cardinalis primary hairy root cultures

Full-length cDNA encoding the hDAT (1.8-kb) was PCR amplified from human brain total reference RNA (**Figure 6.1**), sequenced and authenticity confirmed. Subsequently, the cDNA coding for the hDAT was ligated into an expression cassette downstream of the constitutively active CaMV 35S promoter and upstream of the rbcs 3' terminator sequence (**Figure 6.2**). AR1000-hDAT was obtained by transforming AR1000 with pCambia1301-hDAT, created by sub-

cloning the hDAT expression cassette within the T-DNA borders of the binary vector pCambia1301.

Hairy roots were generated from hypocotyl segments of *L. cardinalis* seedlings. Initial studies were performed to determine whether hairy roots could be induced from *L. cardinalis* hypocotyl explants using AR1000-C. Ctrl-1°HRs were successfully obtained. The transformation frequency for *L. cardinalis* hypocotyl explants was ~53% (46 out of 86 explants produced Ctrl-1°HRs that tested positive for GUS reporter gene expression). A total of 129 Ctrl-1°HRs, as confirmed GUS reporter gene expression, were generated from the 46 explants (mean Ctrl-1°HRs per explant, 2.8). Images of Crtl-1°HRs subject to GUS histochemical staining clearly demonstrate the presence of a blue precipitate (**Figure 6.3**), indicative of successful transformation. Subsequently, hypocotyl explants were transformed with AR1000-hDAT generating hDAT-1°HRs, and successful integration of T-DNA was confirmed based on GUS reporter gene expression. A schematic summarizing the approach utilized to induce Ctrl- and hDAT-1HRs is depicted in **Figure 6.4**.

6.4. hDAT-1°HRs tested positive for cDNA encoding the hDAT and hDAT protein expression

The expression of the cDNA encoding the hDAT was examined in hDAT-1°HRs by RT-PCR. As shown in **Figure 6.5 A**, a 1.8-kb PCR amplification product was clearly visible in the sample from hDAT-1°HRs (lane 4), whereas the band was absent in the sample from Ctrl-1°HRs (lane 3). Radioligand binding studies were conducted to determine if the hDAT protein was expressed by hDAT-1°HRs that tested positive for cDNA encoding the transporter. Ctrl- or hDAT-1°HR membranes were incubated with varying concentrations of [^{3}H]-GBR12935 (0 – 250 nM), a highly selective DAT ligand [84, 86]. In hDAT-1°HR membranes, specific binding was saturable (K_d = 2.8 ± 0.7 nM, B_{max} = 22.9 ± 1.0 fmol/mg tissue), and displayed excellent fit (r^2 = 0.9687) to a one-site binding model (**Figure 6.5 B**). The K_d value for [^{3}H]-GBR12935 at the hDAT in plant cell

membranes corresponded well with that reported for the radioligand at the DAT in rat striatal membranes (K_d ~1 – 6 nM) [84, 86]. However, the B_{max} value determined for hDAT-1°HR membranes was substantially lower than that reported for rat striatum (56.9 ± 3.5 pmol/µg tissue) [216]. In Ctrl-1°HR membranes, a non-specific increase in binding was observed. The hDAT-1°HR lines that tested positive for cDNA encoding the hDAT and hDAT protein expression were maintained for use in subsequent experiments.

6.5. [^{3}H]-DA Uptake in 1°HRs: the hDAT expressed in hDAT-1°HRs is functional

Radiotracer uptake studies were performed to determine if the hDAT was functional when expressed in transgenic plant cells. Initially, [^{3}H]-DA uptake was measured at a single time point (4 minutes; **Figure 6.6 A**). The rate of [^{3}H]-DA uptake was significantly greater in hDAT-1°HRs, as compared to Ctrl-1°HRs (5.9 ± 0.5 and 2.8 ± 0.3 DPM/mg tissue/minute, respectively; $p = 0.0008$). In hDAT-1°HRs, the rate of [^{3}H]-DA uptake was significantly reduced by GBR12909 (100 µM) or under Na^+-free conditions (3.1 ± 0.2 and 2.4 ± 0.4 DPM/mg tissue/minute, $p = 0.0018$ and $p = 0.0002$, respectively), both of which reduced the rate of radiotracer uptake to that observed in Ctrl-1°HRs. The rate of [^{3}H]-DA uptake in Ctrl-1°HRs was unaffected by GBR12909 pretreatment or under Na^+-free conditions. Next, the time course of [^{3}H]-DA uptake was examined in Ctrl- and hDAT-1°HRs (**Figure 6.6 B**). Two-way ANOVA revealed a significant effect of phenotype ($p < 0.001$), a significant effect of time ($p < 0.001$), and a significant time x phenotype interaction ($p < 0.001$). The magnitude of [^{3}H]-DA uptake in Ctrl- and hDAT-1°HRs was significantly different at 4-minutes (16.8 ± 0.9 and 24.7 ± 1.1 CPM/mg tissue, respectively, $p = 0.0257$), and remained significant thereafter. Of note, [^{3}H]-DA uptake in Ctrl- and hDAT-1°HRs was time-dependent and saturable, albeit the V_{max} was significantly lower ($p = 0.0006$) in Ctrl-1°HRs (V_{max} = 94.1 ± 2.7 CPM/mg tissue/minute), as compared to hDAT-1°HRs (V_{max} = 131.8 ± 2.6 CPM/mg tissue/minute). A one-way ANOVA followed by Dunnett's post-hoc analysis was performed to determine the time points at which [^{3}H]-DA

uptake was significantly greater than that measured at 1-minute in Ctrl- or hDAT-1°HRs. In Ctrl- and hDAT-1°HRs, the magnitude of [^{3}H]-DA uptake at 5-minutes (25.6 ± 0.1 and 36.0 ± 1.0 CPM/mg tissue, respectively) was significantly greater ($p < 0.001$ and $p = 0.0007$, respectively) than that measured at 1-mintue (15.6 ± 0.4 and 18.6 ± 0.8 CPM/mg tissue, respectively). These data indicate that both Ctrl- and hDAT-1°HRs express transporters with the capacity for [^{3}H]-DA uptake, in agreement with previous studies reporting transporter-mediated biogenic amine uptake in plants [217, 218]. However, hDAT expression significantly increased [^{3}H]-DA uptake in hDAT-1°HRs demonstrating that the transporter was functional in transgenic plant cells. Additionally, the increase in [^{3}H]-DA uptake in hDAT-1°HRs was abolished by GBR12909 or under Na^+-free conditions indicating that hDAT expressed in plant cells retains its sensitivity to pharmacologic and ionic manipulations known to influence DAT function in mammalian cells [54, 84-88].

To confirm hDAT-1°HR's increased capacity for [^{3}H]-DA uptake was attributable to hDAT expression beyond 4-minutes, radiotracer uptake was measured in Ctrl- and hDAT-1°HRs pretreated with vehicle or GBR12909 (100 μM) at two time points (5- and 25-mintues; **Figure 6.6 C**). Two-way analysis of variance revealed a significant effect of time ($p < 0.001$), and a significant effect of phenotype ($p < 0.001$), and a significant time x phenotype interaction ($p < 0.001$). [^{3}H]-DA uptake measured at 5- and 25-mintues in hDAT-1°HRs was significantly greater ($p < 0.001$) than that observed in all of the corresponding Ctrl-1°HR treatment groups at 5- and 25-minutes. In Ctrl- and hDAT-1°HRs, the magnitude of [^{3}H]-DA uptake was significantly greater ($p < 0.001$) at 25-minutes, as compared uptake measure in corresponding treatment groups at 5-mintues. An additional two-way ANOVA revealed a significant effect of phenotype ($p < 0.001$), a significant effect of treatment ($p < 0.001$), and a significant phenotype x treatment interaction ($p < 0.001$). GBR12909 pretreatment did not affect [^{3}H]-DA uptake in Ctrl-1°HRs at either time point. In contrast, [^{3}H]-DA uptake in hDAT-1°HRs was significantly decreased ($p < 0.001$) by GBR12909 at 5- and 25-minutes (19.9 ± 0.1 and 76.2 ± 1.6 CPM/mg, respectively), as compared to

vehicle pretreated hDAT-1°HRs (36.0 ± 1.0 and 127.2 ± 1.1 CPM/mg tissue, respectively). At 5- and 25-minutes, the magnitude of [^{3}H]-DA uptake in hDAT-1°HRs pretreated with GBR12909 was reduced to that observed in Ctrl-1°HRs. These data indicate that hDAT expression enhances [^{3}H]-DA uptake in hDAT-1°HR's, although radiotracer uptake occurs via two components: 1) hDAT-mediated uptake, which is Na^+-dependent and GBR12909-sensitive, and 2) Na^+-independent transporter-mediated uptake that was GBR-insensitive. The latter, which was observed in Ctrl- and hDAT-1°HRs, is consistent with previous studies in rice and Arabidopsis demonstrating Na^+-independent biogenic amine uptake via system L amino acid transporters [217-219].

6.6. Differential cytotoxic effects of MPTP and 6-OHDA in Ctrl- and hDAT-1°HRs

L. cardinalis wild-type roots (WT-Rs), Ctrl- and hDAT-1°HRs were treated with MPTP or 6-OHDA (final concentration, 100 and 50 µM, respectively; 24-hour treatment) to determine whether hairy root phenotype and/or hDAT expression altered root's susceptibility to cytotoxic DAT substrates. MPTP's oxidative metabolite, MPP+, is a cytotoxic DAT substrate [89, 90]. In initial studies, cell viability was normalized to that of WT-Rs treated with cytotoxins (**Figure 6.7**). MPTP significantly reduced cell viability in hDAT-1°HRs (54.1% decrease, $p < 0.0001$), as compared to WT-Rs. MPTP reduced cell viability in Ctrl-1°HRs (15.8% decrease), as compared to WT-Rs, but the effect was not significant ($p = 0.2762$). Cell viability in MPTP-treated hDAT-1°HRs was also significantly reduced (38.3% decrease, $p = 0.0016$), as compared to Ctrl-1°HRs. In contrast, 6-OHDA significantly decreased cell viability in Ctrl-1°HRs (32.8% reduction, $p = 0.0060$) and hDAT-1°HRs (58.4% reduction, $p < 0.001$), as compared to WT-Rs. Cell viability in hDAT-1°HRs exposed to 6-OHDA was significantly reduced (25.7% reduction, $p = 0.0034$), as compared to Ctrl-1°HRs. These findings indicated hairy root phenotype alone increased susceptibility to 6-OHDA, and vulnerability to 6-OHDA was augmented by hDAT expression. On the other hand, MPTP susceptibility was only significantly increased by hDAT expression. Thus,

hDAT expression increased susceptibility to MPTP and 6-OHDA, but MPTP was more selective for hDAT-1°HRs. These findings are consistent with studies reporting DAT-independent 6-OHDA-induced toxicity, whereas MPTP is highly selective for DAT-expressing cells [89, 90, 214].

Subsequent experiments examining GBR12909's ability to attenuate MPTP- and 6-OHDA-induced cytotoxicity in Ctrl- and hDAT-1°HRs ensued (**Figure 6.8**). GBR12909 is a potent, selective DAT inhibitor which prevents MPTP toxicity in mammalian cells expressing the DAT [84-90, 124]. Cell viability was normalized to that of Ctrl-1°HRs treated with vehicle alone (i.e. no exposure to MPTP or 6-OHDA). Prior to being exposed to MPTP or 6-OHDA (final concentration, 100 and 50 μM, respectively; 24-hour treatment), hDAT-1°HRs were pretreated (1 hour) with vehicle or GBR12909 (final concentration, 10 or 100 μM). MPTP and 6-OHDA significantly reduced cell viability ($p = 0.0003$ and $p < 0.001$, respectively) in vehicle pretreated hDAT-1°HRs (51.3% and 52.0% reduction, respectively), as compared to vehicle treated Ctrl-1°HRs. In hDAT-1°HRs, GBR12909 dose-dependently attenuated MPTP-induced cytotoxicity. Cell viability was increased by 10 μM GBR12909 (25.3% increase, $p = 0.0619$), and was significantly increased by 100 μM GBR12909 (38.0% increase, $p = 0.0088$), as compared to vehicle pretreated hDAT-1°HRs. In fact, cell viability in hDAT-1°HRs pretreated with 100 μM GBR12909 was not significantly different from that of Ctrl-1°HRs. However, GBR12909 pretreatment failed to attenuate cytotoxicity caused by 6-OHDA in hDAT-1°HRs. Similar to PC12 cells, cytotoxicity caused by 6-OHDA in 1°HRs is not entirely dependent on the DAT, nor is it abolished by selective DAT inhibition [214]. In contrast, MPTP-induced cytotoxicity was selective for transgenic plant cells expressing the hDAT, and was dose-dependently attenuated by GBR12909, in agreement with previous reports in mammalian models [84-90, 124].

6.7. Discussion

The hDAT was functionally expressed in transgenic *L. cardinalis* hDAT-1°HRs via *A. rhizogenes*-mediated genetic transformation. The expression and function of the hDAT protein in transgenic plant cells was confirmed by performing radioligand binding and radiotracer uptake studies, respectively. Expression of the hDAT in transgenic plant cells increased their susceptibility to the DAergic neurotoxins MPTP, which is oxidized to the cytotoxic DAT substrate MPP^+, and 6-OHDA [43, 89-91, 214]. Cytotoxicity caused by MPTP in hDAT-1°HRs was attenuated by the highly selective DAT inhibitor GBR12909 [84-88].

Initially, full-length cDNA coding for the hDAT was reverse transcribed from human brain total reference RNA, PCR amplified, and cloned into the vector p-GEMT. Authenticity of the gene was confirmed via sequencing. Full-length cDNA encoding the hDAT was sub-cloned into the expression cassette depicted in **Figure 6.2**, which was mobilized into the T-DNA borders of the binary vector pCambia1301, creating pCambia1301-hDAT. A. *Rhizogenes* strain R1000 was transformed with pCambia1301-hDAT, thus obtaining AR1000-hDAT. Subsequently, hypocotyl explants from *L. cardinalis* seedlings were transformed with AR1000-hDAT, inducing the formation of hDAT-1°HRs. Successful transformation of hDAT-1°HRs was confirmed using the GUS histochemical assay.

Radioligand binding studies were performed in 1°HR membranes determine if the hDAT protein was expressed in transgenic plant cells. Membranes preparations from Ctrl- and hDAT-1°HRs were incubated with the highly selective DAT ligand [^{3}H]-GBR12935 [84, 86]. Binding in hDAT-1°HRs was saturable and consistent with binding to a single site, whereas a non-specific increase in [^{3}H]-GBR12935 binding was observed in controls, confirming that the hDAT protein was expressed in hDAT-1°HR cells. The affinity of [^{3}H]-GBR12935 at the hDAT in hDAT-1°HRs (K_d = 2.7 ± 0.7 nM) corresponded well with that reported for the radioligand at the DAT in rat striatal membranes (K_d ~1 – 6 nM) [84, 86]. These data indicated that the hDAT cDNA was effectively translated,

transcribed, and the hDAT protein was trafficked to the cell membrane where it assumed a structural conformation similar to that in mammalian cells, thereby enabling similar ligand-transporter interactions [213]. However, the expression level of the hDAT protein expression (B_{max} = 22.9 ± 1.0 fmol/mg tissue) in hDAT-1°HRs was substantially lower than that reported in rat striatal tissue (B_{max} = 56.9 ± 3.5 pmol/µg tissue), likely due to differences in codon preference, protein trafficking, and/or protein turnover [213, 216]. A significant increase in [^{3}H]-DA uptake was observed in hDAT-1°HRs, as compared to Ctrl-1°HRs, indicating the transporter was functional. The hDAT expressed in transgenic plant cells also retained its sensitivity to pharmacologic and ionic manipulations known to influence DAT function in mammalian cells [54, 84-88]. Uptake of [^{3}H]-DA was saturable and time-dependent in Ctrl- and hDAT-1°HRs, indicating the presence of endogenous transporters with the capacity for [^{3}H]-DA uptake. GBR12909 and Na^+-free conditions reduced radiotracer uptake in hDAT-1°HRs to that observed in Ctrl-1°HRs, suggesting the endogenous transporter is structurally distinct from the hDAT and Na^+-independent. This is consistent with studies performed in rice and Arabidopsis, wherein biogenic amine uptake was mediated by a Na^+-independent system L amino acid transporter [217-219].

Expression of the hDAT protein in hDAT-1°HRs significantly increased toxicity caused by the DAergic neurotoxins MPTP and 6-OHDA [43, 89-92, 114, 214]. Cell viability in Ctrl-1°HRs was significantly reduced by 6-OHDA, but not MPTP, indicating toxicity caused by 6-OHDA was not dependent on hDAT expression. This is consistent with 6-OHDA's ability to induce cytotoxicity extracellularly in PC12 cells [214]. The highly selective DAT inhibitor GBR12909 dose-dependently attenuated MPTP-induced cytotoxicity in hDAT-1°HRs, but did not reduce toxicity caused by 6-OHDA [84-88]. Again, this is in agreement with previous reports of DAT-independent toxicity caused by 6-OHDA, whereas MPTP toxicity is highly dependent on DAT expression and is attenuated by DAT inhibitors [89, 90, 214, 220]. Alternatively, endogenous transporters present in the hairy roots may be capable of transporting 6-OHDA. Since [^{3}H]-DA uptake attributed to an endogenous transporter/s was not inhibited by GBR12909, the

DAT inhibitor would not be expected attenuate 6-OHDA's cytotoxic effects. On the other hand, the endogenous transporter/s putatively present in Ctrl- and hDAT-1°HRs may lack the capacity to efficiently translocate MPP^+. In the latter case, toxicity caused by MPTP's oxidative metabolite MPP^+, would be highly dependent on DAT-mediated transport in hDAT-1°HRs, explaining GBR12909's ability to attenuate its cytotoxic effects. Based on these observations, gain-of-function mutations that increase biosynthesis of lobinaline and/or "novel" DAT inhibitors in hDAT-1°HRs should confer resistance to MPTP only. Therefore, MPTP was chosen as a selection agent for future studies.

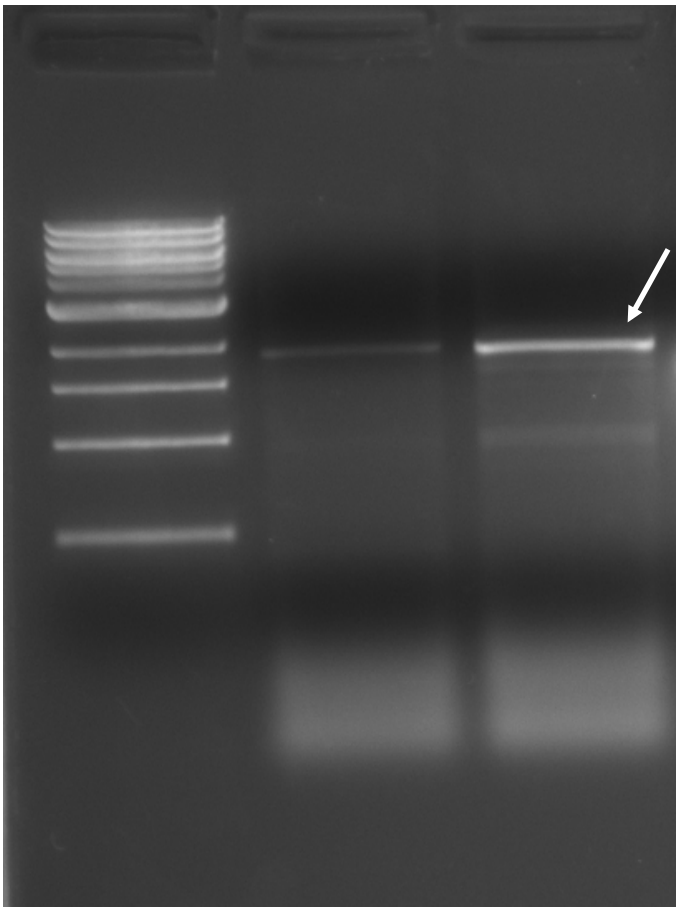

Figure 6.1. Full-length cDNA encoding the hDAT cloned into the multiple cloning site of the vector p-GEMT. Sample DNA was PCR amplified with hDAT specific primers. Lane 1 – ladder; Lane 2 – empty p-GEMT vector; Lane 3 – p-GEMT vector containing full-length cDNA encoding the hDAT; A 1.8-kb band (indicated by the white arrow) is clearly visible in the sample from p-GEMT containing full-length cDNA coding for the hDAT indicating the presence of cDNA coding for the hDAT, which is absent in the sample from empty p-GEMT vector. The hDAT cDNA was sequenced and authenticity confirmed.

Figure 6.2. Diagram of the hDAT expression cassette. Full-length cDNA encoding the hDAT was flanked by the constitutively actively CaMV 35S promoter (35S P) at it’s 5’-end and the rbcs terminator at it’s 3’-end. The expression cassette was sub-cloned into the T-DNA borders of the binary vector pCambia-1301, creating pCambia1301-hDAT.

Figure 6.3. *L. cardinalis* hypocotyl explant successfully transformed with AR1000-C. Hairy roots can been seen emerging the explant which tested positive for the GUS reporter gene, as indicating by the formation of blue precipitate following GUS histochemical staining.

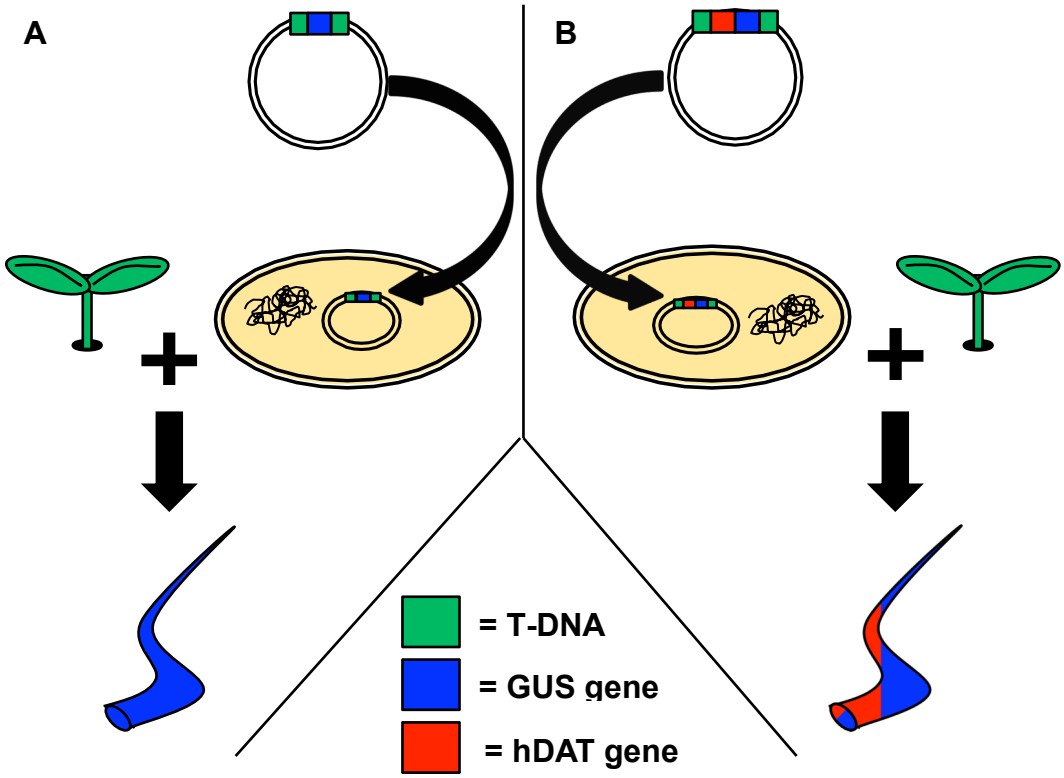

Figure 6.4. Induction of Ctrl- and hDAT-1°HRs. A) An empty binary vector (pCambia1301) was mobilized into *A. rhizogenes* strain AR1000 creating AR1000-C. *L. cardinalis* seedlings were transformed with AR1000-C inducing the formation of Ctrl-1°HRs. B) The binary vector pCambia1301-hDAT, carrying the hDAT expression cassette within the borders of its transfer DNA (T-DNA), was mobilized into *A. rhizogenes* strain AR1000 creating AR1000-hDAT. *L. cardinalis* seedlings were transformed with AR1000-hDAT inducing the formation of hDAT-1°HRs. The GUS reporter gene was present in pCambia1301 and pCambia1301-hDAT enabling the conformation of successful transformation using the GUS histochemical staining assay. T-DNA refers to DNA present in *A. rhizogenes*' root inducing plasmid that is transferred and integrated into the plant genome, which also encodes genes responsible for the induction of hairy roots. A hairy root arises from a single transformed plant cell and consists of cells that are clonal in nature, each expressing the gene/s present within the T-DNA borders.

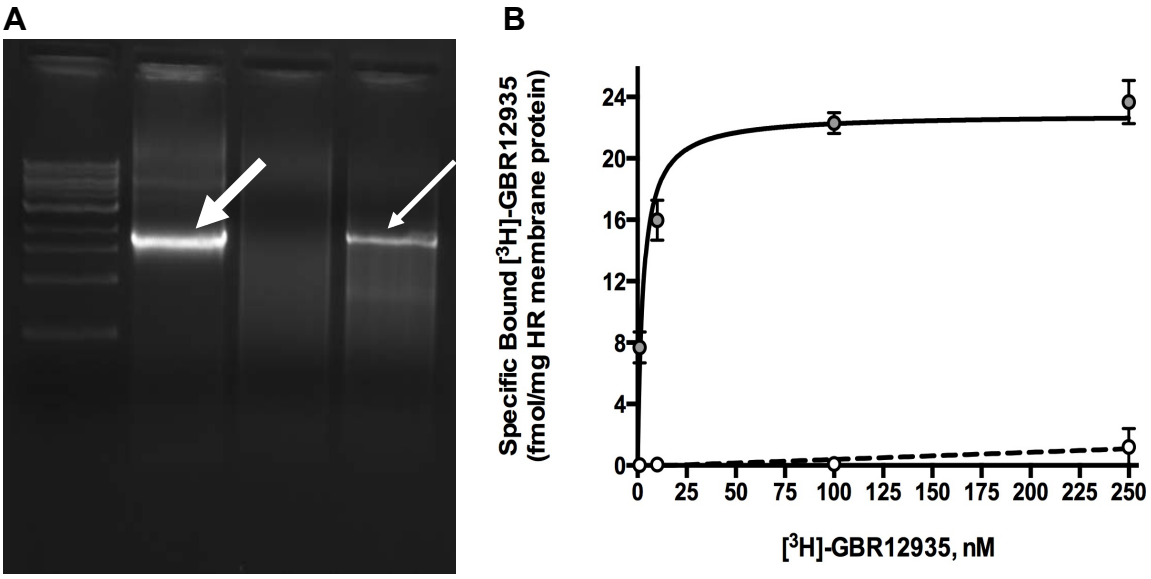

Figure 6.5. Detection of cDNA encoding the hDAT and the hDAT protein in *L. cardinalis* hDAT-1°HRs. A) DNA samples PCR amplified with hDAT specific primers (Lane 1 – ladder; Lane 2 – pCambia1301-hDAT; Lane 3 – sample from Ctrl-1°HRs; Lane 4 – sample from hDAT-1°HRs). A 1.8-kb band representing the full-length cDNA encoding the hDAT is clearly visible in samples from hDAT-1°HRs (small arrow; Lane 4) and pCambia1301-hDAT (large arrow; Lane 2), but is absent in the sample from Ctrl-1°HRs (Lane 3). B) Radioligand binding was performed in Ctrl- and hDAT-1°HRs (dashed line with open circle markers and solid line with gray circle markers, respectively) with the highly selective DAT ligand [^{3}H]-GBR12935. In hDAT-1°HR membranes, specific binding was saturable (K_d = 2.773 ± 0.7304 nM, B_{max} = 22.87 ± 0.9704 fmol/mg tissue) and displayed excellent fit to a one-site binding model (r^2 = 0.8956). In Ctrl-1°HR membranes, only a non-specific increase in binding was observed.

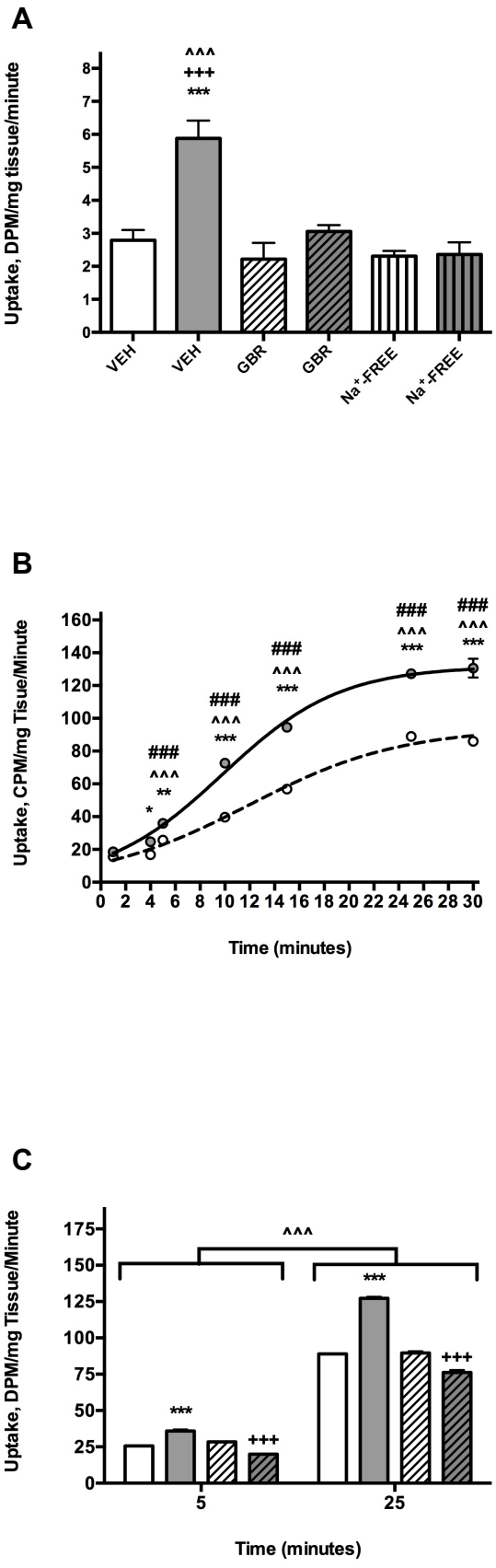

Figure 6.6. [^{3}H]-DA uptake in *L. cardinalis* 1°HRs. A) [^{3}H]-DA uptake performed at a single time point in Ctrl- (white fill) and hDAT-1°HRs (gray fill). [^{3}H]-DA uptake in vehicle (VEH) pretreated hDAT-1°HRs was significantly greater than that in VEH pretreated Ctrl-1°HRs. GBR12909 (GBR) pretreatment and Na^+-free conditions significantly reduced uptake in hDAT-1°HRs. GBR pretreatment and Na^+-free conditions did not affect uptake in Ctrl-1°HRs. *** $p < 0.001$ vs. VEH treated Ctrl-1°HRs, +++ $p < 0.001$ vs. GBR pretreated hDAT-1°HRs, $p < 0.001$ vs. hDAT-1°HRs under Na^+-free conditions; One-way ANOVA, Tukey's post-hoc test. B) Time course of [^{3}H]-DA uptake in Ctrl- (dashed line) and hDAT-1°HRs (solid line). [^{3}H]-DA uptake was significantly greater in hDAT-1°HRs, as compared to Ctrl-1°HRs by 4 minutes. [^{3}H]-DA uptake in Ctrl- and hDAT-1°HRs was significantly greater than that observed within the same group at 1 minute, and thereafter. * $p < 0.05$, ** $p < 0.01$, *** $p < 0.001$ vs. Ctrl-1°HRs; Two-way ANOVA, Bonferroni's post-hoc test. ^^^ $p < 0.001$ vs. Ctrl-1°HRs at 1 minute, ### $p < 0.001$ vs. hDAT-1°HRs at 1 minute; One-way ANOVA, Dunnett's post-hoc test. C) [^{3}H]-DA uptake Ctrl- and hDAT-1°HRs at 5- and 25 minutes pretreated with VEH (no lines) or GBR (diagonal lines). [^{3}H]-DA uptake in hDAT-1°HRs was significantly greater than that observed in Ctrl-1°HRs, and was significantly reduced by GBR pretreatment. [^{3}H]-DA uptake in all treatment groups at 25-minutes was significantly greater than that observed at 5-minutes in corresponding treatment groups. *** $p < 0.001$ vs. Ctrl-1°HRs, +++ $p < 0.001$ vs. GBR, ^^^ $p < 0.001$ vs. corresponding group; Two-way ANOVA, Bonferroni's post-hoc test. n = 3.

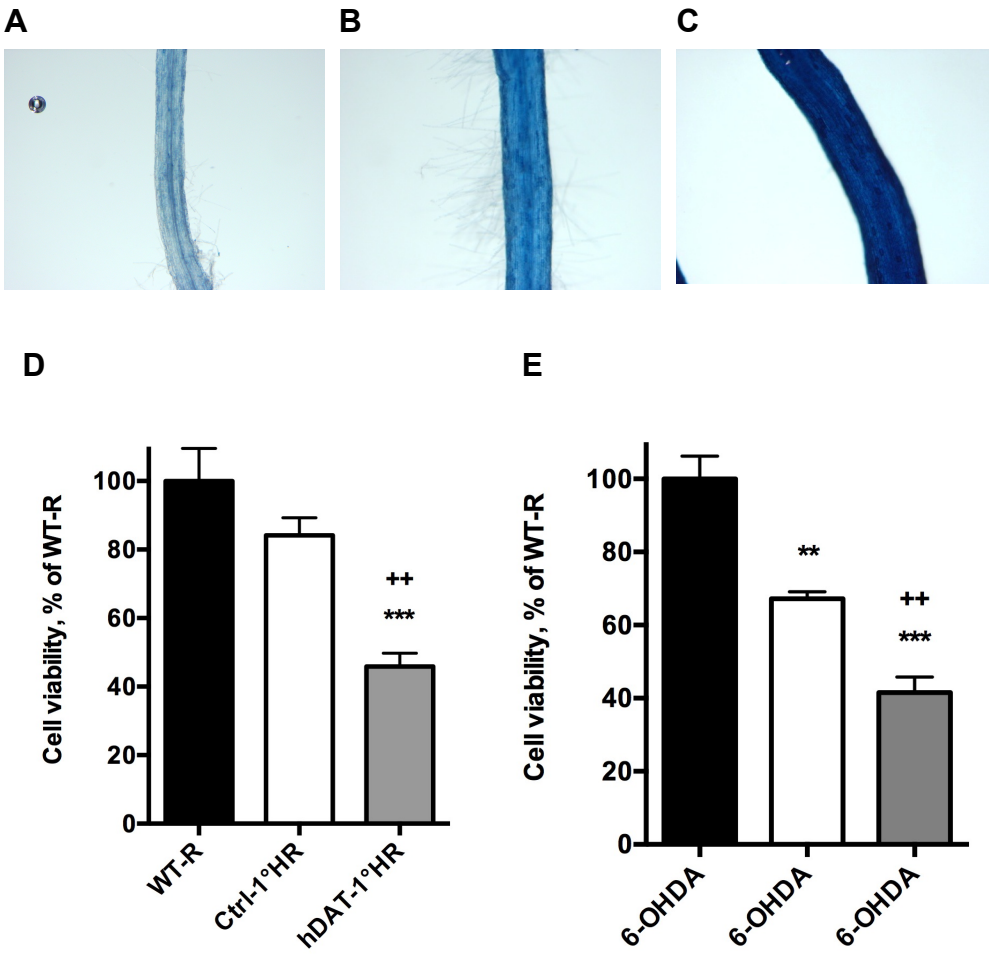

Figure 6.7. MPTP- and 6-OHDA-induced cytotoxicity in *L. cardinalis* roots. Representative images of MPTP treated A) WT-Rs, B) Ctrl-, and C) hDAT-1°HRs stained with trypan blue. D) MPTP significantly reduced cell viability in hDAT-1°HRs, but not Ctrl-1°HRs, as compared to WT-Rs. MPTP significantly reduced cell viability in hDAT-1°HRs, as compared to Ctrl-1°HRs. D) 6-OHDA significantly reduced cell viability in Ctrl- and hDAT-1°HRs, as compared to WT-Rs. Cell viability was significantly reduced by 6-OHDA in hDAT-1°HRs, as compared to Ctrl-1°HRs. ** $p < 0.01$, *** $p < 0.001$ vs. WT-Rs; ++ $p < 0.01$ vs. Ctrl-°HRs; One-way ANOVA, Tukey's post-hoc test. n = 5.

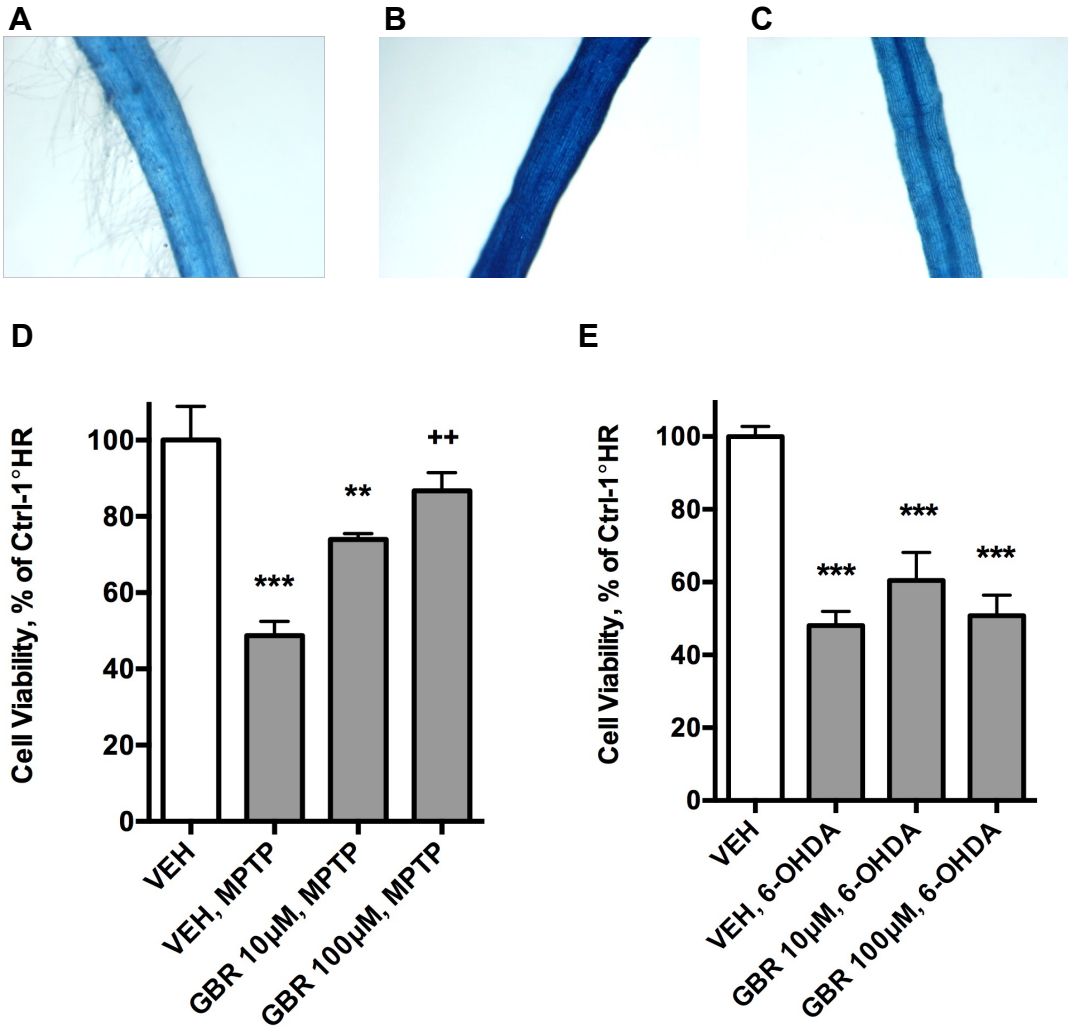

Figure 6.8. GBR-12909 dose-dependently attenuates toxicity caused by MPTP, but not 6-OHDA, in *L. cardinalis* hDAT-1°HRs. A – C) Representative images of vehicle treated Ctrl-1HRs (A), and hDAT-1°HRs pretreated with vehicle (B), or 100 μM GBR12909 (C) prior to being exposed to MPTP, then stained with trypan blue. D) MPTP significantly reduced cell viability in vehicle pretreated hDAT-1°HRs (gray fill) and hDAT-1°HRs pretreated with 10 μM GBR 12909, as compared to vehicle treated Ctrl-1°HRs. Cell viability in hDAT-1°HRs pretreated with GBR12909 prior to MPTP exposure was not significantly different than that of vehicle treated Ctrl-1°HRs. Cell viability measured after exposure to MPTP was significantly increased hDAT-1°HRs pretreated with 100 μM GBR12909, as compared to vehicle pretreated hDAT-1°HRs. E) 6-OHDA significantly reduced cell viability in all hDAT-1°HR treatment groups, as compared to vehicle treated Ctrl-1°HRs, and GBR12909 failed to attenuate toxicity caused by 6-OHDA in hDAT-1°HRs. ** $p < 0.01$, *** $p < 0.001$ vs. vehicle treated Ctrl-1°HRs; ++ $p < 0.01$ vs. MPTP treated hDAT-1°HRs following pretreatment with vehicle. One-way ANOVA, Tukey's post-hoc test. n = 5.

Chapter 7

Sequential hairy root transformation (proof-of-concept): induction of gain-of-function hairy roots, initial pharmacological, and chemical assessments

7.1. Introduction

The hDAT was functionally expressed in transgenic *L. cardinalis* hDAT-1°HRs via *A. rhizogenes*-mediated genetic transformation. Expression of the transporter in hDAT-1°HRs increased their susceptibility to the selective DAergic neurotoxin MPTP. Given DAT inhibition attenuated MPTP-induced cytotoxicity in hDAT-1°HRs, gain-of-function mutations which increase biosynthesis of lobinaline and/or "novel" DAT inhibitor should confer resistance to MPTP. However, intact transgenic plants are traditionally regenerated from hairy roots prior to further genomic modification. Regeneration can be particularly time consuming in plants species, such as *L. cardinalis*, for which a standardized regeneration protocol has not been developed. In order to circumvent the need for regeneration, a novel method to induce hairy roots directly from hairy root explants was developed, referred to as sequential hairy root transformation. Subsequently, hDAT-1°HR explants were sequentially transformed with AR1000-ATM harboring the activation tagging vector pPCVICE4hpt, inducing the formation of gain-of-function transgenic hairy roots expressing the hDAT [16, 19, 221]. One population of ATMhDAT-2°HRs was generated under selection on medium containing MPP^+, such that only individuals having beneficial gain-of-function mutations engendering MPP^+-resistance should survive. The resultant population of TR-2°HRs was enriched with mutants with mutants overproducing lobinaline and/or putatively "novel" inhibitors of the hDAT. Additionally, TR-2°HRs were identified which survived selection via mechanisms other than DAT inhibition.

7.2. Sequential Transformation of L. cardinalis hairy roots: secondary hairy root induction

In the present study, a novel method was developed to accelerate the generation of gain-of-function transgenic hairy roots expressing the hDAT. Essentially, hairy roots are induced directly from hairy root explants, herein referred to as sequential transformation, leading the induction of 2°HRs. The proof-of-application was demonstrated using AR1000-C and AR1000-GFP. *L. cardinalis* hypocotyl explants were transformed with AR1000-C, and the resultant Ctrl-1°HRs that tested positive for GUS reporter gene expression were transformed with AR1000-GFP. In **Figure 7.1 A**, 2°HRs can be seen emerging from a transformed Ctrl-1°HR explants. As shown in **Figure 7.1**, 2°HRs expressing GFP (**Figure 7.1 B**) and the GUS reporter gene (**Figure 7.1 D**), via integration of T-DNA from AR1000-C and AR1000-GFP, respectively, were successfully obtained. On average, ~25 2°HRs were obtained from each Ctrl-1°HR explant with a transformation frequency of ~32% (12 out of 37 tested positive for both reporter genes). In theory, the process could be repeated to induce successive hairy root "generations", thus generating secondary, tertiary, quaternary, etc. hairy roots. To the best of our knowledge, this is the first report of sequential hairy root transformation.

7.3. Generation of secondary gain-of-function transgenic hairy roots expressing the hDAT

Explants from hDAT-1°HRs were transformed with AR1000-ATM. Nodules signifying the initiation of developing secondary gain-of-function transgenic hairy roots expressing the hDAT (ATMhDAT-2°HRs) became visible on transformed explants within ~2 weeks. Explants were then placed on selection medium containing MPP^+ (final concentration, 100 μM). Nodules were allowed to initiate before placing explants on selection medium to allow adequate time for

alterations in gene expression, resulting from the integration of the CaMV 35S enhancer tetramer, to manifest at the cellular level prior to selection. Therefore, only nodules representing developing ATMhDAT-2°HRs with beneficial gain-of-function mutations conferring MPP^+-resistance were able to survive, differentiate, and form mature hairy roots (**Figure 7.2**, schematic of selection process and predicted mechanism/s underlying MPP^+-resistance). Explants from hDAT-1°HRs transformed with AR1000-ATM and emerging activation tagged 2°HRs on medium lacking or containing MPP+, as well as TR-2°HRs emerging from hDAT-1°HR explants, are depicted in **Figure 7.3 A – C**. ATMhDAT-2°HRs resistant to MPP^+ (MRGFhDAT-2°HRs) were maintained on selection medium for 4 months to ensure genotype/phenotypes stability. A total of ~1500 hDAT-1°HR explants were transformed with AR1000-ATM, which should theoretically yield ~12,000 activation tagged 2°HRs. However, only 120 TR-2°HRs were obtained, equating to a survival rate of 1.0% in the presence of MPP^+. After maintaining TR-2°HRs on selection medium for ≥ 4 months, TR-2°HRs were transferred to growth medium lacking MPP^+. Only tissue from TR-2°HRs that had been removed from selection medium for ≥ 2 months was used to prepare methanolic (MeOH) extracts. Of note, 11 TR-2°HRs failed to survive after being removed from medium containing MPP^+, and were not included in pharmacological or chemical analyses as they did not pass the 2 month "washout" period. MPP^+ could detected in MeOH extracts prepared from TR-2°HR tissue collected up to 6 weeks after removal from selection medium. Thus, the 2-month "washout" period was essential to avoid confounds arising from the presence of MPP^+ in TR-2°HR extracts. A second population of ATMhDAT-2°HRs was generated (n = 72), but was not selected on medium containing MPP^+.

7.4. Pharmacological analysis of hairy root MeOH extracts: evaluation of DAT inhibition in vitro

In vitro [^{3}H]-DA uptake studies in rat striatal synaptosomes were performed to measure the DAT inhibitory activity of hairy root extracts. Four

populations were examined: 1) Ctrl-1°HRs (n = 68), 2) hDAT-1°HRs (n = 77), 3) ATMhDAT-2°HRs (n = 72), and 4) TR-2°HRs (n = 109). The DAT inhibitory activity of each hairy root extract was expressed as lobinaline equivalents, extrapolated from lobinaline's DAT inhibition dose-response curve. The DAT inhibitory activity of each population were (summarized in **Table 7.1**; n, mean, S.E.M., min., and max.) as follows (mean ± S.E.M): Ctrl-1°HRs, 2.9 ± 0.3 µg/ml; hDAT-1°HRs, 2.3 ± 0.2 µg/ml; ATMhDAT-2°HRs, 3.6 ± 0.3 µg/ml; TR-2°HRs 2,632 ± 791 µg/ml. The mean DAT inhibitory activity of the Ctrl-1°HR, hDAT-1°HR, and ATMhDAT-2°HR populations were not significantly different. However, the mean DAT inhibitory activity of the TR-2°HR population was significantly greater than that of Ctrl-1°HR, hDAT-1°HR, and ATM-hDAT-2°HR populations ($p = 0.0024$, $p = 0.0015$, and $p = 0.0019$, respectively). Additionally, the frequency of "highly active DAT inhibitors" in the TR-2°HR population (64.2%) was significantly greater ($p < 0.001$) than that of the ATMhDAT-2°HR population (12.5%). Frequency distributions of each population are depicted in **Figure 7.4**. These data indicate that hDAT expression does not increase DAT inhibitory activity of hairy root extracts. Although ATM alone was capable of generating mutants with increased inhibitory activity at the DAT (max. = 11.9 µg/ml), the frequency at which such mutants were generated was not sufficient to significantly increase the mean DAT inhibitory activity of the ATMhDAT-2°HR population. As predicted, the TR-2°HR population displayed a significant increase in the frequency of mutants with increased inhibitory activity at the DAT, thereby significantly increasing the mean DAT inhibition of the population. Furthermore, TR-2°HR cultures were obtained which displayed a remarkable increase in DAT inhibitory activity, exceeding that which could be expressed as lobinaline equivalents. Therefore, the activity of 10 TR-2°HRs was expressed as the maximum amount of lobinaline equivalents which could be extrapolated from lobinaline's DAT inhibition dose-response curve (i.e. 28,496 µg/ml). A single TR-2°HR mutant's extract did not produce DAT inhibition of sufficient magnitude, and was expressed as the minimum amount of lobinaline equivalents that could be extrapolated from lobinaline's DAT inhibition dose-response curve (i.e. 1.2×10^{-4}

μg/ml). DAT inhibitory activity of extracts from individuals of all other populations could be expressed as lobinaline equivalents. These observations indicate that target-directed biosynthesis is a feasible approach to optimize a plant's pharmacological activity at a specific molecular target.

7.5. GC-MS analysis of hairy root extracts

Hairy root MeOH extracts were analyzed via GC-MS to quantify lobinaline content and to acquire a chromatographic "fingerprint" of the metabolite profile of each hairy root. The lobinaline content of each population are as follows: 1) Ctrl-1°HRs, 41.3 ± 1.9 μg/mL; hDAT-1°HRs, 38.3 ± 1.8 μg/mL; ATMhDAT-2°HRs, 56.5 ± 1.8 μg/mL; TR-2°HRs 59.2 ± 2.5 μg/mL (summarized in **Table 7.2**; n, mean, S.E.M, min., and max.). The mean lobinaline content of the Ctrl- and hDAT-1°HR populations was not significantly different. In contrast, the mean lobinaline content of ATMhDAT- and TR-2°HR populations was significantly greater than that of the Ctrl- ($p < 0.001$ and $p < 0.001$, respectively) and hDAT-1°HR ($p < 0.001$ and $p < 0.001$, respectively) populations. Although the mean lobinaline content of ATMhDAT- and TR-2°HR populations were not significantly different, the frequency of "lobinaline overproducers" in the TR-2°HR population (33.9%) was significantly greater ($p = 0.0267$) than that of the ATMhDAT-2°HR population (18.1%). Frequency distributions of each population are depicted in **Figure 7.5**. Qualitative analysis of the GC traces acquired from Ctrl- and hDAT-1°HRs revealed an excellence correspondence between the chromatographic peaks present and their relative abundances when comparing traces within and between populations. An overlay of representative GC traces obtained from Ctrl- and hDAT-1°HRs can be seen in **Figure 7.6**. These findings indicate that hDAT expression does not significantly increase lobinaline biosynthesis. Greater variation was observed in GC traces acquired from ATMhDAT- and TR-2°HRs with regards to the chromatographic peaks present (*see below*) and their relative abundances. The use of ATM alone did generate ATMhDAT-2°HRs with a marked increased in lobinaline content (max. = 92.9 μg/ml), however the

frequency at which such mutants were generated was insufficient to significantly increase the mean of the population. As predicted, the frequency of “lobinaline overproducers” was significantly increased in the TR-2°HR population, thus leading to a significant increase in the mean lobinaline content of the population. The lobinaline content of 14 TR-2°HRs was greater than the maximum of the ATMhDAT-2°HR population. The frequency of “lobinaline overproducers” and the maximum increase in lobinaline biosynthesis (max. = 117.0 µg/ml) was greater in the TR-2°HR population, owing to the use of selection favoring mutants of interest. These observations indicate that target-directed biosynthesis is a feasible approach to genetically optimize medicinal plants to increase yields of therapeutically valuable, structurally complex bioactive plant metabolites.

7.6. Discussion

Agrobacterium-mediated ATM creates stable gain-of-function mutations in plant cells via integration of an enhancer tetramer into the plant genome, activating genes 10-kb upstream and downstream of the integration site [14, 18]. Activation tagging has previously been demonstrated as a means to increase the yields of bioactive plant metabolites and/or cause synthesis of putatively “novel” metabolites with similar bioactivity [14, 15]. However, the use of ATM requires the generation and maintenance of thousands of mutants to saturate the plant genome, and subsequent preparation and screening of extracts from each culture [14, 15]. As such, ATM alone is inefficient, timely, and laborious if used for the purpose of drug discovery [14, 15]. Target-directed biosynthesis circumvents these limitations by generating gain-of-function mutants under selection conditions favoring the survival of individuals of interest. First, a human target protein is functionally expressed in transgenic plant cells, corresponding to hDAT-1°HRs expressing the hDAT in the current study. Next, gain-of-function mutants functionally expressing the human target protein are generated on selection medium such that survival is dependent upon enhanced activity at the human target protein, described below.

Traditionally, after obtaining transgenic plant cell cultures, intact plants are regenerated and the T3 progeny is obtained to ensure plants are homozygous for the transgene before inducing additional mutations in the transgenic plants. However, the process can problematic when time constraints are an issue, especially if the plant species is difficult to regenerate and/or has a long life cycle. Since there is no standardized regeneration protocol for *L. cardinalis* hairy roots, and the plant takes a minimum of ~3 months to mature and produce seed, a considerable amount of time would have been invested to obtain the T3 progeny. In order to circumvent the need to regenerate and obtain T3 progeny prior to activation tagging, a novel method referred to as sequential hairy root transformation was developed, wherein hairy roots are induced directly from hairy roots. Proof-of-concept was demonstrated by transforming Ctrl-1°HR explants, which expressed the GUS reporter gene, with AR1000-GFP, inducing the formation of GUS/GFP-2°HRs. The GUS/GFP-2°HRs expressed both reporter genes, as confirmed via fluorescence microscopy and GUS histochemical staining, respectively. To the best of our knowledge, this is the first report of sequential hairy root transformation, a feasible approach rapidly obtain transgenic plant cell cultures expressing multiple transgenes. In theory, hairy roots could be sequentially transformed repeatedly, inducing successive hairy root "generations" introducing additional transgenes with each round of transformation. This possibility remains to be explored in future studies.

One goal of the current study was to obtain gain-of-function hairy root cultures with mutations leading to increased inhibitory modulation of the hDAT predicted to arise via increased biosynthesis of lobinaline and/or "novel" DAT inhibitors of greater potency. Activation tagged hDAT-1°HR explants were placed on selection medium containing the cytotoxic DAT substrate MPP^+ once nodules representing the initiation of ATMhDAT-2°HRs became visible [89, 90]. As such, only nodules representing ATMhDAT-2°HRs with beneficial gain-of-function mutations conferring resistance to MPP^+ should survive selection. Given GBR12909 prevented toxicity caused by MPTP in hDAT-1°RHs, gain-of-function mutations that increase inhibitory activity at the hDAT should confer resistance to

the toxin. MPP^+ was utilized as a selection agent, rather than its precursor MPTP, given resistance to the latter could have arisen due to mutations that decreased MPTP oxidation. Monoamine oxidase inhibitors and DAT inhibitors attenuate MPTP-induced cytotoxicity, whereas the former do not reduce toxicity caused by MPP^+ [89, 90, 124]. Thus, selection on medium containing MPP^+ should theoretically engender greater selectivity for mutations that enhance inhibitory activity at the hDAT. However, MPP^+-resistance could potentially arise via other mechanisms. The selective DAergic neurotoxin MPP^+, which is used to model PD, is generally accepted to cause neurotoxicity as follows: 1) MPP^+ is transported to the cell interior by the DAT, 2) MPP^+ inhibits complex-I of the electron transport chain, 3) mitochondrial dysfunction leads to depletion of ATP and excessive free radical production, and 4) resultant caspase activation leads to initiation of apoptotic signaling, ultimately culminating in cell death [92]. Gain-of-function mutations that directly and/or indirectly interfere with any of the aforementioned steps preceding cell death should confer resistance to MPP^+, given pharmacological agents acting at any of these stages attenuate toxicity caused by MPP^+ in mammalian cells [89, 90, 92, 107-126].

Indeed, 109 TR-2°HRs were obtained which expressed the hDAT, yet were MPP^+-resistant. In order to obtain this quantity of TR-2°HRs, ~1500 hDAT-1°HR explants were activation tagged, which should have theoretically produced ~12,000 ATMhDAT-2°HRs, equating to a survival rate of 1.0%. Three other populations of *L. cardinalis* hairy roots were generated: Ctrl-1°HRs, hDAT-1°HRs, and ATMhDAT-2°HRs. Extracts prepared from every individual of each population were evaluated for their ability to inhibit DAT-mediated [^{3}H]-DA uptake in rat striatal synaptosomes. Additionally, extracts were subject to GC-MS analysis to quantify their lobinaline content, examine GC traces for the present of "novel" chromatographic peaks undetectable in controls, and to identify peaks present in controls that may have been up-regulated in other experimental groups, as described below.

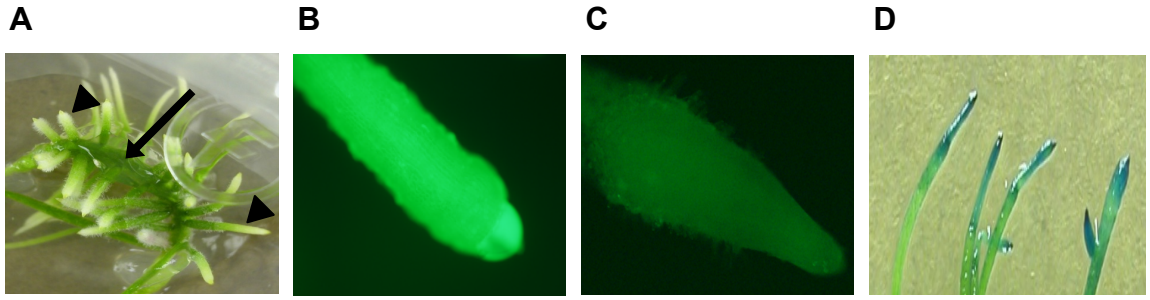

Figure 7.1. Sequential hairy root transformation in *L. cardinalis*. A) GUS/GFP-2°HRs (arrowheads) emerging from a Ctrl-1°HR explant (arrow) transformed with AR1000-GFP. B) GFP expression in a GUS/GFP-2°HR. C) Background observed in Ctrl-1°HRs. D) GUS/GFP-2°HRs that tested positive for GFP expression, which express the GUS reporter gene, as indicated by the formation of blue precipitate.

1st	Express the hDAT in plant cells	Allow selection of cells based on activity at the hDAT
2nd	Activation tagging mutagenesis	Create a heterogeneous population of gain-of-function mutants
3rd	Selection on medium containing MPP+	Survival of mutants of interest

Predicted Outcome: A) Survival of mutants that "overproduce" inhibitors of DAT or B) molecules that interfere with toxins intracellular mechanisms of cell death

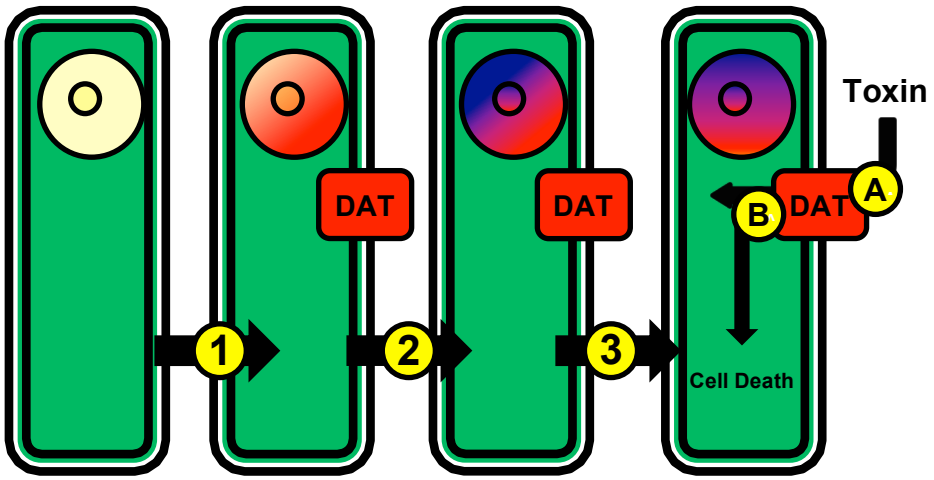

Figure 7.2. Schematic of the selection process and mechanisms predicted to confer resistance to MPP^+.

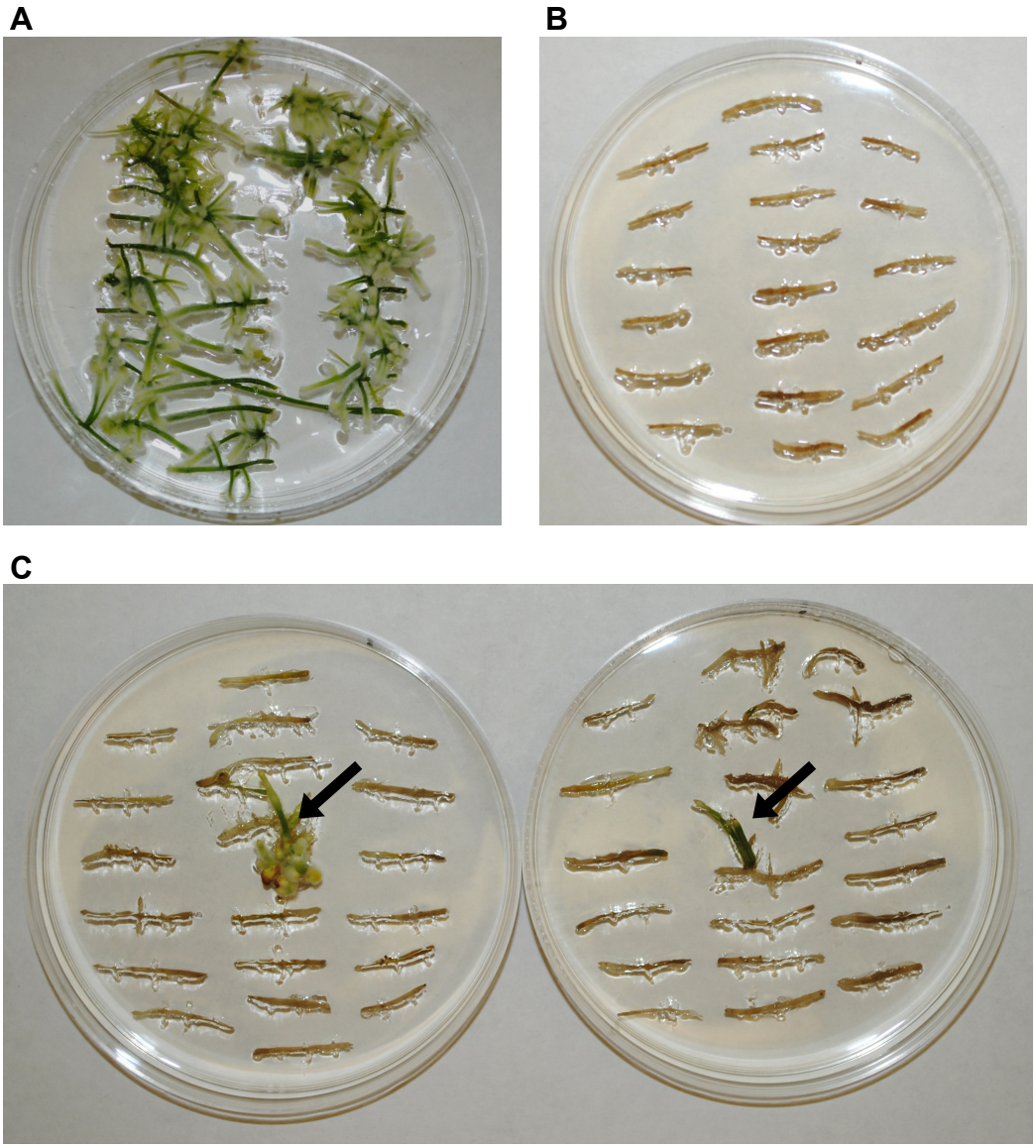

Figure 7.3. Activation tagged hDAT-1°HR explants and emerging activation tagged 2°HRs on medium containing and lacking MPP^+. A) On medium lacking MPP^+, hDAT-1°HR explants and ATMhDAT-2°HRs thrive. B) On selection medium containing MPP^+, all hDAT-1°HR explants, and the vast majority of activation tagged 2°HRs, fail to survive. C) If sufficient quantities of hDAT-1°HR explants are activation tagged and placed on selection medium containing MPP^+, TR-2°HRs that express the hDAT, yet are resistant to MPP^+ (indicated by arrows), can be obtained. However, hDAT-1HR explants never survived selection.

Table 7.1.
DAT inhibitory activity of hairy root populations*

Population	n	Mean	S.E.M.	Min.	Max.
Ctrl-1°HRs	68	2.9	0.3	0.2	10.7
hDAT-1°HRs	77	2.3	0.2	1.1×10^{-2}	9.0
ATMhDAT-2°HRs	72	3.6	0.3	0.3	11.9
TR-2°HRs	109	2,632	791	1.2×10^{-4}	28496

*DAT inhibitory activity expressed as lobinaline equivalents (µg/ml)

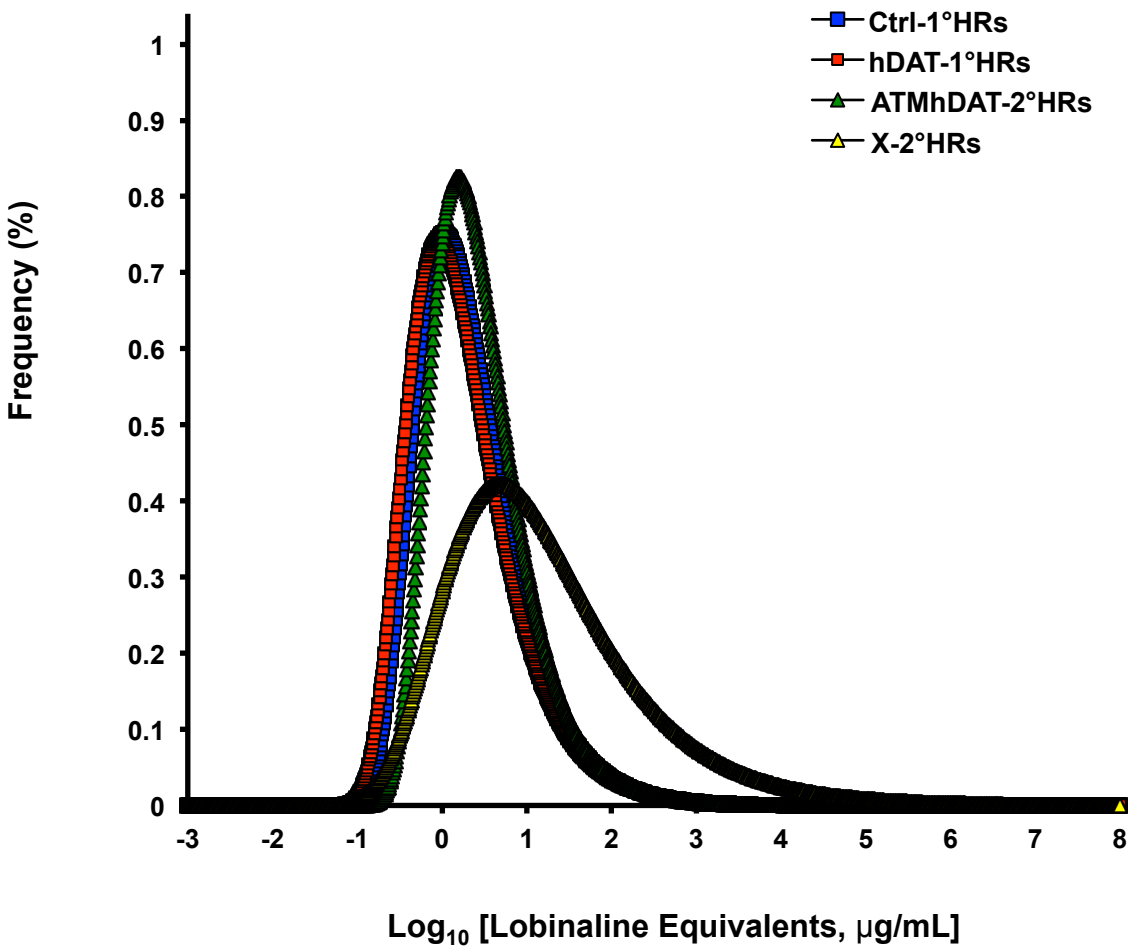

Figure 7.4. Frequency distributions of the hairy root populations' DAT inhibitory activity. As depicted above, Ctrl-1°HR, hDAT-1°HR, and ATMhDAT-2°HRs frequency distributions were not significantly different. However the frequency of individuals that were "highly active inhibitors of the DAT" was significantly increased in the X-2°HR population.

Table 7.2
Lobinaline content of hairy root populations*

Population	n	Mean	S.E.M	Min.	Max.
Ctrl-1°HRs	68	41.3	1.9	13.7	70.3
hDAT-1°HRs	77	38.3	1.8	11.0	76.8
ATMhDAT-2°HRs	72	56.5	1.8	12.2	92.9
TR-2°HRs	109	59.2	2.4	9.9	117.0

*Lobinaline content expressed as (µg/ml)

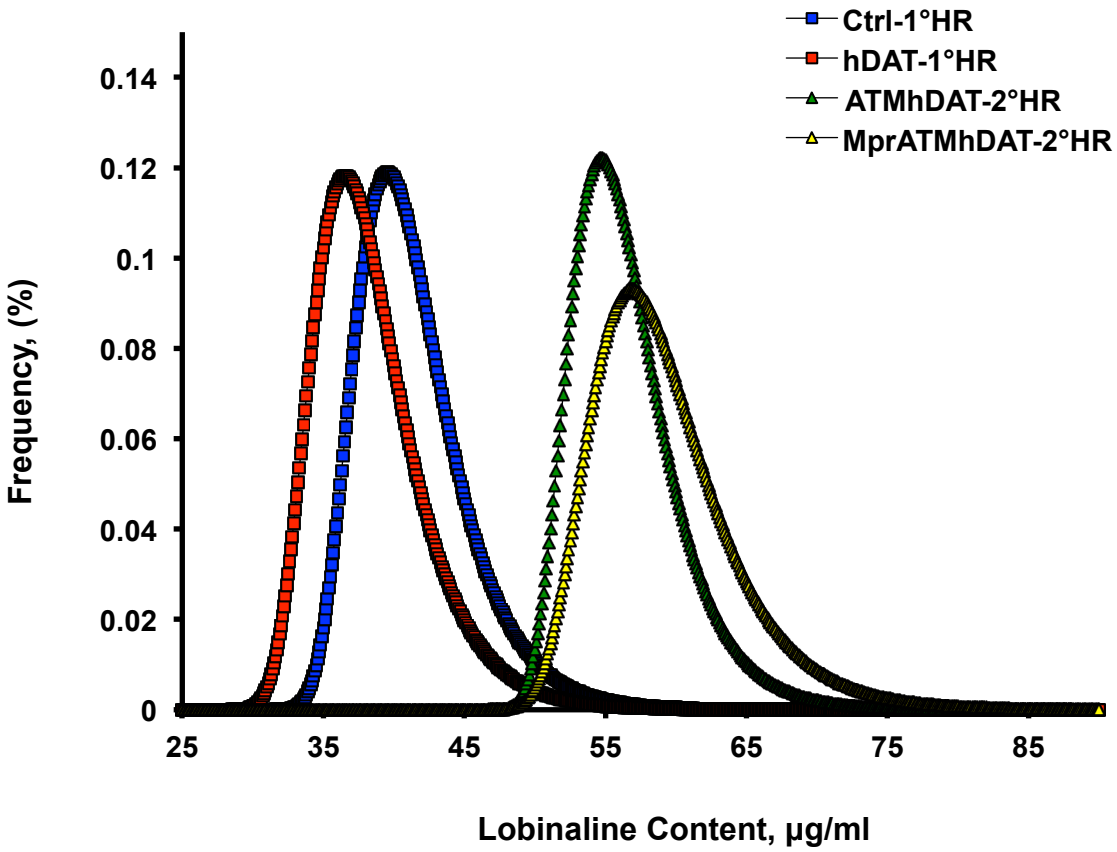

Figure 7.5. Frequency distributions of the hairy root populations' lobinaline content. The frequency of "lobinaline overporducers" in Ctrl- and hDAT-1°HR populations was not significantly different. The frequency of "lobinaline overproducers" present in the ATMhDAT- and X-2°HR populations was significanly greater than that of Ctrl- or hDAT-1°HRs. Additionally , the frequency of "lobinaline overproducers " present in the X-2°HR population was significantly greater than that of the ATMhDAT-2°HR population.

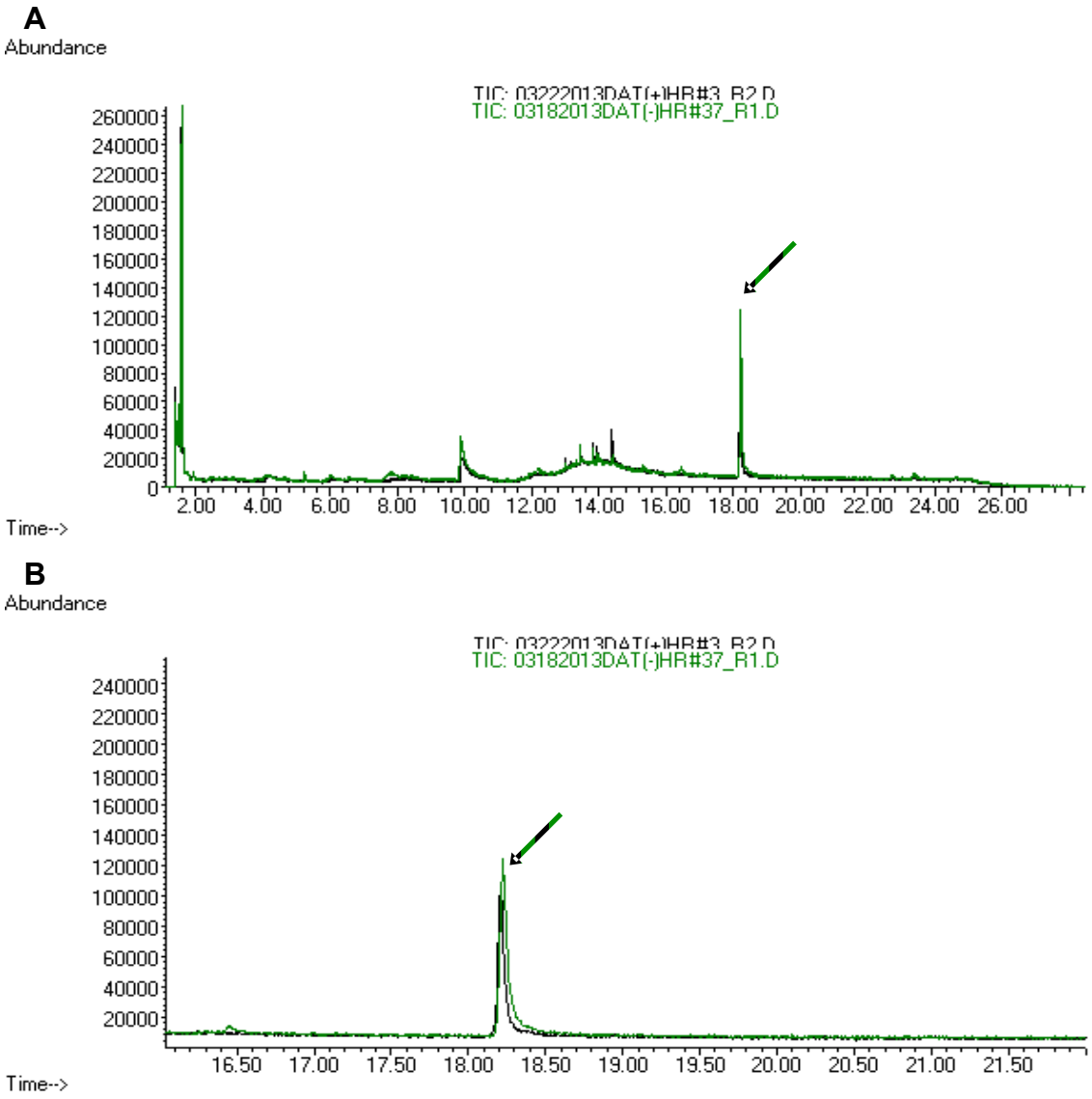

Figure 7.6. Overlay of a representative GC trace from a Ctrl- (green trace) and a hDAT-1°HR (black trace). A) An overlay of a representative GC trace from a Ctrl- and hDAT-1°HR reveals major differences with regards to the chromatographic peaks present and their relative abundances. B) Closer examination reveals no difference in the relative abundance of lobinaline in Ctrl- and hDAT-1°HRs. This was also confirmed quantitatively for Ctrl- and hDAT-1°HR populations. The green and black striped arrow in each of the GC traces indicates the chromatographic peak corresponding to lobinaline.

Chapter 8

Characterization of gain-of-function subpopulations

8.1. Introduction

In previous studies, a population of MPP^+-resistant gain-of-function mutant transgenic secondary hairy roots expressing the human dopamine transporter (TR-2°HRs) was generated. After analyzing extracts from MPP^+-resistant TR-2°HRs for their ability to in inhibit the DAT, and via GC-MS, it became apparent that the TR-2°HR population consisted of multiple "subpopulations", summarized in **Table 8.1**. The selection agent utilized in the present study, MPP^+, is generally accepted to cause cytotoxicity by the following steps: 1) DAT-mediated MPP^+ uptake to the cytosol, 2) mitochondrial dysfunction arising from inhibition of complex-1 by MPP^+, 3) consequential depletion of ATP and excess free radical production, 4) activation of caspases and associated apoptotic signaling cascades, and 5) ensuing cell death [92]. As such, molecules that inhibit the DAT, preserve mitochondrial function, prevent ATP depletion, prevent free radical damage, or prevent activation of caspases attenuate MPP^+-induced cytotoxicity [89, 90, 92, 107-126]. The various "subpopulations" of TR-2°HRs, and their respective mechanisms of MPP^+-resistance, are described in greater detail below.

Table 8.1
TR-2°HR Subpopulations

Number	Mechanism of Resistance	n, (frequency)
1	DAT inhibition	42, (38.5%)
2	Increased biosynthesis of cytoprotective lipids	33, (30.3%)
3	Increased biosynthesis of cytoprotective metabolites	24, (22.0%)
4	Induction of cytoprotective genes	10, (9.2%)

Chapter 9

TR-2°HR Subpopulation-1: increased inhibitor modulation of the hDAT

9.1. Introduction

The DAT transporter is exclusively expressed on DAergic neurons in the CNS, and has been implicated as a "gateway" allowing neurotoxins to access the intracellular compartment of nigrostriatal neurons [43, 50, 52, 95, 97, 98, 220, 222-224]. Upon gaining entry to the interior of DAergic neurons, selective DAergic neurotoxins have been reported to cause cell death by a variety of mechanisms, such as inhibition of mitochondrial function and inducing excessive free radical production [43, 50, 52, 92, 95, 97, 98, 220, 222-224]. Given DAT-mediated uptake plays a pivotal role in the selective vulnerability of DAergic neurons to the neurotoxin MPP^+, it is not surprising that numerous DAT inhibitors have been reported to attenuate MPP^+-induced cytotoxicity *in vitro* and *in vivo* [50, 52, 89, 90, 95, 97, 98, 220, 222-224]. As such, increased inhibition of the hDAT was predicted to be the primary mechanism underlying MPP^+-resistance in in the TR-2°HR population. Pharmacological analysis of TR-2°HRs' methanolic (MeOH) in [^{3}H]-DA uptake studies revealed that DAT inhibition was the primary mechanism underlying MPP^+ resistance in the TR-2°HR population.

9.2. Criteria indicating that MPP^+-resistance was the result of beneficial gain-of-function mutations that increased inhibitory modulation of the DAT

The designation of TR-2°HRs to Subpopulation-1 (mechanism of survival, increased inhibitory modulation of the hDAT) was made based on the following criteria: 1) DAT inhibitory modulation of TR-2°HR extract could not be expressed as lobinaline equivalents and/or 2) the TR-2°HR's extract produced DAT

inhibition greater than three standard deviations above the mean of the ATMhDAT-2°HR population (*see* **Table 9.1**). DAT inhibition produced by the TR-2°HRs' extracts was attributed to a "novel" DAT inhibitor if the extract's activity could not be expressed as lobinaline equivalents.

9.3. TR-2°HR Subpopulation-1: DAT inhibitory activity is attributable to lobinaline and putatively "novel" inhibitors of the DAT

The majority of TR-2°HRs (n = 42, frequency = 38.5%) were resistant to MPP^+ via increased inhibitory modulation of the DAT, and therefore were designated to Subpopulation-1. In Subpopulation-1, 22 TR-2°HRs' extracts exhibited increased DAT inhibition that was attributed to lobinaline, as indicated by a corresponding increase in DAT inhibition and lobinaline content. However, 20 TR-2°HRs in Subpopulation-1 displayed a marked increase in DAT inhibitory activity that was not accompanied by a corresponding increase in lobinaline. In fact, DAT inhibition produced by extracts from 10 TR-2°HRs could not be expressed as lobinaline equivalents. These observations, and the presence of chromatographic peaks in GC traces acquired from the latter TR-2°HRs' extracts, which were absent/undetectable in controls, suggested the extracts contained "novel" metabolites that where presumably highly potent DAT inhibitors.

9.4. Discussion

In the present study, *L. cardinalis* TR-2°HRs expressing the hDAT were generated on medium containing the cytotoxic DAT substrate MPP^+ [89, 90]. As predicted, the presence of beneficial gain-of-function mutations that increased DAT inhibitory activity were the primary explanation for MPP^+-resistance in the TR-2°HR population. The underlying reasons for this were two-fold: 1) *L. cardinalis* has the biosynthetic machinery necessary to synthesize DAT inhibitors and 2) DAT inhibitors are known to ameliorate the cytotoxic effects of MPP^+ *in vitro* and *in vivo* [75, 89, 90, 94, 124]. Increased yields of lobinaline explained

DAT inhibition produced by roughly half (n = 22) of the TR-2°HRs designated to Subpopulation-1. A representative GC trace obtained from an TR-2HR whose DAT inhibitory activity was explained by increased yields of lobinaline is depicted in **Figure 9.1**. However, the quantity of lobinaline present in the remaining TR-2°HRs was not sufficient to account for DAT inhibition produced by their extracts, indicating the presence of putatively "novel" DAT inhibitors of greater potency.

Lobinaline is a complex binitrogenous decahydroquinoline alkaloid present in *L. cardinalis* that inhibits the DAT, activates nicAchRs, and scavenges free radicals (*see* ***Chapter 4***). Considering MPP^+ treatment increases free radical production, which contributes to its cytotoxic effects, lobinaline should attenuate the deleterious effects of the toxin via two mechanisms: 1) preventing uptake of the MPP^+ via inhibition of the hDAT, and 2) scavenging free radicals produced by MPP^+ that may have gained access to the cell interior through hDAT proteins unoccupied by lobinaline. The potential cytoprotective effects of lobinaline in models of neurodegeneration in mammalian cells utilizing MPTP/MPP^+ remain to be explored in future studies.

In Subpopulation-1, roughly half (n = 20) of the TR-2°HRs' extracts inhibitory activity at the DAT was not attributed to lobinaline. In fact, the potency of 10 TR-2°HRs' extracts produced DAT inhibition equivalent to the positive control GBR12909, a highly potent and selective DAT inhibitor [84-88]. DAT inhibition produced by extracts from the aforementioned hairy roots could not be expressed as lobinaline equivalents. Therefore, their activity was expressed as the maximum amount of lobinaline equivalents that could be extrapolated from the lobinaline dose-response curve. GC trace acquired via analysis of TR-2°HRs' extracts for which lobinaline was not responsible for DAT inhibition are depicted in **Figure 9.2** and **Figure 9.3**. These TR-2°HRs represent a "library" of genomically optimized plant cultures whose evolution was redirected to favor biosynthesis of DAT inhibitors meant to interact with the hDAT. This is in contrast to DAT inhibitors that occur naturally in plants, which evolved to target the DAT and/or other monoamine transporters present in organisms other than humans. Given the TR-2°HRs putatively contain "novel" DAT inhibitors that evolved to

interact with the human target protein, leads isolated form the cultures may require less optimization than those found in nature. This is particularly advantageous from a drug discovery perspective, since their extracts known to contain highly potent DAT inhibitors whose structure may require only minor modifications, thus streamlining their discovery and development.

Pharmacological and chemical analysis of extracts from TR-2°HR designated to Subpopulation-1 demonstrated that the technology is a viable option to increase yields of bioactive metabolites present in the wild-type plant. Furthermore, target-directed biosynthesis represents a means to tap a plant's inherent biosynthetic capacity to generate "novel" bioactive metabolites active at a specific human target protein, here the hDAT. If lobinaline proves to be a valuable therapeutic, and/or derivatives of lobinaline prove to be valuable therapeutics, TR-2°HRs which overproduce lobinaline could be used as a production system to obtain bulk quantities of the complex alkaloid. The hairy roots containing novel DAT inhibitors represent a repository of metabolites that could be mined to identify "novel" DAT inhibitors and/or leads for the development of novel DAT inhibitors. Given natural products are often more "druggable" than synthetics, target-directed biosynthesis may prove to be an effective approach to generate leads with greater potential to be successfully developed as therapeutics. It's also advantageous in that leads generated using this system "evolve" in an aqueous environment, akin to that of human cells. This is in contrast to synthetics, which "evolve" in organic solution, which may partly contribute to lower druggability of the synthetic molecules.

Table 9.1
DAT inhibitory modulation of the ATMhDAT-2°HR population*

Mean	Standard Deviation (S.D.)	Mean + 3x S.D.
3.6	2.5	11.3

*DAT inhibition expressed as lobinaline equivalents (µg/ml)

A

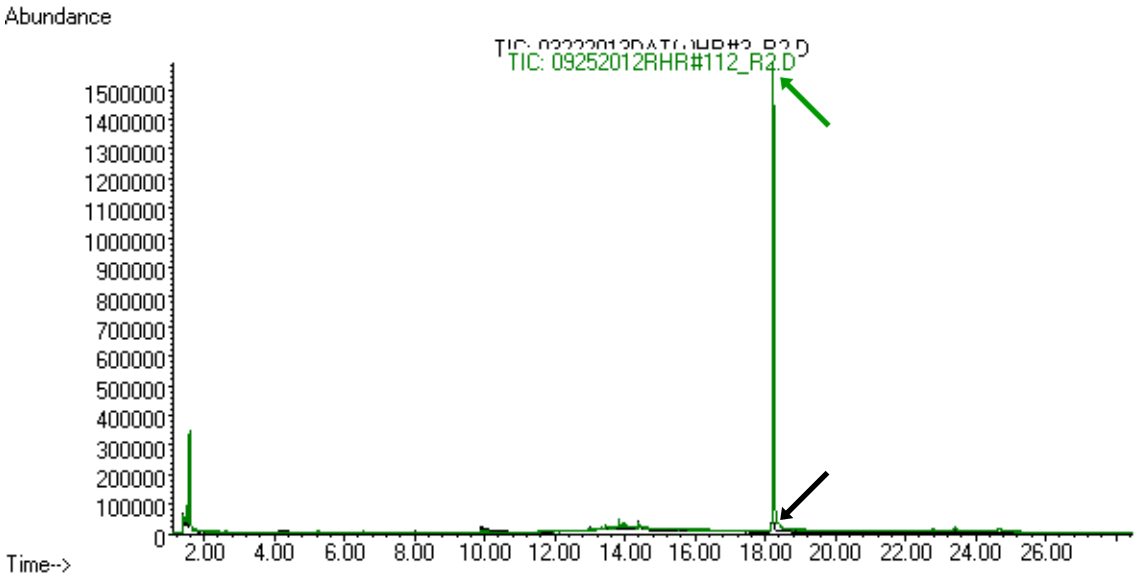

B

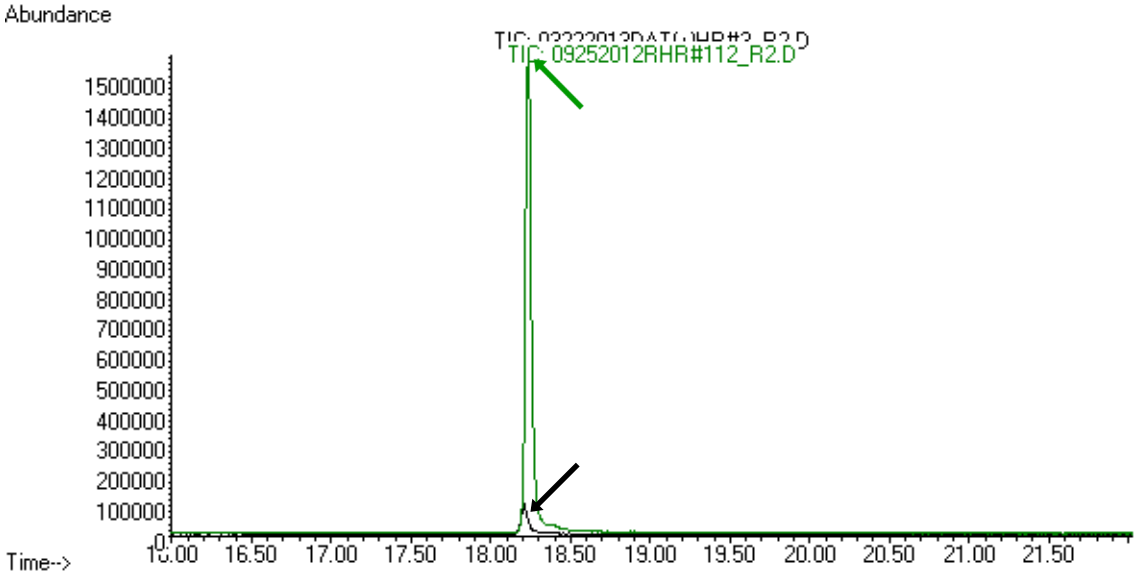

Figure 9.1. Overlay of a representative GC trace from a hDAT-1°HR (black trace) and a TR-2°HR (green trace) overproducing lobinaline. A) An overlay of a representative GC trace from a hDAT-1°HR and a TR-2°HR with increased yields of lobinaline clearly shows a marked increase in the latter, as compared the former. B) A closer examination demonstrates the pronounced increase in lobinaline content in the TR-2°HR, as compared to a representative hDAT-1°HR. The black and green arrows indicate the chromatographic peak corresponding to lobinaline in the GC traces from a hDAT-1°HR and a TR-2°HR, respectively.

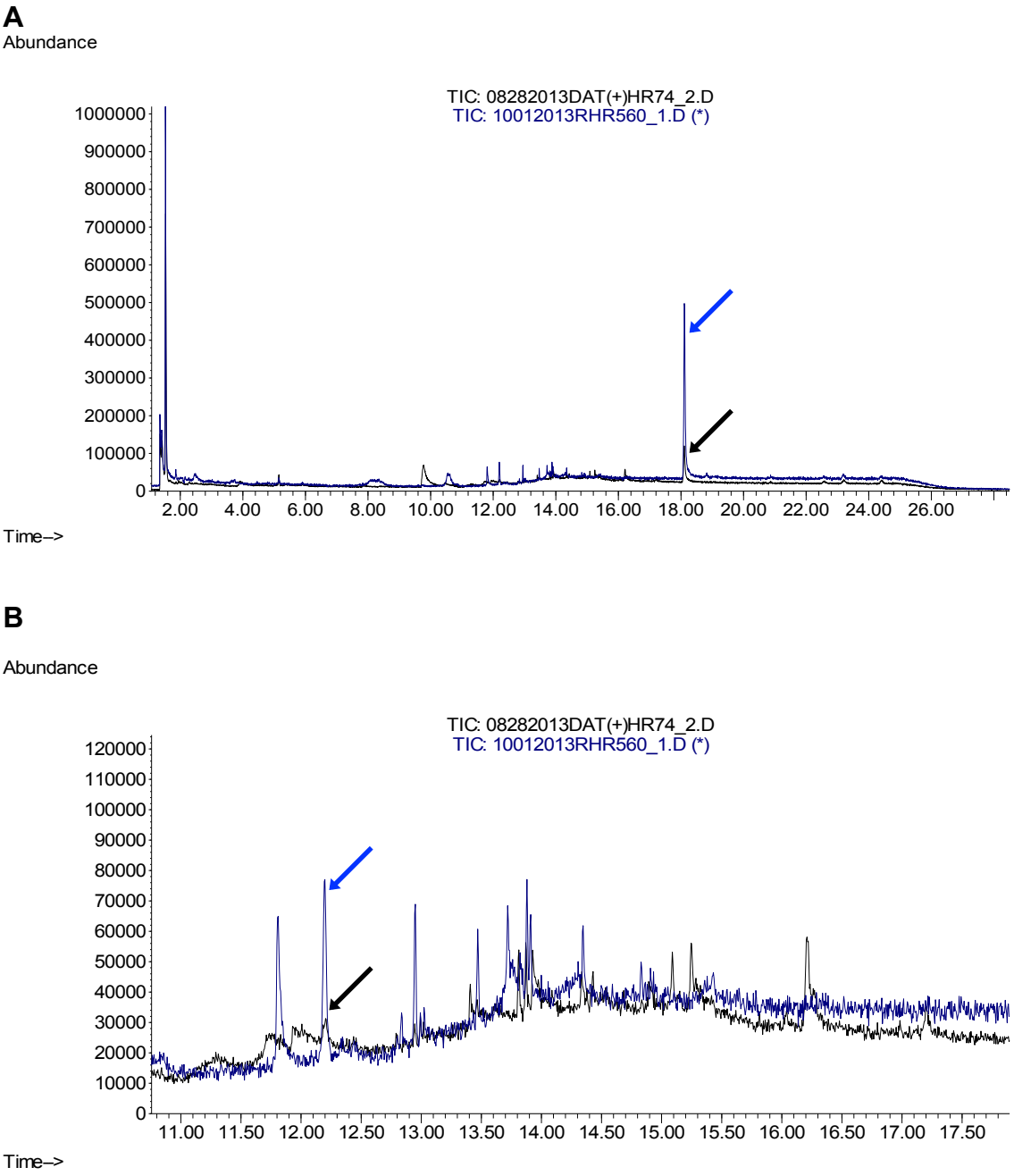

Figure 9.2. Overlay of GC traces from a representative hDAT-1°HRs (black trace) and a TR-2°HR with increased yields of a putatively "novel" DAT inhibitor (blue trace). A) An overlay of a representative GC trace from a hDAT-1°HR and a TR-2°HR with increased yields of a putatively "novel" DAT inhibitor demonstrates a marked increase in the latter (blue arrow), as compared the former (black arrow). B) A closer examination demonstrates the pronounced increase in the TR-2°HR, as compared to a representative hDAT-1°HR.

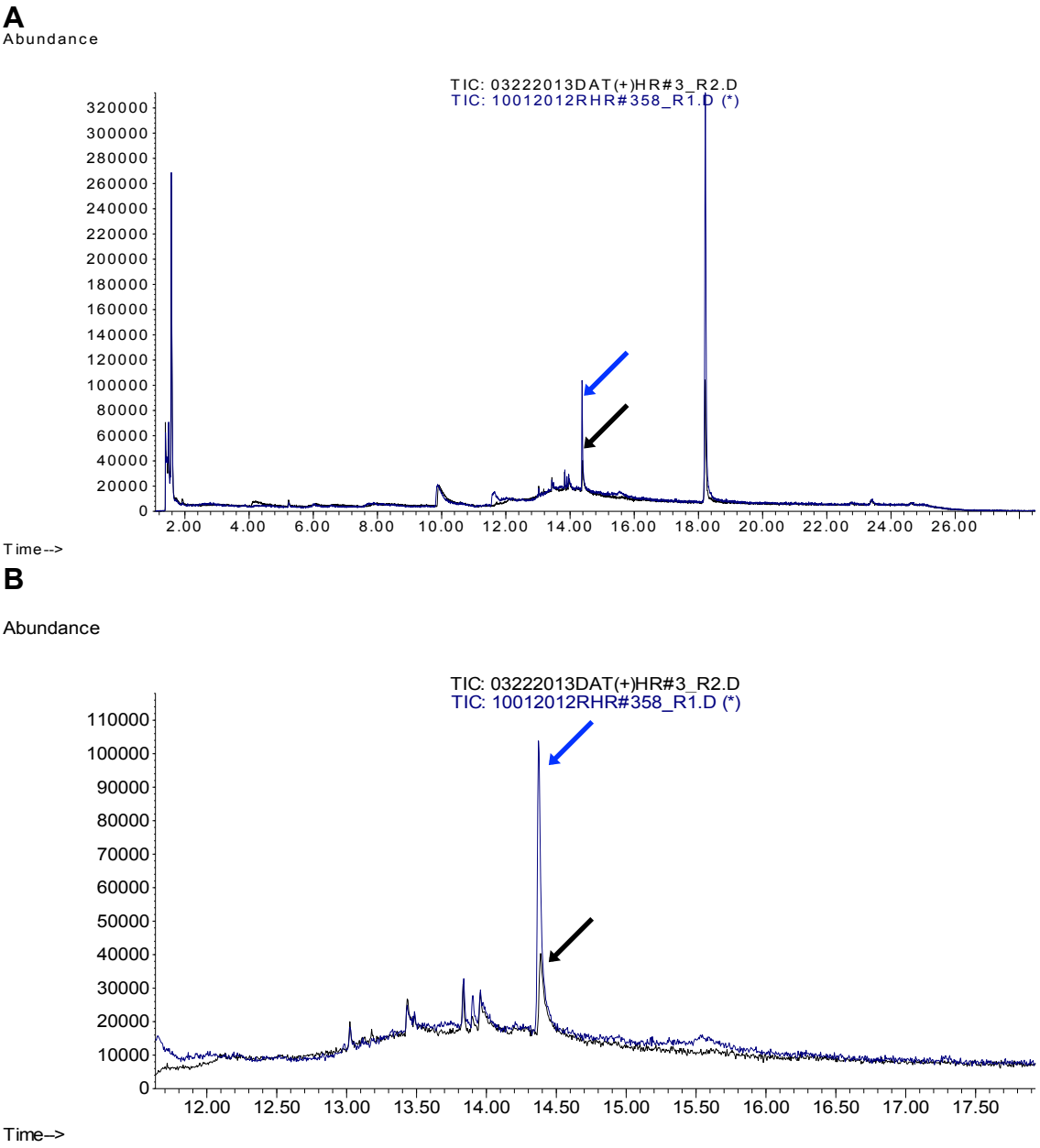

Figure 9.3. Overlay of GC traces from a representative hDAT-1°HRs and a TR-2°HR with increased yields of a putatively "novel" DAT inhibitor. A) An overlay of a representative GC trace from a hDAT-1°HR and a TR-2°HR with increased yields of a putatively "novel" DAT inhibitor demonstrates a marked increase in the latter (green arrow), as compared the former (black arrow). B) A closer examination demonstrates the pronounced increase in the TR-2°HR, as compared to a representative hDAT-1°HR.

Chapter 10

Subpopulation-2: Increased biosynthesis of cytoprotective lipids

10.1. Introduction

Lipids are hydrophobic molecules that serve diverse physiological functions in eukaryotic cells [225]. For example, lipids are the primary structural components of cellular membranes, serve as substrates that can be metabolized to produce energy in the form of ATP, function as intracellular and extracellular signaling molecules, and modulate gene expression [225]. The four primary classes of lipids are fatty acids, triglycerides, phospholipids, and steroids [225].

A variety of naturally occurring lipids have been demonstrated to attenuate the cytotoxicity caused by a variety of insults [75, 94, 226, 227]. As described above, MPP^+-resistance in TR-2°HRs was predicted to arise from increased inhibitory modulation of the hDAT and/or increased biosynthesis of cytoprotective metabolites that prevent MPP^+-induced cytotoxicity intracellularly. A variety of lipids have been reported to attenuate cytotoxicity caused by cytotoxic substrates of the DAT, such as squalene, lanosterol, and polyunsaturated fatty acids [93, 94, 227]. In the TR-2°HR population, increased biosynthesis of cytoprotective lipid was the second most common mechanism explaining MPP^+-resistance, as described below.

10.2. Criteria indicating MPP^+-resistance was attributable to increased biosynthesis of cytoprotective lipids

The designation of TR-2°HRs to Subpopulation-2 (mechanism of survival, increased biosynthesis of cytoprotective lipids) was made based on the following criteria: 1) DAT inhibitory modulation produced by the TR-2°HRs' extracts was

less than three standard deviations above the mean of the ATMhDAT-2°HR population (*see* **Table 9.1**) and 2) chromatic peaks in the TR-2°HRs' GC traces were "positively identified" as lipids previously reported to attenuate cytotoxicity caused by cytotoxic DAT substrates. Here, "positive identification" refers to the identification of lipids based on the MS spectra extracted from their corresponding chromatographic peak (quality of match ≥ 99%).

10.3. Subpopulation-2: increased biosynthesis of squalene, polyunsaturated fatty acids, and/or sterols engenders resistance to MPP^+

MPP^+-resistance arose from increased biosynthesis of cytoprotective lipids in 33 TR-2°HRs (frequency = 30.3%). In TR-2°HRs designated to Subpopulation-2, squalene was the most common lipid present in increased quantities (n = 23, 69.70%), followed by linoleic acid (n = 21, 63.64%). In Subpopluation-2, both squalene and linoleic were present in increased yields in 9 TR-2°HRs (frequency = 27.27%). Each of these lipids has previously been reported to attenuate the deleterious effects of cytotoxic DAT substrates [93, 94, 227].

10.4. Discussion

A heterogeneous population of *L. cardinalis* gain-of-function mutant transgenic hairy roots expressing the hDAT was generated on medium containing MPP^+. Upon completing pharmacological and chemical analysis of TR-2°HRs extracts, it became evident that MPP^+-resistance in a large portion of the population arose from increased biosynthesis of cytoprotective lipids. In fact, increased biosynthesis of cytoprotective lipids was the second most frequent mechanism underlying MPP^+-resistance in TR-2°HRs.

Squalene was the most frequently observed lipid present in increased quantities in extracts from TR-2°HRs designated to Subpopulation-2. MPP^+ is commonly utilized to model DAergic neurotoxicity observed in PD, and the hDAT

was expressed in TR-2°HRs such that their phenotype resembled that of DAergic neurons at a fundamental level in that DAT expression is restricted to DAergic neurons [43, 52]. Thus, a literature search was performed to determine whether squalene was reported to exert cytoprotective effects in models of PD. Indeed, previous studies demonstrated that squalene attenuated DAergic neurotoxicity observed in the 6-OHDA model of PD in rats [93]. This finding supported the hypothesis that cytoprotective metabolites that prevent the cytotoxic effects of selective DAergic neurotoxins would also exert similar effects in mammalian cells. The neuroprotective effects of squalene in the 6-OHDA model of PD were attributed to its ability to stabilize cell membranes, scavenge singlet oxygen radicals, and reduce inflammation [93, 228]. Lastly, squalene is a precursor for the biosynthesis of plant phytosterols and sterols present in human cells [227, 229]. Given lanosterol exerts cytoprotective effects in *in vitro* and *in vivo* models of PD, increased yields of squalene may led to greater levels of phytosterols that exert effects analogous to lanosterol in plant cells (i.e. induction of mitochondrial uncoupling proteins) [227].

Linoleic acid has previously been reported to abolish the cytotoxic effects of MPP^+ in PC12 cells [94]. Polyunsaturated fatty acids (PUFAs), such as arachidonic acid, attenuate H_2O_2- and glutamate-induced cytotoxicity in hippocampal slices [94]. PUFAs also reduce cell death caused by ischemia and ethanol in the cardiac myocytes and gastrointestinal epithelia cells, respectively [94]. Furthermore, PUFAs have been reported to inhibit the DAT [74, 75]. Elongation of hydrocarbon tail and a higher degree of unsaturation increases the inhibitory potency of PUFAs [75]. The inhibitory action of PUFAs is dependent upon the presence of a terminal carboxylic acid group, given esters of PUFAs fail to inhibit DAT function [75]. Given PUFAs are reported to inhibit DAT, and exert antioxidant, anti-inflammatory, and anti-apoptotic effects, their ability to inhibit cytotoxicity caused by MPP^+ is not surprising [74, 75, 94, 226]. Additionally, MPTP toxicity was reduced in mice via dietary supplementation with PUFAs [226].

Resistance to MPP^+ in TR-2°HR Subpopulation-2 arose from beneficial gain-of-function mutations which increased the biosynthesis of cytoprotective lipids. Both squalene and linoleic acid were present in increased quantities in TR-2°HRs, each of which has been reported to exert neuroprotective effect in models of PD [93, 94]. The ability of cytoprotective lipids to prevent the cell death caused by MPP^+ in plant cells, in addition to their cytoprotective effects in mammalian models of PD, supports the hypothesis that cytoprotective metabolites will protect human and plant cells challenged with similar insults [93, 94]. As such, similar approaches could be utilized to drive the production of cytoprotective metabolites for the treatment of other human diseases. For example, the generation of gain-of-function mutants plant cell resistant to 3-nitropropionic acid, which is utilized to model Huntington's disease (HD), would be predicted to favor biosynthesis of metabolites with therapeutic applications in HD [230-233]. The utilization of target-directed biosynthesis may potentially revitalize plant-based drug discovery and accelerate the discovery of therapeutics and/or "druggable" leads for the treatment of numerous human diseases.

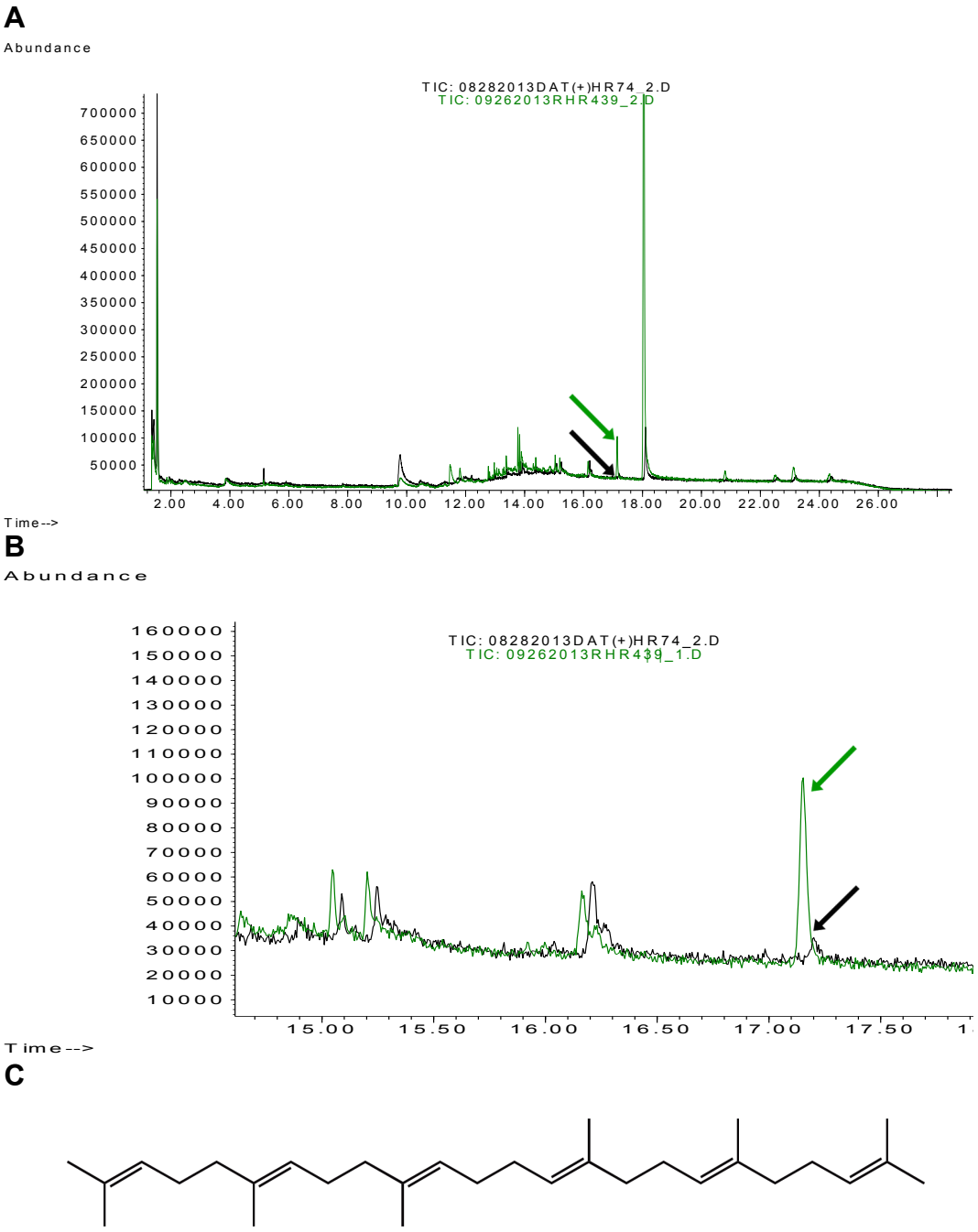

Figure 10.1. Overlay of a representative GC trace from a hDAT-1°HR (black line) and a TR-2°HR (green line) overproducing squalene. A) An overlay of a representative GC trace from a hDAT-1°HR and a TR-2°HR with increased yields squalene demonstrates the marked increase in the latter, as compared the former. B) A closer examination demonstrates the pronounced increase squalene content in the TR-2°HR, as compared to a representative hDAT-1°HR. The black and green arrows indicate the chromatographic peak corresponding to squalene in the GC traces from a hDAT-1°HR and a TR-2°HR, respectively. C) The structure of squalene.

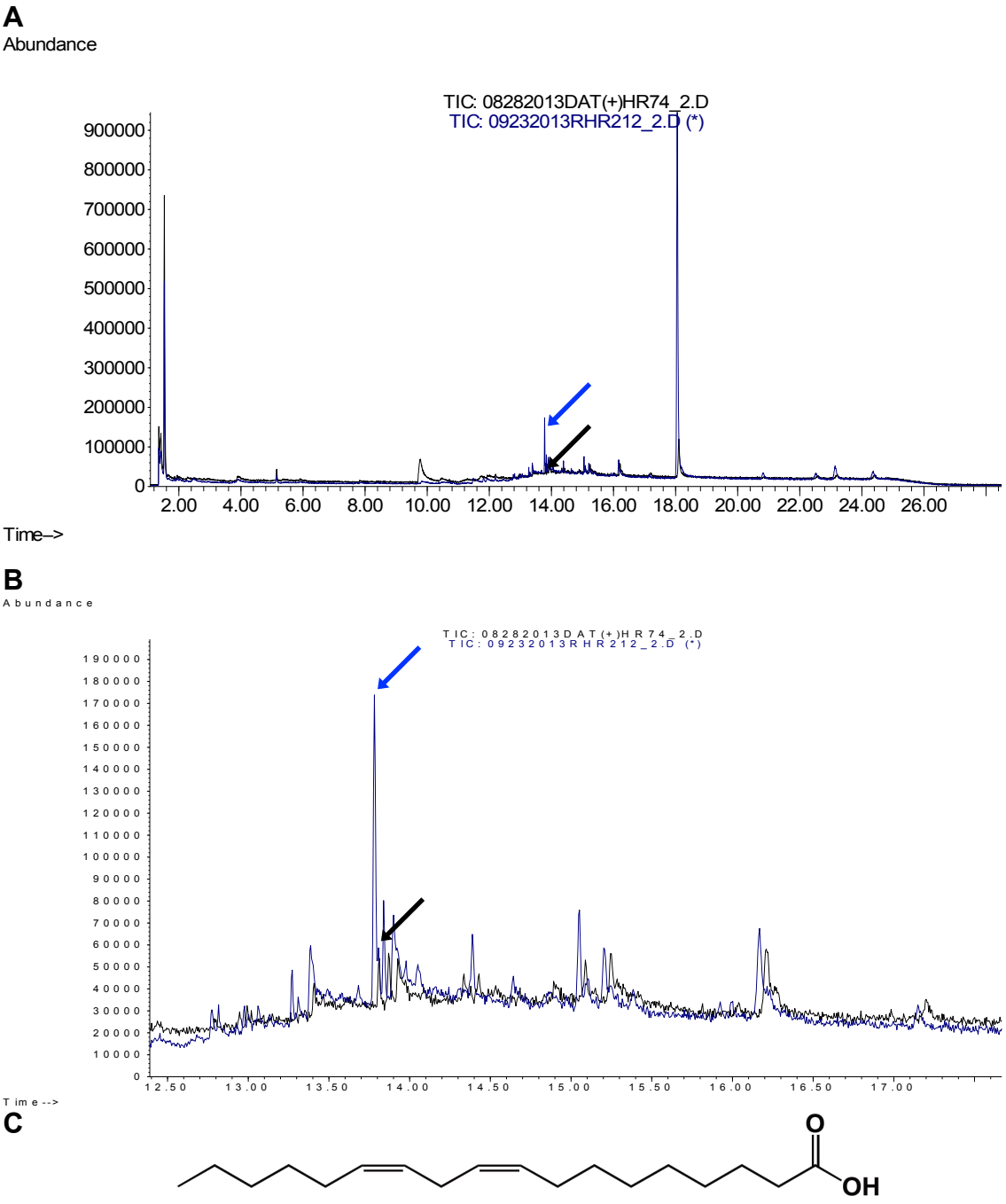

Figure 10.2. Overlay of a representative GC trace from a hDAT-1°HR (black trace) and a TR-2°HR (blue trace) overproducing linoleic acid. A) An overlay of a representative GC trace from a hDAT-1°HR and a TR-2°HR with increased yields linoleic acid demonstrates the marked increase in the latter, as compared the former. B) A closer examination demonstrates the pronounced increase in the TR-2°HR, as compared to a representative hDAT-1°HR. The black and blue arrows indicate the chromatographic peak corresponding to squalene in the GC traces from a hDAT-1°HR and a TR-2°HR, respectively. C) The structure of linoleic acid.

A

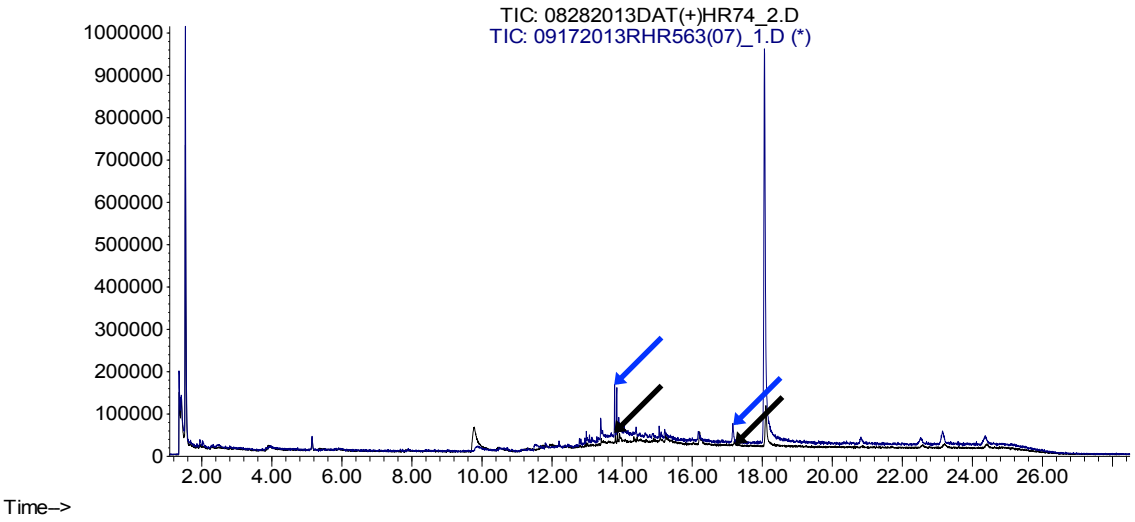

B

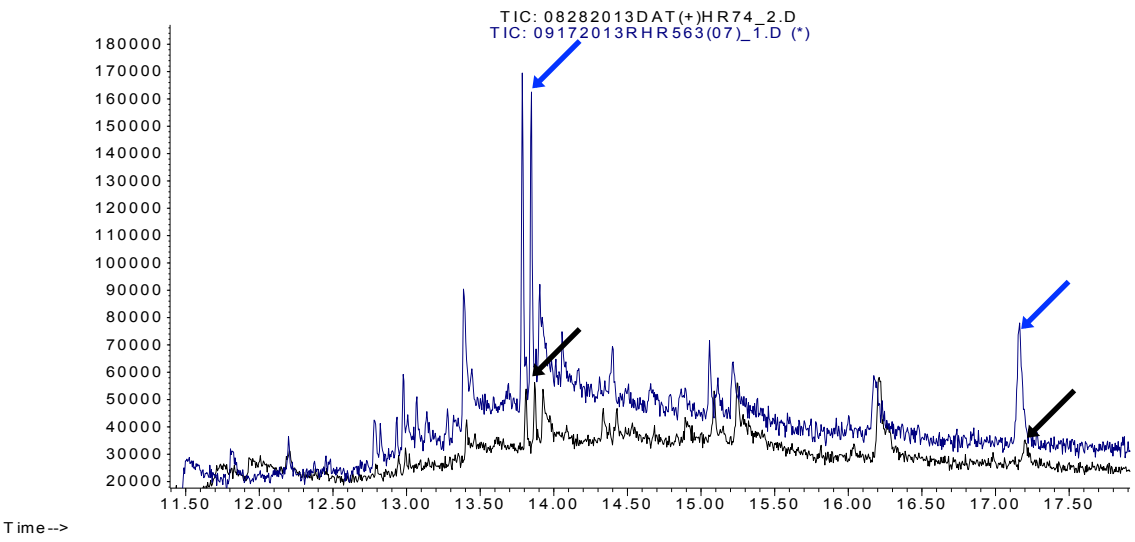

Figure 10.3. Overlay of a representative GC trace from a hDAT-1°HR (black trace) and a TR-2°HR (blue trace) overproducing linoleic acid and squalene. A) An overlay of a representative GC trace from a hDAT-1°HR and a TR-2°HR with increased yields linoleic acid and squalene demonstrates the marked increase in the latter, as compared the former. B) A closer examination demonstrates the pronounced increase in the TR-2°HR, as compared to a representative hDAT-1°HR. The black and blue arrows indicate the chromatographic peaks corresponding to linoleic acid and squalene (chromatographic peaks indicated by arrows on the left and right, respectively) in the GC traces from a hDAT-1°HR and a TR-2°HR, respectively.

Chapter 11

Subpopulation 3: Increased biosynthesis of putatively "novel" cytoprotective metabolites

11.1. Introduction

Numerous phytochemicals and other small molecule natural products (SMNPs) have been investigated for their ability to attenuate MPP^+-induced cytotoxicity *in vitro* and *in vivo* [108, 109, 112, 113, 115-118, 120-122, 125]. MPP^+-induced DAergic neurotoxicity is widely accepted as a useful tool to model PD [92, 123, 124]. The efficacy of phytochemicals and SMNPs at preventing DAergic neuron loss in models of PD has spiked interest in their use as potential therapeutics and/or drug leads for the development of anti-PD therapeutics, as covered in recent reviews [234, 235]. Chrysotoxine, salvianolic acid B, lycopene, and neoechinulin A, amongst other SMNPs, have been reported reduce cytotoxicity caused by MPP^+ (select phytochemicals and SMNPs reported to reduce MPP^+-induced cytotoxicity are summarized **Table 11.1**) [108, 109, 112, 113, 115-118, 120-122, 125]. The cytoprotective effects of the aforementioned plant metabolites were not reported to occur via inhibition of the DAT, nor have they been reported to inhibit the DAT [108, 109, 112, 113, 115-118, 120-122, 125]. In fact, salvianolic acid B was reported to lack inhibitory activity at the DAT, and was shown to increase Nrf2 expression and glial-cell derived neurotrophic factor (GDNF) release [122]. Therefore, it is conceivable that TR-2°HRs' resistance to MPP^+ may have arisen due to increased biosynthesis cytoprotective metabolites that exert effects similar to those of the abovementioned phytochemicals. Extracts from TR-2°HRs designated to Subpopulation-3 did not display a marked increased in DAT inhibitory modulation, and GC-MS analysis of their extracts indicated no discernable increase in cytoprotective lipids. However, GC-MS analysis of extracts from TR-

2°HRs designated to Subpopulation-3 revealed the presence of chromatographic peaks that were detectable in trace amounts and/or were undetectable in controls, and were predicted to represent putatively "novel" cytoprotective metabolites.

11.2. Criteria indicating MPP^+-resistance was attributable to increased biosynthesis of "novel" cytoprotective metabolites

The designation of TR-2°HRs to Subpopulation-3 (mechanism of survival, increased biosynthesis of "novel" cytoprotective metabolites) was made based on the following criteria: 1) DAT inhibitory modulation produced by the TR-2°HRs' extracts was less than three standard deviations above the mean of the ATMhDAT-2°HR population (*see* ***Table 9.1***), 2) chromatographic peaks representing cytoprotective lipids were not identified in the TR-2°HRs' GC traces, and 3) prominent chromatographic peaks were present in the TR-2°HRs' GC traces that were only detectable in trace amounts and/or were undetectable in controls.

11.3. Subpopulation 3: increased biosynthesis of "novel" cytoprotective metabolites putatively underlies resistance to MPP^+

Increased biosynthesis of putatively "novel" cytoprotective metabolites that prevent MPP^+ intracellularly, rather than preventing DAT-mediated toxin uptake or via increased biosynthesis of cytoprotective lipids, was the third most frequently observed mechanism underlying MPP^+-resistance (n = 24, frequency = 22.0%). Chemical structures were not assigned to the putatively "novel" cytoprotective metabolites present TR-2°HRs designated to Subpopulation-3. The inability to assign chemical structures the aforementioned metabolites presumably arose from the utilization of a GC-MS method aimed to separate and identify alkaloids, specifically those structurally related to lobinaline. Considering "novel" metabolites present in the TR-2°HRs were predicted to have structures

related to lobinaline, the method employed for GC-MS analysis was developed accordingly with the aim of separating and identifying such alkaloids.

11.4. Discussion

A population of *L. cardinalis* TR-2°HRs was generated, which consisted of mutants resistant to MPP^+ despite expressing the hDAT. The most common mechanism explaining resistance to the cytotoxin in the TR-2°HRs was increased inhibitory modulation of the hDAT, followed by increased biosynthesis of cytoprotective lipids. However, TR-2°HRs were identified which did not display increased inhibitory activity at the DAT, nor did their extracts contain increased amounts of cytoprotective lipids previously reported to attenuate MPP^+-induced cytotoxicity. Chemical analysis of the aforementioned TR-2°HR extracts via GC-MS led to the identification of chromatographic peaks that were absent and/or present in trace amounts in controls. The peaks were predicted to indicate the presence of putatively "novel" cytoprotective metabolites that conferred resistance to MPP^+.

Structural elucidation of the putatively "novel" cytoprotective metabolites via analysis of the MS extracted from their corresponding chromatographic peaks proved unavailing. However, the GC-MS method employed in the current study was developed to enable the detection, separation, and structural identification of lobinaline (*see* ***Figure 3.3***) and lobinaline-like alkaloids. Considering alkaloids structurally related to lobinaline, which were active at the DAT, were predicted to be the primary metabolites present in TR-2°HRs, the GC-MS method utilized was logical. If an alternate GC-MS method was utilized the quantification of lobinaline present in hairy root extracts may not have been achieved, which would have prevented the attribution of DAT inhibition to lobinaline and/or a novel DAT inhibitor/s. However, the GC-MS method utilized generated data essential for one develop hypotheses pertaining to the class of metabolites present in the TR-2°HR extracts, thus allowing the future utilization of analytical instrumentation necessary for structural elucidation.

In future studies, analytical instrumentation that is less likely to decompose metabolites prior to reaching the mass selective detector (MSD), which also acquires superior MS data, could be utilized in combination with MS libraries of greater breadth. For example, flavonoids are decomposed when analyzed via GC-MS prior to reaching the MSD, precluding structural elucidation [236]. Liquid chromatographic techniques (i.e. HPLC or UPLC) coupled to tandem mass spectroscopy (LC-MS/MS) may prove to be an effective alternative to elucidate the structures of unidentified metabolites present in TR-2°HRs [236]. The TR-2°HRs represent a repository of putatively "novel" small molecule natural products (SMNPs) with a high probability of exerting cytoprotective effects awaiting to be mined for such metabolites if reasonable manpower and resources are dedicated to this task. Given squalene and linoleic acid were present in TR-2°HRs designated to Subpopulation-2, each of which protects TR-2°HR and neuronal cells from similar insults, this is truly a possibility of high likelihood [93, 94].

That said, a coumarin-like compound (8-methyloctahydrocoumarin) was amongst the hits that arose in the while performing library searches of the MS data, albeit the quality of the match was low (quality of match, 41%). This may indicate that increased biosynthesis of molecules similar to coumarins and/or flavonoids, which share a degree of structural similarity, and are reported to attenuate MPP^+-induced cytotoxicity, led to MPP^+-resistance in TR-2°HRs designated to Subpopulation-3 [112, 114, 116, 117, 119]. Especially considering *L. cardinalis* contains complex flavonoid-anthocyanin glycosides, and both flavonoids and anthocyanins have been shown to attenuate MPP^+-induced cytotoxicity [112, 114, 116, 117, 119, 237]. Although other classes of metabolites cannot be ruled out, increased biosynthesis of flavonoid- or anthocyanin-like metabolites is a plausible explanation underlying MPP^+-resistance in Subpopulation-3.

A wide variety of phytochemicals and SMNPs have been identified that attenuate the deleterious effects of cytotoxic DAT substrates in mammalian systems *in vitro* and *in vivo* [108, 109, 112, 113, 115-118, 120-122, 125]. Most of

the aforementioned natural products reduce MPP^+-induced formation of reactive oxygen species, prevent opening of the mitochondrial permeability transition pore, reduce the Bax/Bcl-2 ratio, and decrease caspase-3 activity, all effects which reduce MPP^+-induced apoptosis [108, 109, 112, 113, 115-118, 120-122, 125]. Lycopene, salvianolic acid B, sulforaphane, and carnosic acid cause Nrf2 translocation to the nucleus, which is believed to function as a master regulator of antioxidant systems within cells responsible for the induction of detoxification and antioxidant enzymes [108, 113, 118, 122, 238]. Furthermore, Nrf2 signaling activated by salvianolic acid B increases GDNF release *in vitro*, and increases GNDF levels *in vivo* [122]. GDNF exerts neuroprotective effects in a wide variety of *in vitro* and *in vivo* models, and is particularly effective at restoring DAergic function in animal models of PD [122].

Homologs of Nrf2's upstream regulator, Keap1, have been identified in plants [238-241]. It is conceivable that phytochemicals such as salvianolic acid B, sulforaphane, and carnosic acid, which activate Nrf2, bind to homologs of Keap1 in plant cells, but disrupt the Keap1-Nrf2 interaction in animal cells thereby allowing Nrf2 translocation to the nucleus. Considering plant homologs of Keap1 have been identified, plants and animals may share similar signaling pathways to induce the expression of antioxidant defenses [13, 239]. Subpopulation-3 may be enriched with TR-2°HRs containing molecules that activate plant cells' antioxidant defense systems, thereby providing protection from toxicity caused by MPP^+. Supporting this notion, an isothiocyanate (2-heptane isothiocyanate) was the top match identified after performing a library search on the MS extracted from a chromatographic peak present in increased abundance in an TR-2°HR's extract present in Subpopulation-3. Isothiocyanates that occur naturally in plants, sulforaphane representing a prime example, have been shown activate Nrf2 thereby exerting neuroprotective effects [118, 241, 242]. Subpopulation-3 could essentially be viewed as a chemical repository that likely contains SMNPs capable of promoting Nrf2 translocation to the nucleus, thereby exerting cytoprotective and neuroprotective effects.

Table 11.1
Phytochemicals and other SMNPs shown to reduce the toxic effects of cytotoxic DAT substrates and/or selective DAergic neurotoxins*

SMNP	Source	Cytotoxin, model system	Mechanism of Action
Chrysotoxine[1]	*Dendrobium* species	6-OHDA, SH-SY5Y cells	Reduce ROS formation Preserve ΔΨm Attenuate increase in $[Ca^{2+}]_i$ Prevent cytochrome c release Reduce Bax/Bcl-2 ratio Prevent caspase-3 activation Reduce p38 MAPK and ERK1/2 phosphorylation Inhibit NF-κB translocation Prevent iNOS up-regulation Reduce NO production
Kaempferol[2]	*Glycine max*	Rotenone, SH-SY5Y cells	Reduce ROS formation Preserve ΔΨm Restore ΔΨm (<12 post-treatment) Reduce lipid peroxidation Induce mitophagy
Lycopene[3]	*Solanum lycopersicum*	MPP+, SH-SY5Y cells	Reduce ROS formation Reduce lipid peroxidation Preservation of mitochondrial morphology Prevent opening of mPTP Prevent ATP depletion Prevent reduction in mtDNA
Neoechinulin A[4]	*Eurotium rubrum*	MPP+, PC12 cells	Reduce free radical levels Reduce activation of caspase-3 Increase NADH production

Table 11.1 (continued)
Phytochemicals and other SMNPs shown to reduce the toxic effects of cytotoxic DAT substrates and/or selective DAergic neurotoxins*

Osthole[5]	*Cnidium monnieri*	MPP+, PC12 cells	Reduce ROS formation Induction of SOD activity Induction of catalase activity Reduce lipid peroxidation Reduce Bax/Bcl-2 ratio Reduce caspase-3 activity
S-Allylcysteine[6]	*Allium sativum*	MPP+, C57BL/6J mice	Reduce ROS formation Reduce lipid peroxidation Enhance CuZn-SOD activity Enhance glutathione reductase activity
Salvianic acid A[7]	*Salvia miltiorrhiza*	MPP+, SH-SY5Y cells	Reduce ROS formation Reduce Bax/Bcl-2 ratio Preserve ΔΨm Inhibit cytochrome c release Reduce caspase-3 activity
Salvianolic acid B[8]	*Salvia miltiorrhiza*	MPP+, neuron-microglia cultures	Reduce glial TNF-a release Reduce IL-1b release Reduce NO production Increase GDNF mRNA Increase GDNF release
		MPP+, mouse midbrain neuron-glia cultures	Increase Nrf2 expression Increase Nrf2 translocation Reduce glial TNF-a release Reduce IL-1b release Reduce NO production Increase GDNF mRNA Increase GDNF release
		MPTP, C57BL/6J mice	Reduce glial TNF-a release Reduce IL-1b release Reduce NO production Increase GDNF content

Table 11.1 (continued)
Phytochemicals and other SMNPs shown to reduce the toxic effects of cytotoxic DAT substrates and/or selective DAergic neurotoxins*

Tetrahydroxystilbene glucoside[9]	*Polygonum multiflorum*	MPP+, SH-SY5Y cells	Reduce ROS formation Preserve ΔΨm Reduce Bax/Bcl-2 ratio Reduce capase-3 activity
Licopyranocoumarin[10]	*Glycyrrhiza* species	MPP+, PC12 cells	Reduce ROS formation Preserve ΔΨm Attenuate JNK activity
Glycyrurol[10]			

*The list provided is non-exhaustive and is intended to provide select examples of phytochemicals and other SMNPs that reduce MPP+- and/or 6-OHDA-induced cytotoxicity

Small molecule natural product, SMNP; 6-hydroxydopamine, 6-OHDA; 1-methyl-4-phenylpyridinium, MPP+; reactive oxygen species, ROS; mitochondrial membrane potential, ΔΨm; inducible nitric oxide synthase, iNOS; nitric oxide (NO), mitochondrial permeability transition pore; adenosine triphosphate, ATP; mitochondrial DNA, mtDNA; superoxide dismutase, SOD; copper-zinc superoxide dismutase, CuZn-SOD

[1]Song et al. (2013) [109]
[2]Filomeni et al. (2012) [116]
[3]Yi et al. (2013) [113]
[4]Kajimura et al. (2008) [115]
[5]Liu et al. (2010) [117]
[6]Rojas et al. (2011) [120]
[7]Wang et al. (2015) [121]
[8]Zhou et al. (2014) [122]
[9]Sun et al. (2011) [125]
[10]Fujimaki et al. [112]

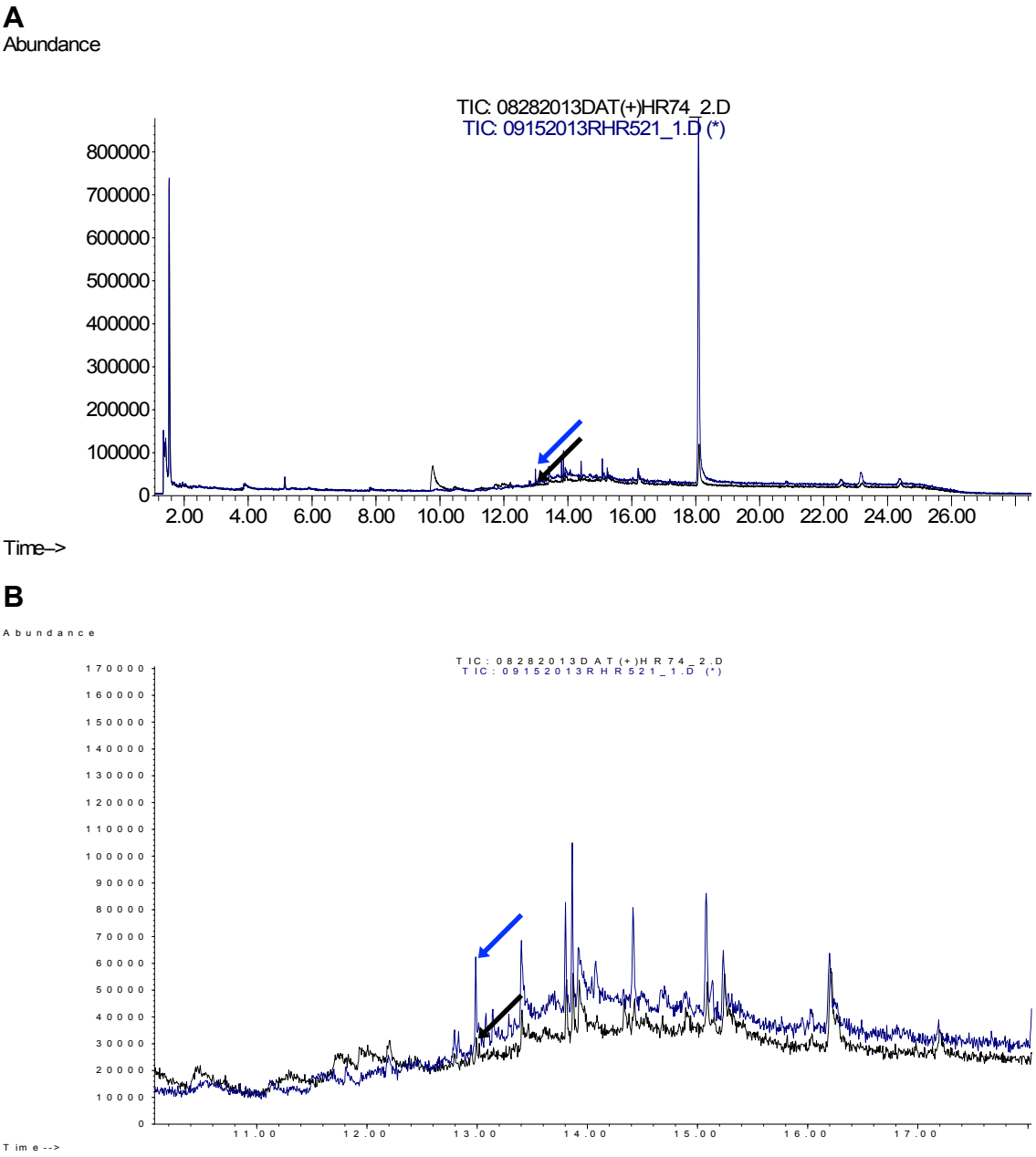

Figure 11.1. Overlay of GC traces from a representative hDAT-1°HR extract (black trace) and a TR-2°HR with increased yields of a putatively "novel" cytoprotective metabolite/s (blue trace), in this case a coumarin-like metabolite. A) An overlay of a representative GC trace from a hDAT-1°HR and a TR-2°HR with increased yields of a putatively "novel" cytoprotective metabolite demonstrates the marked increase in the latter (blue arrows), as compared the former (black arrows). B) A closer examination demonstrates the pronounced increase in the TR-2°HR, as compared to a representative hDAT-1°HR.

Chapter 12

Subpopulation 4: Mechanism of MPP^+-resistance undetermined

12.1. Introduction

The DAT has been implicated to play a role in DAergic neurodegeneration seen in PD, functioning as a "gateway" allowing cytotoxic substances to access the cytosol of nigrostriatal neurons [50, 52, 95, 97, 98, 220, 222-224]. Cytotoxic substrates of the DAT include endogenous and exogenous compounds, such as salsolinol and MPP^+, respectively [95]. Upon accessing the cytosol of DAergic neurons, the aforementioned compounds cause cell death by disrupting mitochondrial function, increasing free radical production, and/or depleting ATP levels, ultimately inducing apoptosis and/or necrosis [50, 52, 92, 95, 97, 98, 110, 220, 222-224]. In the present study, the hDAT was expressed in *L. cardinalis* hairy root cells, which were subsequently "activation tagged" and selected on medium containing MPP^+. Methanolic extracts from the resulting population of MPP^+-resistant TR-2°HRs were subject to pharmacologic and chemical analysis (*see sections 7.4 and 7.5*). MPP^+-resistance in the TR-2°HR Subpopulations 1 – 3 was explained by the presence of beneficial gain-of-function mutations that increased inhibitory modulation of the hDAT, increased biosynthesis of cytoprotective lipids, or increased biosynthesis of other cytoprotective metabolites, respectively. However, resistance to MPP^+ in Subpopulation-4 did not arise via the aforementioned mechanisms.

12.2. Criterion leading to the designation of TR-2°HRs to Subpopulation-4

The designation of TR-2°HRs to Subpopulation-4 (mechanism of survival undetermined) was made based on the following criteria: 1) DAT inhibitory modulation produced by the TR-2°HRs' extracts was less than three standard

deviations above the mean of the ATMhDAT-2°HR population (*see* **Table 9.1**), 2) chromatographic peaks representing cytoprotective lipids were not identified in the TR-2°HRs' GC traces, and 3) chromatographic peaks that were detectable in trace amounts and/or were undetectable in controls were not present in greater abundance in GC traces acquired from the TR-2°HRs' extracts.

12.3. Subpopulation 4: mechanism of MPP^+-resistance undetermined

In Subpopulation-4, the mechanism/s underlying TR-2°HRs' resistance to MPP^+ was undetermined. This was the least common type of TR-2°HR encountered (n = 10, frequency = 9.17%). As seen in **Figure 12.1**, GC traces acquired via analysis of the aforementioned TR-2°HRs' extracts were devoid of chromatographic peaks other than that which corresponded to lobinaline.

12.4. Discussion

A population of *L. cardinalis* TR-2°HRs that express the hDAT, yet are resistant to MPP^+, was generated. The vast majority of TR-2°HRs were resistant to the toxin owing to increased inhibitory modulation of the hDAT (Subpopulation-1) or increased biosynthesis of cytoprotective metabolites (Subpopulations 2 and 3). However, a small portion of the population survived selection on medium containing MPP^+ via a mechanism/s independent of DAT inhibition and increased biosynthesis of metabolites capable of attenuating the deleterious effects of the toxin. These TR-2°HRs were designated to Subpopulation-4. At present, the mechanism/s underlying MPP^+-resistance in this subpopulation is undetermined. One could speculate that resistance to the toxin arose via enhanced expression of cytoprotective genes that were capable of mitigating MPP^+-induced cytotoxicity. However, increased biosynthesis of cytoprotective metabolites that were undetectable using the analytical instrumentation and methodology employed in the present study cannot be ruled out. The former is predicted to explain MPP^+-resistance in these TR-2°HRs, as described below.

The Arabidopsis genome was sequenced in 2000, and subsequent analyses led to the realization that plant homologs exist for 71% of the genes linked to human neurological disorders [243, 244]. Although the evolution of plants and humans diverged roughly 1.6 billion years ago, plant orthologs exist for the majority of genes linked to human disease [243, 244]. Furthermore, the aforementioned genes serve related functions in plant and human cells, despite differences the organisms' morphological structure, cellular requirements for the production of energy (i.e. autotrophs and heterotrophs, respectively), and challenges encountered during their existence [243]. These observations have spiked interest in the use of plants to model human disease, including neurodegenerative diseases [243-245]. In fact, knowledge relating to the function of plant genes, and their respective proteins products, facilitated the discovery of genes associated with several neuropathological disorders, including PD, Alzheimer's disease, Rett syndrome, and Friedreich's ataxia [243-245]. Plant models may be particularly well-suited to delineate certain genetic defects that contribute to the manifestation of PD, considering plant orthologs exist for all PD-linked genes, with the exception of PARK1 and PARK3 [244]. Furthermore, aberrant gene variants, such as mutant SPK1-like1-1 (ask1-1), produce similar cellular defects in human and plant cells [246]. Ask1-1 is homologous to SPK1 present in mammalian cells [246]. Downregulation of SPK1 in mouse embryonic substantia nigra-derive DAergic cells produces a phenotype that resembles that of sporadic PD [246]. A loss-of-function mutant form of ask1-1 produces cellular defects in *Arabidopsis* analogous to those observed in mammalian cells, including the formation of intracellular aggregates, aberrant cell division, and ultimately cell death [246]. Given plants such as *Arabidopsis* have shot life-spans, are easily maintained in the laboratory at relatively low costs, can be genetically modified rapidly using well-established methodology, and ethical constraints are less of an issue, plants represent an excellent alternative to model neurological disorders [244].

A variety of genes have been demonstrated exert cytoprotective effects in models of DAergic neurodegeneration, including models of PD wherein lesions

are created via the administration of cytotoxic DAT substrates [247-251]. For example, DJ-1 reduces oxidative stress caused by MPP^+ and paraquat in SH-SY5Y cells via activation of superoxide dismutase (SOD) [247]. The plant ortholog of DJ-1, AtDJ-1a, also increases SOD activity, thereby playing a role cellular defense system that prevent the deleterious effects of reactive oxygen species [244, 252, 253]. Overexpression of the vesicular monoamine transporter type-2 (VMAT-2) decreases the neurotoxic effects of MPP^+ in a mouse model of PD [248]. Undifferentiated SH-SY5Y cells are less vulnerable to MPP^+, compared to SH-SY5Y cells differentiated toward a DAergic phenotype, which is believed to arise due to differences in the DAT: VMAT-2 expression ratio [124]. The DAT: VMAT-2 expression ratio is lower in the former, which is believed reduce uptake and enhance vesicular sequestration of the toxin thereby reducing cytotoxicity caused by MPP^+ [124]. Plant express transporters for auxins, hormones that influence the growth and differentiation of plant cells, and auxin transporters and VMAT-2 share homology with p-glycoprotein [254-258]. Therefore, overexpression of transporters for auxins, or structurally related molecules, may lead to the sequestration of MPP^+ in storage organelles present in plant cells, thereby abrogating MPP^+-induced cytotoxicity. Plant also express homologs of Keap1, which regulates the activity of Nrf2 (*see section 11.4*), the latter of which has been proposed as the master regulator of antioxidant defense systems [238, 239]. Given Keap1's role in the regulation of Nrf2, induction of genes whose protein products reduce Keap1 activity may lead increased expression of antioxidant defense systems, which would also be predicted to attenuate the cytotoxic effects of MPP^+ [238, 240, 241]. Lastly, plants and mammals express the anti-apoptotic protein Bcl-2, which has been reported to attenuate toxicity caused by MPP^+ [251, 259]. Clearly, a vast array of genes present in plants may lead to MPP^+ resistance if their genes were directly or indirectly "activated" by gain-of-function mutations introduced in TR-2°HRs via ATM.

The induction of cytoprotective genes was predicted to explain resistance to MPP^+ in Subpopulation-4, although the presence of cytoprotective metabolites that were undetectable using the analytical techniques employed in the current

study cannot be ruled out. Plants express a variety of genes that are homologous to human genes linked to neurological disorders, and which serve similar functions in plant and animal cells [243-245]. Since the “activation tag” allows one to identify and rescue genes up-regulated via ATM, the TR-2°HRs designated to Subpopulation-4 are a potential source of putatively “novel” cytoprotective genes capable of reducing the effects of the DAergic neurotoxin MPP^+. DAergic neurodegeneration caused by MPP^+ recreates many of the symptoms observed in PD, such as rigidity and bradykinesia [89-91]. Considering many genes linked to human neuropathological disorders (e.g. PD) share homology with those present in plants, human homologs of cytoprotective genes capable of mitigating the deleterious effects of MPP^+ in TR-2°HRs may exist [243-245]. Future studies examining genes flanking the “activation tag” in TR-2°HRs remain to be performed. If “novel” cytoprotective genes are identified in these TR-2°HRs, their sequences could be utilized to identify homologous human genes, thereby accelerating the identification of new molecular targets for the development of therapeutics to treat and/or prevent PD.

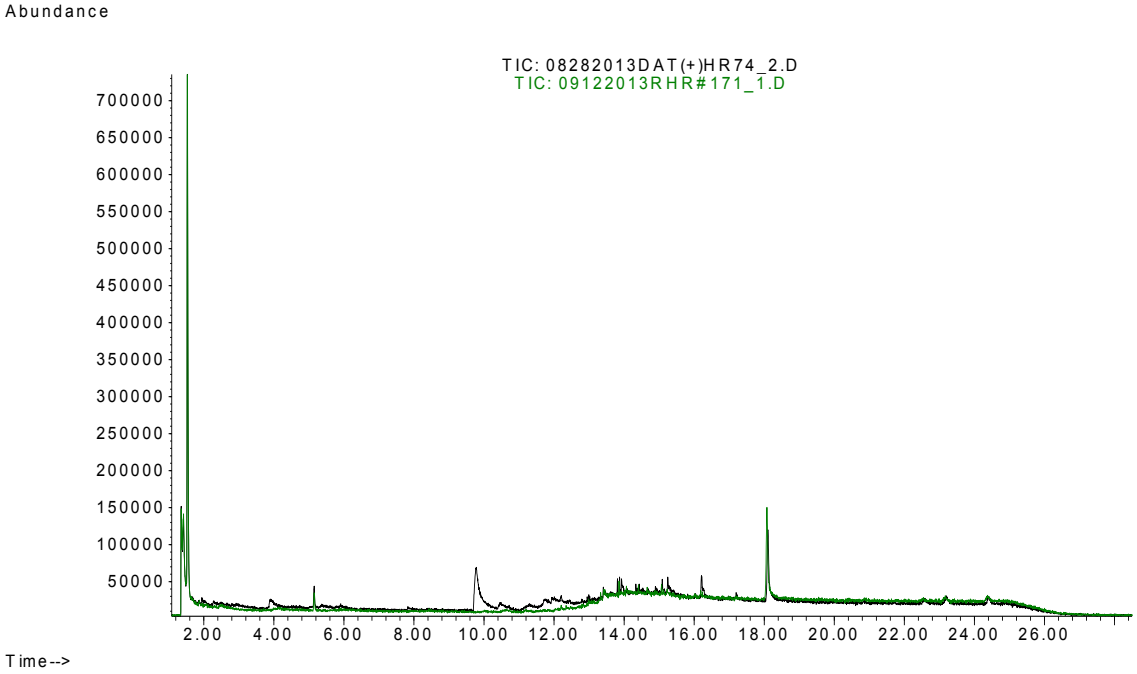

Figure 12.1. Overlay of GC traces from a representative hDAT-1HRs and a TR-2°HR in which a cytoprotective gene/s has putatively been activated. No appreciable difference was apparent upon comparison, however the TR-2°HR survived selection, suggesting survival due to the induction of a cytoprotective gene/s.

Chapter 13

Evaluation of TR-2°HR extracts for the presence of putatively "novel" DAT inhibitors and/or potentially neuroprotective metabolites

13.1 Introduction

In the present dissertation, the fundamental principles underlying evolution by natural selection were applied to develop a novel plant-based drug discovery platform. The innovative biotechnology described herein, referred to as target-directed biosynthesis, essentially redirects plant evolution favoring the biosynthesis of metabolites meant to interact with a specific human target protein. Here, the hDAT was used as an example to demonstrate the application of the technology.

Two fundamental requirements for evolution via natural selection are: 1) genetic/phenotypic heterogeneity within a given population, and 2) environmental selection pressures favoring the survival of individuals with the greatest reproductive fitness [12]. In nature, genetic heterogeneity within a plant population arises from sexual reproduction and germline mutations, whereas environmental selection pressures arise from a vast array of abiotic and biotic sources [12-14]. For example, ultraviolet (UV) radiation favored the survival of plants whose genome encoded the biosynthetic machinery responsible for the synthesis of carotenes and flavonoids, metabolites capable of absorbing UV energy and scavenging free radicals thereby abrogating the deleterious effects of UV radiation [13, 14]. As described above (*see section 1.2*), the presence of herbivorous insects favored the survival of plants having genomes that encoded biosynthetic pathways responsible for the synthesis of secondary metabolites, such as nicotine or cocaine, which function as natural insect deterrents [13, 14].

We sought to emulate the process of evolution via natural selection in the laboratory setting to revolutionize and revitalize drug discovery from plant sources. This was accomplished by creating an artificial environment wherein survival was dependent upon the biosynthesis of plant metabolites with a required bioactivity at a specific human protein. The hDAT, a molecular target for therapeutics in drug abuse and Parkinson's disease, was chosen as an example to illustrate the application of target-directed biosynthesis [59, 60, 65, 66, 70, 79, 95-101]. *A. rhizogenes*-mediated genetic transformation was utilized to express the hDAT in *L. cardinalis*, which contains the relatively weak DAT inhibitor lobinaline. Transgenic *L. cardinalis* plant cells expressing the hDAT displayed increased sensitivity to MPP^+, a cytotoxic DAT substrate [89, 90]. MPP^+-induced toxicity in the aforementioned cells was prevented via pharmacological blockade of the transporter with GBR12909, a highly potent and selective DAT inhibitor [84-88]. As such, one requirement for evolution in the laboratory setting was fulfilled: selection of transgenic *L. cardinalis* plant cells expressing the hDAT on medium containing MPP^+ favoring survival of individuals that synthesized 1) DAT inhibitors of sufficient potency, or at a concentration to prevent MPP^+ uptake and ensuing toxicity and/or 2) metabolites that interfere with MPP^+-induced toxicity downstream of DAT-mediated uptake. Furthermore, the former favored biosynthesis of metabolites that were optimized for activity at a human target protein, i.e. the hDAT. Given DAT inhibitors present in plants evolved to target the insect variant of the transporter, the artificial selection conditions created should "redirect" plant evolution favoring biosynthesis of molecules meant to target the hDAT [30].

Next, agrobacterium-mediated ATM was performed on transgenic *L. cardinalis* plant cells expressing the hDAT to create a heterogeneous population of gain-of-function mutants. ATM produces dominant, gain-of-function mutations in plant cells via integration of T-DNA containing a tetramer of the CaMV 35S promoter enhancer sequence "activating" genes 10-kb upstream and downstream of its integration site [221]. Since the integration of agrobacterial T-DNA occurs randomly throughout the plant genome, each mutant generated has

a unique gain-of-function mutation [14, 16-19]. Thus, the utilization of ATM fulfilled the second fundamental requirement needed for evolution via natural selection. ATM was already shown to have the capacity to alter plant metabolism in studies conducted in *Nicotiana tabacum*, wherein mutant cultures with increased yields of nicotine, or novel nicAchR ligands, were successfully obtained [14, 260]. If ATM increased yields of lobinaline, a novel DAT inhibitor of greater potency, and/or induced biosynthesis of cytoprotective metabolites that were capable of mitigating intracellular events preceding MPP^+-induced cell death, then the gain-of-function mutants should be resistant to the toxin.

Indeed, MPP^+-resistant transgenic gain-of-function *L. cardinalis* plant cells expressing the hDAT were obtained. Additionally, TR-2°HRs were resistant to MPP^+ via both of the predicted mechanisms: 1) increased inhibitory modulation of the DAT and 2) biosynthesis of cytoprotective metabolites that prevent the deleterious effects of MPP^+ via a mechanism independent of DAT inhibition (i.e. prevent MPP^+-induced cytotoxicity intracellularly). To provide proof-of-concept, two studies were performed: 1) a MeOH extract from a TR-2°HR that survived via DAT inhibition was sub-fractionated via pHPLC in an effort to identify a novel DAT inhibitor, and 2) a MeOH extract from a TR-2°HR was evaluated for its ability to attenuate MPP^+-induced cytotoxicity in SH-SY5Y cells. In the former study, a MeOH extract from a TR-2°HR that displayed DAT inhibitory activity, exceeding that which could be expressed as lobinaline equivalents, was chosen to increase the probability of identifying a novel DAT inhibitor. In the latter study, the cytoprotective effect of a TR-2°HR aqueous extract was compared to that of an aqueous extract from a hDAT-1°HR. Treatment of SH-SY5Y cells with MPP^+ is widely accepted as an *in vitro* model of DAergic neurodegeneration seen in PD [92, 107-126]. In the latter study, it was predicted that cytoprotective metabolites that attenuated MPP^+-induced cytotoxicity in TR-2°HRs would also exert cytoprotective effects in mammalian cells challenged with the toxin.

13.2. Study 1: Methods

13.2.1. Chemicals and supplies

Methanol, acetonitrile, and o-phosphoric acid were purchased from Sigma Aldrich (St. Louis, MO, USA). [^{3}H]-DA (S.A. = 60 Ci/mmol) was purchased from American Radiolabeled Chemicals, Inc. (St. Louis, MO, USA). All other chemicals and materials were purchased from Fisher Scientific (Pittsburgh, PA, USA), unless otherwise stated.

13.2.2. pHPLC sub-fractionation of L. cardinalis hairy root methanolic extracts

Hairy root tissue was collected and MeOH extracts were prepared as described above (*see sections 5.15 and 5.16, respectively*). Hairy root MeOH extracts were sub-fractionated via pHPLC using a Waters XBridge Prep C_{18} (5 µm OBD, 19 x 150 mm) column attached to a Waters 600E Multisolvent Delivery System coupled to a Waters 2998 Photodiode Array Detector and Waters 2767 Sample Manager, Injector, and Collector. The pHPLC instrument was operated using Waters MassLynx Software (Version 4.1) and FractionLnyx Collection Control Software (Version 4.1). The mobile phase consisted of a mixture of Solvent A (100% acetonitrile, pHPLC grade) Solvent B (0.1% o-phosphoric acid in Milli-Q water, pH = 1.890), and Solvent C (100% Milli-Q water, pH 7.0). Dried hairy root MeOH extract samples were dissolved in a mixture of Solvents A – C (20% A, 1% B, 79% C) to achieve a final concentration of 20 mg/ml. Samples were vortex briefly (~30 seconds), sonicated (~45 seconds), and then syringe filtered (pore size, 0.22 µm) prior to injection (sample injection volume = 200 µl). Separation was performed with the following gradient at a flow rate of 10 ml/minute: initial conditions, 10% A in C; 0 – 3 minutes, gradient curve = 5, 10 – 15% A in C; 3 – 6 minutes, gradient curve = 5, 15 – 20% A in C; 6 – 12 minutes, gradient curve = 7, 20 – 30% A in C; 12 – 24 minutes, gradient curve = 6, 30 – 50% A in C; 24 – 25 minutes, gradient curve = 6, 50 – 84% A in C; 25 – 30

minutes, gradient curve = 6, 84 – 10% A in C; B was held at 1% throughout the entire run. Sub-fractions (SFs) were dried, and then re-suspended in uptake buffer containing 0.1% DMSO (final concentration, 66.7 – 16.7 µg/ml) or methanol (final volume, 150 µl) for [^{3}H]-DA uptake studies and GC-MS analysis, respectively (*see sections 5.17 and 5.18, respectively*). In [^{3}H]-DA uptake studies, lobinaline was evaluated at four concentrations (51.5 – 6.4 µg/ml) in each 96-well plate to allow comparison to pHPLC SFs, and to ensure consistency between experiments.

13.2.3 Data Analysis

Graphical presentation of data were performed using GraphPad Prism software (Version 6.0; GraphPad Software, San Diego, CA, USA). Data were expressed as the mean ± S.E.M.

13.3. Study 2: Methods

13.3.1. Chemicals and supplies

Penicillin (10,000 units/ml), streptomycin (10,000 µg/mL), 2.5% trypsin (10x), heat inactivated fetal bovine serum (FBS), Dulbecco's Modified Eagle Medium (DMEM), and Hanks Balanced Salt Solution (HBSS) were purchased from Life Technologies Corporation (Grand Island, NY, USA). 1-methyl-4-phenylpyridinium (MPP^+) iodide, and 7-hydroxy-3H-phenoxazin-3-one-10-oxide sodium salt (resazurin) were purchased from Sigma-Aldrich (St Louis, MO, USA). All other chemicals and supplies were purchased from Fischer Scientific (Pittsburgh, PA, USA), unless stated otherwise.

13.3.2. Preparation of hairy root aqueous extracts and MPP^+ treatment solutions

L. cardinalis hairy root tissue was collected, flash frozen with liquid

nitrogen, and lyophilized. Immediately after removing tissue from the lyophilizer, freeze-dried plant tissue was ground to a fine powder and extracted with 3 volumes of water for 24-hours in the dark. The following day, *L. cardinalis* hairy root aqueous extracts (LCE) were obtained via vacuum filtration, filter sterilized (pore size, 0.45 µm), frozen, and dried with a lyophilizer. Solutions of LCEs (final concentration, 50.0 µg/ml) were prepared by dissolving the extracts in an appropriate volume of serum-free DMEM containing 0.5% DMSO, then 1:1 serial dilutions were performed (concentration of final dilution, 9.4 – 150.0 µg/ml). A solution of MPP^+ (final concentration, 3.0 mM) was prepared by dissolving the cytotoxin in serum-free DMEM containing 0.5% DMSO. Solutions of LCEs and MPP^+ in serum-free DMEM were prepared fresh on the day of the experiment, and filter sterilized (pore size, 0.45 µm).

13.3.3. SH-SY5Y Cell Culture

SY-SY5Y human neuroblastoma cells were obtained from the American Type Culture Collection (Manassas, VA, USA) and cultured as described previously with minor modifications [113, 124]. Cells were cultured in 60 mm dishes containing DMEM supplemented with 10% FBS (v/v), penicillin (100 units/ml), and streptomycin (100 µg/ml) in humidified 5% CO_2/95% air at 37°C. Culture medium was changed at 3-day intervals, and cells were subcultured roughly twice per week, or upon reaching 80% confluence.

13.3.4. MPP^+ treatment and measurement of cell viability

Experiments assessing the ability of LCEs to inhibit MPP+ toxicity in SH-SY5Y were performed as previously described with minor modifications [113, 124]. SH-SY5Y cells were seeded in 96-well plates at a density of 5 x 10^5 cells/ml (final volume, 100 µl) in DMEM supplemented with 10% FBS (v/v), penicillin (100 units/ml), and streptomycin (100 µg/ml), and maintained at 37°C in humidified 5% CO_2/95% air for ≥ 24 hours prior to further manipulation. After cells

adhered and reached ~80% confluence, cell culture medium was aspirated, cells were gently washed with HBSS, and then 50 µl of serum-free FBS or serum-free FBS containing LCE (final concentration, 3.1 – 50.0 µg/ml) was added to each well. LCEs did not cause toxicity at the concentration used in the present study. 96-well plates were incubated with various treatment solutions for 1 hour at 37°C, after which serum-free FBS containing 3.0 mM MPP^+ was added (final concentration, 1.0 mM), and then 96-well plates were maintained at 37°C in humidified 5% CO_2/95% air for 60 hours prior to assessing cell viability. In each 96-well plate, one column contained serum-free medium only, and a second column contained cells that were subject to all manipulations, but were only challenged with serum-free DMEM (i.e. no MPP^+ and/or LCE treatment). The former was used to subtract background signal, and the latter served as control. After 60 hours, resazurin (final concentration, 100.0 µM) was added to each well, and then 4 hours later fluorescence (excitation wavelength = 560 nm, emission wavelength = 590 nm) was measured using a Wallac 1420 VICTOR plate reader (PerkinElmer, MA, USA). Background fluorescence measured in wells containing serum-free FBS and resazurin only was subtracted from all treatment groups, and cell viability was normalized to that of controls.

13.3.5 Data analysis

Statistical analyses and graphical presentation of data were performed using GraphPad Prism software (Version 6.0; GraphPad Software, San Diego, CA, USA). Two-way ANOVA (treatment type x concentration) followed by Bonferroni's post-hoc analysis was performed to determine whether the extract from the TR-2°HR exerted significantly greater cytoprotection against MPP^+-induced cytotoxicity, compared the hDAT-1°HR extract, and to determine the concentrations at which the difference was significant. Here, treatment type refers to extracts from the hDAT-1°HR or the TR-2°HR. Two-way analysis of variance (treatment x concentration) followed by Tukey's post-hoc analysis was performed to determine the effect of the hDAT-1HR extract and the TR-2°HR

extract significantly attenuated MPP+-induced cytotoxicity as compared to vehicle treated controls, and to determine the concentrations at which each extract significantly attenuated MPP+-induced cytotoxicity. Data are expressed as the mean ± S.E.M. A p-value < 0.05 was defined as statistically significant.

13.4. Study 1: Results

13.4.1. Study 1: pHPLC SFs 1 – 9 from TR-2HR #479 inhibited [^{3}H]-DA uptake and contained negligible quantities of lobinaline

The MeOH extract from TR-2°HR #479 was sub-fractionated via pHPLC, and the SFs thus obtained were evaluated for their ability to inhibit DAT-mediated [^{3}H]-DA uptake in rat striatal synaptosomes. The SFs were also analyzed via GC-MS to identify the metabolites present and to quantify the amount of lobinaline present in each of the SFs.

SF-1 and SFs 3 – 8 dose-dependently inhibited [^{3}H]-DA uptake in rat striatal synaptosomes (**Figure 13.1**). Lobinaline was not detected in any of the SFs indicating that DAT inhibition produced by the SFs was contingent upon the presence of another bioactive metabolite/s. SF-2 and SF-9 also dose-dependently inhibited DAT-mediated [^{3}H]-DA uptake in rat striatal synaptosomes, which contained only trace amounts of lobinaline (AUC = 1.3% and 2.3%, respectively). The lobinaline content of all SFs is depicted in **Figure 13.2**. SFs beyond SF9 contained quantities of lobinaline that were readily detectably. Therefore, these fractions were not included in the present dissertation, since the presence of lobinaline presented a confound. The major metabolites detected in SF-1 and SF-2 were 2,4-bis(1,1-dimethylethyl)phenol (2,4-DTBP) and dodecyl acrylate. The identity of 2,4-DTBP and dodecyl acrylate was determined based on the MS spectra extracted from their respective chromatographic peaks. SFs 3 – 9 contained a mixture of metabolites, the majority of which could not be assigned a chemical structure.

13.5 Study 2: Results

Attenuation of MPP+-induced cytotoxicity in SH-SY5Y cells pretreated with an TR-2°HR aqueous extract was significantly greater than that observed in SH-SY5Y cells pretreated with an hDAT-1°HR extract (**Figure 13.3**). Two-way ANOVA (treatment type x concentration) revealed a significant effect of treatment type ($p < 0.001$), a significant effect of concentration ($p < 0.001$), and a significant treatment type x concentration interaction ($p < 0.05$). The aforementioned two-way ANOVA was performed to determine if the difference between treatment types was significant (i.e. hDAT-1°HR extract vs. TR-2°HR extract). An additional two-way ANOVA (treatment x concentration) revealed a significant effect of treatment ($p < 0.001$), a significant effect of concentration ($p < 0.001$), and a significant treatment by concentration interaction ($p = 0.0255$). This two-way ANOVA was utilized to compare the effect of the hDAT-1°HR extract or the TR-2°HR extract, as compared to vehicle treated controls. MPP^+-induced cytotoxicity in SH-SY5Y cells was significantly reduced by both the hDAT-1°HR and the TR-2°HR extracts, as compared to vehicle pretreated SH-SY5Y cells. However, at concentrations of 3.1, 6.3, and 12.5 µg/mL, the cytoprotective effect the TR-2°HR extract was significantly greater than that produced by the hDAT-1°HR extract ($p = 0.0123$, $p = 0.0288$, and $p = 0.0203$, respectively). At higher concentrations (25.0 and 100 µg/ml), the attenuation of MPP^+-induced cytotoxicity by the hDAT-1°HR and the TR-2°HR extract was not significantly different. The TR-2°HR extract displayed greater efficacy at attenuating MPP^+-induced cytotoxicity in SH-SY5Y cells, given the TR-2°HR extract's cytoprotective effect was significant at 3.1 µg/ml ($p < 0.001$), whereas a concentration ~8-fold greater (25.0 µg/ml, $p = 0.0100$) was required for the hDAT-1°HR extract's cytoprotective effect to reach significance.

13.6. Discussion

Plant cells were made to resemble DAergic neurons on a fundamental

level, i.e. the hDAT was expressed in transgenic plant cells of *L. cardinalis* [43, 52]. The transgenic plant cells were activation tagged creating a heterogeneous population of transgenic plant cells expressing the hDAT. This population was subject to selection on medium containing the neurotoxin MPP^+, which is accumulated via the DAT [89, 90]. Since *L. cardinalis* has the inherent biosynthetic potential to synthesize DAT inhibitors, gain-of-function mutations that enhanced transcription of genes that increased inhibitory modulation of the DAT was predicted to confer resistance to MPP^+. Indeed, the population of MPP^+ resistant mutant was enriched with mutants highly active at the DAT, or which survived selection via increased biosynthesis of cytoprotective compounds.

A gain-of-function mutant that displayed a dramatic increase in DAT inhibitory modulation (TR-2°HR #479) was chosen in an effort to identify a novel DAT inhibitor. A MeOH extracted prepared from the hairy root was sub-fractionated via pHPLC, and the SFs were evaluated for their ability to inhibit DAT-mediated DA uptake in rat striatal synaptosomes. In addition, the SFs were subject to chemical analysis to quantify lobinaline present in each SF. Indeed, SFs that lacked lobinaline, or only contained the alkaloid in trace amounts, inhibited the DAT-mediated [^{3}H]-DA uptake in rat striatal synaptosomes.

The two primary metabolites, if not the only metabolites present in SFs 1 – 2 were 2,4-DTBP and dodecyl acrylate. The former resembles tert-butylhydroquinone (tBHQ), which has previously been reported to activate Nrf2 signaling, which has been shown to exert neuroprotective effects [238, 240-242, 261]. Dodecyl acrylate resembles PUFAs, which may explain DAT inhibition produced by the SFs, considering a variety of PUFAs have been demonstrated to inhibit the DAT [74, 75]. That said, 2,4-DTBPs effects on the DAT cannot be ruled out. Thus, future studies remain to be performed to determine whether DAT inhibition caused by SFs 1 – 2 was attributable to 2,4-DTBP or dodecyl acrylate, or perhaps additive or synergistic actions of the two molecules.

In an additional set of studies, an hDAT-1°HR aqueous extract and a TR-2°HR extract were evaluated for their ability to attenuate MPP^+-toxicity in SH-SY5Y cells. Cytotoxicity caused by MPP^+ in SH-SY5Y cells is commonly utilized

as an in vitro to model DAergic neurodegeneration that occurs in PD, and to evaluate the potential cytoprotective and/or neuroprotective effects of molecules [92, 107-126]. Given TR-2°HRs were made to resemble DAergic neurons via expression of hDAT in the transgenic plant cells, and metabolites present in TR-2°HRs were predicted to exert similar cytoprotective effects in mammalian cells, the TR-2°HR extract was predicted to exert cytoprotection that was superior to that of the hDAT-1°HR extract. Both the hDAT-1°HR extract and the TR-2°HR extract attenuated MPP^+-induced cytotoxicity in SH-SY5Y cells. Furthermore, the cytoprotective effect of the TR-2°HRs' extract attenuated MPP^+-induced cytotoxicity at doses lower than that of the hDAT-1°HR extract. The fact that an ~8-fold higher concentration of the hDAT-1°HR extract was required to reach significance, as compared to the TR-2°HR extract, indicated that selection favored the survival of mutants whose extracts were more effective at preventing insults caused by DAergic neurotoxins. Although these data are preliminary in nature, they warrant further evaluation of the population to identify mutants that synthesize novel neuroprotective agents, given only a single TR-2°HRs' extract was tested.

The selection strategy used in the present study, target-directed biosynthesis, was capable of generating mutant plant cultures optimized for their pharmacological actions at a specific human target protein, here the hDAT. Additionally, mutants were generated whose extracts contained increased yields of cytoprotective metabolites previously reported to attenuate the effects of selective DAergic neurotoxins. Given these limited number of proof-of-concept studies successfully identified SFs that inhibited DAT and lacked lobinaline, and extracts from TR-2°HRs were superior to hDAT-1°HRs extracts with regards to their ability to attenuate MPP^+-induced toxicity, the technology seems very promising indeed. Future evaluation of the aforementioned TR-2°HRs population described in the present dissertation is warranted, such that the potential of target-directed biosynthesis can be truly be realized.

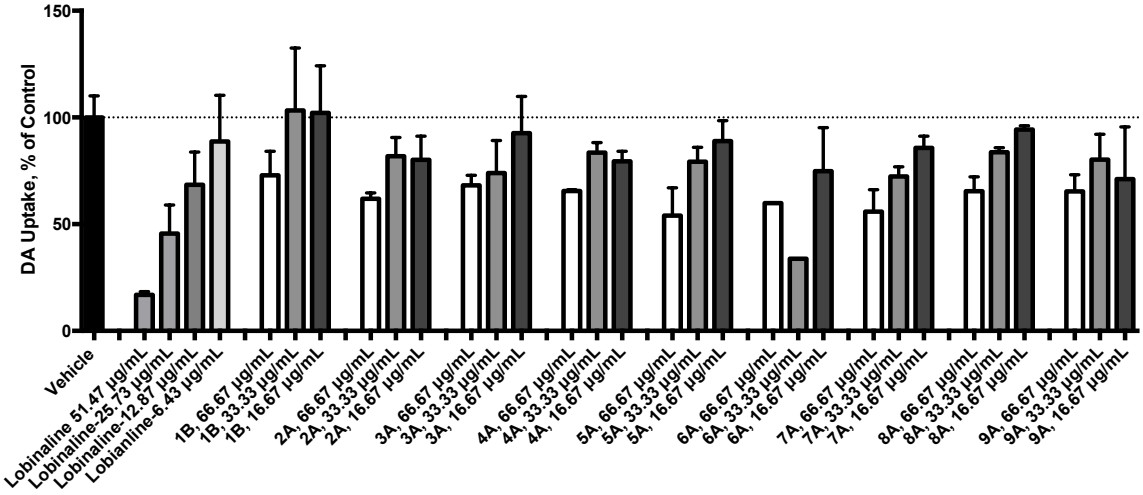

Figure 13.1. Sub-fractions 1 – 9 dose-dependently inhibited DAT-mediated [^{3}H]-DA uptake in rat striatal synaptosomes. Data expressed as the mean ± S.E.M. SFs 1 – 9, which lacked lobinaline or only contained trace amounts of the alkaloid, dose-dependently inhibited the DAT. SF-1 and SFs 3 – 8 lacked lobinaline, indicating DAT inhibition was dependent upon the presence of other bioactive metabolites. SF-1 and SF-9 contained only trace amounts of lobinaline, yet were still capable of inhibiting the DAT. The dotted line indicates the magnitude of specific [^{3}H]-DA uptake observed in rat striatal synaptosomes pretreated with vehicle. n = 3 – 4.

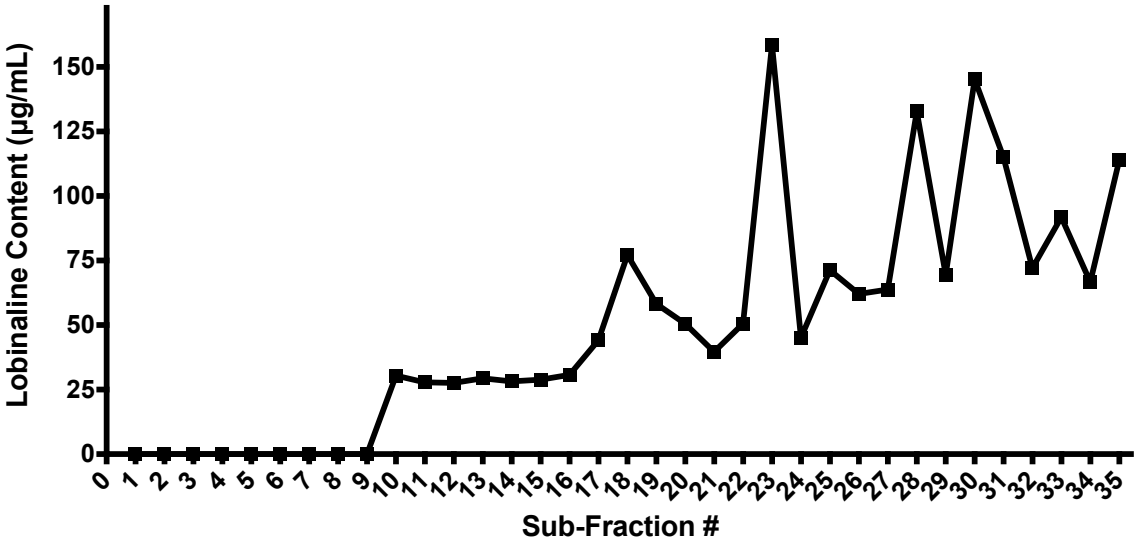

Figure 13.2. Lobinaline content of various pHPLC sub-fractions. Sub-fractions 1 – 9 contained undetectable or trace amounts of lobinaline.

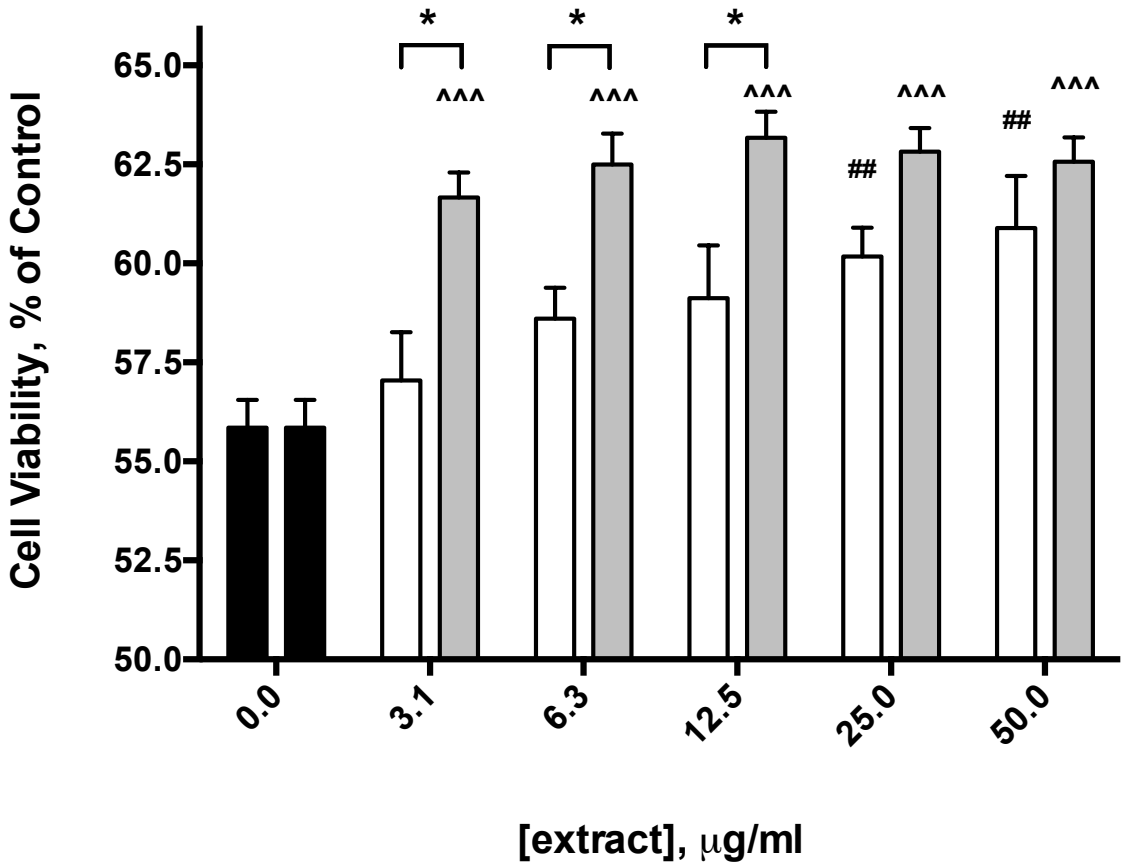

Figure 13.3. The X-2°HR (gray fill) aqueous extract's cytoprotective effect was significantly greater than the hDAT-1°HR (white fill) aqueous extract in SH-SY5Y cells treated with MPP^+. Data are expressed as the mean ± S.E.M. Both the hDAT-1°HR and the X-2°HR extract significantly attenuated MPP^+-induced cytotoxicity as compared to vehicle pretreated cells (black fill), albeit higher concentrations of the hDAT-1°HR extract were required to reach significance. ^^^ $p < 0.001$ vs. vehicle treated cells, ## $p < 0.01$ vs. vehicle treated cells, two-way ANOVA, Tukey's post hoc test. * $p < 0.05$, hDAT-1°HR extract vs. X-2°HR extract, two-way ANOVA, Bonferroni's post-hoc test. n = 6 – 21.

Chapter 14

Major findings and future directions

Herein, principles underlying the evolution of species via natural selection were applied to plant-based drug discovery to develop a novel approach to genomically optimize a plant's pharmacological profile, coined target-directed biosynthesis. The technology enables one to redirect plant evolution such that the biosynthesis of metabolites meant to interact with a specific human target protein is favored.

In the present dissertation, proof-of-concept was demonstrated in the species *Lobelia cardinalis*. The major alkaloid present in *L. cardinalis* was identified as possessing a unique combination of pharmacological effects relevant to the treatment of drug abuse and dopaminergic neurodegeneration [80, 81, 135, 174, 175]. The complex multifunctional decahydroquinoline alkaloid acts as an agonist at nicAchRs, an inhibitor of the DAT, and a relatively potent free radical scavenger [80, 81, 135, 174, 175]. To the best of our knowledge, this combination of multi-target effects has not been reported for any other natural product, representing a structural scaffold with potential for the development of pharmaceuticals with the aforementioned multifunctional pharmacological activities.

The activity of *L. cardinalis* was optimized for activity at the hDAT, a potential target for therapeutics aimed for the treatment of drug abuse and/or neurodegeneration [59, 60, 65, 66, 70, 79, 95-101]. The hDAT was expressed in transgenic *L. cardinalis* plant cells increasing their susceptibility to the cytotoxic DAT substrate MPP^+ [89, 90]. DAT inhibitors prevented the cytotoxic actions of MPP^+ in transgenic *L. cardinalis* plant cells. As such, selection of a population of genetically heterogeneous plant cells on medium containing MPP^+ would be predicted to favor the survival of individuals with a greater capacity to synthesize

DAT inhibitors. Genetic heterogeneity was achieved by creating a population of gain-of-function mutant *L. cardinalis* plant cells expressing the hDAT, each possessing a unique mutation, which enhanced of gene transcription [14, 16-19, 221]. Indeed, selection of the gain-of-function mutant population favored individuals with a marked increase in DAT inhibitory activity. This provides proof-of-concept for the ability of the technology to evolve a plant species toward a desired pharmacological phenotype. In addition, DAT inhibition arose due to increased biosynthesis of lobinaline, in addition to "novel" DAT inhibitors (i.e. active metabolites not readily detectable in the wild-type plant). This provides proof-of-concept for the ability of the technology to act as a plant drug discovery platform targeted on a specific protein. In parallel, subpopulations of gain-of-function mutants resistant to MPP^+ via mechanisms independent of DAT inhibition were generated. This included gain-of-function mutants with increased yields of metabolites previously reported to attenuate the cytotoxic effects of the DAergic neurotoxins, including squalene and polyunsaturated fatty acids, in addition to individuals with increased yields of putatively "novel" cytoprotective metabolites and as yet undetermined mechanisms of MPP^+-resistance [93, 94, 226, 227].

This novel approach to plant-based drug discovery could be applied to numerous molecular targets and plant species, representing a new approach to develop drug leads whose "druggability" may be superior to than that of synthetics. Target-directed biosynthesis could potentially revitalize and revolutionize plant-based drug discovery fueling the parched pipelines of drug discovery programs with leads of increased diversity and complexity. Furthermore, the application of the technology is not limited to the production of pharmaceuticals. Rather, target-directed biosynthesis represents a viable strategy for other avenues such as the production of valuable agrochemicals and the generation of plants suitable for phytoremediation (i.e. those capable of removing accumulating toxins facilitating their removal from contaminated soil). Target-directed biosynthesis has tremendous potential for application to

numerous disciplines. It is a technology which could revolutionize the way in which we view evolution of the plant genome.

References

1. Sulzer, D., *How addictive drugs disrupt presynaptic dopamine neurotransmission.* Neuron, 2011. **69**(4): p. 628-49.
2. De Luca, V., et al., *Mining the biodiversity of plants: a revolution in the making.* Science, 2012. **336**(6089): p. 1658-61.
3. Mishra, B.B. and V.K. Tiwari, *Natural products: an evolving role in future drug discovery.* Eur J Med Chem, 2011. **46**(10): p. 4769-807.
4. Koehn, F.E. and G.T. Carter, *The evolving role of natural products in drug discovery.* Nat Rev Drug Discov, 2005. **4**(3): p. 206-20.
5. Li, J.W. and J.C. Vederas, *Drug discovery and natural products: end of an era or an endless frontier?* Science, 2009. **325**(5937): p. 161-5.
6. Newman, D.J. and G.M. Cragg, *Natural products as sources of new drugs over the 30 years from 1981 to 2010.* J Nat Prod, 2012. **75**(3): p. 311-35.
7. Spainhour, C.B., *Natural Products*, in *Drug Discovery Handbook*. 2005, John Wiley & Sons, Inc. p. 11-72.
8. Feher, M. and J.M. Schmidt, *Property distributions: differences between drugs, natural products, and molecules from combinatorial chemistry.* J Chem Inf Comput Sci, 2003. **43**(1): p. 218-27.
9. Katiyar, C., et al., *Drug discovery from plant sources: An integrated approach.* Ayu, 2012. **33**(1): p. 10-9.
10. Danishefsky, S., *On the potential of natural products in the discovery of pharma leads: a case for reassessment.* Nat Prod Rep, 2010. **27**(8): p. 1114-6.
11. Georgiev, M.I., A.I. Pavlov, and T. Bley, *Hairy root type plant in vitro systems as sources of bioactive substances.* Appl Microbiol Biotechnol, 2007. **74**(6): p. 1175-85.
12. Hartl, D.L. and E.W. Jones, *Genetics : analysis of genes and genomes*. 2005, Sudbury, Mass.: Jones and Bartlett Publishers.
13. Kennedy, D.O. and E.L. Wightman, *Herbal extracts and phytochemicals: plant secondary metabolites and the enhancement of human brain function.* Adv Nutr, 2011. **2**(1): p. 32-50.

14. Littleton, J., *The future of plant drug discovery.* Expert Opinion on Drug Discovery, 2007. **2**(5): p. 673-683.
15. Littleton, J., T. Rogers, and D. Falcone, *Novel approaches to plant drug discovery based on high throughput pharmacological screening and genetic manipulation.* Life Sciences, 2005. **78**(5): p. 467-475.
16. Weigel, D., et al., *Activation tagging in Arabidopsis.* Plant Physiol, 2000. **122**(4): p. 1003-13.
17. Tani, H., et al., *Activation tagging in plants: a tool for gene discovery.* Funct Integr Genomics, 2004. **4**(4): p. 258-66.
18. Fritze, K. and R. Walden, *Gene activation by T-DNA tagging.* Methods Mol Biol, 1995. **44**: p. 281-94.
19. Seki, H., et al., *Hairy root-activation tagging: a high-throughput system for activation tagging in transformed hairy roots.* Plant Mol Biol, 2005. **59**(5): p. 793-807.
20. Salim, A.A., Y.-W. Chin, and A.D. Kinghorn, *Drug Discovery from Plants*, in *Bioactive Molecules and Medicinal Plants*, K.G. Ramawat and J.M. Merillon, Editors. 2008, Springer Berlin Heidelberg. p. 1-24.
21. Leaviss, J., et al., *What is the clinical effectiveness and cost-effectiveness of cytisine compared with varenicline for smoking cessation? A systematic review and economic evaluation.* Health Technol Assess, 2014. **18**(33): p. 1-120.
22. Daly, J.W., *Nicotinic agonists, antagonists, and modulators from natural sources.* Cell Mol Neurobiol, 2005. **25**(3-4): p. 513-52.
23. Vocci, F.J. and N.M. Appel, *Approaches to the development of medications for the treatment of methamphetamine dependence.* Addiction, 2007. **102 Suppl 1**: p. 96-106.
24. Montoya, I.D. and F. Vocci, *Novel medications to treat addictive disorders.* Curr Psychiatry Rep, 2008. **10**(5): p. 392-8.
25. Karila, L., et al., *Pharmacological approaches to methamphetamine dependence: a focused review.* Br J Clin Pharmacol, 2010. **69**(6): p. 578-92.

26. Appendino, G., A. Minassi, and O. Taglialatela-Scafati, *Recreational drug discovery: natural products as lead structures for the synthesis of smart drugs.* Nat Prod Rep, 2014. **31**(7): p. 880-904.
27. Hosztafi, S., *Recent Advances in the Chemistry of Oripavine and Its Derivatives.* Advances in Bioscience and Biotechnology, 2014. **2014**.
28. Balunas, M.J. and A.D. Kinghorn, *Drug discovery from medicinal plants.* Life Sci, 2005. **78**(5): p. 431-41.
29. Steppuhn, A., et al., *Nicotine's defensive function in nature.* PLoS Biol, 2004. **2**(8): p. E217.
30. Nathanson, J.A., et al., *Cocaine as a naturally occurring insecticide.* Proceedings of the National Academy of Sciences of the United States of America, 1993. **90**(20): p. 9645-9648.
31. Barik, J. and S. Wonnacott, *Molecular and cellular mechanisms of action of nicotine in the CNS.* Handb Exp Pharmacol, 2009(192): p. 173-207.
32. Gotti, C. and F. Clementi, *Neuronal nicotinic receptors: from structure to pathology.* Prog Neurobiol, 2004. **74**(6): p. 363-96.
33. Mortensen, O.V. and S.G. Amara, *Dynamic regulation of the dopamine transporter.* Eur J Pharmacol, 2003. **479**(1-3): p. 159-70.
34. Penmatsa, A., K.H. Wang, and E. Gouaux, *X-ray structure of dopamine transporter elucidates antidepressant mechanism.* Nature, 2013. **503**(7474): p. 85-90.
35. Barron, A.B., E. Sovik, and J.L. Cornish, *The roles of dopamine and related compounds in reward-seeking behavior across animal phyla.* Front Behav Neurosci, 2010. **4**: p. 163.
36. Allen, J.M., B.H. Van Kummer, and R.W. Cohen, *Dopamine as an anorectic neuromodulator in the cockroach Rhyparobia maderae.* The Journal of experimental biology, 2011. **214**(22): p. 3843-3849.
37. Bainton, R.J., et al., *Dopamine modulates acute responses to cocaine, nicotine and ethanol in Drosophila.* Curr Biol, 2000. **10**(4): p. 187-94.
38. Volkow, N.D., *Cocaine: Abuse and addiction.* NIH Publication, 2010: p. 10-4166.

39. Hanson, G., *NIDA Research Report Series: Methamphetamine Abuse and Addiction.* Rockville, MD: National Clearinghouse on Alcohol and Drug Information, 2002.
40. Yahyavi-Firouz-Abadi, N. and R.E. See, *Anti-relapse medications: preclinical models for drug addiction treatment.* Pharmacol Ther, 2009. **124**(2): p. 235-47.
41. Tiihonen, J., et al., *A comparison of aripiprazole, methylphenidate, and placebo for amphetamine dependence.* Am J Psychiatry, 2007. **164**(1): p. 160-2.
42. Lile, J.A., *Pharmacological determinants of the reinforcing effects of psychostimulants: relation to agonist substitution treatment.* Exp Clin Psychopharmacol, 2006. **14**(1): p. 20-33.
43. Giros, B., et al., *Hyperlocomotion and indifference to cocaine and amphetamine in mice lacking the dopamine transporter.* Nature, 1996. **379**(6566): p. 606-12.
44. Pontieri, F.E., G. Tanda, and G. Di Chiara, *Intravenous cocaine, morphine, and amphetamine preferentially increase extracellular dopamine in the "shell" as compared with the "core" of the rat nucleus accumbens.* Proc Natl Acad Sci U S A, 1995. **92**(26): p. 12304-8.
45. Pierce, R.C. and V. Kumaresan, *The mesolimbic dopamine system: the final common pathway for the reinforcing effect of drugs of abuse?* Neurosci Biobehav Rev, 2006. **30**(2): p. 215-38.
46. Cass, W.A., et al., *Clearance of exogenous dopamine in rat dorsal striatum and nucleus accumbens: role of metabolism and effects of locally applied uptake inhibitors.* J Neurochem., 1993. **61**(6): p. 2269-78.
47. Williams, J.M. and A. Galli, *The dopamine transporter: a vigilant border control for psychostimulant action.* Handb Exp Pharmacol, 2006(175): p. 215-32.
48. Schmitt, K.C. and M.E. Reith, *Regulation of the dopamine transporter: aspects relevant to psychostimulant drugs of abuse.* Ann N Y Acad Sci, 2010. **1187**: p. 316-40.

49. Zhu, J. and M.E. Reith, *Role of the dopamine transporter in the action of psychostimulants, nicotine, and other drugs of abuse.* CNS Neurol Disord Drug Targets, 2008. **7**(5): p. 393-409.
50. Gainetdinov, R.R., T.D. Sotnikova, and M.G. Caron, *Monoamine transporter pharmacology and mutant mice.* Trends Pharmacol Sci, 2002. **23**(8): p. 367-73.
51. Zahniser, N.R. and A. Sorkin, *Rapid regulation of the dopamine transporter: role in stimulant addiction?* Neuropharmacology, 2004. **47 Suppl 1**: p. 80-91.
52. Sotnikova, T.D., et al., *Molecular biology, pharmacology and functional role of the plasma membrane dopamine transporter.* CNS Neurol Disord Drug Targets, 2006. **5**(1): p. 45-56.
53. Giros, B. and M.G. Caron, *Molecular characterization of the dopamine transporter.* Trends Pharmacol Sci, 1993. **14**(2): p. 43-9.
54. Schmitt, K.C., R.B. Rothman, and M.E. Reith, *Nonclassical pharmacology of the dopamine transporter: atypical inhibitors, allosteric modulators, and partial substrates.* J Pharmacol Exp Ther, 2013. **346**(1): p. 2-10.
55. Eriksen, J., T.N. Jorgensen, and U. Gether, *Regulation of dopamine transporter function by protein-protein interactions: new discoveries and methodological challenges.* J Neurochem, 2010. **113**(1): p. 27-41.
56. Baumann, M.H., et al., *Preclinical evaluation of GBR12909 decanoate as a long-acting medication for methamphetamine dependence.* Ann N Y Acad Sci, 2002. **965**: p. 92-108.
57. Chen, R., et al., *Abolished cocaine reward in mice with a cocaine-insensitive dopamine transporter.* Proc Natl Acad Sci U S A, 2006. **103**(24): p. 9333-8.
58. Wu, H., et al., *Restoration of cocaine stimulation and reward by reintroducing wild type dopamine transporter in adult knock-in mice with a cocaine-insensitive dopamine transporter.* Neuropharmacology, 2014. **86**: p. 31-7.

59. Rothman, R.B., et al., *Dopamine transport inhibitors based on GBR12909 and benztropine as potential medications to treat cocaine addiction.* Biochem Pharmacol, 2008. **75**(1): p. 2-16.
60. Desai, R.I., et al., *Pharmacological characterization of a dopamine transporter ligand that functions as a cocaine antagonist.* J Pharmacol Exp Ther, 2014. **348**(1): p. 106-15.
61. Smith, M.P., et al., *Dopaminergic agents for the treatment of cocaine abuse.* Drug Discov Today, 1999. **4**(7): p. 322-332.
62. Velazquez-Sanchez, C., et al., *The dopamine uptake inhibitor 3 alpha-[bis(4'-fluorophenyl)metoxy]-tropane reduces cocaine-induced early-gene expression, locomotor activity, and conditioned reward.* Neuropsychopharmacology, 2009. **34**(12): p. 2497-507.
63. Xi, Z.X. and E.L. Gardner, *Hypothesis-driven medication discovery for the treatment of psychostimulant addiction.* Curr Drug Abuse Rev, 2008. **1**(3): p. 303-27.
64. Vocci, F.J., J. Acri, and A. Elkashef, *Medication development for addictive disorders: the state of the science.* Am J Psychiatry, 2005. **162**(8): p. 1432-40.
65. Batman, A.M., et al., *The selective dopamine uptake inhibitor, D-84, suppresses cocaine self-administration, but does not occasion cocaine-like levels of generalization.* Eur J Pharmacol, 2010. **648**(1-3): p. 127-32.
66. Howell, L.L. and K.M. Wilcox, *The dopamine transporter and cocaine medication development: drug self-administration in nonhuman primates.* J Pharmacol Exp Ther, 2001. **298**(1): p. 1-6.
67. Perez-Mana, C., et al., *Efficacy of indirect dopamine agonists for psychostimulant dependence: a systematic review and meta-analysis of randomized controlled trials.* J Subst Abuse Treat, 2011. **40**(2): p. 109-22.
68. Elkashef, A., et al., *Pharmacotherapy of methamphetamine addiction: an update.* Subst Abus, 2008. **29**(3): p. 31-49.

69. Agoston, G.E., et al., *Novel N-substituted 3 alpha-[bis(4'-fluorophenyl)methoxy]tropane analogues: selective ligands for the dopamine transporter.* J Med Chem, 1997. **40**(26): p. 4329-39.
70. Li, L., et al., *The stereotypy-inducing effects of N-substituted benztropine analogs alone and in combination with cocaine do not account for their blockade of cocaine self-administration.* Psychopharmacology (Berl), 2013. **225**(3): p. 733-42.
71. Chi, K.R., *Revolution dawning in cardiotoxicity testing.* Nat Rev Drug Discov, 2013. **12**(8): p. 565-7.
72. Tanda, G., et al., *Relations between stimulation of mesolimbic dopamine and place conditioning in rats produced by cocaine or drugs that are tolerant to dopamine transporter conformational change.* Psychopharmacology (Berl), 2013. **229**(2): p. 307-21.
73. Gether, U., et al., *Neurotransmitter transporters: molecular function of important drug targets.* Trends Pharmacol Sci, 2006. **27**(7): p. 375-83.
74. Ingram, S.L. and S.G. Amara, *Arachidonic acid stimulates a novel cocaine-sensitive cation conductance associated with the human dopamine transporter.* J Neurosci, 2000. **20**(2): p. 550-7.
75. Chen, N., et al., *Inhibition by arachidonic acid and other fatty acids of dopamine uptake at the human dopamine transporter.* Eur J Pharmacol, 2003. **478**(2-3): p. 89-95.
76. Farhan, H., M. Freissmuth, and H.H. Sitte, *Oligomerization of neurotransmitter transporters: a ticket from the endoplasmic reticulum to the plasma membrane.* Handb Exp Pharmacol, 2006(175): p. 233-49.
77. Gorentla, B.K. and R.A. Vaughan, *Differential effects of dopamine and psychoactive drugs on dopamine transporter phosphorylation and regulation.* Neuropharmacology, 2005. **49**(6): p. 759-68.
78. Cass, W.A. and G.A. Gerhardt, *Direct in vivo evidence that D2 dopamine receptors can modulate dopamine uptake.* Neurosci Lett., 1994. **176**(2): p. 259-63.

79. Schmitt, K.C., et al., *INTERACTION OF COCAINE-, BENZTROPINE-, AND GBR12909-LIKE COMPOUNDS WITH WILDTYPE AND MUTANT HUMAN DOPAMINE TRANSPORTERS: MOLECULAR FEATURES THAT DIFFERENTIALLY DETERMINE ANTAGONIST BINDING PROPERTIES.* Journal of neurochemistry, 2008. **107**(4): p. 928-940.
80. Gupta, R.N. and I.D. Spenser, *Biosynthesis of Lobinaline.* Canadian Journal of Chemistry, 1971. **49**(3): p. 384-397.
81. Manske, R.H.F., *LOBINALINE, AN ALKALOID FROM LOBELIA CARDINALIS L.* Canadian Journal of Research, 1938. **16b**(12): p. 445-448.
82. Schapira, A.H.V., *Mitochondrial dysfunction in Parkinson's disease.* Cell Death and Differentiation, 2007. **14**(7): p. 1261-1266.
83. Cass, W.A., et al., *Clearance of exogenous dopamine in rat dorsal striatum and nucleus accumbens: role of metabolism and effects of locally applied uptake inhibitors.* J Neurochem, 1993. **61**(6): p. 2269-78.
84. Berger, P., et al., *[3H]GBR-12935: a specific high affinity ligand for labeling the dopamine transport complex.* Eur J Pharmacol, 1985. **107**(2): p. 289-90.
85. Heikkila, R.E. and L. Manzino, *Behavioral properties of GBR 12909, GBR 13069 and GBR 13098: specific inhibitors of dopamine uptake.* Eur J Pharmacol, 1984. **103**(3-4): p. 241-8.
86. Andersen, P.H., *Biochemical and pharmacological characterization of [3H]GBR 12935 binding in vitro to rat striatal membranes: labeling of the dopamine uptake complex.* J Neurochem, 1987. **48**(6): p. 1887-96.
87. Boos, T.L., et al., *Structure-activity relationships of substituted N-benzyl piperidines in the GBR series: Synthesis of 4-(2-(bis(4-fluorophenyl)methoxy)ethyl)-1-(2-trifluoromethylbenzyl)piperidine, an allosteric modulator of the serotonin transporter.* Bioorg Med Chem, 2006. **14**(11): p. 3967-73.

88. Rothman, R.B., et al., *Tight binding dopamine reuptake inhibitors as cocaine antagonists. A strategy for drug development.* FEBS Lett, 1989. **257**(2): p. 341-4.
89. Pifl, C., B. Giros, and M.G. Caron, *Dopamine transporter expression confers cytotoxicity to low doses of the parkinsonism-inducing neurotoxin 1-methyl-4-phenylpyridinium.* J Neurosci, 1993. **13**(10): p. 4246-53.
90. Kopin, I.J., *MPTP: an industrial chemical and contaminant of illicit narcotics stimulates a new era in research on Parkinson's disease.* Environ Health Perspect, 1987. **75**: p. 45-51.
91. Di Monte, D.A., et al., *Relationship among nigrostriatal denervation, parkinsonism, and dyskinesias in the MPTP primate model.* Mov Disord, 2000. **15**(3): p. 459-66.
92. Fall, C.P. and J.P. Bennett, Jr., *Characterization and time course of MPP+ -induced apoptosis in human SH-SY5Y neuroblastoma cells.* J Neurosci Res, 1999. **55**(5): p. 620-8.
93. Kabuto, H., et al., *Effects of squalene/squalane on dopamine levels, antioxidant enzyme activity, and fatty acid composition in the striatum of Parkinson's disease mouse model.* J Oleo Sci, 2013. **62**(1): p. 21-8.
94. Tang, K.S., *Protective effect of arachidonic acid and linoleic acid on 1-methyl-4-phenylpyridinium-induced toxicity in PC12 cells.* Lipids Health Dis, 2014. **13**: p. 197.
95. Storch, A., A.C. Ludolph, and J. Schwarz, *Dopamine transporter: involvement in selective dopaminergic neurotoxicity and degeneration.* J Neural Transm, 2004. **111**(10-11): p. 1267-86.
96. Fleming, S.M., Y. Delville, and T. Schallert, *An intermittent, controlled-rate, slow progressive degeneration model of Parkinson's disease: antiparkinson effects of Sinemet and protective effects of methylphenidate.* Behav Brain Res, 2005. **156**(2): p. 201-13.
97. Cicchetti, F., J. Drouin-Ouellet, and R.E. Gross, *Environmental toxins and Parkinson's disease: what have we learned from pesticide-induced animal models?* Trends Pharmacol Sci, 2009. **30**(9): p. 475-83.

98. Hornykiewicz, O., *Biochemical aspects of Parkinson's disease.* Neurology, 1998. **51**(2 Suppl 2): p. S2-9.
99. Marek, G.J., G. Vosmer, and L.S. Seiden, *Dopamine uptake inhibitors block long-term neurotoxic effects of methamphetamine upon dopaminergic neurons.* Brain Res, 1990. **513**(2): p. 274-9.
100. Dekundy, A., et al., *Effects of dopamine uptake inhibitor MRZ-9547 in animal models of Parkinson's disease.* J Neural Transm, 2014.
101. Huot, P., et al., *UWA-121, a mixed dopamine and serotonin re-uptake inhibitor, enhances L-DOPA anti-parkinsonian action without worsening dyskinesia or psychosis-like behaviours in the MPTP-lesioned common marmoset.* Neuropharmacology, 2014. **82**: p. 76-87.
102. Sandoval, V., et al., *Methylphenidate alters vesicular monoamine transport and prevents methamphetamine-induced dopaminergic deficits.* J Pharmacol Exp Ther, 2003. **304**(3): p. 1181-7.
103. Schmidt, C.J. and J.W. Gibb, *Role of the dopamine uptake carrier in the neurochemical response to methamphetamine: effects of amfonelic acid.* Eur J Pharmacol, 1985. **109**(1): p. 73-80.
104. Cadet, J.L. and I.N. Krasnova, *Molecular bases of methamphetamine-induced neurodegeneration.* Int Rev Neurobiol, 2009. **88**: p. 101-19.
105. Luo, Y., et al., *Mitochondria: A Therapeutic Target for Parkinson's Disease?* Int J Mol Sci, 2015. **16**(9): p. 20704-30.
106. Fernandez-Moriano, C., E. Gonzalez-Burgos, and M.P. Gomez-Serranillos, *Mitochondria-Targeted Protective Compounds in Parkinson's and Alzheimer's Diseases.* Oxid Med Cell Longev, 2015. **2015**: p. 408927.
107. Storch, A., et al., *6-Hydroxydopamine toxicity towards human SH-SY5Y dopaminergic neuroblastoma cells: independent of mitochondrial energy metabolism.* Journal of Neural Transmission, 2000. **107**(3): p. 281-293.
108. Wu, C.R., et al., *Carnosic acid protects against 6-hydroxydopamine-induced neurotoxicity in in vivo and in vitro model of Parkinson's disease: involvement of antioxidative enzymes induction.* Chem Biol Interact, 2015. **225**: p. 40-6.

109. Song, J.X., et al., *Chrysotoxine, a novel bibenzyl compound, inhibits 6-hydroxydopamine induced apoptosis in SH-SY5Y cells via mitochondria protection and NF-kappaB modulation.* Neurochem Int, 2010. **57**(6): p. 676-89.
110. Martins, J.B., et al., *Differential Effects of Methyl-4-Phenylpyridinium Ion, Rotenone, and Paraquat on Differentiated SH-SY5Y Cells.* J Toxicol, 2013. **2013**: p. 347312.
111. Ridley, D.L., J. Pakkanen, and S. Wonnacott, *Effects of chronic drug treatments on increases in intracellular calcium mediated by nicotinic acetylcholine receptors in SH-SY5Y cells.* Br J Pharmacol, 2002. **135**(4): p. 1051-9.
112. Fujimaki, T., et al., *Identification of licopyranocoumarin and glycyrurol from herbal medicines as neuroprotective compounds for Parkinson's disease.* PLoS One, 2014. **9**(6): p. e100395.
113. Yi, F., X. He, and D. Wang, *Lycopene protects against MPP(+)-induced cytotoxicity by maintaining mitochondrial function in SH-SY5Y cells.* Neurochem Res, 2013. **38**(8): p. 1747-57.
114. Kim, H.G., et al., *Mulberry fruit protects dopaminergic neurons in toxin-induced Parkinson's disease models.* Br J Nutr, 2010. **104**(1): p. 8-16.
115. Kajimura, Y., et al., *Neoechinulin A protects PC12 cells against MPP+-induced cytotoxicity.* J Antibiot (Tokyo), 2008. **61**(5): p. 330-3.
116. Filomeni, G., et al., *Neuroprotection of kaempferol by autophagy in models of rotenone-mediated acute toxicity: possible implications for Parkinson's disease.* Neurobiol Aging, 2012. **33**(4): p. 767-85.
117. Liu, W.B., et al., *Neuroprotective effect of osthole on MPP+-induced cytotoxicity in PC12 cells via inhibition of mitochondrial dysfunction and ROS production.* Neurochem Int, 2010. **57**(3): p. 206-15.
118. Jazwa, A., et al., *Pharmacological targeting of the transcription factor Nrf2 at the basal ganglia provides disease modifying therapy for experimental parkinsonism.* Antioxid Redox Signal, 2011. **14**(12): p. 2347-60.

119. Bournival, J., P. Quessy, and M.G. Martinoli, *Protective effects of resveratrol and quercetin against MPP+ -induced oxidative stress act by modulating markers of apoptotic death in dopaminergic neurons.* Cell Mol Neurobiol, 2009. **29**(8): p. 1169-80.
120. Rojas, P., et al., *S-Allylcysteine, a garlic compound, protects against oxidative stress in 1-methyl-4-phenylpyridinium-induced parkinsonism in mice.* J Nutr Biochem, 2011. **22**(10): p. 937-44.
121. Wang, X.J. and J.X. Xu, *Salvianic acid A protects human neuroblastoma SH-SY5Y cells against MPP+-induced cytotoxicity.* Neurosci Res, 2005. **51**(2): p. 129-38.
122. Zhou, J., et al., *Salvianolic acid B attenuates toxin-induced neuronal damage via Nrf2-dependent glial cells-mediated protective activity in Parkinson's disease models.* PLoS One, 2014. **9**(7): p. e101668.
123. Xie, H.R., L.S. Hu, and G.Y. Li, *SH-SY5Y human neuroblastoma cell line: in vitro cell model of dopaminergic neurons in Parkinson's disease.* Chin Med J (Engl), 2010. **123**(8): p. 1086-92.
124. Presgraves, S.P., et al., *Terminally differentiated SH-SY5Y cells provide a model system for studying neuroprotective effects of dopamine agonists.* Neurotox Res, 2004. **5**(8): p. 579-98.
125. Sun, F.L., et al., *Tetrahydroxystilbene glucoside protects human neuroblastoma SH-SY5Y cells against MPP+-induced cytotoxicity.* Eur J Pharmacol, 2011. **660**(2-3): p. 283-90.
126. Takahashi, T., et al., *Uptake of a neurotoxin-candidate, (R)-1,2-dimethyl-6,7-dihydroxy-1,2,3,4-tetrahydroisoquinoline into human dopaminergic neuroblastoma SH-SY5Y cells by dopamine transport system.* J Neural Transm Gen Sect, 1994. **98**(2): p. 107-18.
127. Koylu, E., et al., *Sex difference in up-regulation of nicotinic acetylcholine receptors in rat brain.* Life Sci, 1997. **61**(12): p. PL 185-90.
128. Davies, A.R., et al., *Characterisation of the binding of [3H]methyllycaconitine: a new radioligand for labelling alpha 7-type*

neuronal nicotinic acetylcholine receptors. Neuropharmacology, 1999. **38**(5): p. 679-90.

129. Gattu, M., A.V. Terry, Jr., and J.J. Buccafusco, *A rapid microtechnique for the estimation of muscarinic and nicotinic receptor binding parameters using 96-well filtration plates.* J Neurosci Methods, 1995. **63**(1-2): p. 121-25.
130. Gnadisch, D., et al., *High affinity binding of [3H]epibatidine to rat brain membranes.* Neuroreport, 1999. **10**(8): p. 1631-6.
131. Gerzanich, V., et al., *Comparative pharmacology of epibatidine: a potent agonist for neuronal nicotinic acetylcholine receptors.* Mol Pharmacol, 1995. **48**(4): p. 774-82.
132. Lopez, M.G., et al., *Unmasking the functions of the chromaffin cell alpha7 nicotinic receptor by using short pulses of acetylcholine and selective blockers.* Proc Natl Acad Sci U S A, 1998. **95**(24): p. 14184-9.
133. Hall, M., et al., *Characterization of [3H]cytisine binding to human brain membrane preparations.* Brain Res, 1993. **600**(1): p. 127-33.
134. Saitoh, F., M. Noma, and N. Kawashima, *The alkaloid contents of sixty Nicotiana species.* Phytochemistry, 1985. **24**(3): p. 477-480.
135. Clugston, D.M., D.B. MacLean, and R.H.F. Manske, *The examination of lobinaline and some degradation products by mass spectrometry.* Canadian Journal of Chemistry, 1967. **45**(1): p. 39-47.
136. Lutz, J.A., et al., *A nicotinic receptor-mediated anti-inflammatory effect of the flavonoid rhamnetin in BV2 microglia.* Fitoterapia, 2014. **98**: p. 11-21.
137. Kimura, M., et al., *Syntheses of novel diphenyl piperazine derivatives and their activities as inhibitors of dopamine uptake in the central nervous system.* Bioorg Med Chem, 2003. **11**(8): p. 1621-30.
138. Wada, A., et al., *Inhibition of Na+-pump enhances carbachol-induced influx of 45Ca2+ and secretion of catecholamines by elevation of cellular accumulation of 22Na+ in cultured bovine adrenal medullary cells.* Naunyn Schmiedebergs Arch Pharmacol, 1986. **332**(4): p. 351-6.

139. Gandia, L., et al., *Inhibition of nicotinic receptor-mediated responses in bovine chromaffin cells by diltiazem.* Br J Pharmacol, 1996. **118**(5): p. 1301-7.
140. Grando, S.A., et al., *Activation of keratinocyte nicotinic cholinergic receptors stimulates calcium influx and enhances cell differentiation.* J Invest Dermatol, 1996. **107**(3): p. 412-8.
141. Saw, C.L., et al., *The berry constituents quercetin, kaempferol, and pterostilbene synergistically attenuate reactive oxygen species: involvement of the Nrf2-ARE signaling pathway.* Food Chem Toxicol, 2014. **72**: p. 303-11.
142. Dwoskin, L.P. and N.R. Zahniser, *Robust modulation of [3H]dopamine release from rat striatal slices by D-2 dopamine receptors.* J Pharmacol Exp Ther, 1986. **239**(2): p. 442-53.
143. Teng, L., et al., *Lobeline and nicotine evoke [3H]overflow from rat striatal slices preloaded with [3H]dopamine: differential inhibition of synaptosomal and vesicular [3H]dopamine uptake.* J Pharmacol Exp Ther, 1997. **280**(3): p. 1432-44.
144. Miller, D.K., P.A. Crooks, and L.P. Dwoskin, *Lobeline inhibits nicotine-evoked [(3)H]dopamine overflow from rat striatal slices and nicotine-evoked (86)Rb(+) efflux from thalamic synaptosomes.* Neuropharmacology, 2000. **39**(13): p. 2654-62.
145. Gerhardt, G.A. and A.F. Hoffman, *Effects of recording media composition on the responses of Nafion-coated carbon fiber microelectrodes measured using high-speed chronoamperometry.* J Neurosci Methods, 2001. **109**(1): p. 13-21.
146. Paxinos, G. and C. Watson, *The rat brain in stereotaxic coordinates*. 2007: Academic press.
147. Gerhardt, G.A. and M.R. Palmer, *Characterization of the techniques of pressure ejection and microiontophoresis using in vivo electrochemistry.* J Neurosci Methods, 1987. **22**(2): p. 147-59.

148. Zahniser, N.R., G.A. Larson, and G.A. Gerhardt, *In vivo dopamine clearance rate in rat striatum: regulation by extracellular dopamine concentration and dopamine transporter inhibitors.* J Pharmacol Exp Ther., 1999. **289**(1): p. 266-77.
149. Lipinski, C.A., et al., *Experimental and computational approaches to estimate solubility and permeability in drug discovery and development settings.* Adv Drug Deliv Rev, 2001. **46**(1-3): p. 3-26.
150. Li, Q., et al., *PubChem as a public resource for drug discovery.* Drug Discov Today, 2010. **15**(23-24): p. 1052-7.
151. Information, N.C.f.B. Pubchem Compound Database.
152. Picciotto, M.R. and P.J. Kenny, *Molecular mechanisms underlying behaviors related to nicotine addiction.* Cold Spring Harb Perspect Med, 2013. **3**(1): p. a012112.
153. Bordia, T., et al., *The alpha7 nicotinic receptor agonist ABT-107 protects against nigrostriatal damage in rats with unilateral 6-hydroxydopamine lesions.* Exp Neurol, 2015. **263**: p. 277-84.
154. Ferrea, S. and G. Winterer, *Neuroprotective and neurotoxic effects of nicotine.* Pharmacopsychiatry, 2009. **42**(6): p. 255-65.
155. Piao, W.H., et al., *Nicotine and inflammatory neurological disorders.* Acta Pharmacol Sin, 2009. **30**(6): p. 715-22.
156. Mudo, G., N. Belluardo, and K. Fuxe, *Nicotinic receptor agonists as neuroprotective/neurotrophic drugs. Progress in molecular mechanisms.* J Neural Transm, 2007. **114**(1): p. 135-47.
157. Quik, M., *Smoking, nicotine and Parkinson's disease.* Trends Neurosci, 2004. **27**(9): p. 561-8.
158. Janhunen, S. and L. Ahtee, *Differential nicotinic regulation of the nigrostriatal and mesolimbic dopaminergic pathways: implications for drug development.* Neurosci Biobehav Rev, 2007. **31**(3): p. 287-314.
159. Quik, M., M. O'Neill, and X.A. Perez, *Nicotine neuroprotection against nigrostriatal damage: importance of the animal model.* Trends Pharmacol Sci, 2007. **28**(5): p. 229-35.

160. Quik, M., et al., *Multiple roles for nicotine in Parkinson's disease.* Biochem Pharmacol, 2009. **78**(7): p. 677-85.
161. Buccafusco, J.J., et al., *Long-lasting cognitive improvement with nicotinic receptor agonists: mechanisms of pharmacokinetic-pharmacodynamic discordance.* Trends Pharmacol Sci, 2005. **26**(7): p. 352-60.
162. Stegelmeier, B.L., et al., *The toxicity and kinetics of larkspur alkaloid, methyllycaconitine, in mice.* J Anim Sci, 2003. **81**(5): p. 1237-41.
163. Brust, A., et al., *Differential evolution and neofunctionalization of snake venom metalloprotease domains.* Mol Cell Proteomics, 2013. **12**(3): p. 651-63.
164. Celie, P.H., et al., *Crystal structure of nicotinic acetylcholine receptor homolog AChBP in complex with an alpha-conotoxin PnIA variant.* Nat Struct Mol Biol, 2005. **12**(7): p. 582-8.
165. Nickell, J.R., et al., *Lobelane inhibits methamphetamine-evoked dopamine release via inhibition of the vesicular monoamine transporter-2.* J Pharmacol Exp Ther, 2010. **332**(2): p. 612-21.
166. Felpin, F.-X. and J. Lebreton, *History, chemistry and biology of alkaloids from Lobelia inflata.* Tetrahedron, 2004. **60**(45): p. 10127-10153.
167. Brown, J.M. and B.K. Yamamoto, *Effects of amphetamines on mitochondrial function: role of free radicals and oxidative stress.* Pharmacol Ther, 2003. **99**(1): p. 45-53.
168. Sheet, P.F. and G.C. Page, *CARDINAL FLOWER.*
169. Villarroya, M., et al., *Measurement of Ca2+ Entry Using 45Ca2+*, in *Calcium Signaling Protocols*, D. Lambert, Editor. 1999, Humana Press. p. 137-147.
170. Chatterjee, S., et al., *Partial agonists of the alpha3beta4* neuronal nicotinic acetylcholine receptor reduce ethanol consumption and seeking in rats.* Neuropsychopharmacology, 2011. **36**(3): p. 603-15.
171. Clarke, P.B. and M. Reuben, *Release of [3H]-noradrenaline from rat hippocampal synaptosomes by nicotine: mediation by different nicotinic*

receptor subtypes from striatal [3H]-dopamine release. Br J Pharmacol, 1996. **117**(4): p. 595-606.

172. Mihalak, K.B., F.I. Carroll, and C.W. Luetje, *Varenicline is a partial agonist at alpha4beta2 and a full agonist at alpha7 neuronal nicotinic receptors.* Mol Pharmacol, 2006. **70**(3): p. 801-5.
173. Zhu, B.T., *Mechanistic explanation for the unique pharmacologic properties of receptor partial agonists.* Biomed Pharmacother, 2005. **59**(3): p. 76-89.
174. Robison, M.M., et al., *The skeletal structure of lobinaline.* J Org Chem, 1966. **31**(10): p. 3206-13.
175. Robison, M.M., et al., *The stereochemistry and synthesis of the lobinaline ring system.* J Org Chem, 1966. **31**(10): p. 3220-3.
176. Gomes, N.G., et al., *Plants with neurobiological activity as potential targets for drug discovery.* Prog Neuropsychopharmacol Biol Psychiatry, 2009. **33**(8): p. 1372-89.
177. Koeberle, A. and O. Werz, *Multi-target approach for natural products in inflammation.* Drug Discov Today, 2014. **19**(12): p. 1871-82.
178. Virmani, A., F. Gaetani, and Z. Binienda, *Effects of metabolic modifiers such as carnitines, coenzyme Q10, and PUFAs against different forms of neurotoxic insults: metabolic inhibitors, MPTP, and methamphetamine.* Ann N Y Acad Sci, 2005. **1053**: p. 183-91.
179. Virmani, A., et al., *Metabolic syndrome in drug abuse.* Ann N Y Acad Sci, 2007. **1122**: p. 50-68.
180. Kita, T., et al., *Protective effects of phytochemical antioxidants against neurotoxin-induced degeneration of dopaminergic neurons.* J Pharmacol Sci, 2014. **124**(3): p. 313-9.
181. Phillipson, O.T., *Management of the aging risk factor for Parkinson's disease.* Neurobiol Aging, 2014. **35**(4): p. 847-57.
182. Karuppagounder, S.S., et al., *Quercetin up-regulates mitochondrial complex-I activity to protect against programmed cell death in rotenone model of Parkinson's disease in rats.* Neuroscience, 2013. **236**: p. 136-48.

183. Francis, M.M., et al., *Specific activation of the alpha 7 nicotinic acetylcholine receptor by a quaternary analog of cocaine.* Mol Pharmacol, 2001. **60**(1): p. 71-9.
184. Gerhardt, G.A. and J.J. Burmeister, *Voltammetry In Vivo for Chemical Analysis of the Nervous System*, in *Encyclopedia of Analytical Chemistry*. 2006, John Wiley & Sons, Ltd.
185. Gerhardt, G.A., et al., *Nafion-coated electrodes with high selectivity for CNS electrochemistry.* Brain Research, 1984. **290**(2): p. 390-395.
186. Rose, G.M., et al., *Age-related alterations in monoamine release from rat striatum: an in vivo electrochemical study.* Neurobiol Aging, 1986. **7**(2): p. 77-82.
187. Gerhardt, G.A., G.M. Rose, and B.J. Hoffer, *Release of monoamines from striatum of rat and mouse evoked by local application of potassium: evaluation of a new in vivo electrochemical technique.* J Neurochem, 1986. **46**(3): p. 842-50.
188. Thomas, B. and M.F. Beal, *Parkinson's disease.* Hum Mol Genet, 2007. **16 Spec No. 2**: p. R183-94.
189. Riddle, E.L., A.E. Fleckenstein, and G.R. Hanson, *Mechanisms of methamphetamine-induced dopaminergic neurotoxicity.* AAPS J, 2006. **8**(2): p. E413-8.
190. Hojahmat, M., et al., *Lobeline esters as novel ligands for neuronal nicotinic acetylcholine receptors and neurotransmitter transporters.* Bioorg Med Chem, 2010. **18**(2): p. 640-9.
191. Rueter, L.E., et al., *A-85380: a pharmacological probe for the preclinical and clinical investigation of the alphabeta neuronal nicotinic acetylcholine receptor.* CNS Drug Rev, 2006. **12**(2): p. 100-12.
192. Green, B.T., et al., *Plant toxins that affect nicotinic acetylcholine receptors: a review.* Chemical research in toxicology, 2013. **26**(8): p. 1129-1138.
193. Middleton, L.S., W.A. Cass, and L.P. Dwoskin, *Nicotinic receptor modulation of dopamine transporter function in rat striatum and medial prefrontal cortex.* J Pharmacol Exp Ther, 2004. **308**(1): p. 367-77.

194. Hoffman, A.F. and G.A. Gerhardt, *In vivo electrochemical studies of dopamine clearance in the rat substantia nigra: effects of locally applied uptake inhibitors and unilateral 6-hydroxydopamine lesions.* J Neurochem, 1998. **70**(1): p. 179-89.
195. Gulley, J.M., G.A. Larson, and N.R. Zahniser, *Using High-Speed Chronoamperometry with Local Dopamine Application to Assess Dopamine Transporter Function.*
196. Joyce, B.M., P.E. Glaser, and G.A. Gerhardt, *Adderall produces increased striatal dopamine release and a prolonged time course compared to amphetamine isomers.* Psychopharmacology (Berl), 2007. **191**(3): p. 669-77.
197. Glaser, P.E., et al., *Differential effects of amphetamine isomers on dopamine release in the rat striatum and nucleus accumbens core.* Psychopharmacology (Berl), 2005. **178**(2-3): p. 250-8.
198. Inamdar, A.P., *Ligand-based pharmacophore studies in the dopaminergic system.* 2011.
199. Enyedy, I.J., et al., *Pharmacophore-based discovery of substituted pyridines as novel dopamine transporter inhibitors.* Bioorg Med Chem Lett, 2003. **13**(3): p. 513-7.
200. Kem, W.R., et al., *Anabaseine is a potent agonist on muscle and neuronal alpha-bungarotoxin-sensitive nicotinic receptors.* J Pharmacol Exp Ther, 1997. **283**(3): p. 979-92.
201. Tsuneki, H., et al., *Marine alkaloids (-)-pictamine and (-)-lepadin B block neuronal nicotinic acetylcholine receptors.* Biol Pharm Bull, 2005. **28**(4): p. 611-4.
202. Daly, J.W., et al., *Decahydroquinoline alkaloids: noncompetitive blockers for nicotinic acetylcholine receptor-channels in pheochromocytoma cells and Torpedo electroplax.* Neurochem Res, 1991. **16**(11): p. 1207-12.
203. Hill, E.R., et al., *Potencies of cocaine methiodide on major cocaine targets in mice.* PLoS One, 2009. **4**(10): p. e7578.

204. Hopkins, A.L., *Network pharmacology: the next paradigm in drug discovery.* Nat Chem Biol, 2008. **4**(11): p. 682-90.
205. Kola, I. and J. Landis, *Can the pharmaceutical industry reduce attrition rates?* Nat Rev Drug Discov, 2004. **3**(8): p. 711-5.
206. Lipinski, C.A., *Drug-like properties and the causes of poor solubility and poor permeability.* J Pharmacol Toxicol Methods, 2000. **44**(1): p. 235-49.
207. Di Paolo, T., et al., *AQW051, a novel and selective nicotinic acetylcholine receptor alpha7 partial agonist, reduces l-Dopa-induced dyskinesias and extends the duration of l-Dopa effects in parkinsonian monkeys.* Parkinsonism Relat Disord, 2014. **20**(11): p. 1119-23.
208. Leung, E.L., et al., *Network-based drug discovery by integrating systems biology and computational technologies.* Brief Bioinform, 2013. **14**(4): p. 491-505.
209. Hojahmat, M., et al., *Lobeline esters as novel ligands for neuronal nicotinic acetylcholine receptors and neurotransmitter transporters.* Bioorganic & Medicinal Chemistry, 2010. **18**(2): p. 640-649.
210. Gunjan, S.K., et al., *Hairy root cultures and plant regeneration in Solidago nemoralis transformed with Agrobacterium rhizogenes.* American Journal of Plant Sciences, 2013. **2013**.
211. Yonemitsu, H., et al., *Lobeline production by hairy root culture of Lobelia inflata L.* Plant cell reports, 1990. **9**(6): p. 307-310.
212. Yamanaka, M., et al., *Polyacetylene glucosides in hairy root cultures of Lobelia cardinalis.* Phytochemistry, 1996. **41**(1): p. 183-185.
213. Mu, J.H., N.H. Chua, and E.M. Ross, *Expression of human muscarinic cholinergic receptors in tobacco.* Plant Mol Biol, 1997. **34**(2): p. 357-62.
214. Hanrott, K., et al., *6-hydroxydopamine-induced apoptosis is mediated via extracellular auto-oxidation and caspase 3-dependent activation of protein kinase Cdelta.* J Biol Chem, 2006. **281**(9): p. 5373-82.
215. van Wees, S., *Phenotypic analysis of Arabidopsis mutants: trypan blue stain for fungi, oomycetes, and dead plant cells.* CSH Protoc, 2008. **2008**: p. pdb prot4982.

216. Wilson, J.M., et al., *Heterogeneous subregional binding patterns of 3H-WIN 35,428 and 3H-GBR 12,935 are differentially regulated by chronic cocaine self-administration.* J Neurosci, 1994. **14**(5 Pt 2): p. 2966-79.
217. Mulangi, V., et al., *Functional analysis of OsPUT1, a rice polyamine uptake transporter.* Planta, 2012. **235**(1): p. 1-11.
218. Fujita, M. and K. Shinozaki, *Identification of polyamine transporters in plants: paraquat transport provides crucial clues.* Plant Cell Physiol, 2014. **55**(5): p. 855-61.
219. Kanai, Y. and H. Endou, *Functional properties of multispecific amino acid transporters and their implications to transporter-mediated toxicity.* J Toxicol Sci, 2003. **28**(1): p. 1-17.
220. Pifl, C., B. Giros, and M.G. Caron, *Dopamine Transporter Expression Confers Cytotoxicity to Low-Doses of the Parkinsonism-Inducing Neurotoxin 1-Methyl-4-Phenylpyridinium.* Journal of Neuroscience, 1993. **13**(10): p. 4246-4253.
221. Fritze, K. and R. Walden, *Gene activation by T-DNA tagging.* Methods Mol Biol, 1995. **44**: p. 281-294.
222. Sossi, V., et al., *Dopamine transporter relation to dopamine turnover in Parkinson's disease: a positron emission tomography study.* Ann Neurol, 2007. **62**(5): p. 468-74.
223. Miller, G.W., et al., *Dopamine transporters and neuronal injury.* Trends Pharmacol Sci, 1999. **20**(10): p. 424-9.
224. Masoud, S.T., et al., *Increased expression of the dopamine transporter leads to loss of dopamine neurons, oxidative stress and l-DOPA reversible motor deficits.* Neurobiol Dis, 2015. **74**: p. 66-75.
225. Widmaier, E.P., et al., *Vander's human physiology : the mechanisms of body function*. 2008, Boston: McGraw-Hill Higher Education.
226. Bousquet, M., et al., *Beneficial effects of dietary omega-3 polyunsaturated fatty acid on toxin-induced neuronal degeneration in an animal model of Parkinson's disease.* FASEB J, 2008. **22**(4): p. 1213-25.

227. Lim, L., et al., *Lanosterol induces mitochondrial uncoupling and protects dopaminergic neurons from cell death in a model for Parkinson's disease.* Cell Death Differ, 2012. **19**(3): p. 416-27.
228. Kohno, Y., et al., *Kinetic study of quenching reaction of singlet oxygen and scavenging reaction of free radical by squalene in n-butanol.* Biochim Biophys Acta, 1995. **1256**(1): p. 52-6.
229. Piironen, V., et al., *Plant sterols: biosynthesis, biological function and their importance to human nutrition.* Journal of the Science of Food and Agriculture, 2000. **80**(7): p. 939-966.
230. Brouillet, E., et al., *3-Nitropropionic acid: a mitochondrial toxin to uncover physiopathological mechanisms underlying striatal degeneration in Huntington's disease.* J Neurochem, 2005. **95**(6): p. 1521-40.
231. Garcia, M., et al., *The mitochondrial toxin 3-nitropropionic acid induces striatal neurodegeneration via a c-Jun N-terminal kinase/c-Jun module.* J Neurosci, 2002. **22**(6): p. 2174-84.
232. Kumar, P. and A. Kumar, *Possible neuroprotective effect of Withania somnifera root extract against 3-nitropropionic acid-induced behavioral, biochemical, and mitochondrial dysfunction in an animal model of Huntington's disease.* J Med Food, 2009. **12**(3): p. 591-600.
233. Brouillet, E., et al., *Replicating Huntington's disease phenotype in experimental animals.* Prog Neurobiol, 1999. **59**(5): p. 427-68.
234. Kumar, G.P. and F. Khanum, *Neuroprotective potential of phytochemicals.* Pharmacogn Rev, 2012. **6**(12): p. 81-90.
235. Houghton, P.J. and M.J. Howes, *Natural products and derivatives affecting neurotransmission relevant to Alzheimer's and Parkinson's disease.* Neurosignals, 2005. **14**(1-2): p. 6-22.
236. Nolvachai, Y. and P.J. Marriott, *GC for flavonoids analysis: Past, current, and prospective trends.* J Sep Sci, 2013. **36**(1): p. 20-36.
237. Vodopivec, B.M., et al., *Differences in the structure of anthocyanins from the two amphibious plants, Lobelia cardinalis and Nesaea crassicaulis.* Nat Prod Res, 2013. **27**(7): p. 654-64.

238. Sykiotis, G.P., et al., *The role of the antioxidant and longevity-promoting Nrf2 pathway in metabolic regulation.* Curr Opin Clin Nutr Metab Care, 2011. **14**(1): p. 41-8.
239. Gacesa, R., W.C. Dunlap, and P.F. Long, *Bioinformatics analyses provide insight into distant homology of the Keap1-Nrf2 pathway.* Free Radic Biol Med, 2015.
240. Stefanson, A.L. and M. Bakovic, *Dietary regulation of Keap1/Nrf2/ARE pathway: focus on plant-derived compounds and trace minerals.* Nutrients, 2014. **6**(9): p. 3777-801.
241. Bryan, H.K., et al., *The Nrf2 cell defence pathway: Keap1-dependent and -independent mechanisms of regulation.* Biochem Pharmacol, 2013. **85**(6): p. 705-17.
242. Miller, D.M., et al., *Administration of the Nrf2-ARE activators sulforaphane and carnosic acid attenuates 4-hydroxy-2-nonenal-induced mitochondrial dysfunction ex vivo.* Free Radic Biol Med, 2013. **57**: p. 1-9.
243. Jones, A.M., et al., *The impact of Arabidopsis on human health: diversifying our portfolio.* Cell, 2008. **133**(6): p. 939-43.
244. Xu, X.M. and S.G. Moller, *The value of Arabidopsis research in understanding human disease states.* Curr Opin Biotechnol, 2011. **22**(2): p. 300-7.
245. Gama Sosa, M.A., R. De Gasperi, and G.A. Elder, *Modeling human neurodegenerative diseases in transgenic systems.* Hum Genet, 2012. **131**(4): p. 535-63.
246. Wang, Y. and M. Yang, *The Arabidopsis skp1-like1-1 (ask1-1) mutant and the mouse cells of a sporadic Parkinson's disease model created with downregulation of SKP1 share similar cellular defects.* Parkinsonism Relat Disord, 2012. **18**(1): p. 102-3.
247. Wang, Z., et al., *DJ-1 modulates the expression of Cu/Zn-superoxide dismutase-1 through the Erk1/2-Elk1 pathway in neuroprotection.* Ann Neurol, 2011. **70**(4): p. 591-9.

248. Lohr, K.M., et al., *Increased vesicular monoamine transporter enhances dopamine release and opposes Parkinson disease-related neurodegeneration in vivo.* Proc Natl Acad Sci U S A, 2014. **111**(27): p. 9977-82.
249. Haque, M.E., et al., *Cytoplasmic Pink1 activity protects neurons from dopaminergic neurotoxin MPTP.* Proc Natl Acad Sci U S A, 2008. **105**(5): p. 1716-21.
250. Lee, M.A., et al., *Overexpression of midbrain-specific transcription factor Nurr1 modifies susceptibility of mouse neural stem cells to neurotoxins.* Neurosci Lett, 2002. **333**(1): p. 74-8.
251. O'Malley, K.L., et al., *Targeted expression of BCL-2 attenuates MPP+ but not 6-OHDA induced cell death in dopaminergic neurons.* Neurobiol Dis, 2003. **14**(1): p. 43-51.
252. Xu, X.M., et al., *The Arabidopsis DJ-1a protein confers stress protection through cytosolic SOD activation.* J Cell Sci, 2010. **123**(Pt 10): p. 1644-51.
253. Xu, X.M. and S.G. Moller, *ROS removal by DJ-1: Arabidopsis as a new model to understand Parkinson's Disease.* Plant Signal Behav, 2010. **5**(8): p. 1034-6.
254. Gopalakrishnan, A., M. Sievert, and A.E. Ruoho, *Identification of the substrate binding region of vesicular monoamine transporter-2 (VMAT-2) using iodoaminoflisopolol as a novel photoprobe.* Molecular pharmacology, 2007. **72**(6): p. 1567-1575.
255. Staal, R.G., et al., *Interactions of 1-methyl-4-phenylpyridinium and other compounds with P-glycoprotein: relevance to toxicity of 1-methyl-4-phenyl-1, 2, 3, 6-tetrahydropyridine.* Brain research, 2001. **910**(1): p. 116-125.
256. Saier Jr, M.H., et al., *The major facilitator superfamily.* J Mol Microbiol Biotechnol, 1999. **1**(2): p. 257-279.
257. Yelin, R. and S. Schuldiner, *The pharmacological profile of the vesicular monoamine transporter resembles that of multidrug transporters.* FEBS letters, 1995. **377**(2): p. 201-207.

258. Verrier, P.J., et al., *Plant ABC proteins–a unified nomenclature and updated inventory.* Trends in plant science, 2008. **13**(4): p. 151-159.
259. Lord, C.E. and A.H. Gunawardena, *Programmed cell death in C. elegans, mammals and plants.* Eur J Cell Biol, 2012. **91**(8): p. 603-13.
260. Falcone, D., et al. *A functional genomics strategy to identify genes that regulate the production of biologically active metabolites in plants*. in *Plant biotechnology 2002 and beyond. Proceedings of the 10th IAPTC&B Congress, Orlando, Florida, USA, 23-28 June, 2002*. 2003. Kluwer Academic Publishers.
261. Miller, D.M., et al., *Nrf2-ARE activator carnosic acid decreases mitochondrial dysfunction, oxidative damage and neuronal cytoskeletal degradation following traumatic brain injury in mice.* Exp Neurol, 2015. **264**: p. 103-10.

Vita

Dustin Paul Brown
Graduate Student
The University of Kentucky
Department of Anatomy and Neurobiology
Lexington, Kentucky

Education

University of Kentucky Graduate School **August 2010 – 2015**
Department of Anatomy and Neurobiology
G.P.A 4.000
University of Kentucky Graduate School
Lexington, KY 40506-0033

University of Kentucky Medical School **August 2008 - Present**
Promotion with High Distinction (2008-2009)
Promotion with Distinction (2009-2010)
G.P.A. 3.873
University of Kentucky College of Medicine
Lexington, KY 40536-0298

Bachelor of Arts **August 2005 – May 2008**
University Honors: Summa Cum Laude
Biology
G.P.A. 3.88
University of Kentucky
Lexington, KY 40506

Owensboro Community and Technical College **August 2004 – July 2005**
Undetermined
G.P.A 3.79
Owensboro, KY 42303

University of Kentucky Medical School **August 2003 – May 2004**
Pre-Pharmacy
G.P.A 3.67
Lexington, KY 40506

High School Diploma **August 1999 –May 2003**
Salutatorian
G.P.A 3.95
McLean County High
Calhoun, KY 42327

Presentations and Posters/Abstracts

Presentations

Brown DP. Back to the Roots of Drug Discovery: Development of Novel Pharmacotherapies for Drug Abuse. University of Kentucky Department of Anatomy and Neurobiology, Departmental Seminar, Lexington, KY, May 15, 2014

Brown DP. Plant-Based Drug Discovery Aimed at the Development of Novel Ligands for the Dopamine Transporter. University of Kentucky Department of Anatomy and Neurobiology, Departmental Seminar, Lexington, KY, May 2, 2013

Brown DP. Applying Evolutionary Concepts to Plant-Based Drug Discovery. Center for Clinical and Translational Science Seminar Series, Lexington, KY, November 14, 2012

Brown DP. The Evolution of (Plant) Species (for Smoking Cessation) by Natural Selection. 35th Annual Research Society on Alcoholism Scientific Meeting, San Francisco, CA, June 23-27, 2012

Brown DP. Plant-Based Drug Discovery Aimed at the Development of Novel Ligands for the Dopamine Transporter. University of Kentucky Department of Anatomy and Neurobiology, Departmental Seminar, Lexington, KY, April, 26, 2012

Brown DP. Plant-Based Drug Discovery Aimed at the Development of Novel Ligands for the Dopamine Transporter. University of Kentucky Department of Anatomy and Neurobiology, Departmental Seminar, Lexington, KY, September 15, 2011

Brown DP, Lutz J. Persuading Plants to Make Neuroprotective Compounds. Kentucky Tobacco Research and Development Center, Lexington, KY, February 23, 2011

Posters/Abstracts

Brown DP, Rogers DT, Siripurapu KB, Gerhardt GA, Littleton JM. Lobinaline: The Major Bioactive Alkaloid Present in *Lobelia cardinalis* and a Promising Lead to Develop Novel Multifunctional Anti-Parkinsonian Agents. Alpha Omega Alpha Groves Memorial and M.D./Ph.D Program Student Research Symposium, Lexington, KY, February 3, 2015

Brown DP, Rogers DT, Gunjan S, Siripurapu KB, Gerhardt GA, Littleton JM. Target-Directed Biosynthesis of Multifunctional Plant Metabolites as Potential

Therapeutics for Alcohol and Nicotine Co-Dependence. 37th Annual Research Society on Alcoholism Scientific Meeting, Bellevue, WA, June 21-25, 2014

Brown DP, Rogers DT, Gunjan S, Siripurapu KB, Gerhardt GA, Littleton JM. Back to the "Roots" of Plant Drug Discovery: Natural Selection of Transgenic Root Cells for Novel Bioactive Metabolites. Alpha Omega Alpha Groves Memorial and M.D./Ph.D. Program Student Research Symposium, Lexington, KY, February 21, 2014

Brown DP, Rogers DT, Gunjan S, Gerhardt GA, Littleton JM. Directed Evolution of Plant Metabolites as Leads for the Treatment of Comorbid Alcohol and Nicotine Use Disorders. 36th Annual Research Society on Alcoholism Scientific Meeting, Orlando, FL, June 22-26, 2013

Brown DP, Rogers DT, Gunjan S, Gerhardt GA, Littleton JM. Pharmacological Optimization of Plant Species by Directed Evoltuion. Alpha Omega Alpha Groves Memorial and M.D./Ph.D. Program Student Research Symposium, Lexington, KY, February 20, 2013

Brown DP, Rogers DT, Gunjan S, Gerhardt GA, Littleton JM. The Evolution of Plant Metabolites for Smoking Cessation in Alcoholics. 35th Annual Research Society on Alcoholism Scientific Meeting, San Francisco, CA, June 23-27, 2012

Brown DP, Rogers DT, Gunjan S, Gerhardt GA, Littleton JM. The Evolution of Plant Metabolites for Smoking Cessation in Alcoholics. Alpha Omega Alpha Groves Memorial and M.D./Ph.D. Program Student Research Symposium, Lexington, KY, March 1, 2012

Brown DP, Rogers DT, Gunjan S, Littleton JM. Expression of Mammalian CNS Proteins in Plant Systems: A Step Toward the Development of 'Directed Evolution' of Plant Metabolomes to Produce Medicinal Compounds. Alpha Omega Alpha Groves Memorial and M.D./Ph.D. Program Student Research Symposium, Lexington, KY, February 2, 2011

Honors and Awards

NIDA T32 Training Grant: "Training in Drug Abuse and Related Research", 2014 - 2015
NIA T32 Training Grant: "The Cellular and Molecular Basis of Aging", 2012 - 2014
Kentucky Opportunity Fellowship, 2010 - 2012
MD/PhD Scholarship at the University of Kentucky College of Medicine, 2008 - Present
Promotion with Distinction, University of Kentucky Medical School, 2009 - 2010

Promotion with High Distinction, University of Kentucky Medical School, 2008 - 2009
John B. and Brownie Young Memorial Scholarship, 2003 – 2015
University Honors: Summa Cum Laude, University of Kentucky, 2008
Deans' List, University of Kentucky, 2005 – 2008
Deans' List, Owensboro Community and Technical College, 2004 – 2005
McLean County High School: Science Award in Chemistry and Physics, Math Award, Recognition as Participant With Distinction in Biology and Chemistry by the National Science League, Recognition as Participating with Distinction in Chemistry by the National Science Olympiad, Certificate of Recognition by the Kentucky Administrative Support Skills Standards for successfully mastering Administrative Support Standards